

Technical Report Documentation Page

| | | | | | |
|---|--|--|--|--|-----------|
| 1. Report No. UMTA-MA-06-0025-74-3 | | 2. Government Accession No. PB 233 016/AS | | 3. Recipient's Catalog No. | |
| 4. Title and Subtitle ASSESSMENT OF DESIGN TOOLS AND CRITERIA FOR URBAN RAIL TRACK STRUCTURES Volume I. At-Grade Tie-Ballast Track | | | | 5. Report Date Reprint: July 1974 | |
| | | | | 6. Performing Organization Code | |
| 7. Author(s) Robert H. Prause, Howard C. Meacham, et al* | | | | 8. Performing Organization Report No. DOT-TSC-UMTA-74-5 | |
| 9. Performing Organization Name and Address Battelle-Columbus Laboratories 505 King Ave. Columbus OH 43201 | | | | 10. Work Unit No. (TRAIS) UM404/R4734 | |
| | | | | 11. Contract or Grant No. DOT-TSC-563 | |
| 12. Sponsoring Agency Name and Address Department of Transportation Urban Mass Transportation Administration Office of Research and Development Washington DC 20590 | | | | 13. Type of Report and Period Covered Final Report March 1973 - March 1974 | |
| | | | | 14. Sponsoring Agency Code | |
| 15. Supplementary Notes Department of Transportation *Under contract to: Transportation Systems Center Cambridge MA 02142 Vol. II is subtitled "At-Grade Slab Track" | | | | | |
| 16. Abstract The development of techniques and criteria for track design is an important part of the Rail Supporting Technology Program that is being managed for the Urban Mass Transportation Administration by the Transportation Systems Center (TSC). This report presents the results of a critical review of the technical factors which govern the design and performance of at-grade tie-ballast track for urban rail systems. The assessment of current design practice is based on a review of the literature and discussions with experienced track design personnel. The evaluation includes design loads and the criteria for selecting rail size, tie size and spacing, ballast depth, and subgrade parameters. The major track problems identified were rail joints, rail wear and noise on curves, rail fasteners, and rail corrugation. Detailed technical evaluations were made to determine those areas where the track design procedures are inadequate. The report includes detailed information for the engineering design of track and recommendations for both short and long-range program plans for future research pertaining to the improvement of track performance. Volume II of this two volume report, entitled "At-Grade Slab Track", gives similar results for at-grade concrete slab track construction. | | | | | |
| 17. Key Words Track, track design, track loading, rapid transit systems, ballast, cross ties, fastenings, rail, rail defects, rail joints, rail wear, stresses, noise, soil mechanics | | | | 18. Distribution Statement DOCUMENT IS AVAILABLE TO THE PUBLIC THROUGH THE NATIONAL TECHNICAL INFORMATION SERVICE, SPRINGFIELD, VIRGINIA 22151. | |
| 19. Security Classif. (of this report) UNCLASSIFIED | | 20. Security Classif. (of this page) UNCLASSIFIED | | 21. No. of Pages 250 | 22. Price |

PREFACE

This report presents the results of a program to review the technical factors which govern the design and performance of at-grade urban rail track structures. The report has been prepared by Battelle-Columbus Laboratories (BCL) under Contract DOT-TSC-563 for the Transportation Systems Center (TSC), Systems Manager for the Urban Mass Transportation Administration's Rail Supporting Technology Program. The program was conducted under the technical direction of Dr. Leonard Kurzweil, Code TMP, at the Transportation Systems Center.

The report is presented in two volumes. Volume I gives results related to the design and performance of tie-ballast track construction and Volume II is an evaluation of the technical requirements for designing track constructed from concrete slab.

The cooperation and assistance provided by Dr. Leonard Kurzweil and Dr. Herbert Weinstock of TSC and Mr. Ronald Melvin of BCL is gratefully acknowledged. Dr. Kamran Majizadeh, Professor of Civil Engineering at The Ohio State University, deserves recognition for his contribution as a consultant on soil mechanics.

This report is necessarily quite dependent on previous work which has been reported in the literature, and the authors are grateful to the several authors and publishers who granted permission for the use of copyrighted material.

TABLE OF CONTENTS

| <u>SECTION</u> | <u>Page</u> |
|---|-------------|
| 1.0 INTRODUCTION | 1 |
| 2.0 SUMMARY OF CONCLUSIONS AND RECOMMENDATIONS FOR FUTURE RESEARCH | 3 |
| 3.0 CURRENT DESIGN PRACTICE FOR CONVENTIONAL AT-GRADE TRACK STRUCTURES | 10 |
| 3.1 Design Loads | 12 |
| 3.1.1 Vertical Design Loads | 14 |
| 3.1.2 Lateral Design Loads | 14 |
| 3.1.3 Longitudinal Design Loads | 15 |
| 3.2 Track Design Procedures | 15 |
| 3.2.1 Beam on Elastic Foundation Analysis | 15 |
| 3.2.2 Rail Size | 25 |
| 3.2.3 Rail Fasteners | 37 |
| 3.2.4 Cross Ties | 49 |
| 3.2.5 Ballast | 61 |
| 3.2.6 Subgrade | 75 |
| 3.3 Comparison of Track Design Parameters for Recent Track Construction | 85 |
| 3.4 Lateral Track Strength | 88 |
| 3.4.1 Lateral Track Strength on Curves | 89 |
| 3.4.2 Track Lateral Shift | 91 |
| 3.4.3 Rail Rollover | 94 |
| 3.4.4 Wheel Derailment | 95 |
| 3.4.5 Wheel Flange Clearance | 95 |
| 4.0 DISCUSSION OF CURRENT TRACK PROBLEMS AND RECOMMENDATIONS FOR FUTURE RESEARCH | 97 |
| 4.1 Literature Survey | 97 |
| 4.1.1 Noise | 98 |
| 4.1.2 Ride Quality | 99 |
| 4.1.3 Derailment | 99 |
| 4.2 Priority Ranking of Urban Rail Track Problems | 100 |
| 4.2.1 Industry Interviews | 100 |

TABLE OF CONTENTS (Continued)

| <u>SECTION</u> | <u>Page</u> |
|---|-------------|
| 4.3 Rail Joints | 104 |
| 4.3.1 Technical Evaluation | 106 |
| 4.3.2 Summary of Conclusions and Recommendations | 123 |
| 4.4 Rail Wear and Lubrication | 125 |
| 4.4.1 Technical Evaluation of Rail Wear and Lubrication | 126 |
| 4.4.2 Summary of Conclusions and Recommendations | 136 |
| 4.5 Rail Fasteners | 137 |
| 4.5.1 Summary of Conclusions and Recommendations | 138 |
| 4.6 Rail Corrugation | 139 |
| 4.6.1 Technical Evaluation | 141 |
| 4.6.2 Summary of Results and Conclusions | 151 |
| 4.7 Rail Field Welds. | 152 |
| 4.7.1 Conclusions and Recommendations | 153 |
| 4.8 Track Geometry | 155 |
| 4.8.1 Technical Evaluation | 156 |
| 4.8.2 Conclusions and Recommendations | 158 |
| 4.9 Community Noise and Vibration | 159 |
| 4.10 Track Buckling | 159 |
| 4.11 Track Maintenance Equipment | 160 |
| 4.12 Rail Failures | 161 |
| 4.12.1 Rail Shelling | 161 |
| 4.12.2 Transverse Fissures | 164 |
| 4.12.3 Engine-Burn Fractures | 165 |
| 4.12.4 Horizontal Split Head | 165 |
| 4.12.5 Vertical Split Head | 167 |
| 4.12.6 Piped Rail | 167 |
| 4.12.7 Compound Fissure | 167 |
| 4.12.8 Weeping Cracks | 167 |
| 4.12.9 Flowed Head and Head Check | 169 |
| 4.12.10 Head and Web Separation | 169 |
| 4.12.11 Split Web and Bolt Hole Crack | 169 |

TABLE OF CONTENTS (Continued)

| | <u>Page</u> |
|---|-------------|
| REFERENCES | 171 |
| APPENDIX A RAIL PRODUCTION DATA | A-1 |
| APPENDIX B BEAM ON ELASTIC FOUNDATION ANALYSIS OF TIE DEFLECTIONS AND BALLAST PRESSURES | B-1 |
| APPENDIX C BALLAST PYRAMID MODEL. | C-1 |
| APPENDIX D SOIL CLASSIFICATION | D-1 |
| APPENDIX E TRACK STRUCTURE SETTLEMENT | E-1 |
| APPENDIX F REPORT OF INVENTIONS. | F-1 |
| INDEX | G-1 |

LIST OF ILLUSTRATIONS

| <u>Figure</u> | | <u>Page</u> |
|---------------|---|-------------|
| 3-1 | Flow Chart for Conventional At-Grade Track Structure Design | 11 |
| 3-2 | Normalized Rail Deflection and Bending Moment Curves | 18 |
| 3-3 | Track Modulus Measurement Procedure | 20 |
| 3-4 | Comparison of Several Formulas Used to Predict the Effect of Train Speed on Rail Stress | 30 |
| 3-5 | Lumped Parameter Model Representing Portion of Car and Track Structure Associated with one Truck | 46 |
| 3-6 | Effect of Rail Pad Stiffness K_p on Response of Car and Track to a 1/4-Inch Step in the Rail Profile | 47 |
| 3-7 | Pressure Distribution Along Tie Length | 53 |
| 3-8 | Ballast Pressure Under an Oak Tie (6" x 8" x 8'6", $E_p =$ 1.15×10^6 psi) For Various Values of Ballast Foundation Modulus k_o . The Rail Seat Load $q_o = 17,500$ lbs | 59 |
| 3-9 | Ballast Pressure Under 6" x 8" x 8'6" Wood and Concrete Ties. Ballast Foundation Modulus $k_o = 5,000$ psi and the Rail Seat Load $q_o = 17,500$ lbs | 60 |
| 3-10 | Average Vertical Pressure Distribution on the Subgrade Using the Principle of Superposition for Different Ballast Depths | 68 |
| 3-11 | Average Vertical Pressure Distribution at Depths up to 30 Inches of Ballast Below the Center-Line of a Single Tie . . | 69 |
| 3-12 | Comparison of Ballast Pressure Predictions with Measured Data by Salem and Hay. | 70 |
| 3-13 | Average Vertical Pressure Distribution on the Subgrade at a Depth of 18 Inches of Ballast Below a Single Tie | 72 |
| 3-14 | Vertical Pressure Distribution at Depths up to 30 Inches of Ballast Below the Center-Line of a Single Tie, Tie Load = 20,000 lbs | 73 |
| 3-15 | Pyramid Model for Ballast Pressure Distribution | 74 |
| 3-16 | AASHTO Compaction Curves | 78 |

LIST OF ILLUSTRATIONS (Continued)

| <u>Figure</u> | | <u>Page</u> |
|---------------|---|-------------|
| 3-17 | Load-Penetration Curves for Typical Soils Tested by the CBR Method | 80 |
| 3-18 | Approximate Correlation of the Casagrande, R. R. and C.A.A. Classification on the Basis of Bearing Capacity | 81 |
| 3-19 | Relationship Between Modulus of Subgrade Reaction and Diameter of Bearing Plate. | 82 |
| 3-20 | Cumulative Strain Resulting from Repeated Loading Tests of London Clay | 84 |
| 3-21 | Design Chart for Determining Ballast Depth and Soil Strength Requirements | 86 |
| 4-1 | Typical Failure at Rail Joint Through the First Bolt Hole. | 107 |
| 4-2 | Bending Moment and Rail Depression for a Single Wheel Load at a Joint | 110 |
| 4-3 | Division of Moment Between Rail and Joint Bars | 112 |
| 4-4 | Illustration of Stresses Acting Between Joint Members | 113 |
| 4-5 | Effect of Bolt Tension on Joint Bar Stresses for Lateral Bending Moments | 114 |
| 4-6 | Cantilevered Beam with a Hole | 115 |
| 4-7 | Stress Concentration Factor Around a Bolt Hole | 117 |
| 4-8 | Photoelastic Model of Loaded Rail End | 118 |
| 4-9 | Sketch of Fringe Orders on Photoelastic Model of Rail End. Fringe Constant is 160 psi/Fringe, The Load Q is 130.9 lb. | 120 |
| 4-10 | Joint Bar and Receiving Rail Impact-Load Comparison at Low and High Speed, Compromise Joint | 122 |
| 4-11 | Conventional Coned and Worn Contour Wheels | 132 |
| 4-12 | Servocontrolled Laboratory Machine to Produce Both Vertical Loading and Longitudinal Rocking of the Rail, for Evaluating Rail Anchors | 140 |
| 4-13 | Typical Rail Corrugations | 142 |
| 4-14 | Rail Profile Measurement Apparatus | 146 |

LIST OF ILLUSTRATIONS (Continued)

| <u>Figure</u> | | <u>Page</u> |
|---------------|--|-------------|
| 4-15 | Profile of Typical Corrugation on Shaker Heights Rapid Transit Lines (East Bound Track) | 147 |
| 4-16 | Profile of Corrugations on Shaker Heights Rapid Transit Lines (West Bound Track) | 148 |
| 4-17 | Effect of Train Velocity on Corrugation Wavelength for Typical Contact Resonant Frequencies | 149 |
| 4-18 | Summary of Corrugation Wavelength Versus Estimated Train Speed Measurements at Shaker Heights | 150 |
| 4-19 | Typical Shelly Failures | 162 |
| 4-20 | Rail Head Showing Transverse Fissure Defect | 166 |
| 4-21 | Horizontal Split-Head Defect | 166 |
| 4-22 | Vertical Head and Web Defects. | 166 |
| 4-23 | Flowed Head and Head Check | 168 |
| 4-24 | Head and Web Separation | 168 |
| 4-25 | Split Web Originating Around Bolt Holes | 168 |
| A-1 | Percentage of Total Rail Rolled in North America by Year for the Four Rail Sections of Major Interest | A-3 |
| A-2 | Bending Stiffness and Relative Efficiency of Various Rail Sections | A-6 |
| B-1 | Illustration of a Beam on an Elastic Foundation | B-2 |
| B-2 | Ballast Pressure under an Oak Tie (6" x 8" x 8'6", $E_p = 1.15 \times 10^6$ psi) for Various Values of Ballast Foundation Modulus, k_o . The Rail Seat Load $q_o = 17,500$ lbs | B-6 |
| B-3 | Ballast Pressure under 6" x 8" x 8'6" Wood and Concrete Ties. Ballast Foundation Modulus $k_o = 5000$ psi and the Rail Seat Load $q_o = 17,500$ lbs | B-8 |
| C-1 | Ballast Pyramid Model | C-2 |
| C-2 | Lines of Equal Vertical Pressure in Ballast for a Single Loaded Tie | C-4 |
| C-3 | Effective Bearing Area as a Function of Ballast Depth Beneath Tie Base | C-5 |

LIST OF ILLUSTRATIONS (Continued)

| <u>Figure</u> | | <u>Page</u> |
|---------------|--|-------------|
| E-1 | Effect of Confining Pressure and Number of Load Cycles On the Axial Strain | E-4 |
| E-2 | Typical Stress-Strain Curve for a Soil | E-5 |
| E-3 | Stress-Strain Diagram of an Elastic, Perfectly Plastic Material | E-6 |
| E-4 | Typical Deformation-Load Cycles, N. Curve | E-8 |
| E-5 | Contours of Vertical Stress | E-12 |
| E-6 | Idealized Load-Initial Settlement Curve | E-14 |
| E-7 | Terzaghi's Problem - One Dimensional Consolidation . . . | E-18 |
| E-8 | Biot's Problem - Previous Strip Load on Halfspace (Spatial Distribution of Surface Settlements) | E-18 |
| E-9 | Viscoelastic and Elastic Models for Soil Consolidation . | E-19 |

LIST OF TABLES

| <u>Table</u> | | <u>Page</u> |
|--------------|--|-------------|
| 3-1 | Weights of Typical Rail Cars | 13 |
| 3-2 | Typical Data for Characteristic Lengths X_1 and X_2 | 18 |
| 3-3 | Typical Track Modulus Data | 22 |
| 3-4 | Comparison of Stress Factors from the Literature | 31 |
| 3-5 | Rail Wear Factors for Predicting Rail Life on Curves | 34 |
| 3-6 | Wear Factors for Calculating Rail Head Wear by the Couard Method | 36 |
| 3-7 | Comparison of Rail Wear Predictions by AREA and Couard Methods | 38 |
| 3-8 | Summary of Typical Vertical and Lateral Rail Fastener Design Loads | 42 |
| 3-9 | Effective Tie Bearing Areas and Lengths | 54 |
| 3-10 | Safe Average Bearing Pressures of Soils | 65 |
| 3-11 | Ballast Depth Required to Reduce 65 psi Pressure to 20 psi | 67 |
| 3-12 | Comparison of Selected Track Design Parameters for Rapid Transit Track. | 87 |
| 4-1 | Priority Ranking of Rapid Transit Industry Problems | 97 |
| 4-2 | Organizations and Personnel Interviewed About Track Design and Track Problems. | 102 |
| 4-3 | Priority Ranking of Track Structure Problems | 103 |
| A-1 | Quantities of AREA Recommended Rail Sections Rolled in North America from 1962 to 1971 | A-2 |
| A-2 | Rail Section Properties | A-5 |
| D-1 | ASTM Soil Classification | D-2 |
| D-2 | Soil Components-USCS System | D-2 |
| D-3 | Soil Strength and Density for Penetration Test | D-4 |

1.0 INTRODUCTION

The development of urban rail systems is an important factor in meeting the transportation requirements of large cities in the coming years. In addition, the rapidly changing economic and technological environment makes it necessary to continually reevaluate the criteria used to design all components of the transportation system.

The objective of this program was to evaluate the technical factors which govern the design and performance of urban rail track structures. This report includes information that is useful for the engineering design of track as well as recommendations to be used for the development of both short and long-range program plans for future track research.

These results will be used to develop standard techniques and criteria for track design as a part of the Urban Mass Transportation Administration's Rail Supporting Technology Program that is being managed by TSC.

The results of this program are presented in two volumes. This report, Volume I, gives the results pertaining to the design and performance of at-grade tie-ballast track construction. Volume II gives an evaluation of the technical requirements for designing at-grade track constructed from concrete slab.

The major conclusions and recommendations resulting from the work reported in Volume I are summarized in Section 2. Detailed results are presented in Sections 3 and 4.

Section 3 of this report is a critical review of current design practice for at-grade track structures, including the design loads and the criteria for selecting rail size, tie size and spacing, ballast depth, and subgrade parameters. The discussion of the design criteria includes a critical evaluation of the governing assumptions and recommendations for improving the design procedures where they appear deficient. The review of current design practice is based on the results of a relatively extensive review of available literature and discussions with persons experienced in track design.

Section 4 of this report discusses the major track problems which were identified from the literature review and during meetings with track design and maintenance personnel from several urban rail operating properties. Detailed technical evaluations have been made of several of the high priority track

problems to determine those areas where the design procedures are inadequate and to determine what additional research is needed to improve track performance.

In an effort to make this report easier to use, information about very specific topics of interest for track structures can be located by referring to the Volume I Index.

2.0 SUMMARY OF CONCLUSIONS AND RECOMMENDATIONS FOR FUTURE RESEARCH

The current practice for designing at-grade track is based on satisfying several criteria for the strength of individual track components. These criteria include rail stresses, tie bending stress, pressure on the ballast, and pressure on the subgrade. The key factor in evaluating these criteria is the beam on elastic foundation analysis model, whereby a continuous elastic support for the rail is used to represent the discrete tie supports for actual track.

This simplified analytical model yields accurate results for the deflections and bending moments in the rail for existing track where measured data can be obtained on the effective track modulus. The principal deficiency of this design procedure, however, is that there is not sufficient information available, either analytical or experimental to accurately evaluate the contribution of individual track components to the overall track performance. Furthermore, the design criteria for the individual track components are not based on indices which represent the important track performance criteria such as safety, ride quality, maintenance, and the noise and vibration transmitted to the community. A prime example of this deficiency is that while the deterioration of track geometry (vertical profile, lateral alignment, crosslevel, gauge) is a governing factor for all aspects of track performance, there is no way to quantitatively evaluate the effect of changing track design parameters such as ballast depth, tie size, or tie spacing on the deterioration of track geometry in service.

The development of a track design procedure that is directly related to the significant track performance criteria is recommended as a high-priority, long-term objective that will require considerable research in all aspects of track performance. Many of the specific topics for research that are needed to reach this objective are described briefly in this section, and they are discussed in greater detail in the indicated sections of the report. Additional information on specific topics can be located by using the Index.

Statistical Description of Track Forces. The actual forces in track structures from the train wheels and from the environment are quite complex. A more detailed, statistical description of track loading is needed to evaluate the reliability of track components and provide a basis for developing improved track performance criteria. Specific areas where a statistical load description is

needed include the development of design criteria and evaluation tests for improved rail fasteners for concrete ties and for direct fixation to concrete invert and slab track structures; the development of fatigue criteria for the design and evaluation of concrete ties; the development of realistic models for the differential settlement of track; and the development of improved design criteria for bolted rail joints. Additional information is given in Sections 3.1, 3.2, 4.3, and 4.5.

Characteristics of Ballast and Subgrade. The effect of ballast and subgrade characteristics on tie loads, rail deflection and stresses, and subgrade pressures is not known with sufficient accuracy to evaluate changes in track design. Measured data on the performance of ballast and subgrade in track are needed to develop improved analytical models of the track roadbed. See Sections 3.0, 3.2, and 4.8 for more detail.

Rail Wear Prediction. Existing methods for predicting rail wear are based on empirical results for existing track, and they do not include sufficient information for evaluating the effect of vehicle or track design changes on wear rate. Improved analytical models which account for such parameters as contact stresses, curve geometry, rail material, vehicle design, operating speed, environmental conditions, etc., are needed for predicting rail wear on curves as a first step for making a significant reduction in wear rates. Detailed wear and traffic data for particular track locations are needed to correlate with analytical models. Sections 3.2.2 and 4.4 give additional data.

Rail Fastener Loads. Rail fasteners are a key component for improved track designs, and a better definition of service loads is needed as a basis for fastener design and for developing realistic accelerated life tests. See Sections 3.2.3 and 4.5.

Concrete Ties. Several types of concrete ties are now performing satisfactorily in transit track, and the recent increased cost and reduced availability of wood ties makes the concrete tie a more attractive alternative. However, additional information is needed to determine if concrete ties really have significant advantages in durability and performance. Also, concrete ties

should be designed specifically for rapid transit use where the support of guard rails, restraining rails, and a contact rail are important requirements. Additional information is given in Section 3.2.4.

Track Subgrade. The effect of subgrade properties and the preparation of the subgrade during track construction is a critical factor for track performance, but this is the least understood and the most neglected part of track design. Additional information on the effect of the subgrade on track differential settlement in service is needed to demonstrate the importance of the subgrade in obtaining improved track performance. The development of laboratory soil tests based on the static and cyclic loading for track needs further evaluation. See Sections 3.2.6 and 4.8.

Track Model for Lateral Loads. The current track design practice is based almost entirely on vertical load requirements. However, many of the safety related aspects of track performance such as thermal buckling, train derailment, track lateral shift, and rail roll-over are functions of the track response to combined lateral and vertical loading and to longitudinal loading. In order to evaluate the effects of design changes on lateral track response, an analytical model backed by experimental data is needed to include the characteristics of individual track parameters such as tie geometry, tie weight, ballast type, and the dimensions of the ballast section. Additional detail can be found in Section 3.4.

The identification of the major track problems in the rail rapid transit industry was an important task in this program, and it is evident that many of the track problems are given little consideration in the track design procedures. Discussions with track design and maintenance personnel and previous experience by the Battelle-Columbus staff were used as a basis for establishing a priority ranking of the most important track problems. The top six track problems identified, in order of priority, were:

- (a) Rail joints
- (b) Rail wear and noise on curves
- (c) Rail fasteners
- (d) Rail corrugation

- (e) Rail field welds
- (f) Track geometry maintenance.

It should be cautioned, however, that this is a subjective ranking rather than a quantitative ranking based on maintenance costs, safety, or community acceptance criteria. It is quite possible that track geometry maintenance may require the largest part of the track maintenance budget. However, loose bolts in joints and rail fasteners or community and passenger complaints about noise from rail corrugations may be a greater "annoyance" factor, and therefore they would have a higher subjective ranking based on discussions with track design and maintenance personnel. The major conclusions and recommendations for research in each of these track problem areas are discussed in the following paragraphs.

Bolted Rail Joints. Corrosion and wear at the contact surfaces between the rail and joint bars are the major cause of loose bolts and loose joints for standard bolted rail joints. The degradation of the joint increases rapidly as the bolts become loose, and the increased loading on the tie is a major factor in the degradation of track profile. The need for higher bolt clamping forces to reduce wear conflicts with the requirements for the bolted joint to alleviate rail thermal stresses. However, these requirements have not been fully evaluated.

It is recommended that typical joints in new track construction should be instrumented to obtain a statistical description of joint loads, displacements, and stresses under traffic. These data should be used as a basis for laboratory tests under controlled conditions to determine the effects of bolt preload on contact surface wear, joint stresses and longitudinal slip forces. These data are necessary for the development of new or modified joint design concepts for improved life. See Sections 4.3 for more detail.

Insulated Rail Joints. Insulated rail joints are a particularly important problem for the rapid transit industry because signal block lengths are relatively short and a failed (electrically shorted) joint delays train operations immediately. It is not unusual to have to rebuild insulated joints as frequently as every three months because the standard materials used for electrical insulation have inadequate structural properties. However, there

are several new commercial designs for insulated joints that promise improved life, and these are being installed for trial by several properties. Appropriate instrumentation and a detailed evaluation of these test installations would provide valuable data for the industry. A coordinated program is needed to reduce duplication of effort and to make the data available to the industry as quickly as possible. Accelerated life tests that correlate well with service life are needed for both standard and insulated bolted joints. Additional information is given in Section 4.3.

Improved Guidance on Curves. The negotiation of short radius curves is such an important requirement and such a major source of noise and wheel/rail wear problems that the development of improved transit car truck designs to provide primary guidance without flange contact should be given a high priority. The achievement of this objective would provide substantial benefits in terms of improved ride quality, reduced noise, higher average train speeds, and reduced train and track maintenance. Additional data are given in Section 4.4.

Rail Wear on Curves. Some limited improvements in rail wear on curves should be possible with less effort than that required for developing new truck designs. Several recommendations related to wear prediction and the reduction of rail wear on curves include (see Section 4.4)

- The development of improved wear prediction techniques based on wear data obtained from simulated wheel-rail contact.
- A lubricant evaluation program combining field and laboratory measurements is recommended to determine the properties needed for an improved lubricant. The lubricants now used for curve lubrication do reflect recent progress in lubrication science.
- Wheel and rail lubricators are not sufficiently reliable for rapid transit use. Design improvements are needed to maintain constant lubricant delivery rates for a wide range of temperatures and lubricant properties.

- Continued evaluation of the effect of rail metallurgy and heat treatment on rail wear is needed to provide a sound basis for developing more durable rail for use in rapid transit track.

Rail Corrugation. Rail corrugations are an important track problem because they cause objectionable noise and vibration, and the resulting wheel/rail dynamic forces cause increased wear of the rail and vehicle suspension components. However, there are no provisions in track or vehicle design procedures related to rail corrugations. Some recently developed theoretical models for contact resonance phenomena show promise for explaining the initiation and development of corrugations. But these models must be validated before they can be used with confidence as a basis for reducing or eliminating rail corrugations by changing track or vehicle design procedures.

A program to evaluate the critical mechanisms for the initiation of rail corrugations should include (Section 4.6)

- A study of the combined effect of normal loads and shear loads on the deformation and wear processes producing corrugations using controlled laboratory tests to identify critical parameters and evaluate the effectiveness of design changes.
- A field evaluation of the effect of vehicle traffic on rail surface roughness starting with new rail and continuing through the development of a well-defined pattern of corrugation. The track should be instrumented to measure wheel/rail contact forces at track locations selected to include curves and constant speed tangent track for both low speed and high speed train operation.
- Metallurgical analyses of corrugated rail should be made to aid determining the roles of wear, plastic flow and material phase changes on corrugation development.

Rail Field Welds. The availability of effective methods for field welding sections of rails together is particularly important because bolted rail joints are such a major source of track problems. It appears that the

most frequently used method for field welding, the thermit process, is capable of producing welds with sufficient strength for the rapid transit industry. However, the principal problem is the difficulty in obtaining consistent weld quality with unskilled labor.

It is recommended that new concepts for field welding and improvements to the thermit process be investigated to improve the reliability of field welds. It is important to evaluate weld integrity under realistic dynamic loading conditions because fatigue failures originating in the weld or the heat-affected zone are the most important cause of weld failure. Additional discussion can be found in Section 4.7.

Track Settlement. The review of current track design practice indicated that there were no design criteria directly related to the degradation of track geometry which results from differential settlement along the track route. Furthermore, very little work has been done on track settlement except for the development of a relatively simplified roadbed settlement model by TRW. However, there has been considerable research on the response of soils to dynamic loading that provides a good foundation for developing settlement models that adequately represent the complex state of stress and service conditions found in actual track structures. It is apparent that the analysis of track settlement will require considerable research on the characterization of ballast and subgrade materials subjected to repeated loads, and this must include field measurements of ballast and subgrade performance. Considerable field data on track settlement are needed to determine the validity of theoretical assumptions and to correlate with the results of theoretical analyses. See Section 4.8 for more detail.

3.0 CURRENT DESIGN PRACTICE FOR CONVENTIONAL AT-GRADE TRACK STRUCTURES

The majority of railroad track and a large part of urban rail track consists of steel rails supported by wood ties which rest on a roadbed of stone ballast on top of a soil subgrade. The basic function of a track is to support and guide the trains. However, the important track performance criteria are the safety and ride quality for train passengers, the noise and vibration transmitted to the community, and the maintenance problems and costs for the operating property. It is significant to note, though, that the technical factors on which the current track design practice is based are only indirectly related to these performance criteria.

The current design practice for at-grade track is based on satisfying a number of design criteria for the strength of individual track components. These criteria include the following:

- (1) Bending stress in the rail base
- (2) Tie bending stress
- (3) Pressure on the ballast surface under a tie
- (4) Pressure on the soil subgrade.

The flow chart shown in Figure 3-1 illustrates the most important steps in the track design procedure. It is apparent that the beam on elastic foundation analysis model of track is the key factor in evaluating the track components. This model utilizes a uniform track modulus representation of the ties and roadbed to predict the deflection and bending moment of the rail due to the vertical forces from the train wheels. The rail deflections and bending moment are then used to calculate all of the design parameters.

Although it might be expected that the rail size would depend on some type of stress criteria, other system requirements such as wear life, electrical resistance, cost, and future availability more frequently govern the rail size selection. This means that tie size and spacing are the remaining design parameters which can be varied to satisfy the component design criteria, and tie size and spacing are the major parameters in track design trade-off studies.

One of the most significant factors in the design procedure is the way in which the ballast section is sized. The ballast depth is selected based on its capability to reduce the pressure from individual ties to meet an

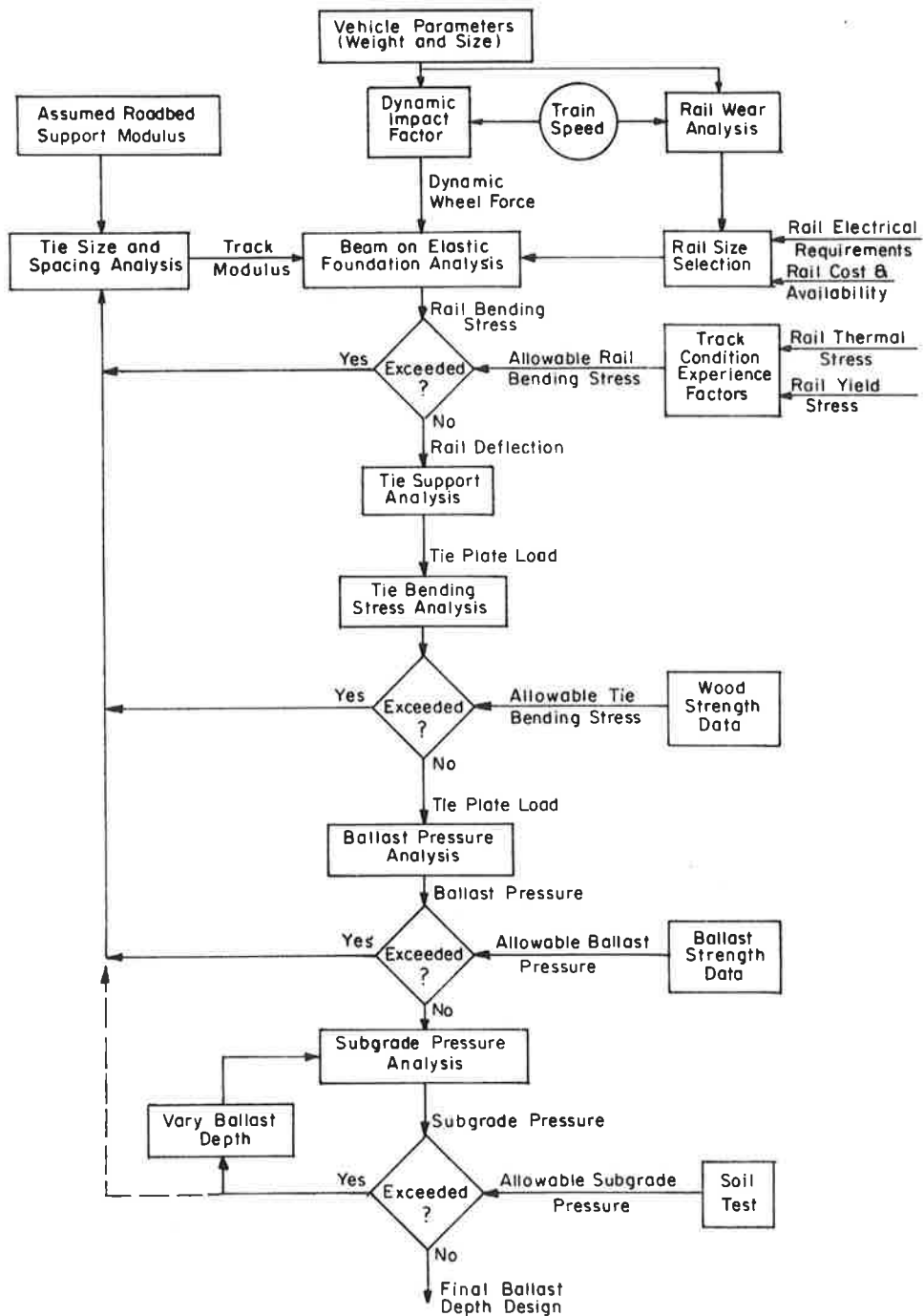


FIGURE 3-1. FLOW CHART FOR CONVENTIONAL AT-GRADE TRACK STRUCTURE DESIGN

allowable pressure limit for the subgrade. However, although it is generally recognized that increasing ballast depth and compacting and stabilizing the subgrade results in a stiffer and more durable roadbed, this effect is not included as a part of the major iteration loop for track design. Consequently, track design is restricted considerably by the initial assumption of a roadbed support modulus based on average data from typical track.

The technical factors used for evaluating the individual track components are reviewed in some detail in the following sections of this report. However, the flow chart does demonstrate some of the important relationships which might not be as clear when they are discussed on a component-by-component basis.

3.1 DESIGN LOADS

The basic function of a track structure is to support and guide trains. Vertical, lateral, and longitudinal forces are developed at the wheel-rail interface as this function is performed. The track structure is also subjected to continuously changing thermal expansion and contraction forces.

The forces transmitted through the wheel-rail interface are:

- (1) Vertical forces due to static weight and dynamic forces from the response of the car to deviations in track geometry and external disturbances.
- (2) Lateral forces due to the car's response to track geometry deviations and external disturbances, forces from self-excited hunting motions, and the forces necessary to guide the train through curves.
- (3) Longitudinal forces due to traction and braking.

The actual forces transmitted to the track are quite complex, and a statistical description of the loads is needed in order to evaluate the reliability of any particular design. However, current design practices for track are based on using representative design loads developed from empirical data, and these have been continually revised based on observations of track performance. Therefore, the resulting design loads do, in effect, represent a type of statistical design, although there is no explicit relation between

TABLE 3-1. WEIGHTS OF TYPICAL RAIL CARS

| Light Rail Cars | Total Car Weight (lbs) | | Average Wheel Load (lbs) | |
|-----------------------------|------------------------|---------|--------------------------|---------|
| | Empty | Maximum | Empty | Maximum |
| MBTA ⁽¹⁾ | 32,000 | 47,000 | 4,000 | 5,800 |
| Shaker Heights | 42,000 | 60,600 | 5,300 | 7,600 |
| <u>Rapid Transit Cars</u> | | | | |
| BART ⁽²⁾ | 61,000 | 98,000 | 7,600 | 12,200 |
| PATCO ⁽³⁾ | 75,000 | 98,200 | 9,400 | 12,300 |
| CTA ⁽⁴⁾ | 84,000 | 106,000 | 10,500 | 13,300 |
| NYCTA (R-42) ⁽⁵⁾ | 74,500 | 116,500 | 9,300 | 14,500 |
| NYCTA (R-44) | 83,000 | 132,000 | 10,400 | 16,500 |
| SOAC ⁽⁶⁾ | 90,000 | 135,000 | 11,300 | 16,900 |
| <u>Railroad Cars</u> | | | | |
| Passenger (Typ.) | 131,500 | 144,000 | 16,400 | 18,000 |
| Metroliner | 158,000 | 170,000 | 19,800 | 21,200 |
| Freight (Large) | 80,000 | 280,000 | 10,000 | 35,000 |
| Cooper E72 | - | - | - | 36,000 |

- (1) Massachusetts Bay Transportation Authority
- (2) San Francisco Bay Area Rapid Transit
- (3) Port Authority Transit Corporation
- (4) Chicago Transit Authority Stress Analysis Loading
- (5) New York City Transit Authority
- (6) State-of-the-Art Car

the design loads and a statistical prediction of track performance in terms of safety, ride quality, durability, or life-cycle costs.

3.1.1 Vertical Design Loads

The vertical force from the static weight of the car on the rails is the starting point for track design, and the car weights and average wheel loads for several types of rail vehicles are listed in Table 3-1. The maximum loads for passenger-carrying cars are based on the seated capacity for railroad passenger cars, but the maximum seated and standing passenger load (crush load) is listed for the transit vehicles because this is a frequent operating condition.

The maximum wheel loads range from a low of 5800 pounds for a light rail car (street car) to as high as 36,000 pounds for the Cooper E72 locomotive wheel loading recommended by the American Railway Engineering Association (AREA) as a design load for railroad structures. However, the maximum wheel loads for rapid transit cars are less than half of the maximum wheel loads for railroad cars.

The standard practice for track design is to use something close to the maximum expected static wheel load and increase this by a speed dependent impact factor (typically 50 to 100 percent) to arrive at a design wheel load that includes dynamic effects. Axle spacing and the distance between truck centers for the adjacent ends of two coupled cars are also data which are needed to superimpose the effect of adjacent wheels. Axle spacings normally range from 5 to 9 feet, and the truck center spacing between cars ranges from about 14 feet to 28 feet.

3.1.2 Lateral Design Loads

The track and vehicle parameters which affect lateral wheel forces are too complex to use as a basis for determining lateral design loads. Consequently, the maximum lateral forces are usually derived as a percentage of the vertical load based on "experience". The ratio of lateral-to-vertical wheel force is known as the "derailment quotient". A derailment quotient of about 0.8 can be used to estimate the maximum expected lateral force based on

the nominal static wheel load. The way in which the effect of lateral forces is included in the current track design practice is discussed in later sections of the report.

3.1.3 Longitudinal Design Loads

Longitudinal forces caused by temperature changes are the only longitudinal loads that are included in track design procedures. However, the wheel forces from traction and braking do contribute to rail wear and rail failures, and fatigue cracks are started and propagated by the stresses from the combined vertical and longitudinal wheel loading.

Longitudinal wheel forces are transmitted to the rail by friction, and the maximum longitudinal force is limited by the coefficient of friction and the vertical wheel force. The AREA recommends a longitudinal force equal to 15 percent of the live load (static wheel load without dynamic effects) for design purposes. Maximum values for friction coefficients on dry rail are in the range of 0.25 to 0.33.

3.2 TRACK DESIGN PROCEDURES

3.2.1 Beam on Elastic Foundation Analysis

It is not surprising that the well-known theory for a beam on an elastic foundation was first used by Zimmermann (Berlin, 1888) to calculate the stresses and deflections of railroad tracks [3-1]*. Later work by Talbot [3-2], starting in 1913 and continuing through 1942, and contributions by Timoshenko and Langer [3-3] demonstrated the accuracy of the elastic foundation theory for predicting rail deflections and rail bending stresses due to vertical wheel loads. The results from much of this work has been summarized by Clarke [3-4] to form the basis for current track design procedures.

* Numbers in brackets designate references listed in Reference Section.

The basic differential equation for the vertical deflection y of a rail having flexural rigidity EI supported continuously by an elastic foundation and loaded by a point load P at the origin is

$$EI \frac{d^4 y}{dx^4} + Uy = P\delta(x) \quad (3-1)$$

where U is the track modulus for a Winkler foundation defined as the load per inch of rail length required to depress the foundation one inch (lb/in/in or psi).

Equation (3-1) does not include several additional factors which are known to affect the stresses and deflections in railroad track such as longitudinal loads from thermal stresses, a restoring moment proportional to the rotation of the rail and ties, the eccentricity of the vertical load on the rail head, or any track dynamic effects such as inertial and damping forces. However, this simplified analytical model has proven to be quite useful for design purposes, and various empirically developed relations have been used to compensate for the limitations in the analytical model and the uncontrolled nonuniformities observed in actual track structures.

Professor A. D. Kerr of New York University has evaluated some of these effects [3-5,3-6] and his work is being continued under sponsorship of the U.S. Department of Transportation. Additional results from Kerr's study should be available by the end of 1973.

The solution of Equation (3-1) for a single point load results in the well-known relations for rail deflection $y(x)$ and rail bending moment $M(x)$

$$y(x) = (P/K_r) e^{-\beta x} (\cos \beta x + \sin \beta x) \quad (3-2)$$

$$M(x) = (P/4\theta) e^{-\beta x} (\cos \beta x - \sin \beta x) \quad (3-3)$$

where

$$\beta = \left(\frac{U}{4EI} \right)^{1/4}, \quad (3-4)$$

$$K_r = \frac{2U}{\beta} \quad (3-5)$$

and where K_r represents the track stiffness, or spring rate (lb/in), for a vertical point load applied to the rail head.

The normalized curves for the rail deflection and the rail bending moment are shown in Figure 3-2. The distance from the loading point to the point of zero bending moment is a convenient reference distance. This can be calculated for the condition $M=0$ from Equation (3-3) as

$$X_1 = \frac{\pi}{4\beta} \quad , \quad (3-6)$$

and the distance from the load to the point of zero rail deflection X_2 is

$$X_2 = 3X_1 \quad . \quad (3-7)$$

For reference purposes, Table 3-2 lists typical data for the characteristic lengths X_1 and X_2 for the range of rail sizes normally used by the rapid transit industry. As a rule, the discrete tie supports can be approximated satisfactorily by a continuous foundation as long as the tie spacing does not exceed X_1 . Table 3-2 indicates that the tie spacings of 22 to 30 inches used by the rapid transit properties for at-grade track meet this criteria for most of the expected range for track modulus.

The solutions for the rail bending moment and deflection due to a point load can be superimposed to obtain the total deflections and bending moments resulting from the wheel loads of single or multiple cars. Typical axle spacings for rapid transit cars range from 6 to 8 feet, which is equivalent to a distance of about $2X_1$ to $3X_1$. The curves in Figure 3-2 show that adjacent wheel loads will usually increase the rail deflection but reduce the bending moment under the reference wheel. This coupling effect is often accounted for by using a "Zimmermann" load to calculate rail deflections and a "Talbot" load to calculate rail bending stresses. These equivalent single loads give the same maximum deflections and bending stresses that would be obtained for a particular car or train configuration, and they include the influence factors from adjacent wheels obtained from Figure 3-2.

It is generally accepted that rail deflections and bending stresses can be predicted with acceptable accuracy for uniform track conditions if the

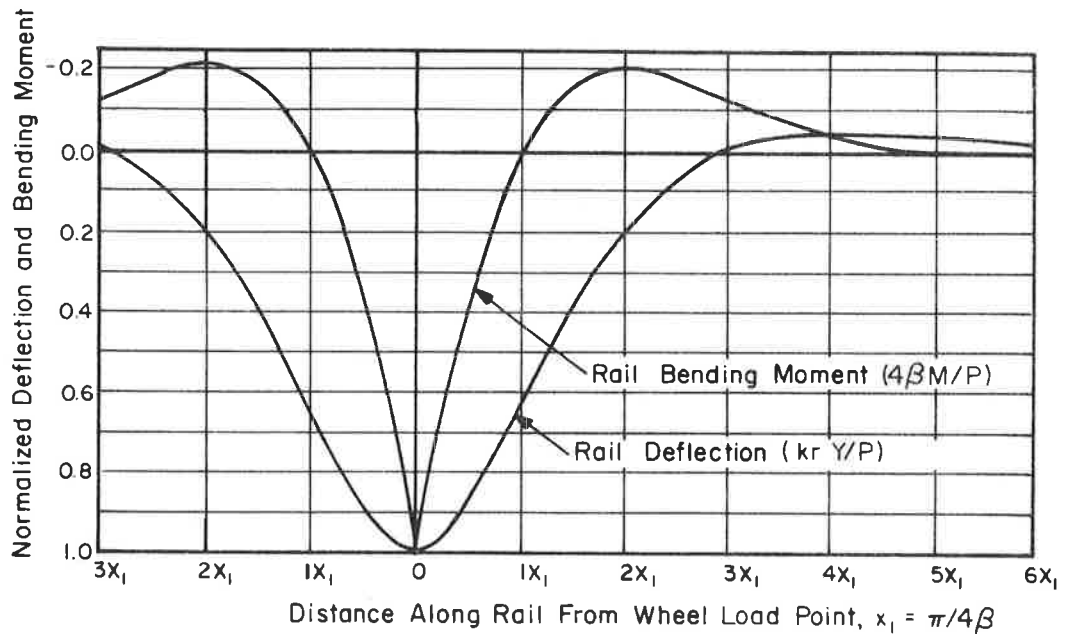


FIGURE 3-2. NORMALIZED RAIL DEFLECTION AND BENDING MOMENT CURVES

TABLE 3-2. TYPICAL DATA FOR CHARACTERISTIC LENGTHS X_1 AND X_2^*

| Track Modulus, (psi) | 100# Rail | | 115# Rail | | 132# Rail | |
|----------------------|-------------|-------------|-------------|-------------|-------------|-------------|
| | X_1 (in.) | X_2 (ft.) | X_1 (in.) | X_2 (ft.) | X_1 (in.) | X_2 (ft.) |
| 500 | 45.9 | 11.5 | 49.4 | 12.3 | 53.1 | 13.3 |
| 1000 | 38.6 | 9.7 | 41.5 | 10.4 | 44.7 | 11.2 |
| 1500 | 34.9 | 8.7 | 37.5 | 9.4 | 40.4 | 10.1 |
| 2000 | 32.4 | 8.1 | 34.9 | 8.7 | 37.6 | 9.4 |
| 3000 | 29.3 | 7.3 | 31.5 | 7.9 | 34.0 | 8.5 |
| 4000 | 27.2 | 6.8 | 29.3 | 7.3 | 31.6 | 7.9 |

* See Equations (3-6) and (3-7).

track modulus is determined by measurements. If the rail is loaded by a single axle, the measured track stiffness K_r could be used to calculate an effective track modulus from Equation (3-5). An alternative approach that has been used frequently is to load the track with either a single axle or several axles (a car), measure the deflection of the rail at each tie for a sufficient distance on both sides of the loaded track to include all significant deflections, and calculate the effective stiffness for the support of each tie based on static equilibrium conditions for the applied load.

This procedure is illustrated in Figure 3-3 for a single wheel load P . The equilibrium condition is

$$P = K_t \sum_i y_i \quad (3-8)$$

where it is assumed that the stiffness K_t is the same at each tie, and that the stiffness is equally effective for downward or upward rail deflections. The use of a loaded car is preferable to a single load for this type of measurement because the effect of rail "uplift" is reduced, thereby improving the accuracy of K_t in calculating deflections and stresses for cars with similar wheel loads and axle spacing.

An important deficiency of using the beam on elastic foundation theory for railroad track consisting of ballast on top of a subgrade is that the Winkler foundation model neglects any continuity or coupling in the foundation. This model assumes that a pressure applied to one area of the foundation does not cause any deflection outside the loaded area. This leads to the conclusion that the stiffness calculated from measured data using Equation (3-8) in the form

$$K_t = \frac{P}{\sum_i y_i} \quad (3-9)$$

should be the same as the stiffness obtained by loading a single tie (with no rail attached). However, Hetenyi reports [3-1] that data obtained by A. Wasiutynski in 1937 indicates the effective stiffness obtained by Equation (3-9) is about half the stiffness measured for a single tie because of the coupling effects of neighboring ties through the ballast and subgrade.

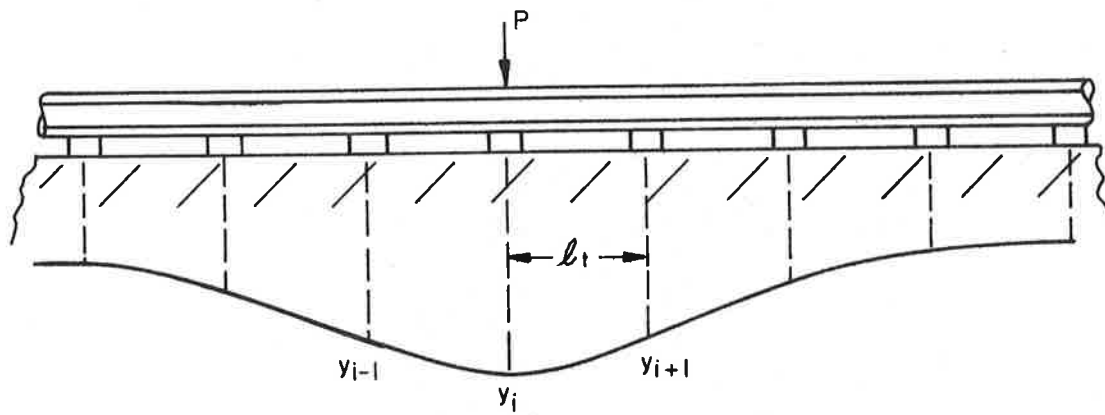


FIGURE 3-3. TRACK MODULUS MEASUREMENT PROCEDURE

An approximate analysis by Kurzweil [3-8] using the theory for a viscoelastic halfspace indicates the effective stiffness is related to the measured stiffness for a single tie by K_t/\sqrt{n} , where n is the number of ties that are deflected by a point load applied to the rail. This conclusion results from the assumption that the equivalent stiffness for a single tie is proportional to the square root of the bearing area of the tie on the ballast, which is theoretically correct for a rigid circular plate on an elastic halfspace. This assumption only approximates the interaction of adjacent ties, the effect of the rectangular contact area geometry, and the behavior of ballast and subgrade materials. However, Kurzweil indicates that n is typically ≤ 10 , so the possible range for the effective tie stiffness in track would be from K_t to $K_t/\sqrt{10}$. Therefore, $K_t/2$ represents a reasonable value for this range.

It is apparent that the magnitude of this coupling effect must depend on the tie spacing and size, the ballast depth, and subgrade properties, but no additional measured data on these effects were located in the literature. These coupling effects are tacitly included if measured data are used and the track design does not deviate much from the measurement conditions. However, this empirical approach cannot be used to accurately evaluate new track designs where measured data are not available. The influence of the continuity in the ballast and subgrade may have important implications on the validity of results from design trade-off studies involving the effect of tie spacing on rail deflections and stresses and pressures in the ballast and subgrade.

The standard design equation for including the effect of tie spacing l_t on track modulus is

$$U = K_t/l_t \quad (3-10)$$

K_t , and hence U , would be obtained from data measured on typical track.

Table 3-3 summarizes some typical track modulus data from W. W. Hay [3-7]. It is apparent that track modulus can vary by an order of magnitude (from $U = 500$ to 5000 psi) depending on the track and roadbed. However, design values of either $1,500$ psi or $2,000^*$ psi are typically used for sizing

* Track modulus values as high as $7000-8000$ psi have been observed in the literature from Japan and the USSR.

TABLE 3-3. TYPICAL TRACK MODULUS DATA

| <u>Rail Size</u> | <u>Tie Size</u> | <u>Tie Spacing</u> | <u>Track and Ballast</u> | <u>Track Modulus (psi)</u> |
|------------------|-----------------|--------------------|---|----------------------------|
| 85 lb | 7" x9" x8'6" | 22 in. | 6" Fine cinder ballast, in poor condition on loam and clay subgrade | 530 |
| 85 lb | 7" x9" x8'6" | 22 | 6" Cinder ballast, in fair condition on loam and clay subgrade | 750 |
| 85 lb | 6" x8" x8'0" | 22 | 6" Limestone on loam and clay roadbed. Good condition before tamping | 970 |
| 85 lb | 6" x8" x8'0" | 22 | 6" Limestone on loam and clay roadbed. After tamping | 1080 |
| 85 lb | 7" x9" x8'0" | NA | 12" Limestone on loam and clay roadbed. Good condition before tamping | 1065 |
| 85 lb | 7" x9" x8'0" | NA | 12" Limestone on loam and clay roadbed. After tamping | 1090 |
| 85 lb | 7" x9" x8'6" | 22 | 24" Crushed limestone on loam and clay | 1200 |
| 130 lb RE | 7" x9" x8'6" | 22 | 24" Gravel ballast plus 8" of heavy limestone on well packed roadbed | 3000 |
| 110 lb RE | 7" x9" x8'0" | 22(G.E.O.) | Flint gravel ballast on wide, stable roadbed | 2900 |
| 110 lb RE | 7" x9" x8'0" | 22 " | Limestone ballast on wide, stable roadbed | 5100 |

new track for either railroad or rapid transit. For example, the design study for the Washington Metropolitan Area Transit Authority [3-9] is based on the premise that ballast track with 7" x 9" x 8'6" wood ties spaced at 20 inches will have a track modulus of $U = 2,000$ psi. This initial design value is used to evaluate the effect of tie type (wood or concrete) and size, tie spacing and rail size on rail deflections and rail stresses using the beam on elastic foundation analysis. Although the additional track design parameters such as ballast depth and subgrade preparation are considered, their effect is not included in the overall track modulus. This results in the erroneous conclusion that rail deflections and stresses are independent of the ballast depth and subgrade parameters used for the final design.

For the WMATA design values discussed in the previous paragraph ($U = 2000$ psi for 7" x 9" x 8'6" wood ties with $\ell_t = 20$ inches), the effective tie support stiffness of $K_t = 40,000$ lb/in. would then be assumed constant in evaluating the effect of different tie spacings. Therefore, the soil coupling effects for a 20-inch tie spacing would be used automatically, even though the final track design might have $\ell_t = 30$ inches or greater.

Fortunately, however, a 100 percent error in U (and K_t) is the maximum error that will occur if the ties are spaced sufficiently far apart so that the factor of 2 included for the foundation coupling at 20 inch spacing can be neglected. It is also fortunate that a 100 percent increase in U causes only a 16.5 percent reduction in the maximum bending stress, and a 40 percent conservative error in predicted rail deflections and pressures on the ballast and subgrade. However, there are no reliable analytical techniques or sufficient measured data to accurately include these foundation coupling effects.

Tie type and size are also important design parameters which affect the deflections and bending stress in the rail and the pressure transmitted to the ballast and subgrade. The use of the elastic foundation model results in the conclusion that the average pressure transmitted to the top of the ballast P_b by the maximum rail seat load q_o is

$$P_b = \frac{q_o}{A_b} \quad (3-10a)$$

where $q_o = K_t y_{\max} = U \ell_t y_{\max} \quad (3-11)$

and A_b is the effective bearing area of one half of a tie.

The actual calculation of an effective bearing area for wood and concrete ties and the distribution of the resulting pressure through the ballast will be discussed in later sections. However, it is useful to define a modulus of roadbed reaction $k \equiv K_t/A_b = U\ell_t/A_b$ to represent the support provided by the roadbed. For a roadbed with specified subgrade and ballast, it is sometimes assumed that k is the constant, so that

$$k = \frac{U\ell_t}{A_b} = \frac{U'\ell_t'}{A_b'} \quad , \quad (3-11a)$$

where the primes designate a control situation. For this case, the effective track modulus depends only on the tie spacing and tie bearing area, as shown by equation (3-11a), and is given by the equation

$$U = \left(\frac{\ell_t'}{\ell_t} \right) \left(\frac{A_b}{A_b'} \right) U' = \frac{A_b}{\ell_t} \left(\frac{K_t}{A_b'} \right) \quad . \quad (3-12)$$

The control situation used for the WMATA track design [3-9] was $U' = 2,000$ psi, $\ell_t' = 20$ inches, and $A_b' = 312 \text{ in}^2$ for 7" x 9" x 8'-8" wood ties.

It is questionable whether the effective tie support stiffness K_t for real track is actually proportional to the bearing area, or to some other function of the tie dimensions. The elastic foundation theory gives the area relation, whereas the theory for a rigid circular plate on a continuous elastic medium [3-8, 3-10] indicates the stiffness is proportional to the plate radius, or the square root of the area for a circular plate. Thus it is apparent that the actual flexibility of the tie and the elastic behavior of the ballast material will affect the relation between tie size and track modulus. The practical significance of this relation is that the apparent advantage possessed by a concrete tie with its larger bearing area that permits wider tie spacing for comparable track modulus may not be as great as has been assumed.

A second shortcoming of this design approach is that the effect of variations in subgrade or ballast characteristics are not included in the analysis of rail deflections, rail stresses, or the pressure on top of the ballast.

Ballast depth is included in the standard design procedure as a factor in reducing the pressure transmitted to the subgrade, but the effect of variation of ballast depth on ballast and subgrade deflection is not included in the formulation for U or K_t .

Previous work done by Battelle [3-11] utilized an approximate model to include the stiffness of the subgrade K_s and ballast K_b as springs in series to arrive at an overall tie stiffness of

$$K_t = \frac{K_b K_s}{K_b + K_s} \quad (3-13)$$

This is a useful approach for including the track roadbed characteristics in a direct formulation to replace the empirical approach used currently, but considerable additional research is needed to develop a model with sufficient accuracy to cover a broad range of track design parameters. These requirements will be discussed in greater detail in Sections 3.2.5 and 3.2.6 on ballast and subgrade.

3.2.2 Rail Size

The selection of a particular rail size for a new track design depends on an evaluation of the structural requirements, the electrical requirements, current and future availability from rail suppliers, and the economic influence of support spacing, rail wear, and maintenance costs. These factors are evaluated in considerable detail for the WMATA track design [3-9], and the considerations which led to the final selection of a 115 lb. RE rail size are summarized as follows:

- The use of three different structural design equations based on axle loads, train speed, dynamic impact, track conditions, and track support showed that a rail section weighing 90 pounds per yard would be adequate.
- The desirability for having a rail section with sufficient cross-sectional area to meet the electrical requirements for negative return of traction power without using additional copper cables, which have recently increased in cost, showed that a 100 pound per yard rail section was needed.

- The accessibility of mills on the East Coast and the previous requirements resulted in the selection of 100 pound RE, 115 pound RE and 132 pound RE rail for economic analysis.
- Detailed cost analysis plus intangible judgment factors resulted in the final selection of 115 pound RE rail for all track. It was decided that assumptions regarding the spacing of rail fasteners and ties were important factors in the cost comparisons as were the life predictions based on rail wear on curves and tangent track.

While it is beyond the scope of this report to consider the economic factors for rail selection, design procedures used for the structural evaluation of rail size and rail wear analysis will be discussed in the following sections. Considerable data on the production and availability of rail sizes currently being used for new track construction by the rapid transit industry are included in Appendix A.

3.2.2.1 Rail Structural Requirements

Determining an appropriate rail size based on structural requirements is governed primarily by the wheel loads. The value for wheel load is affected by static weight, truck wheel base, maximum design speed, and anticipated irregularities in the track structure and the wheel profile. Most of these factors, either expressed or implied, are incorporated into the three design equations used in Reference [3-9]. All three equations have been successfully applied to determine, structurally, an appropriate rail size.

Equations (3-14) and (3-15) were developed empirically, and as a result, will probably work best on conventional track where the various implicit assumptions still hold. Equation (3-16) was derived analytically from the beam on elastic foundation theory and it allows for more explicit variations of the design parameters.

$$W_o = 314 - \frac{47.0 (10^6)}{(2P)K + 147.2 (10^3)} \quad (3-14)$$

$$W_o = 17 \left[\frac{P + 0.0001 PV^2}{2000} \right]^{2/3} \quad (3-15)$$

$$Z_b = \frac{0.318 (PK) X_1}{f_o} \quad (3-16)$$

where

W_o = rail weight (lb/yd.)

P = static wheel load (lbs.)

K = impact factor (ratio of dynamic to static wheel load)

V = trail speed (mph)

Z_b = rail base section modulus (in³)

X_1 = distance from wheel load to point of zero bending moment (in.)

f_o = maximum allowable bending stress in the rail base (psi)

A calculation using typical values from the WMATA design of $P = 15,000$ lbs, $K = 2$, $V = 75$ mph, $X_1 = 34$ inches, and $f_o = 25,000$ psi confirms the conclusion that 90 lb/yd. rail was adequate for structural strength.

$W_o = 87$ lbs/yd. (from Equation 3-14)

$W_o = 87.5$ lbs/yd. (from Equation 3-15)

$Z_b = 13$ in.³ (90 lb/yd.) (from Equation 3-16).

The use of an allowable bending stress of 25,000 psi for continuous welded rail is based on standard American and European design procedures [3-4, 3-7], whereby the bending stress calculated from the beam on elastic foundation analysis for static vertical loads is increased by appropriate factors for the effects of temperature, speed, rail wear, unbalanced superelevation, lateral bending, and track condition. A simultaneous combination of these assumed "average" factors represents a relatively severe condition, and a yield stress of 70,000 psi is used as a limiting stress for the total allowable stress in the rail base. The development of these factors, discussed below, is largely dependent on the work by Talbot [3-2].

Impact Factor. The impact factor, or speed factor, is frequently included directly in the stress and deflection calculations by using a "dynamic" wheel load as demonstrated in Equations (3-14) and (3-16). Actual dynamic wheel forces are caused by a complex combination of effects that depend on the dynamics of both the track and the vehicle. For example, typical measurements of the rail bending stress resulting from wheel flats show that the rail stresses increase rapidly with speed, reaching a maximum between 15 and 30 mph, and then decrease slightly to about 40 mph. The stresses increase again at higher speeds, but they seldom exceed the peak stress reached at 15-30 mph. On the other hand, dynamic forces from track geometry irregularities and from wheel unbalance tend to increase rather continuously with increasing speed.

The procedure used throughout the railroad industry is to apply an empirically-derived, speed-dependent impact factor to the static wheel load that represents this general trend for dynamic wheel loads.

The Indian Railways [3-12] uses a speed factor K given by

$$K = 1 + \frac{V}{3U^{1/2}} \quad (3-17)$$

where V is train speed in miles per hour and U is the track modulus in psi.

Some other equations used for the impact factor by European railroads show a V^2 relation [3-13], but most of the available data indicate the speed factors predicted using the V^2 relation are excessive at high train speeds. Measured data indicate that rail flexural stresses vary with train speed, the proportionality lying between V and $V^{1.2}$ [3-4].

An equation used in [3-9] and included implicitly in Equation (3-15) is

$$K = [1 + 0.0001V^2]^{2/3} \quad (3-18)$$

The speed factor recommended by the AAR and used by Magee [3-14] to determine rail stresses is

$$K = 1 + \frac{33V}{100D} \quad (3-19)$$

where D is the wheel diameter in inches.

Figure (3-4) shows that the results using these different equations are quite similar. However, considering the variability for the speed dependent

factors and the other empirical factors used for rail stress calculations, it is not surprising that a dynamic wheel load equal to twice the static wheel load is often used as a convenient factor for designing rapid transit track where the maximum speeds are 75 to 80 mph.

Table 3-4, compares empirical factors from several references. These factors are used to estimate maximum rail stresses and are discussed below.

Locomotive Factor. Variations in static weight distribution in cars or locomotives produce actual wheel loadings which may exceed a uniform distribution by about 5 percent.

Lateral Bending Factor. Although the basic track design analysis considers only vertical loads, this factor accounts for a lateral wheel load component producing bending stresses in the outer edge of the rail base which will add directly to the vertical bending stresses on one side or the other. The same factor is used for curved or tangent track.

Temperature Stress Factor. In jointed track, the tensile stresses caused by low temperature depend on maintenance procedures, joint bar resistance, and rail anchor restraints. A greater allowance is needed for CWR to allow for rail temperatures as much as 100 degrees below the rail laying temperature.

Rail Wear and Corrosion Factor. Corrosion effects and rail wear on curves reduce the rail section modulus.

Unbalanced Superelevation. AREA recommendations limit operating speeds on curves to 3 inches of unbalanced superelevation. This produces a 15 percent increase in wheel load on the outer rail for a vehicle with a center of gravity 84 inches above the rails. Higher unbalances can occur when operating very slowly on high-speed curves (high superelevation), but this would be offset by the reduced impact factor for the low speed.

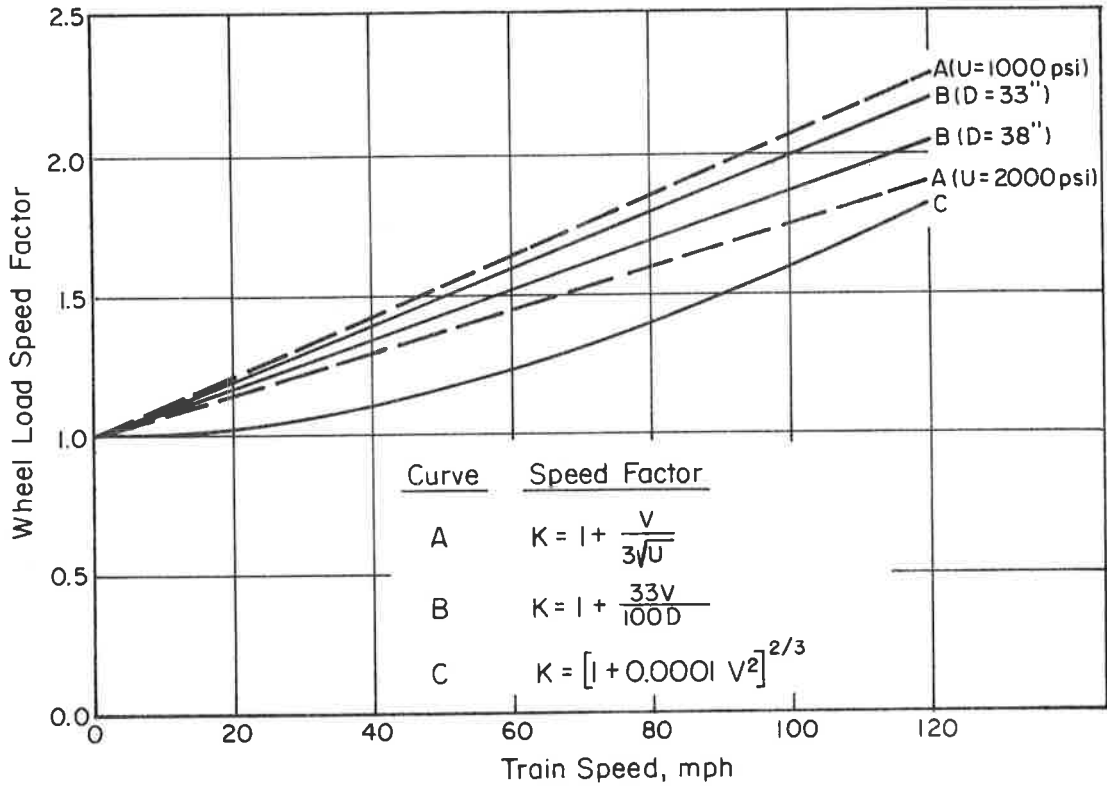


FIGURE 3-4. COMPARISON OF SEVERAL FORMULAS USED TO PREDICT THE EFFECT OF TRAIN SPEED ON RAIL STRESS

TABLE 3-4. COMPARISON OF STRESS FACTORS FROM THE LITERATURE

| Stress Factor | Hay [3-7] | Clark [3-4] | Magee [3-14] |
|------------------------------|-----------------------|-----------------------|--|
| Locomotive | 5% | 5% | 0 |
| Lateral Bending | 15% | 15% | 20% |
| Temperature | 7000 psi (Jointed) | 7000 psi (Jointed) | 5,000 psi (B-J) ⁽¹⁾ 10,000 psi (M-J) 20,000 psi (CWR) |
| Rail Wear | 10% | 10% | 15% |
| Unbalanced Superelevation | 15-20% | 15% | 15% |
| Track Condition | 25% | 25% | 25% (M) 35% (B) |
| Rail Yield Strength, psi | 60,000 | 60,000 | 70,000 |

(1) Branch - Jointed Track (B-J), Main - Jointed Track (M-J), Continuous Welded Rail (CWR).

Track Condition. Increased bending stresses result from the occasional worn, deteriorated or low ties, or soft spots in the roadbed.

Using the factors in Table 3-4 recommended by Magee, the calculation below demonstrates the procedure of multiplying the stress factors to obtain the maximum allowable bending stress for vertical loads on CWR with a 70,000 psi yield stress.

$$\frac{70,000 - 20,000}{(1.20)(1.25)(1.15)(1.15)} = 25,000 \text{ psi}$$

British rail has lower carbon content and therefore it has a lower yield stress of about 60,000 psi. British practice is to limit flexural stress to 50 percent of the yield stress. [3-4]. However, it is not clear if this includes CWR temperature-related stresses. If the 20,000 psi temperature stress were not included in the above equation, then the same 50 percent value (35,000 psi) would be allowed for flexural stress.

German rail design practice [3-13] limits flexural stress based on the class of track and type of traffic (implying a compensation for endurance limit). The stress values range from 21,300 psi (1500 kp/cm²) for Class I track to 28,500 psi (2000 kp/cm²) for Class III track. These values apply to rail steel with a yield stress ranging from 48,400 psi (34 kp/mm²) to 74,000 psi (52 kp/mm²). Using the lower limit for yield stress, a Class I track is allowed 44 percent of yield for flexural stress. Other stresses are allowed as follows:

| | |
|----------------------------------|---------------|
| Temperature stress - 40 percent | (19,400 psi) |
| Lateral bending - 44 percent | (21,300 psi) |
| Wheel flat stresses - 46 percent | (22,300 psi). |

The total exceeds the yield point by almost 75 percent, and this is rationalized by the low probability that all of these maximum values will occur simultaneously at one location on the rail.

The fact that rail structural failures are not a significant problem for the older rapid transit properties in the U. S., which generally use 90-lb or 100-lb rail, substantiates that rail of this size is structurally adequate. This also shows the increased structural safety margin associated with the new constructions where 119-lb rail is being used in San Francisco and 115-lb rail is being installed in Washington.

3.2.2.2 Rail Wear Analysis

Predictions for rail wear based on AREA recommended formulas and the Couard method were reviewed and compared in the WMATA Trackwork Study [3-9]. Both of these analysis procedures are empirical formulations based on railroad (rather than urban rail) experience.

AREA Method. The AREA [3-15] method is based on predicting rail life λ_A for tangent track in years by

$$\lambda_A = \frac{T}{B} \left(\frac{\theta}{3/16} \right) \quad (3-20)$$

$$T = CW_o B^{0.565} \quad (3-21)$$

where

T = rail life in million gross tons of traffic (M.G.T.)

θ = permissible rail wear (inches)

B = annual traffic (M.G.T./year)

C = 0.545 (constant based on railroad experience)

W_o = rail weight, lbs/yd.

The life of rail on curves is estimated as a percentage of the rail life predicted for tangent track using the factors listed in Table 3-5.

This type of formulation does not include specific conditions such as vehicle speed or configuration, unbalanced superelevation, track grade, rail type (standard or heat-treated), or metallurgical properties, or the type of lubricant used. Consequently, the predicted results can be used as estimates for existing track design, but they provide no useful guides for improving either vehicle or track designs to reduce wear, particularly on the very short radius curves (90 to 150-ft radius) that are of greatest concern for present urban rail transit properties.

No detailed explanation or derivation of Equations (3-20) and (3-21) was found in the literature other than an indication that they are based on an allowable vertical head wear of 3/16 inch on tangent track. The value for C should be determined from experience under operating conditions similar to a new installation for which a rail life estimate is needed. However, the validity of this entire procedure is questionable.

TABLE 3-5. RAIL WEAR FACTORS FOR PREDICTING
RAIL LIFE ON CURVES [3-9]

| Degree of Curve | Curves Radius, ft. | Percent of Tangent Rail Life | |
|--------------------|-----------------------|------------------------------|---------------------|
| | | Without Lubricators | With Lubricators |
| 0 | | 100 | 100 |
| 1 | 5730 | 87 | 100 |
| 2 | 2865 | 73 | 89 |
| 3 | 1910 | 60 | 79 |
| 4 | 1433 | 48 | 70 |
| 5 | 1146 | 38 | 62 |
| 6 | 955 | 30 | 55 |
| 7 | 819 | 22 | 49 |
| 8 | 717 | 16 | 44 |
| 9 | 637 | 12 | 40 |
| 10 | 574 | 10 | 37 |

Couard Method [3-9, 3-16]. The Couard method for calculating rail wear is based on the following equations for annual wear rate.

Vertical Rail Head Wear on Tangent Track

$$W_v = 5(10^{-6}) C_1 (1 + 0.23 g^{1.7}) BV + 0.0025 \quad (3-22)$$

Vertical Rail Head Wear on the High Rail of Curved Track

$$W_v = 5.5(10^{-6}) C_1 (1 + 0.1 U_b + 0.23 g^{1.7}) BV + 0.0025 \quad (3-23)$$

Side Head Wear on the High Rail of Curved Track

$$W_s = 8(10^{-6}) C_2 D_c (1 + 0.1 U_b + 0.23 g^{1.7}) BV + 0.0025 \quad (3-24)$$

Side Head Wear on Curves with Rail Lubricators

$$W_{sl} = 0.7 (W_s - 0.0025) + .0025 \quad (3-25)$$

where

W_v = annual vertical head wear (inches/year)

W_s = annual side head wear (inches/year)

W_{sl} = annual side head wear on lubricated rail (inches/year)

g = track gradient (percent)

B = annual traffic density (M.G.T./year)

V = operating speed (mph)

U_b = unbalanced superelevation (inches)

D_c = degree of curve (degrees)

C_1 = ratio of rail head width to that for 140-lb. RE rail

C_2 = ratio of rail head depth to that for 140-lb. RE rail.

These equations were developed for 140-lb. RE rail, and Table 3-6 lists correction factors C_1 and C_2 for several smaller rail sizes. The calculated values of W_v and W_s are used to predict the rail life λ_c (in years) by the Couard method by dividing the annual wear into the permissible wear θ

$$\lambda_c = \frac{\theta}{W_v \text{ (or } W_s)} \quad (3-26)$$

TABLE 3-6. WEAR FACTORS FOR CALCULATING RAIL
HEAD WEAR BY THE COUARD METHOD

| Rail Size | Wear Factor | |
|-----------|----------------|----------------|
| | C ₁ | C ₂ |
| 100-1b RE | 1.1163 | 1.2452 |
| 115-1b RE | 1.1034 | 1.2222 |
| 132-1b RE | 1.0 | 1.1786 |
| 140-1b RE | 1.0 | 1.0 |

The Couard method does include a more detailed description of the track geometry and an allowance for train speed that are not considered by the AREA method, but additional information is needed to evaluate substantial changes in the vehicle or rail parameters which might reduce rail wear significantly.

An examination of the Couard equations indicates that train speed and track grade have an important effect on estimated rail life. A comparison of rail life predictions in Table 3-7 indicates that the two methods give similar predictions for tangent track, but there is considerable difference in the side wear predicted for curves. Detailed wear and traffic data for particular track locations are needed in order to better evaluate the accuracy of either of these two methods. However, the Couard method certainly has the best potential because it includes a greater number of the significant operating parameters.

Additional discussion about rail wear can be found in Section 4.4

3.2.3. Rail Fasteners

From the earliest days of railroading, the rail fastener-the element holding the rail to the tie or other support-has been a key element in the track structure. As track structures become more sophisticated, it is the fastener, perhaps more than any other component, where the requirements will increase the most. In this section of the report, therefore, the role of the rail fastener for various types of track structure will be examined briefly, and the methods for defining the rail fastener requirements will be discussed.

The earliest type of track, and the one which accounts for the majority of track construction even at the present time, is the classical wood tie and ballast track. The basic role of the fastener in this type of track is to maintain gauge. This was done in the earliest days by driving cut steel spikes into the wood ties with the spikes bearing directly against the edges of the rail base. Today, most track includes a steel tie plate between the rail and the tie to provide a broader seating area and a shoulder for improved lateral restraint.

TABLE 3-7. COMPARISON OF RAIL WEAR PREDICTIONS
BY AREA AND COUARD METHODS [3-9]

| Rail Size | Allowable Rail Wear (inches) | RAIL LIFE (Years) | | | | | | | |
|--------------|---------------------------------|-------------------|------|---------------|-----------|-----------|-----------|-----------|-----------|
| | | Vertical Wear | | Tangent Track | | Side Wear | | Side Wear | |
| | | Vertical | Size | AREA(1) | Couard(2) | AREA(3) | Couard(4) | AREA(3) | Couard(4) |
| 100-1b RE | 1/2 | 1/2 | 49 | 52 | 9 | 3.4 | 23 | 4.9 | |
| 115-1b RE | 17/32 | 17/32 | 60 | 55 | 11 | 3.7 | 28 | 5.3 | |
| 132-1b RE | 19/32 | 21/32 | 77 | 67 | 13 | 4.8 | 35 | 6.8 | |

(1) $B = 12.2 \text{ M.G.T./yr.}$,

(2) $B = 12.2 \text{ M.G.T./yr.}$, $V = 50 \text{ mph}$, $g = 2.5 \text{ percent}$

(3) $B = 12.2 \text{ M.G.T./yr.}$, Curve = 7.59 degrees ($R = 755'$)

(4) $B = 12.2 \text{ M.G.T./yr.}$, $V = 40 \text{ mph}$, $g = 4.0 \text{ percent}$, $D_c = 7.59^\circ$ ($R = 755'$), $U_b = 4.5 \text{ in.}$

In this common type of track construction the maintenance of gauge is the only function which the rail fastener (spikes) performs. The rail fasteners do not supply a hold-down force to the rail, they do not provide a friction force to prevent longitudinal creep, they do not provide lateral or vertical resilience in the track structure, and they do not provide electrical insulation.

The more recent use of concrete ties has required the adoption of some fastener other than a steel spike. In the earlier applications, an insert utilizing a steel bolt-type member and a steel clip replaced the traditional cut or screw-type steel spike. The need for additional electrical insulation to replace the insulating properties inherent in the wood tie led to more complicated fastener designs utilizing elastomeric or fiber type pads beneath the rail. This introduced the potential for varying the rail support stiffness while maintaining the same tie type and spacing.

With this more complicated fastener, necessitated by the use of concrete ties, it became logical to incorporate a means for restraining the rail longitudinally in the fastener. The net result for many existing concrete tie fasteners is a fastener that not only maintains lateral alignment, but also provides complete electrical insulation, provides restraint to longitudinal motion of the rail, supplies a positive vertical hold-down force, and provides lateral and vertical resilience to compensate for the increased stiffness sometimes obtained because of the larger bearing area of the concrete ties (for a fixed tie spacing).

The use of continuous longitudinal beams or slab for at-grade track and direct fixation to concrete in tunnels and subways and on elevated structures represents additional important applications for more sophisticated rail fasteners. Direct fixation fastenings are being increasingly utilized in tunnels to reduce the required tunnel size by eliminating the space required for ballast.

Two major changes in the rail fastener requirements are necessitated for direct fixation to these types of structures. First, these structures are inherently stiffer than ballast track. Although this increase in stiffness is a desirable feature for at-grade track structures to reduce the magnitude and frequency of the pressure pulses transmitted to the subgrade, this increase in stiffness is undesirable from the standpoint of the dynamic forces generated at

the wheel/rail interface. If the track alignment and profile were perfect, and the wheels and other running gear of the cars were also perfect, there would be no problem. However, the imperfections which realistically are present on both the rail and vehicle generate dynamic forces which adversely affect the ride of the vehicle and the maintenance of both the vehicle and the track. Previous studies by Battelle [3-11, 3-17] and others have shown that it is desirable to introduce resilience into the rail fastener to compensate for this increased stiffness, and this becomes a major fastener design requirement. Resilience is also desirable for reducing groundborne vibration transmitted to the surrounding communities.

Another important fastener requirement for direct fixation is that of providing vertical and lateral adjustment. As long as cross ties are used, they can be moved both vertically and laterally to align the track, although this becomes increasingly difficult with heavy concrete ties. It is also important that the fastener be relatively easy to install and maintain, and provide the capability for removing and replacing rail without disturbing the horizontal or vertical alignment. This is particularly significant for rapid transit use where rails are replaced frequently on tight curves.

With regard to the selection of rail fasteners, the role of the track designer is frequently restricted to writing specifications which can be met by available fasteners. In view of the increased requirements for rail fasteners as track structures improve, it is not surprising that there have been problems obtaining commercial fasteners to meet these specifications. In essence, fasteners are still in an early stage of development in this country, although in Europe where concrete ties have seen more service- the development of fasteners is also further along. Work is needed to develop fasteners which meet the demands imposed by the railroad and rapid transit properties in this country.

3.2.3.1 Development of Fastener Design Requirements

The relative simplicity of conventional wood tie track construction combined all too often with a poor state of repair belies the fact that high forces of a complex nature are repetitively transmitted through the rail-tie

interface. Most important, of course, are the vertical forces which are transmitted from the train wheels into the track structure. An interesting aspect of the vertical load pattern is the presence of upward motions ("wave action") both ahead and behind the wheel that must be accommodated by the rail fastener. In conventional track, where spikes are either not completely driven in or partially pulled out during service, the "wave action" is virtually unrestricted and the rail lifts freely from the tie. But a resilient rail fastener must be capable of withstanding these uplift forces continuously without fatigue failures in structural components or extensive degradation of the resilient materials.

In addition to the vertical loads, large lateral loads are developed by the trains on curves, by vehicle hunting, and also by the rail forces due to thermal expansion and contraction. With conventional construction, lateral loads are transmitted into the shoulder of the tieplate and through the spike into the ties. If a resilient element, such as an elastomeric-type rail fastener, is used between the rail and the main support, this resilient element must be stiff enough to prevent excessive lateral motion of the rail; otherwise, derailments will occur due to excessive gauge spread or rail rollover.

A third and equally important type of load which must be resisted by the rail fastener is the longitudinal load which is generated by the acceleration and braking of the trains, and by thermal expansion and contraction forces which exist even in the absence of trains. In conventional tie-type construction, rail "anchors" are used to transmit longitudinal rail loads to the ties. This is another component that disappears for direct fixation track, and the longitudinal restraint must be provided by the rail fastener.

In order to determine reasonable design loads for individual rail fasteners, it is first necessary to consider the actual transit car wheel loads, and then to determine how the wheel loads will be distributed on the rail fastener supports. Table 3-8 summarizes some typical results for vertical and lateral rail fastener design loads for "maximum" and "frequent" loading conditions. The "maximum" condition relates to the ultimate strength of the fastener for a single load application; the "frequent" loading condition represents reasonable average service loads for fatigue design considerations and endurance tests. These data are included to illustrate current procedures for developing

TABLE 3-8. SUMMARY OF TYPICAL VERTICAL AND LATERAL
RAIL FASTENER DESIGN LOADS

-
-
1. Vertical Wheel Loads*
 - a. Maximum Load: 30,000 lb
 - b. Frequent Load: 12,000 lb
 2. Vertical Rail-Fastener Loads
 - a. Maximum Compressive Load: 18,000 lb
 - b. Maximum Uplift Load: 1,100 lb
 - c. Frequent Compressive Load: 7,000 lb
 - d. Frequent Uplift Load: 700 lb
 3. Simultaneous Vertical and Lateral Wheel Loads
 - a. Maximum Vertical/Lateral Load: 30,000 lb/18,000 lb
 - b. Frequent Vertical/Lateral Load: 12,000 lb/5,000 lb
 4. Simultaneous Vertical and Lateral Rail-Fastener Loads
 - a. Maximum Vertical/Lateral Load: 18,000 lb/16,200 lb
 - b. Frequent Vertical Lateral Load: 7,000 lb/4,500 lb
-
-

* Based on normal loaded car weight of 80,000 pounds (10,000 lb nominal static wheel load), and car with crush load weighing 98,000 pounds.

the loading used in rail fastener specifications. The data should not be interpreted as recommendations for any particular railroad or rapid transit application.

The 30,000-pound maximum expected vertical wheel load in Table 3-8 includes a dynamic load factor of 2 applied to a maximum expected single wheel load of 15,000 pounds. The 15,000 pound wheel load is based on one truck carrying 55 percent of a 98,000 pound crush load (13,500 pound nominal wheel load) with a tolerance accumulation allowing one wheel on that truck to carry 15 percent more than the lightest wheel. While this estimate is probably conservative, it represents a reasonable maximum ultimate load condition. The 12,000 pound frequent load represents a 20 percent dynamic factor above a nominal 10,000 pound wheel load (occasional overload condition), and this is a reasonable "frequent" load for fatigue evaluations.

Analyses of track structures using the beam on elastic foundation model indicate that vertical fastener loads will range from 40 to 60 percent of vertical wheel loads, so a 60 percent factor was used to estimate the vertical fastener loads. In addition to the vertical compressive loads, Battelle data from both analyses and track measurements indicated that rail fasteners will be subjected to the uplift forces shown in Table 3-8, both preceding and following wheel passage.

Lateral wheel loads are more difficult to predict than vertical wheel loads. However, frequent lateral wheel loads equal to 40 percent of the vertical wheel load and a maximum lateral wheel load equal to 60 percent* of the maximum expected vertical load are reasonable estimates. Previous Battelle analyses [3-17] indicated that 80 to 90 percent of the lateral wheel load can be transmitted through a single fastener, so the 90 percent factor was used to estimate the frequent lateral loads listed in Table 3-7.

The longitudinal restraint characteristics of a rail fastener replace the role of the rail anchor commonly used with wood ties and determine its effectiveness for maintaining a minimum rail gap resulting from a rail fracture at temperatures below the mean rail-laying temperature.

(*) A lateral wheel force equal to 80 percent of the vertical wheel force is approaching a safety limit for derailment, see Section 3.1.2.

An approximate analysis based on assuming all fasteners apply a maximum slip load, or a more detailed analysis using the fastener longitudinal stiffness characteristics, can be used to predict rail gaps. The high longitudinal holding capacity of most fasteners used for direct fixation keeps the rail gap quite small. For ballast track, however, the holding power of the concrete tie in the ballast determines the rail gap. Some measured data indicate that a concrete tie will actually have a linear load-deflection characteristic for loads below the assumed 1800-pound-per rail slip load (3600 pounds per tie), and that slip begins when the tie has moved about 0.2 inch. Thus, the fasteners adjacent to a rail break will not be loaded to 1800 pounds until the total rail gap exceeds 0.4 inch. At a temperature differential of 60 degrees below the mean rail-laying temperature, the calculated rail gap is 1.18 inches based on an analysis which includes the tie and fastener elasticity. This rail gap is considerably greater than what is predicted by assuming a constant force restraint with no elasticity (simplified analysis). However, even these larger rail gaps predicted using typical fastener characteristics do not appear excessive.

The high longitudinal load capacity of many fasteners, however, indicates that rail stresses resulting from the thermal movement of aerial structures may be much higher than anticipated. The thermal movement of an aerial structure will cause high longitudinal loads on fasteners adjacent to the expansion joints in the aerial structure. Analyses of this type are used to determine an upper limit for rail fastener longitudinal slip forces in order to limit the maximum rail stresses caused by thermal contractions of the aerial structures. In some cases, it is necessary to analyze the thermal stresses throughout entire sections of complex aerial structures to check the rail stresses and fastener loads induced by structural motions.

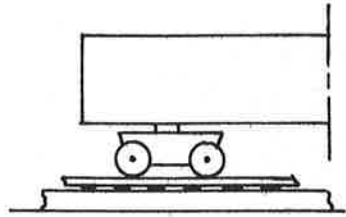
In order to complete fastener performance specifications using the design loads and analysis procedures discussed previously, allowable deflections must be included based on maximum allowable gage spread (typically 1/8 to 1/4 inch) for both ultimate and "frequent" loading conditions. It is also important to evaluate the effect of the vertical fastener stiffness on the rail and roadbed loading and the dynamic forces transmitted to the vehicle.

A lumped-parameter model [3-42] suitable for evaluating the dynamic effects of fastener stiffness is shown in Figure 3-5. The track portion of this model is rather general and the masses and springs can be adjusted to model conventional tie-ballast track or track constructed from concrete slab or twin longitudinal beams.

Figure 3-6 has only been included in this report from Reference [3-42] to illustrate the type of results which can be obtained by modeling the dynamic interactions of the vehicle and track together. This particular analysis is for longitudinal beam track construction, and a 1/4-inch downward step occurring simultaneously in both rails was used to excite vehicle bounce modes. While this type of input represents a severe mismatch at a pair of side-by-side joints (and may be too severe to be realistic), it is a useful input to evaluate the effect of various parameter changes.

In Figure 3-6, the peak accelerations of the car body and axle, the peak displacements of the car body, car axle, and rail, the peak wheel-rail force, and the peak soil pressure are plotted as a function of the rail fastener pad stiffness. These curves show that as the pad stiffness increases, the axle acceleration and the wheel/rail force increase significantly, while the displacement of the car body, axle, and the rail, as well as the peak soil pressure, decrease. The bending moment of the rail will also decrease as the pad stiffness increases. As mentioned earlier, the conclusion from studies of this type, and railroad experience, is that when a relatively stiff support structure is used, resilience must be introduced into the track structure by providing a resilient rail fastener, or the wheel-rail forces and the resulting deterioration of both track and vehicles will be high.

While the particular study used for this illustration was an analog computer time-domain simulation in which the actual profile of the rail was used as the input, other Battelle studies involving frequency domain analysis of random rail profiles have been made using digital computer techniques. These can be used to determine the effect of various parameters-most significantly the resilience of the rail fastener in vertical as well as lateral



Half of Car Body

Two Suspension Springs and Dampers

One Bolster

One Shock Pad

Spider and Sideframes of One Truck

Bearing Sleeves

Four Wheels and Two Axles

Wheel-Rail Contact Forces

Rail Masses

Rail Pads

Beam Masses

Soil and Ballast Foundation

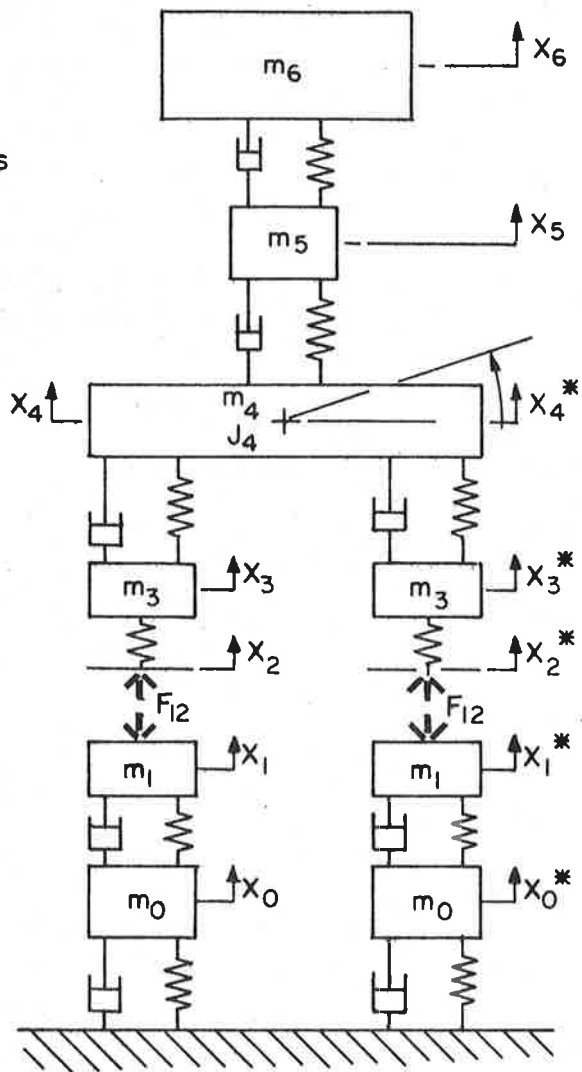


FIGURE 3-5. LUMPED PARAMETER MODEL REPRESENTING PORTION OF CAR AND TRACK STRUCTURE ASSOCIATED WITH ONE TRUCK [3-42]

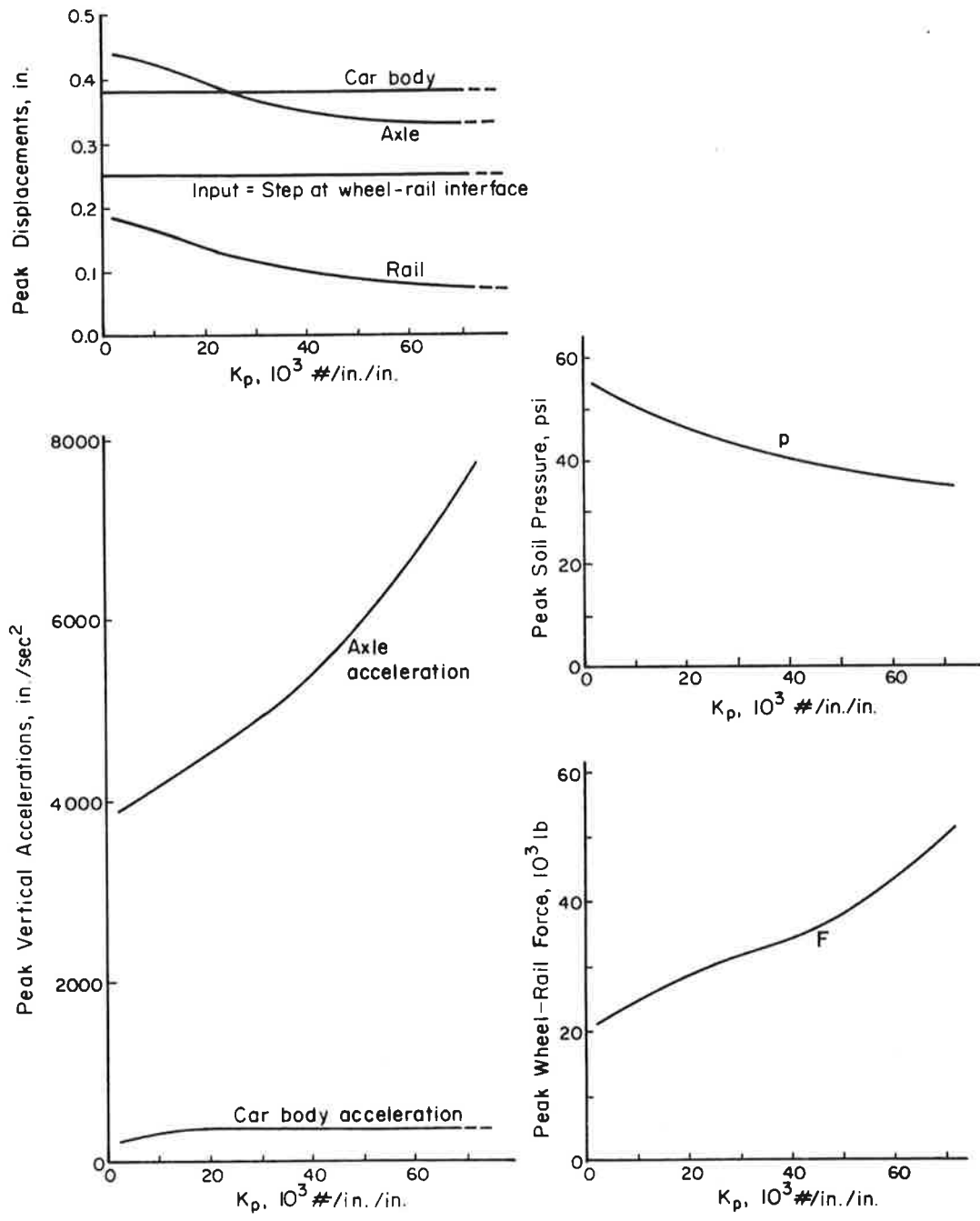


FIGURE 3-6. EFFECT OF RAIL PAD STIFFNESS K_p ON RESPONSE OF CAR AND TRACK TO A 1/4-INCH STEP IN THE RAIL PROFILE [3-42]

directions - on the car ride quality, track deflections and forces, and derailment coefficients.

Based on past experience, one of the major design problems is that of providing sufficient vertical resilience while keeping the lateral resilience within the limits necessary to avoid excessive gage spread. Experience has shown that in designs where rubber is used as the resilient element, it is difficult to obtain the required lateral stiffness unless the base of the rail is effectively widened by attaching a "tie-plate" to it. In other words, if the rail sits directly on a piece of rubber, the torsional stiffness (in response to lateral loads applied at the head of the rail) will be insufficient to prevent rotation and excessive gage spread will result. This can be alleviated by effectively making the rail base wider, but there are certainly other design configurations that would alleviate this problem.

Another basic problem is that the characteristics of almost all elastomers vary considerably with temperature, making it difficult to maintain a specified overall track resilience as ambient temperature changes. Steel, or other metallic springs, do not suffer from this drawback, and perhaps the potential of steel springs in fastener designs has not been fully exploited.

In summary, the design requirements for improved rail fasteners are quite complex, and it is apparent that a better definition of the vertical, lateral, and longitudinal loads to which a fastener is subjected over its design life is needed. The loading definitions should include statistical descriptions suitable for establishing both extreme maximum loads and a realistic simulation of the amplitude and frequency of occurrence distributions to reproduce cumulative fatigue damage. These data can then be used for design and as a basis for realistic laboratory tests. In this way, fastener performance can be evaluated by accelerated life tests that can be correlated with actual service conditions.

3.2.4 Cross Ties

The major functions of the cross ties used for conventional tie-ballast track are to transfer the vertical, lateral, and longitudinal rail seat loads to the ballast and to maintain track gage by providing a reliable support for the rail fastener. Vertical loads subject the tie to a bending moment which is quite dependent on the condition of the ballast underneath the length of the tie. The lateral and longitudinal restraint of the tie are functions of the tie size, shape, surface geometry, and weight. Both wood and concrete ties are now being used by railroad and rapid transit properties in the United States.

3.2.4.1 Wood Ties

Wood has long been used as the standard tie material, and the wood tie has remained basically unchanged in configuration for decades. The 6" x 8" (AREA size 3) and the 7" x 9" (AREA size 5) cross sections are the most widely used. For standard gage track they are normally cut to a length of 8'-6". This length has been selected in an attempt to provide more uniform displacement of ballast between the ends of the tie and the middle, but both longer and shorter ties are also frequently used.

The wood tie represents a "blank" form from which many different assemblies can be built. Thus the incorporation of additional hardware for restraining rail, guard rail, and other special trackwork can be readily accommodated. Additional length is the only special requirement needed for switches and crossovers.

The wood tie also has excellent electrical insulation characteristics, and it is capable of withstanding rough handling during transit, track construction, or from a train derailment. Its light weight makes it relatively easy to handle for spot renewals and new construction.

Some of the major disadvantages of wood ties are their susceptibility to damage by pests, chemicals, and water, and their general deterioration from the weather, from the wear of the rail or tie plates, and from

re-spiking. However, typical data for tie life reported in Reference [3-18] for rapid transit track indicate a life of 25 to 35 years can be expected for wood ties.

The wood tie will generally have a smaller effective bearing area than the concrete tie, and therefore the ties must be spaced closer together in order to maintain comparable bearing pressures and track stiffness. It is generally believed that the greater flexibility of the wood tie contributes to more rapid settlement and/or displacement of the ballast from under the rail seat, but there is little data to justify or refute this observation.

Work has been done recently [3-19] to improve the prospects for future use of wood ties. This work has been directed into two general areas: (1) to improve tie life, and (2) to reduce the initial costs through improved wood usage. Of primary interest from the standpoint of track design is the joining of timber too small for single ties (i.e., 6" x 7") into extra wide ties (7" x 12"), thereby reducing ballast pressures, or permitting an increase in tie spacing which would reduce the overall number of ties and fasteners. Other developments such as laminated and reinforced ties, and "particle board" ties, may have different structural characteristics than wood ties, but their main advantage is expected to be longer life and reduced maintenance.

3.2.4.2 Concrete Ties

The concrete cross tie was originally developed as a substitute for the wood tie in areas of Europe where wood was scarce. Basic economics stimulated the initial development, and this continues to be a dominant factor as the cost for wood increases and the supply diminishes. The concrete tie also offers the greatest hope for a maintenance-free track (at least for the tie-and-ballast type).

In general, there are three factors that have caused resistance to widespread acceptance of the concrete tie by the railroads in this country: (1) the original imported ties were not sized for the heavy loads on American railroads (therefore, failures occurred), (2) several attempts to manufacture ties in this country produced a low-quality produce due to poor manufacturing

techniques and/or poor design, and (3) an attitude of resistance toward new concepts which was somewhat justified by the lack of data indicating significant economic or performance advantages.

The urban rail transit properties have had similar difficulties. Although foreign ties are sized favorably for transit loads, none of the presently available ties, foreign or domestic, have provisions for third rails, guard rails, or restraining rails, and efforts to modify or adapt these ties have frequently been unsatisfactory.

Some of the important advantages that are usually cited for concrete ties are

- Their larger effective bearing area usually permits wider tie spacings; therefore, the number of ties and fasteners which must be purchased, installed and maintained is reduced.
- Their increased weight contributes to greater lateral track stability.
- They provide an opportunity to use a rail fastener that has been designed to provide resilience, adjustability, and improved rail restraint with minimum maintenance. The rail fastener also permits frequent rail replacement or swapping.
- The resistance of concrete ties to chemicals, weather, and abrasion is the basis for claims of long life, but there has been insufficient service time to conclude that concrete ties really have a significant advantage in durability over the wood tie.

Concrete ties also have some disadvantages which, in some cases, result from the same characteristic included as an advantage. The principal disadvantages which are frequently cited for concrete ties are

- Their increased weight makes them difficult to handle and install, particularly for spot renewals
- Attaching rail fasteners to the ties is a critical design problem.

- Their lack of structural resilience makes them more susceptible to major damage by the wheels of derailed cars or from nonuniform ballast support.

3.2.4.3 Tie Strength and Bearing Area

Tie strength and the effective bearing area of the tie on the ballast are the principal factors that are considered in the current track design procedure for either wood or concrete ties. Figure 3-7 shows a single tie supported on ballast and loaded by two equal rail seat loads q_o . The design analysis for determining an effective bearing area for wood ties is based on establishing an "effective bearing length" L centered under each rail seat so that the tie bearing area A_b used previously in Equations (3-10) and (3-12) is given by

$$A_b = bL \quad (3-27)$$

where b is the tie width.

The derivation for the effective bearing length by Clarke [3-4] is not clear, but the equation recommended for wood ties is

$$L = (\ell - c) \left[1 - \frac{0.018 (\ell - c)}{t^{3/4}} \right] \quad (3-28)$$

where Figure 3-7 shows that ℓ is the total tie length (inches), c is the distance between rail seat centers (inches), and t is the tie thickness (inches). For wood tie sizes and the standard track gage used in the United States $c \approx 60$ inches, and the results in Table 3-9 show that Equation (3-28) can be closely approximated by

$$L = \ell/3 \quad (3-29)$$

This effective length may be reasonable based on normal track maintenance practice where ballast is only tamped under each rail seat to prevent "end bound" or "center bound" ties. Consequently, the ballast pressure P_b calculated from $P_b = q_o/A_b$ can be interpreted as an "average" pressure distributed over the tamped ballast region under each rail seat.

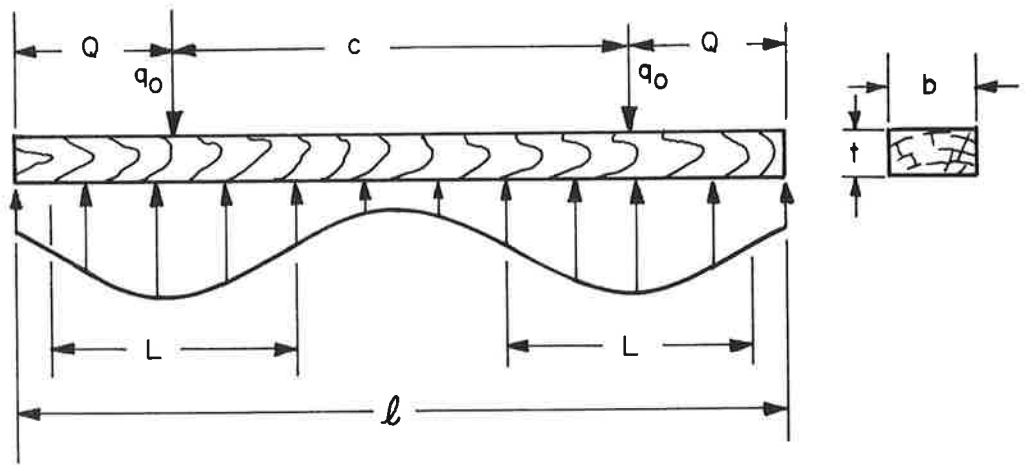


FIGURE 3-7. PRESSURE DISTRIBUTION ALONG TIE LENGTH

TABLE 3-9. EFFECTIVE TIE BEARING AREAS AND LENGTHS

| | Tie Size | Bearing Area, in. | Bearing Length, in. | L/l |
|-------------|--|-------------------|---------------------|------|
| A. Wood | 6" x 8" x 8'-6" | 270 | 33.8 | 0.33 |
| | 6" x 9" x 8'-6" | 304 | 33.8 | 0.33 |
| | 7" x 9" x 8'-6" | 312 | 34.7 | 0.34 |
| B. Concrete | French RS (8.6" x 11.4" x 7'-5.4") | 325 | 28.4 | |
| | German B-58 (7.9" x 11.8" x 7'-10.5")* | 368 | 33.3 | |
| | Gerwick (8" x 12" x 8')** | 380 | 37.5 | |
| | Swedish 101 (8.5" x 12" x 7'-7") | 384 | 32 | |
| | MR-2 (7" x 12" x 8'-6") | 396 | 33 | |

* Tapered Tie, width at rail seat = 11-1/16".

** Tapered Tie, width at rail seat = 10-1/8".

There are no comparable equations for concrete ties which include tie thickness, so it is general practice to base the effective bearing area for concrete ties on the dimensions of the total area in contact with the ballast. The bearing areas and effective bearing lengths for several wood and concrete ties are listed in Table 3-9. These data indicate that the effective bearing length for the concrete ties is about the same as that for wood ties because they have been tapered or are 2-block designs to alleviate center binding. Therefore, the increased bearing area of the concrete ties is mostly due to their 12" width compared to the 8" or 9" width that is typical for wood ties.

Tie strength calculations are based on an approximate analysis of maximum bending moments from the rail seat loads. Clarke [3-4] provides an equation for the tie bending stress under the rail. This equation is supposed to represent the bending moment obtained by applying the average pressure on the effective bearing area under the rail seat to the overhang length of the tie Q. The result given by Clarke for the maximum tie flexural stress f_t under the rail seat is

$$f_t = \frac{6 q_o}{A_b} \left(\frac{Q^2}{bt^2} \right) \quad (3-30)$$

Unfortunately, the units do not check in this equation and it must, therefore, be considered incorrect.

Further analysis to determine the correct form of the Clarke equation indicates that it was probably intended to be

$$f_t = \frac{6 q_o}{A_b} \left(\frac{Q^2}{t^2} \right) \quad (3-31)$$

This corrected equation can be derived by concentrating a force at the end of the tie representing the resultant of the average pressure on the effective bearing area under the rail seat being distributed over the entire overhang length Q. The bending moment M_b at the rail seat for this case is

$$M_b = \left(\frac{q_o}{A_b} \right) bQ^2 \quad (3-32)$$

Equation (3-31) results in tie stress predictions that are b times higher (a factor of 8 to 9 for standard wood ties) than predicted using Equation (3-30). Furthermore, both equations are somewhat inconsistent because an increase in bearing length L (and therefore A_b) will actually increase the tie bending stress rather than reduce it as indicated by the equations.

As a result of this inconsistency in the design equations for tie strength, several alternative formulations were considered. An upper bound for the maximum bending moment M_b that would be expected under the rail seat can be calculated by reacting the entire rail seat load as a point load at the tie end (an end-bound tie). In this case

$$M_b \Big|_{\text{upper bound}} = q_o Q . \quad (3-33)$$

A less conservative and probably more realistic assumption is that half of the tie seat load is distributed uniformly over the tie overhang Q so that

$$M_b = \frac{q_o Q}{4} . \quad (3-34)$$

For an 8' -6" long tie, $Q \approx 21$ inches, and $M_b = 5.25 q_o$.

The bending stress for the rectangular cross-section of the tie would be obtained using

$$f_t = \frac{6M_b}{bt^2} . \quad (3-35)$$

Combining Equations (3-33) and (3-35) gives the upper bound estimate for the tie bending stress as

$$f_t \Big|_{\text{upper bound}} = \frac{6q_o Q}{bt^2} , \quad (3-36)$$

and combining Equations (3-34) and (3-35) gives the more realistic stress estimate of

$$f_t = \frac{3q_o Q}{2bt^2} . \quad (3-37)$$

It can be shown that for the usual case where $\frac{L}{4} < Q < L$, the corrected Clarke Equation (3-31) gives results which lie between those calculated using Equations (3-36) and (3-37).

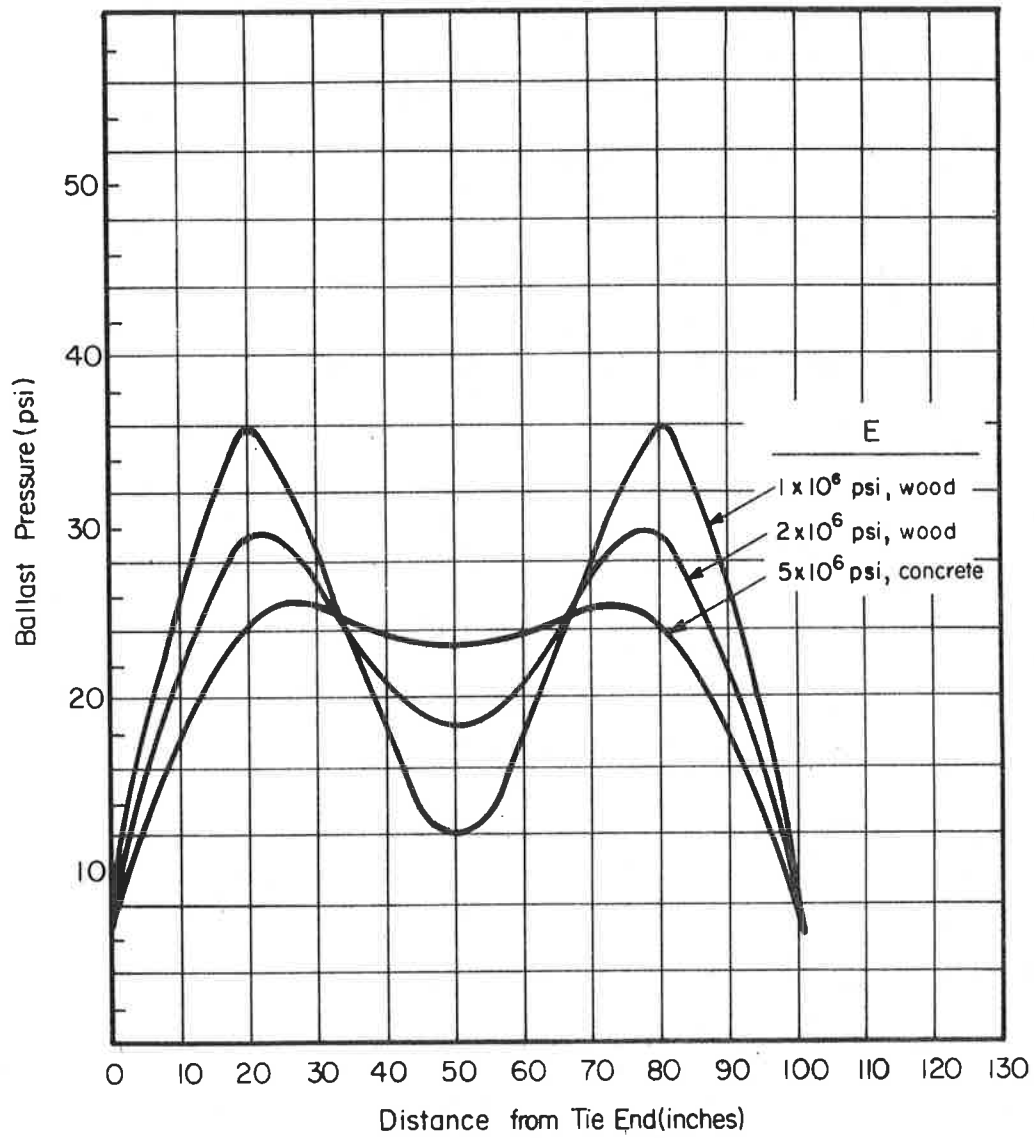


FIGURE 3-9. BALLAST PRESSURE UNDER 6" x 8" x 8' 6" WOOD AND CONCRETE TIES. BALLAST FOUNDATION MODULUS $k_o = 5,000$ psi AND THE RAIL SEAT LOAD $q_o = 17,500$ LBS

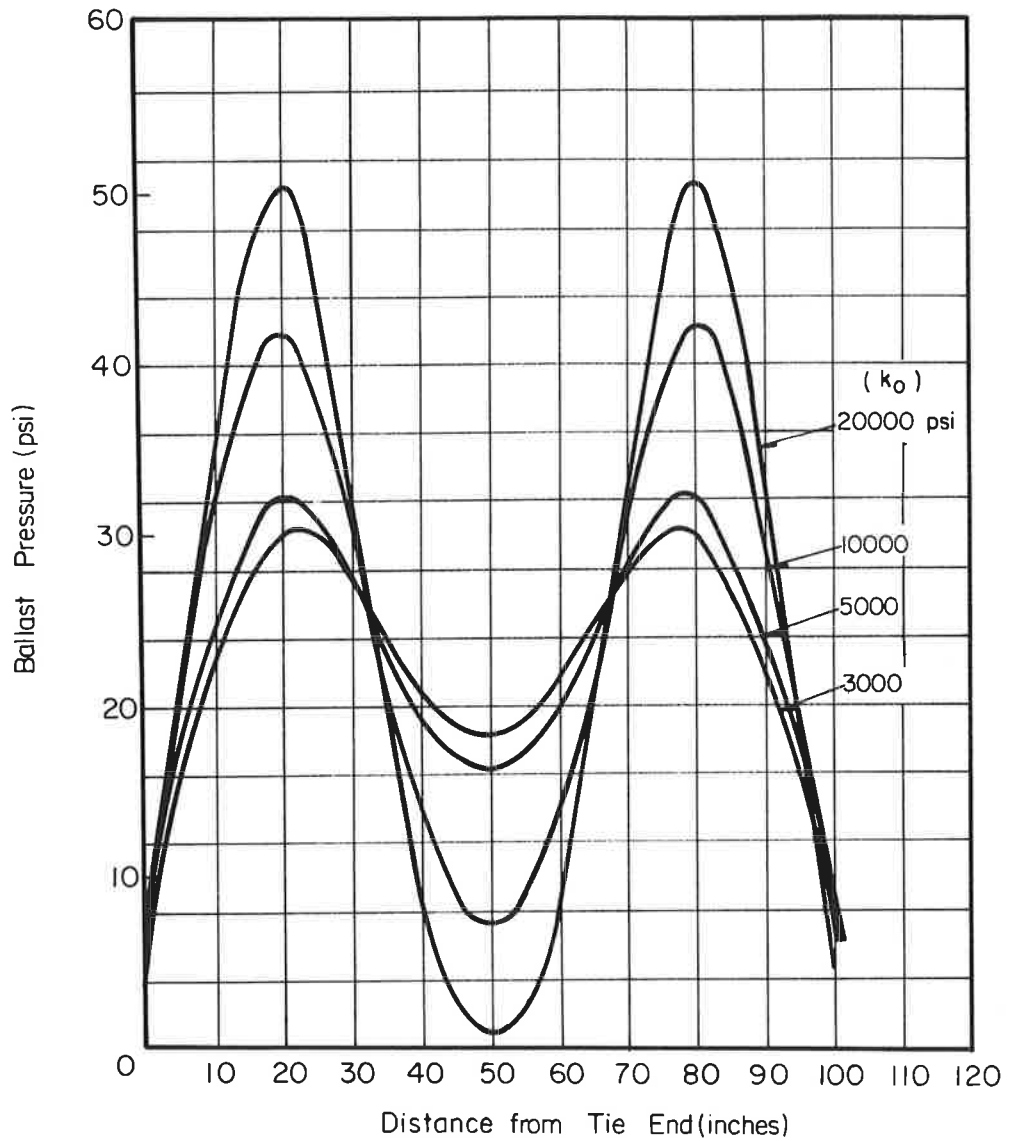


FIGURE 3-8. BALLAST PRESSURE UNDER AN OAK TIE (6" x 8" x 8' 6", $E_b = 1.15 \times 10^6$ psi) FOR VARIOUS VALUES OF BALLAST FOUNDATION MODULUS, k_o . THE RAIL SEAT LOAD $q_o = 17,500$ LBS.

factor) should be less than about 38,000 pounds. For a dynamic impactor of 2, the corresponding allowable static wheel load would be 19,000 pounds, which is greater than the wheel loads for rapid transit cars, but considerably less than the wheel loads for many railroad cars (see Table 3-1).

The need for improved accuracy in predicting the bending loads is demonstrated clearly by the history of the development of concrete ties for the U. S. railroads. The first ties were designed to replace wood ties at the same tie spacing, and they were designed for a bending moment of 100,000 in-lb. under the rail. [3-22] The desire for increased tie spacing resulted in increasing the width of concrete ties to about 12 inches, and the design moments were increased to 150,000 in-lb. under the rail and 200,000 in-lb. of negative bending moment at the center of single block ties. [3-23] Preliminary specifications developed by a special AREA committee on concrete ties [3-24] list similar design values, but it is our understanding that the strength requirements are now being increased to 300,000 in-lb. as a result of field experience.

All of the tie strength analysis that has been discussed has been based on assumed tie loadings from the ballast support, and the effects of the tie bending stiffness and the ballast elasticity are included only indirectly. Consequently, there is no satisfactory way to evaluate the effect of changes in tie materials, an increase in ballast depth, or an improved subgrade on the tie bending stresses.

A first step toward a more comprehensive analytical model with this capability is to consider the tie as a finite length beam on an elastic foundation, and the details of this analysis are included in Appendix B. Figure 3-8 shows the ballast pressure distribution predicted by this model under the length of a 6" x 8" x 8'-6" wood tie for a rail seat load of 17,500 pounds and several values of ballast foundation modulus. These results indicate that variations in foundation modulus, which in practice would result from different types of subgrade and variations in ballast depth, do have a significant effect on the ballast pressure distribution that is not included in the conventional track design procedure.

Figure 3-9 shows the difference between the ballast pressure under wood and concrete ties of the same size and shape (6" x 8" x 8'-6"). These

The bending moment at the center of the tie is also important when the tie becomes centerbound. Under this condition, an upper bound for the maximum bending moment is

$$M_b = \frac{q_o c}{2} \quad (3-38)$$

when it is assumed that the tie is supported by a single load at its center. For the typical case where $c \approx 60$ inches, $M_b = 30 q_o$, which is much higher than the estimate from either Equations (3-36) or (3-37). This justifies the concern for tamping ballast under the rail seat to prevent center-binding.

The maximum allowable bending stress for wood ties is of interest. A working stress of 1100 psi is used for the WMATA design [3-9], and Clarke [3-4] recommends a working stress of 800 psi. These values agree with the "minimum" allowable working stresses recommended by the AREA [3-20] for long duration loading of the lowest grades of oak and pine respectively when the wood is exposed to wet conditions and moderate decay hazard. These working stresses are much lower than the modulus of rupture ($\approx 14,000$ psi for oak and 14,700 psi for pine) or the elastic limit for bending stress ($\approx 3,800$ psi for oak and 9,300 psi for pine) given by Roark [3-21]. However, this reference indicates that an appropriate endurance limit for cyclic loading (reversed bending) is 28 percent of the modulus of rupture, which would be about 4,000 psi.

Using Equation (3-35) and the dimensions for a 6" x 8" wood tie, an allowable stress of 1,100 psi is equivalent to a bending moment of only 52,800 in-lb. This is considerably lower than the data reported by Weber [3-22] that a 400,000 in-lb. moment is required to break an oak tie, or that 100,000 in-lb. moments are frequently measured under the rail seat of end-bound ties. This latter value implies a working stress of about 2,100 psi, assuming wood ties are able to survive repetitive loading equivalent to a 100,000 in-lb. moment. Working backwards, Equation (3-34) indicates a 100,000 in-lb. bending moment (2,100 psi maximum stress) limits the rail seat load to 19,000 pounds for a 6" x 8" x 8'-6" wood tie. Since the rail seat load is typically about 40 to 50 percent of the load applied to the rail for tie spacings up to about 27 inches, this implies that the maximum wheel load (including a dynamic impact

results indicate that the bending deflections of the concrete tie are significant--an effect which is not considered in estimating the effective bearing area for concrete ties. Similar results for the bending moment in the ties show a maximum moment of 78,000 in-lb. for the wood tie ($E = 1 \times 10^6$ psi) compared to 117,200 in-lb. for the concrete tie ($E = 5 \times 10^6$ psi) with these uniform support conditions. This 50 percent increase in bending moment for the same tie size and foundation is not predicted by the approximate design equations. This may explain why initial concrete tie designs based on the bending moments measured for wood ties were inadequate.

3.2.5 Ballast

The primary function of the ballast used for conventional at-grade track is summarized by the following requirements [3-9]

- (1) To provide a firm, even bearing surface for the ties and to spread the load from the rails to the roadbed at acceptable pressures to limit differential settlements between ties, thereby maintaining vertical dimensional stability.
- (2) To provide lateral and longitudinal stability to the track structure, especially due to loads in curves and thermal stresses in CWR.
- (3) To provide drainage for the track structure, draining water away from the loaded portion of the subgrade.
- (4) To provide a material which can readily be worked for surfacing and lining the track and which will remain stable under the action of the elements.
- (5) To eliminate heaving of the track structure by frost action.
- (6) To retard the growth of vegetation which would eventually cause deterioration of the track.
- (7) A layer of sub-ballast under the top ballast will reduce contamination of the top ballast by subgrade soil particles and shield the subgrade from water by draining it to adjacent ditches.

The type of material used for ballast depends on what is locally available, because transportation costs preclude shipment over any great distance. When available, the most desirable materials are crushed rock or mill slag. They are extremely durable and provide a high degree of interlocking action. Gravel is good, but it does not have the rough angular surfaces desirable; therefore, it is usually broken down so that at least 75 percent of the faces are fractured. [3-25] Harder materials are generally better than softer materials because of the improved fragmentation during crushing and greater durability under load.

The gradation of the ballast particles, as well as the absolute size, are important factors that are considered in choosing a ballast. Larger grade sizes are typically more stable, but smaller sizes are easier to work. Nearly all railroads in Europe, Japan, and the U. S. have established a ballast size that includes material between 1 and 2.5 inches in diameter (circular hole).

A ballast depth of 12 inches (30 cm) beneath the tie is usually a minimum design depth for both railroad and rapid transit track in the U. S., but there are some exceptions where less ballast is used. Many properties also use a layer of sub-ballast that is 6 to 8 inches deep, so the total ballast depth varies from a minimum of about 8 inches (a few examples) to a maximum of about 24 inches. There appears to be little difference between the structural performance of ballast and sub-ballast, so only the total ballast depth is of interest in evaluating the distribution of the tie loads to the subgrade.

As discussed in the previous section, the distribution of contact pressure between the tie and the ballast depends on the bending stiffness of the tie as well as the elastic properties of the roadbed (ballast and subgrade). A rigorous approach for predicting the pressure distribution based on an analysis of these elastic layers is too complicated for practical designs. The usual argument for a simplified analysis is that there is insufficient data on the actual mechanics of ballast or on the variations in actual loading and support conditions found in track to justify a very detailed analysis to determine ballast depth requirements.

The conventional design procedure is based on the use of empirical equations to relate the "average" ballast pressure, rather than the maximum pressure, to the ballast depth. The required ballast depth is then determined based on a "safe average bearing pressure" for the soil subgrade. Some consistency is maintained if the safe bearing pressure for the soil is based on a measured subgrade modulus using a 30-inch diameter plate, which at least approximates the pressure loading area on the subgrade under each half tie. The relations between plate diameter, measured modulus, and safe bearing pressure are discussed in greater detail in Section 3.2.6.2.

3.2.5.1 Ballast Pressure

The estimation of an "average" ballast pressure immediately under the tie is based on using Equation (3-10) and an appropriate selection for the effective bearing area of the tie. The pressure calculated using this equation should include a dynamic impact factor (speed effect) and the distribution factor from the beam on elastic foundation analysis for the rail in order to be consistent with standard practice. This can be done by initially increasing the static wheel load to include dynamics and calculate the rail seat load, q_0 , using Equation (3-11).

Typical recommended maximum pressures on the ballast vary considerably. A maximum of 85 psi is recommended in the preliminary concrete tie specifications, [3-24] whereas Magee [3-26] suggests that 65 psi is typical of the ballast pressure under wood ties on 20-inch centers with railroad loads, but he doesn't indicate this as a design goal. Clarke [3-4] recommends a maximum pressure of 35 psi for good stone ballast to avoid excessive deterioration due to crushing. The WMATA design [3-9] was based on Magee's recommendation of 65 psi using twice the rail seat load from the 15,000 pound static wheel load, which is equivalent to using the 30,000 pound dynamic wheel load in the initial calculations. This procedure does not include any additional allowance for variations in tie support which can cause a considerable increase in the loads on particular ties.

3.2.5.2 Subgrade Pressure

There are several empirical relations that are used to determine the depth of ballast, h , below the tie required to obtain a desired subgrade pressure, P_s . The Talbot equation [3-2, Vol. 21]

$$P_s = \frac{16.8 P_b}{h^{1.25}}, \quad (3-39)$$

where pressures are in units of psi and h is given in inches, was developed from field tests with 8-inch wide wood ties.

The Japanese National Railways (JNR) [3-27] use the equation

$$P_s = \frac{50 P_b}{10 + h^{1.35}} \quad (3-40)$$

where h is given in centimeters.

The Love equation, which is an application of Boussinesq theory, is in the form [3-4]

$$P_s = P_b \left[1 - \left(\frac{1}{1 + (r^2/h^2)} \right)^{3/2} \right] \quad (3-41)$$

where r is the radius (in inches) of a uniformly loaded circle whose area equals the effective tie bearing area, A_b , under one rail seat, and h is given in inches.

The usual design practice for determining ballast depth is to limit the pressure on the subgrade to 60 percent of what is considered to be the "safe average bearing pressure". Although the dynamic impact effect is included in the predicted pressure, the 60 percent factor is intended to account for variations in track uniformity. Alternatively, if the normal safe bearing pressure for the soil were used directly, the rail seat load used for the design calculations should be increased to allow for this variation.

Clarke [3-4, p 159] gives the safe average bearing pressures listed in Table 3-10. He recommends that a maximum average subgrade pressure of 12 psi should be used for uncompacted roadbed, and 20 psi or more, depending on the soil, for compacted roadbeds. The WMATA report [3-9, p VII-10] indicates that soil investigations of the proposed route showed a safe subgrade bearing

TABLE 3-10. SAFE AVERAGE BEARING PRESSURES
OF SOILS [3-4]

| Soil Description | Pressure, psi |
|---------------------------------|---------------|
| Alluvial soil | < 10 |
| Made ground not compacted | 11-15 |
| Soft clay, wet or loose sand | 16-20 |
| Dry clay, firm sand, sandy clay | 21-30 |
| Dry gravel soils | 31-40 |
| Compacted soils | > 41 |

capacity of 5,000 psf (35 psi), and therefore 20 psi was used as the allowable subgrade pressure based on the 60 percent guide.

It should be noted that the 60 percent rule is based on Clarke's observation from unreferenced U. S. track data that "individual tie loads can be as high as 2.7 times the normal value computed from elastic theory, and that increases of 66 percent were frequent". It is not stated if the elastic theory calculations referred to here include an allowance for dynamic effects, or if they are based entirely on the static wheel load.

3.2.5.3 Evaluation of Ballast Pressure Equations

In order to illustrate the type of results obtained using the equations for ballast pressure, Table 3-11 lists the ballast depth required for a 20 psi average subgrade pressure when the average pressure on the ballast is 65 psi. These data indicate a 50 percent difference between the minimum ballast depth of 16 inches obtained from the JNR equation and the maximum depth of 24 inches from the Talbot equation.

Some recent work done by Salem and Hay [3-28] using a static test fixture to load single and multiple ties supported on ballast resulted in the measured pressures shown in Figures 3-10 and 3-11. Figure 3-12 shows a comparison of the measured data for a 20,000 pound tie plate load on a 7" x 9" x 8'-6" wood tie with the pressures predicted using the ballast equations discussed previously and a normalized pressure curve developed by the British Railways [3-29] from numerous field tests. The calculated curves are based on an average ballast pressure of 64 psi using $A_b = 312 \text{ in}^2$ for the tie.

This comparison indicates that while the shape of the measured and calculated curves are similar, the calculated pressures are considerably higher than the measured data. The fact that the predicted pressures exceed the measured values is even more significant because it is believed that the equations are supposed to provide "average" pressures, whereas "peak" pressures were measured. Consequently, the prediction techniques can be considered quite conservative.

TABLE 3-11. BALLAST DEPTH REQUIRED TO
REDUCE 65 PSI PRESSURE TO
20 PSI

| Equation | Ballast Depth, inches |
|------------------------|--------------------------|
| Talbot | 24 |
| JNR | 16 |
| Love ($A_b = 270$ in) | 17 |

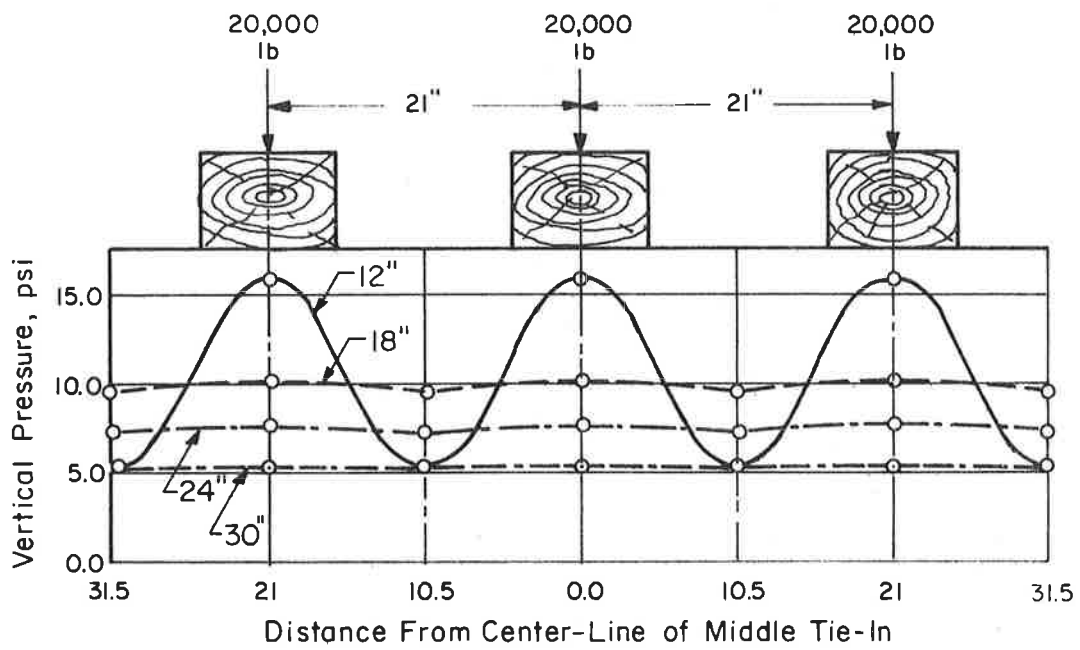


FIGURE 3-10. AVERAGE VERTICAL PRESSURE DISTRIBUTION ON THE SUBGRADE USING THE PRINCIPLE OF SUPERPOSITION FOR DIFFERENT BALLAST DEPTHS [3-28]

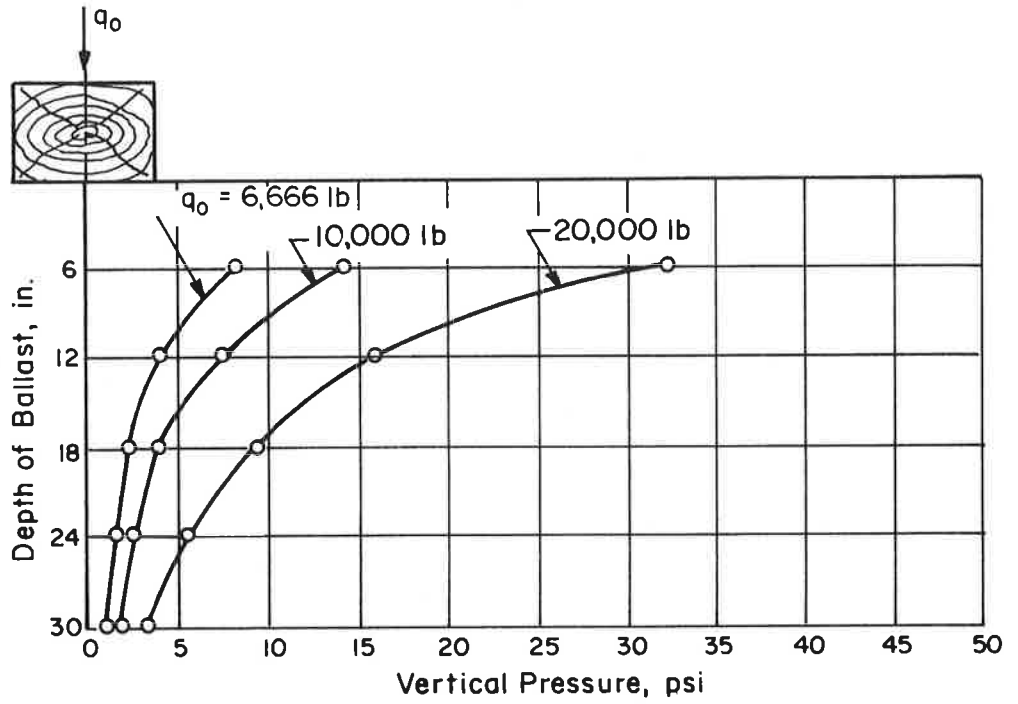


FIGURE 3-11. AVERAGE VERTICAL PRESSURE DISTRIBUTION AT DEPTHS UP TO 30 INCHES OF BALLAST BELOW THE CENTER-LINE OF A SINGLE TIE [3-28]

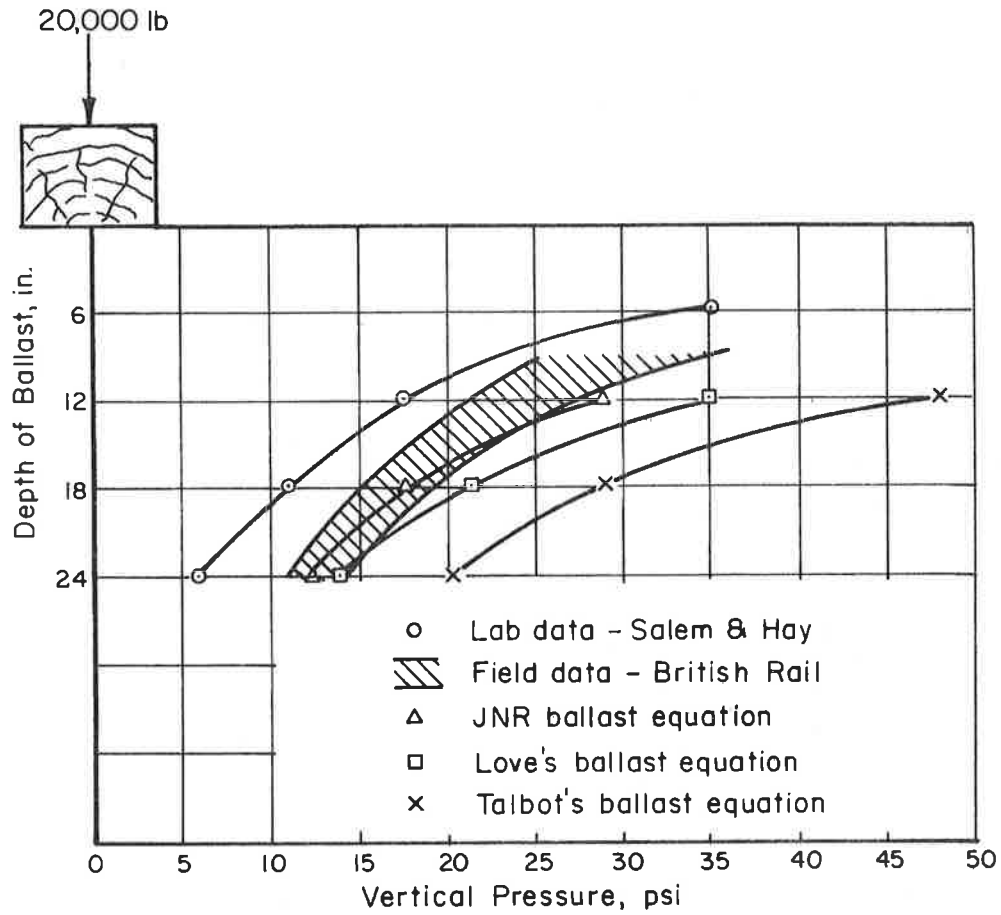


FIGURE 3-12. COMPARISON OF BALLAST PRESSURE PREDICTIONS WITH MEASURED DATA BY SALEM & HAY [3-28]

Figure 3-13 showing the pressure distribution under a wood tie at a depth of 18 inches illustrates another very important factor in track design. The data in Figure 3-10 show that the pressure distribution along the track is very nearly uniform at a depth of 18 inches, and results of this type are the basis for recommendations [3-28] that a ballast depth equal to the tie spacing minus three inches is adequate as long as the safe bearing pressure for the subgrade is not exceeded. However, the fact that the data in Figure 3-13 show a very significant pressure variation under the tie at a depth of 18 inches indicates that even greater depths of ballast may be required to achieve a uniform pressure distribution and reduce differential settlement and the formation of ballast pockets or "ruts" under the rails. This observation has apparently been ignored in track design.

While no extensive data on the structural characteristics of different types or sizes of ballast material is available in the literature, the results shown in Figure 3-14 from Reference [3-2] show that the vertical pressure distribution is identical for crushed slag, pit run gravel, or chat. It is expected that the variations for different ballast materials of similar size and shape are less than the normal variations for other causes of track nonuniformity.

3.2.5.4 Pyramid Model for Ballast Loading

Many ballast designs are based on simplified models of pressure distribution. Figure 3-15 is an example of the pyramid shaped pressure distribution that is commonly used. This simplified model assumes both a uniform deflection and a uniform pressure distribution at every depth in an imaginary pyramid spreading downward through the ballast. It is assumed that the material outside the pyramid is not stressed at all, while the material inside is only under vertical compression. Consequently, Poisson's ratio effects are replaced by the "angle of internal friction". This is a familiar soil mechanics property to describe shearing resistance, and it is closely related to the angle of repose of a free-standing pile of material. It is used in the pyramid model to indicate the inclination of the sides of the pyramid to the vertical and thus determine how the load is distributed as it is transferred downward.

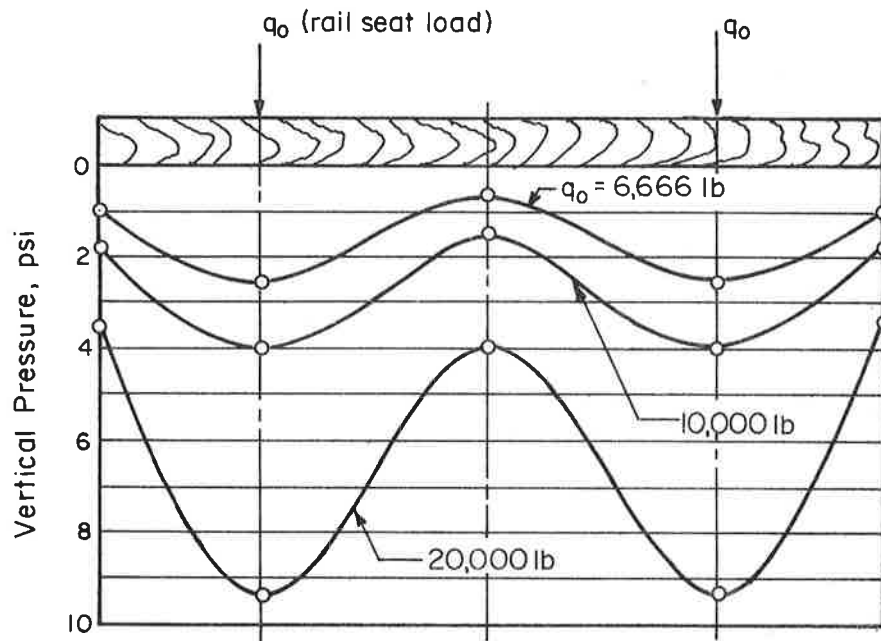


FIGURE 3-13. AVERAGE VERTICAL PRESSURE DISTRIBUTION ON THE SUBGRADE AT A DEPTH OF 18 INCHES OF BALLAST BELOW A SINGLE TIE [3-28]

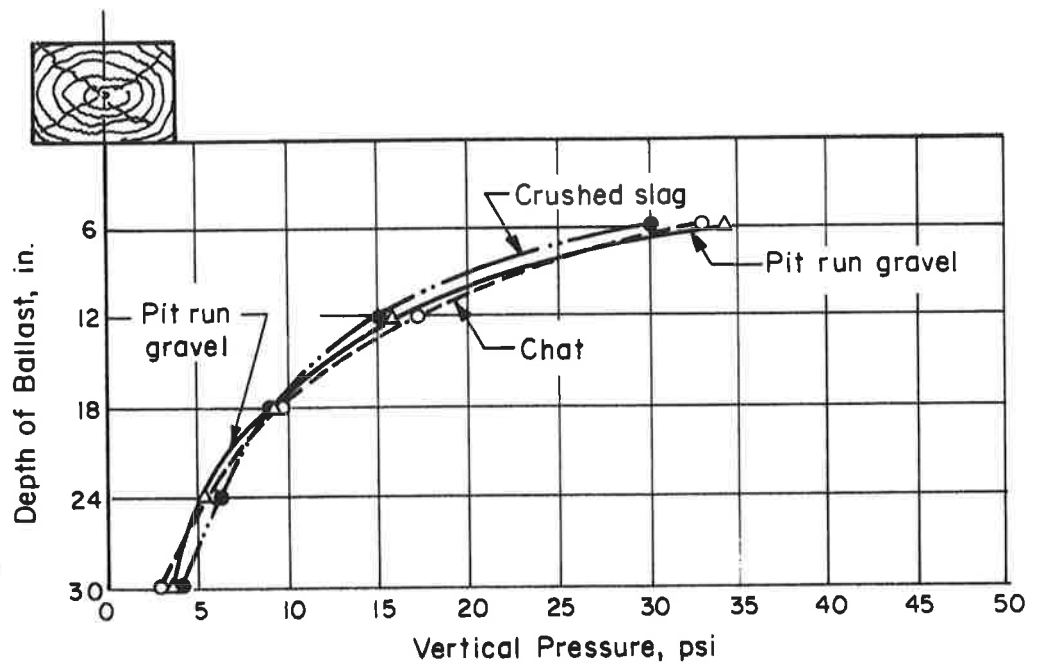


FIGURE 3-14. VERTICAL PRESSURE DISTRIBUTION AT DEPTHS UP TO 30 INCHES OF BALLAST BELOW THE CENTER-LINE OF A SINGLE TIE, TIE LOAD = 20,000 LB [3-28]

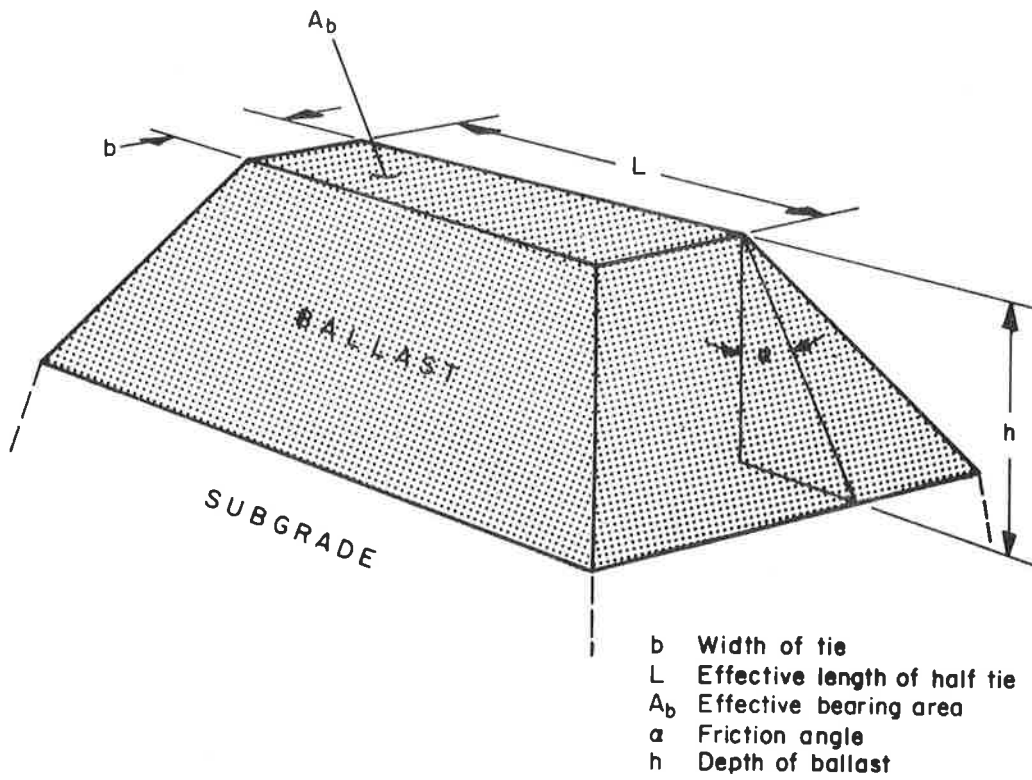


FIGURE 3-15. PYRAMID MODEL FOR BALLAST PRESSURE DISTRIBUTION

The rectangular top of the truncated pyramid is as wide as the width of the base of the tie, and the length is usually that of the effective bearing length of the tie (see Table 3-9). Values for the angle of internal friction which determine the projected base area vary from 45° [3-4] down to 20° . [3-17] Schramm [3-13] indicates that 40° is a good value for high quality ballast and that 30° is indicative of poor ballast.

Although most pyramid models are only concerned with pressure distributions, the Battelle model [3-17] related the ballast stiffness (spring rate) to the modulus of elasticity for ballast as well as predicting average pressures on the subgrade. The capability for deflection predictions is needed in order to evaluate the effect of changes in ballast depth and include these in a more complete model of the track roadbed.

The development and evaluation of the pyramid model approach is discussed in greater detail in Appendix C.

3.2.6 Subgrade

The design of a railroad track ultimately depends on the subgrade, and it is this component that the designer has the least control over, and is probably the least understood. The saving grace is that even if failure occurs, it is unlikely to be catastrophic. This is because the usual mode of failure is excessive vertical settlement occurring gradually in local regions of the track.

A section of roadbed is usually not limited to a single type of soil. Along the right-of-way, it is easy to imagine large changes in the nature of the parent material over short distances due to changes in the geological formations. Conventional track construction is usually based on a uniform track design (constant ballast depth, tie size, tie spacing, etc.), rather than varying the track design to match changes in subgrade properties. Therefore, the track design is based on some "average" subgrade properties, and only those areas of extremely poor subgrade may be replaced, or in some way stabilized, to reduce extreme variations in the roadbed properties. It is important to realize that uniformity is an important goal of the embankment design, because it is not total settlement, but differential settlement which leads to unsatisfactory geometry.

To the best of our knowledge, the construction of new track for either railroad or rapid transit use is based on minimal information about the properties of the soil along the route. However, it is generally recognized that a good subgrade is desirable, and leveling and compacting the subgrade and the ballast before the ties are laid is often a standard procedure. But, it is doubtful if this preparation includes working to any compaction specifications based on soil type and moisture content or to a specification that would improve the uniformity of the subgrade. One of the reasons that subgrade characteristics do not receive greater attention is that no guidelines for relating differential settlement to the subgrade and track design parameters are available for design use. Therefore, there is no way to evaluate the effect of changes in these parameters on overall track performance.

3.2.6.1 Soil Classification

As a prelude to any further discussion on subgrade design, it is appropriate to review some of the basic technical parameters used in soil engineering. Because it is usually necessary to use the soil at or near the work site, it is important to be able to identify the soil type. As a result, several standard classification systems have been developed.

A universal classification system is not desirable in most cases because only certain characteristics of the soil are important in any given application. Most classification systems are based on standard tests which are often made on disturbed samples. Unfortunately, the test values for disturbed samples often vary greatly from the values for undisturbed samples; therefore, it is necessary to supplement the results with information about the soil structure.

The first step in a soil classification is to make a visual survey to obtain geological, climatic, and topographical information. This should be supplemented by test information on the liquid and plastic limits of the soil. Several standard systems used to classify soils are described in Appendix D, together with descriptions and definitions of commonly used terms in soil engineering.

3.2.6.2 Soil Tests

One of the most useful soil tests is a standard compaction test, such as the AASHO compaction test, to determine the relationship between moisture content and dry density. Typical data shown in Figure 3-16 from this test demonstrate how the moisture content during compaction effects the maximum dry density that can be obtained by compaction.

The objective of compacting the subgrade is to increase its stability by increasing the soil density and thereby reducing the sensitivity of the soil strength to variations in moisture. The California Bearing Ratio (CBR), a popular measure of soil strength, is quite dependent on both the density and moisture content, and soil which has been compacted near the optimum moisture content will have the highest CBR. Furthermore, the CBR will be reduced much less by excessive moisture than if the soil had been compacted at a moisture content below or above the optimum. Consequently, a compaction specification should include both the required density and the required moisture content for that particular soil, and it may be necessary to either add moisture during compaction or delay the process if the conditions are unfavorable for compacting at the optimum moisture content.

The California Bearing Ratio is based on a soil test developed originally by the California Division of Highways as an index to soil strength. The CBR test generally requires the following steps.

- (1) Disturbed soil samples with varying moisture contents are compacted into cylindrical steel molds 6 inches in diameter and 8 inches in height.
- (2) The moisture-density curve is plotted and the sample with the greatest dry density is selected.
- (3) The specimen is soaked four days to simulate field water saturation.
- (4) A cylindrical piston with an end area of 3 sq. in. is forced through a 10-pound surcharge ring into the specimen. Load-deformation data are gathered as the specimen is penetrated.

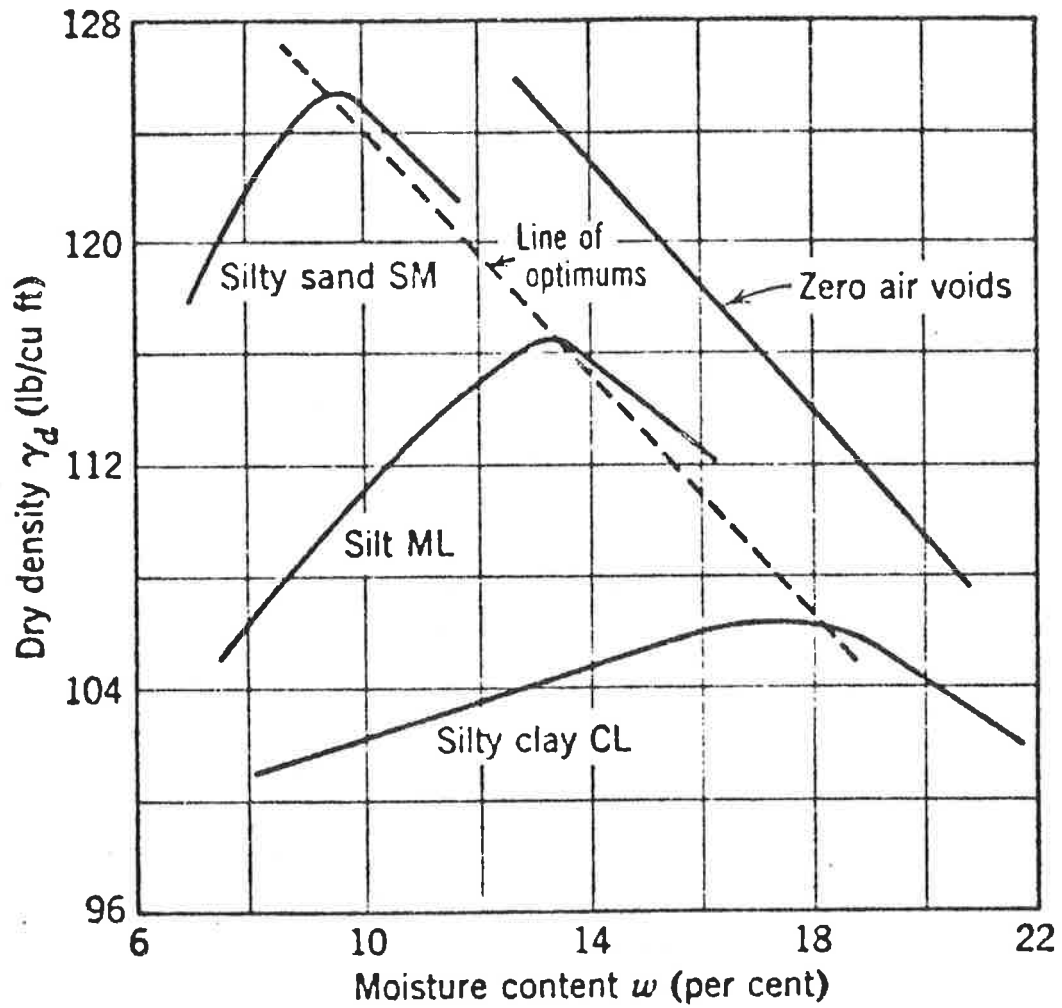


Figure 3-16. AASHTO Compaction Curves [3-30]

- (5) The CBR is then computed from curves similar to those shown in Figure 3-17, or it is calculated by multiplying the ratio of the load carried by the test specimen at 0.1 inch deflection to the load carried by a standard crushed rock base by a factor of 100.

Figure 3-18 gives a very useful approximate correlation between the CBR value, various soil classification systems, and what is considered to be safe bearing pressures for the compacted subgrade.

The modulus of subgrade reaction is also included in this correlation, and this quantity is often used to evaluate the elastic load-deflection characteristics of subgrade. The modulus of subgrade reaction is often obtained from a plate bearing test using a 30-inch diameter circular plate. Figure 3-19 shows that the measured data does depend on the plate size, but a 30-inch diameter plate produces very reliable data for large bearing areas. The rather strong influence of plate area on the data for smaller loading areas indicates that the elastic behavior of actual soil differs considerably from the Winkler foundation model. The theoretical curve is based on results for a rigid circular plate on an elastic continuum where the modulus is proportional to plate radius, and this correlates well with measured data for plate diameters less than 30 inches.

The CBR and the plate bearing tests are the most direct methods for relating design values of subgrade bearing pressure to actual soil characteristics, and these are the basis for most of the empirical highway and airport runway pavement design procedures. However, these methods are all based on rather arbitrary static loading conditions. It is often argued that designs should be based on dynamic properties measured under loading conditions which better approximate the subgrade loading for track. Furthermore, designs based on static data provide no information on subgrade settlement under static or dynamic loading. This is discussed in greater detail in Section 4.8 on track geometry.

Some recent work [3-29, 3-33] in Europe correlating settlement with measured stresses and soil properties demonstrates a reasonable approach toward including subgrade characteristics in track design in a more realistic manner. A triaxial compression test was conducted with clay soil samples to determine

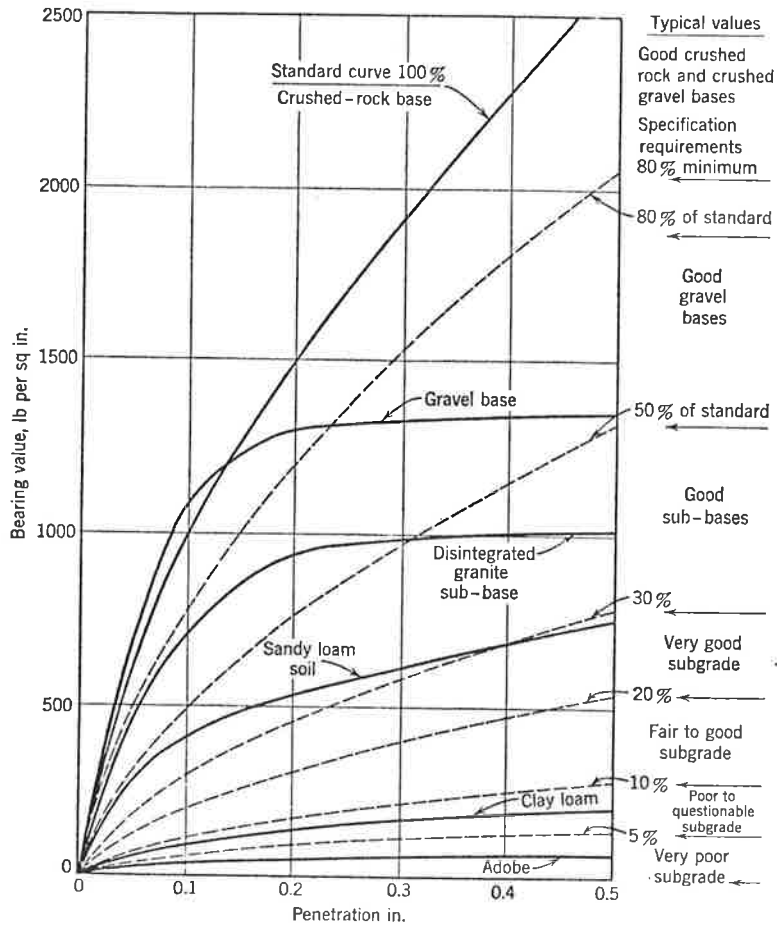


FIGURE 3-17. LOAD-PENETRATION CURVES FOR TYPICAL SOILS TESTED BY THE CBR METHOD [3-31]

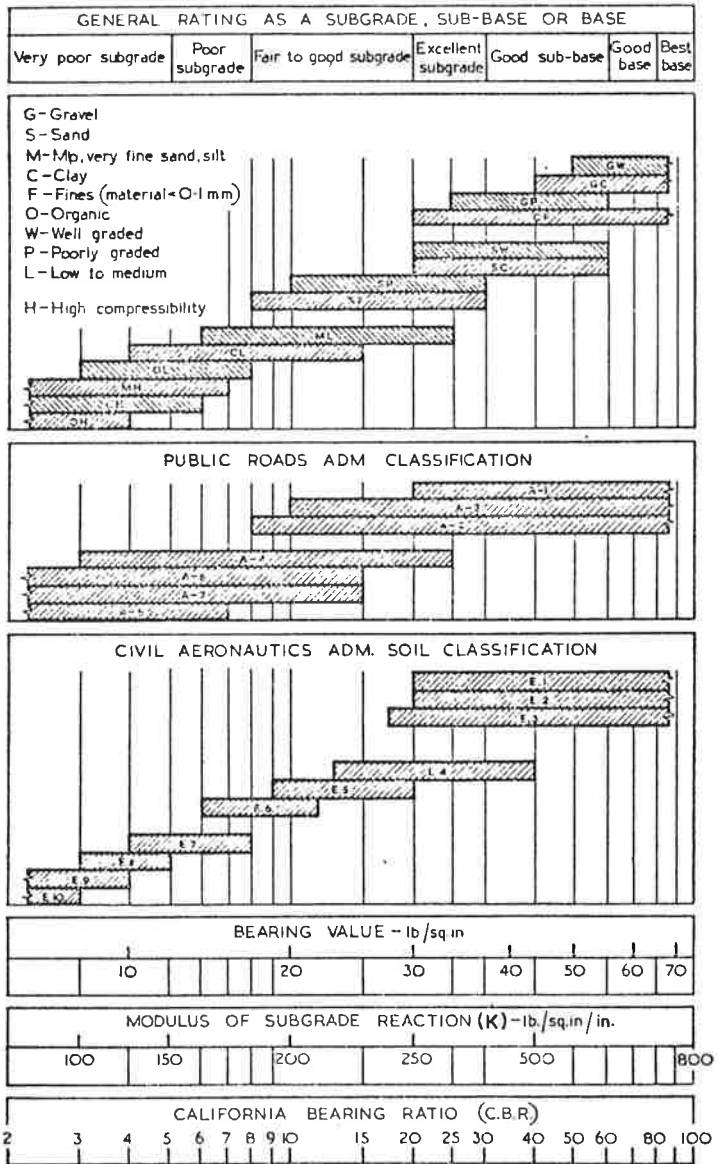


FIGURE 3-18. APPROXIMATE CORRELATION OF THE CASAGRANDE, R.R. AND C.A.A. CLASSIFICATIONS ON THE BASIS OF BEARING CAPACITY [3-32]

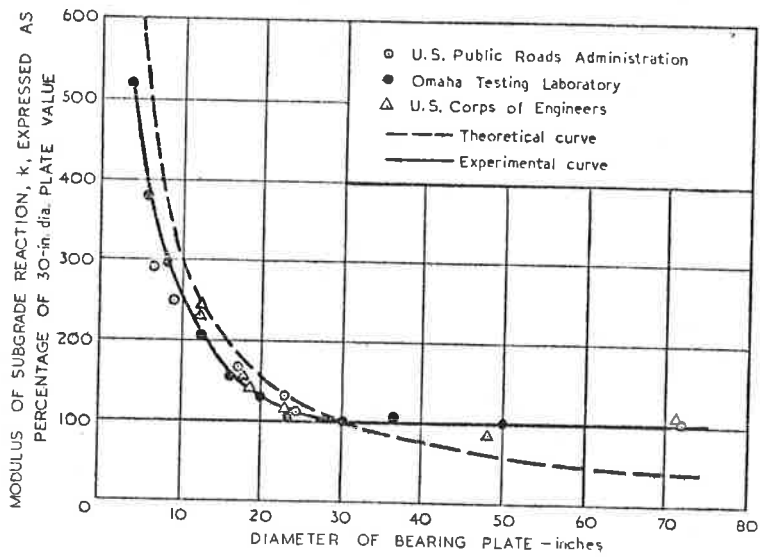


FIGURE 3-19. RELATIONSHIP BETWEEN MODULUS OF SUBGRADE REACTION AND DIAMETER OF BEARING PLATE [3-32]

soil properties under repeated loading along the longitudinal axis of a cylindrical specimen. The radial principal stresses were maintained at a constant confinement pressure typical of the pressure conditions under ballast track while constant amplitude square wave loading was applied to the longitudinal axis at a rate of 30 cycles/min.

Figure 3-20 shows typical results for these repeated load tests. The data for cumulative strain (settlement) versus the number of loading cycles indicate an effective threshold stress difference (endurance limit) such that when the endurance limit stress is exceeded, settlement continues at a high rate. However, when the stress difference (difference in principal stresses) from the applied load is less than the threshold stress, the cumulative settlement reaches equilibrium and very little additional settlement occurs.

Based on these results, the committee proposed a design method for track structures. The inherent assumptions are

- (1) The threshold stress parameters for the subgrade soil may be obtained using the standard repeated loading test.
- (2) Simple elastic theory can be used to predict the stresses in the subgrade from traffic loading.
- (3) The significant stresses are those produced only by the static effect of the heaviest commonly occurring axle load (dynamic load can be included as an effective static load).
- (4) The water table is at the top of the subgrade.

The design method is based on the achievement of a "balanced" design which is obtained when the ballast is sufficiently deep so that the calculated maximum principal stress difference induced in the subgrade by the heaviest commonly occurring axle load is equal to the average threshold principal stress difference established by laboratory soil tests. The use of the principal stress difference as a criterion automatically includes the increase in allowable stress which results from the increase in confinement pressure at greater depths.

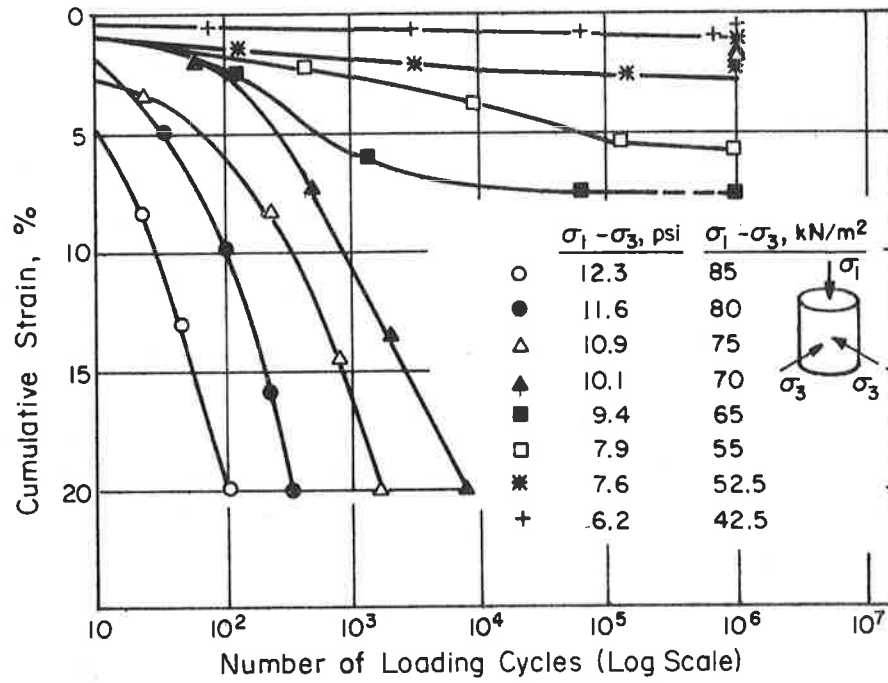


FIGURE 3-20. CUMULATIVE STRAIN RESULTING FROM REPEATED LOADING TESTS OF LONDON CLAY. [3-33]

Figure 3-21 shows a typical design chart for the stresses induced on the subgrade as a function of ballast depth (depth of subgrade/ballast interface below the bottom of the sleeper) for several different axle loads. The threshold stress/depth relationship is superimposed on these curves. Therefore, it is possible to determine the ballast depth required for the stress induced by the axle load to just equal the subgrade threshold stress for soils having different values of threshold stress difference as determined from a standard laboratory test. The intersection points for a particular axle load determine the ballast depth versus soil condition relation needed for track design.

This design method was assessed for ballast track by performing a series of laboratory tests and track measurements. Reduced settlement rates were achieved rather consistently when the ballast depth equaled or exceeded the design depth, and the settlement rates for ballast depths less than the desired depth were significantly higher.

It is important to note, however, that the observation of an apparent threshold stress was made using clay, and there is no assurance that similar results will be obtained for different types of soils with a range of moisture conditions. However, this approach of using a laboratory soil test that closely approximates service loading conditions and yields cumulative settlement data certainly merits further evaluation.

3.3 COMPARISON OF TRACK DESIGN PARAMETERS FOR RECENT TRACK CONSTRUCTION

The current design practice for conventional at-grade track structures is based on formulating design loads as discussed in Section 3.1, and utilizing these with the track design procedures discussed in Section 3.2. However, unless one is a member of the design team, it is often difficult to evaluate a particular track configuration to determine what procedures and criteria were actually used to establish the critical design parameters of rail size, tie size and spacing, ballast depth, and subgrade preparation.

The data listed in Table 3-12 give a brief comparison of the track configurations being used for the most recently designed rapid transit systems.

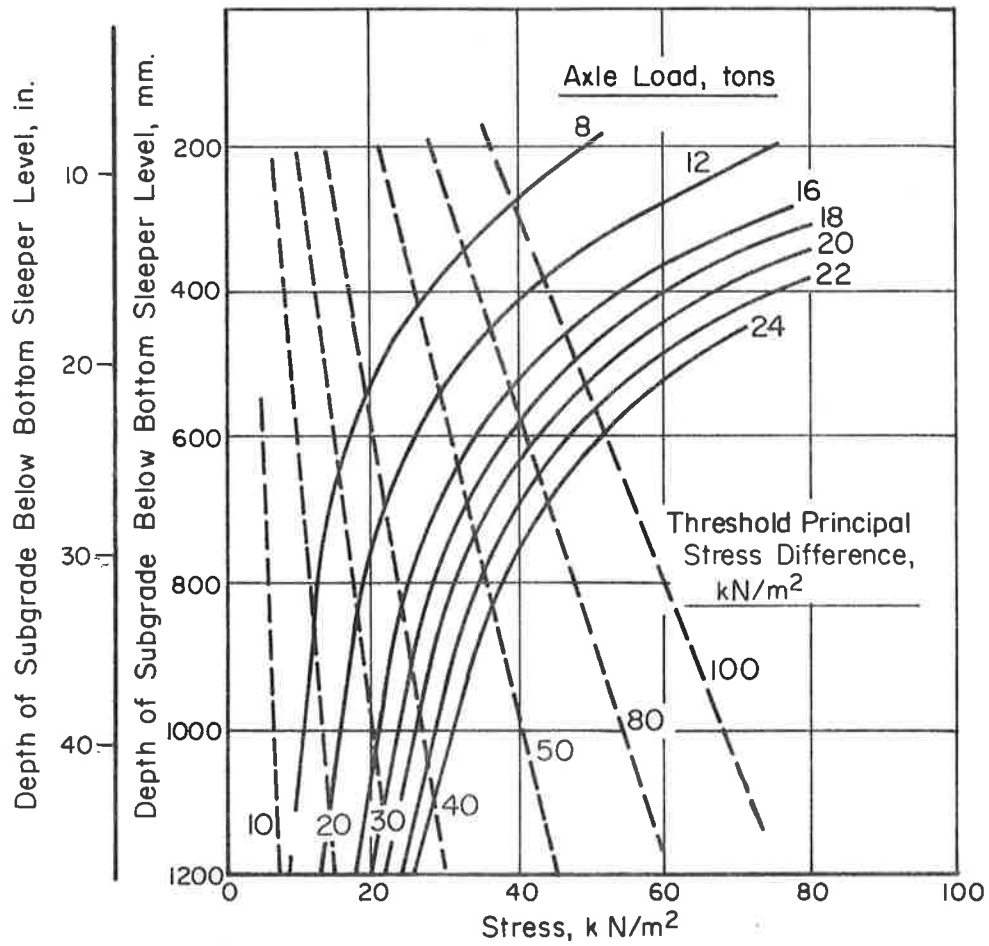


FIGURE 3-21. DESIGN CHART FOR DETERMINING BALLAST DEPTH AND SOIL STRENGTH REQUIREMENTS. [3-33]

TABLE 3-12. COMPARISON OF SELECTED TRACK DESIGN
PARAMETERS FOR RAPID TRANSIT TRACK [3-34]

| Design Parameter | San Francisco | Toronto | Washington, D.C. |
|-------------------------------------|----------------|----------------|------------------|
| Maximum Train Speed, mph | 80 | 55 | 75 |
| Rail Size | 119# CF&I | 100# ARA-A | 115# RE |
| Track Gauge | 5'-6" | 4' 10-7/8" | 4' 8-1/2" |
| Fastener Spacing on Concrete Invert | 36" | 23-3/8" | 30" |
| At-Grade Tie Spacing | | | |
| Wood Ties | 24" | 23-3/8" | 27" |
| Concrete Ties | 30" | | 30" |
| Wood Tie Size (Where used) | 6" x 8" x 9'0" | 7" x 9" x 8'6" | 7" x 9" x 8'6" |
| Depth of Ballast | 12" | 16" | 12" |
| Depth of Sub-ballast | As Needed | 6" | 8" |

Even though the car size and operating conditions are similar for these systems, there are some interesting differences in the track design. The most notable differences are San Francisco's specification of a wide fastener spacing (36 inches) for direct fixation on concrete invert and the use of only 12 inches of ballast for at-grade track compared to a total depth (ballast and sub-ballast) of 22 and 20 inches specified by Toronto and Washington, respectively. This difference in ballast depth represents a factor of 2 difference in the average pressure transmitted to the subgrade, and 12 inches of ballast is considerably less than the depth (tie spacing minus 3 inches) recommended for a uniform subgrade pressure. This difference in design is not surprising, however, because the greatest differences between track designs for either rapid transit or railroad are the ballast depth and the subgrade preparation used for otherwise very similar track configurations and design loads.

It should also be noted that San Francisco uses a track gauge (5'6") that is considerably wider than the 4' 8-1/2" gauge that is standard for other railroad and transit properties in the United States. The technical and economic factors which should be considered in evaluating the advantages and disadvantages of using a nonstandard track gauge are certainly of interest, but they were not included in this report.

3.4 LATERAL TRACK STRENGTH

Conventional track design procedures result in selecting tie size, tie spacing, and rail size for the vertical load requirements. Therefore, the lateral load requirements have relatively little influence on the final track configuration except for the fastener requirements and, in some cases, the width of the ballast shoulder at the tie ends. Urban rail track structures usually follow railroad design practice in providing a 6 to 12-inch ballast shoulder for both tangent track and curves. The lower lateral loads from the short trains of lighter weight transit vehicles (with no locomotives) evidently compensate for the frequent use of tighter curves, because train derailments and track buckling are much lower priority problems for the rapid transit industry than they are for the railroads.

The lateral strength of track is an important factor in maintaining track geometry under continuous traffic and for the safety aspects of train derailments. The lateral strength of unoccupied track must be sufficient to prevent track buckling from rail thermal loads. The resistance to buckling forces is provided primarily by the interaction between the ballast and ties. However, a rail fastener which restrains the rail from rotating in a horizontal plane (rotation about a vertical axis) can significantly increase the track's lateral buckling strength. This represents an additional fastener design parameter.

When the track is occupied by a train, the lateral strength must be sufficient to resist both the thermal loads and the lateral component of the wheel loads. The presence of the vertical wheel loads is an important factor in increasing the effective lateral track strength for these conditions. The possible modes which can cause derailments are

- Lateral track shift
- Rail rollover
- Excessive gauge spread
- Wheel climbing the rail.

The mechanics of lateral track loading is quite complex, and the limited discussion in this section is intended only to illustrate the type of information that is being used for track design. Considerable research on lateral track characteristics has been done in Europe, but there is still much less reliable information available about lateral track characteristics as compared to vertical. In the United States, Dr. Arnold Kerr and several of his students at New York University have been working on vertical and lateral track buckling [3-5, 3-6] and results from some more recent work for the DOT/FRA should be available early in 1974.

3.4.1 Lateral Track Strength on Curves

The lateral resistance provided by a tie in ballast is a principal factor for lateral buckling, and the available data show considerable variation. In Europe [3-35], values of the ultimate lateral resistance for wood ties in 1.2 to 2.5-inch size ballast were between 720 lb. and 1150 lb. per tie

with freshly laid track. After several months of traffic, the lateral resistance often rose by 50 percent or more. Monolithic concrete ties gave results approximately 15 percent greater than wood ties.

In Great Britain [3-35], tests were made with small, soft wood ties and freshly laid ballast, 1.5 - 2.0-inch size, without any consolidation, and lateral resistance was only 440 lb per tie. In Germany, DB tests show lateral resistance for hardwood ties of over 1000 lb. per tie in loose ballast. The differences are due, in part to the size and weight of the ties as indicated below.

| | <u>Weight</u> | <u>Thickness,</u> <u>t</u> | <u>Width,</u> <u>b</u> | <u>Length,</u> <u>l</u> |
|--------|---------------|-------------------------------|---------------------------|----------------------------|
| BR tie | 95-110 lb. | 4.9 in. | 9.9 in. | 101 in. |
| DB tie | 165-175 lb. | 6.3 in. | 10.2 in. | 102 in. |

The end area of the DB tie is about one-third greater than the BR tie, and the side area of the DB tie is almost 30 percent greater than the BR tie, but this does not account for the total discrepancy in values.

Other European experimental work [3-35] on the effect of ballast material has indicated that crushed stone or slag ballast offered greatest resistance, but some carefully conducted tests are needed to fully evaluate the effect of the size and shape of the ballast. For instance, tests with wood on 0.6 - 1.0 inch gravel showed considerably greater resistance than normal 1.2 - 2.7 inch ballast just after the track had been laid. But after 6 months the resistance in gravel had fallen by 22 percent, so it was about the same for the normal 1.2 - 2.7 inch ballast track of the same age.

British Railways made tests with dry ash ballast. The frictional resistance on the bottom of the ties was of similar magnitude to that offered by 1.5 - 2.0 inch crushed stone or slag ballast, but the frictional drag along the sides was only 50 percent that of the stone or slag, and the resistance of the shoulder was negligibly small, however large the shoulder was.

Tests have also been made in Great Britain to find the effect of shoulders of different sizes and shapes in freshly-placed 1.5 - 2.0 inch crushed stone and slag ballasts. Negligibly small improvements in resistance were

obtained if the flat top of the shoulders exceeded 14 inches, and there was only a little reduction in resistance when the flat top of the shoulder was 12 inches. When the flat top was only 7 inches, however, the resistance was 60 to 70 percent of that obtained when the flat top was 12 inches. These data indicate that increasing the ballast shoulder width beyond about 12 to 14 inches is of little value, although some of the design equations assume a linear increase with no specified limits.

The design equation [3-36] frequently used to determine the lateral force produced by CWR on curved track as a result of temperature changes is

$$P_f = 0.441 D_c (\Delta T) \quad (3-42)$$

where P_f is the total lateral track force (pounds per foot of track length), D_c is the degree of curve (degrees), and ΔT is the temperature change ($^{\circ}F$) from the initial rail laying temperature.

If reliable data were available for tie lateral resistance R (pounds per tie) for a specified ballast type and roadbed geometry, the minimum tie spacing given by

$$l_t \leq \frac{R}{P_f} \quad (3-43)$$

can be compared to the spacing determined from the vertical load requirements. If needed, increased lateral resistance can be obtained by reducing tie spacing, increasing the ballast shoulder width or "humping" the ballast above the tie surface at its ends, or by increasing the tie size. Of course, any of these approaches requires information about the relative effect of changes in these design parameters. Some additional information about these effects will be included in the following section on track lateral shift with train loads.

3.4.2 Track Lateral Shift

The net lateral load applied to the track by one axle of a car is the resultant of the flange force at one wheel and the two lateral components of the wheel/rail frictional force at both wheels on the axle. The ratio of this net lateral force to the total vertical axle load is generally considered to be the significant loading quantity governing the lateral shifting of track.

Koci and Marta [3-37] indicate this ratio should be no greater than about .4 for safe operation with regard to lateral track shift on track in poor condition. Other data indicate there is a considerable range in values for the resistance of track to lateral shift. This resistance depends on tie and ballast conditions and maintenance procedures, and the resistance is often very low following lifting of the track or tamping.

The French [3-38] have made extensive measurements using a "Wagon Derailleur" car that has a special axle to apply variable lateral axle loads with a fixed vertical axle load at speeds up to about 25 mph. The critical ratios for track lateral shift range from a low of about 0.5 to as high as 1.25.

Some of the important conclusions from these tests are

- (1) The size of the ballast has little influence on lateral resistance.
- (2) The resistance of the end-face of the tie is important and is improved further by increasing the depth of ballast above the tie base.
- (3) There is a distinct advantage offered by the additional end-face on two-block concrete ties.
- (4) Retamping reduces the lateral resistance of the track structure. The limit of lateral resistance on freshly hand tamped track may occur when [3-39]

$$H_c = \left(1 + \frac{P}{3}\right) 0.85 \quad (3-44)$$

where P is the axle load in metric tons (2205 pounds) and H_c is the critical lateral load in metric tons (applied by an axle). This includes a 15 percent safety factor and is considered to be a practical safety limit for French track. Mechanical tamping will provide

$$H_c = 1.28 + \frac{P}{3} \quad (3-45)$$

and concrete ties will improve the limit to

$$H_c = 2 + \frac{P}{3} \quad (3-46)$$

These equations are useful guides for relating the wheel-rail forces from vehicle operation to safety limits based on the measured resistance of track to lateral shifting, but they are of little value for track design except to indicate typical lateral strength capabilities for resisting thermal loads with unoccupied track ($P=0$).

Amans [3-40] has provided a more thorough empirical design equation to determine the critical lateral force as a function of the combined effects of axle load, radius of curvature, temperature, track modulus and rail stiffness. The empirical reference is a track tested by the S.N.C.F.

$$H_c = \Gamma H'_c \quad (3-47)$$

where H_c is the critical lateral force for track shifting based on measured data for the resistance H'_c of a "reference track". This is frequently given by

$$H'_c = 1 \times 10^4 + \frac{P}{3} \quad (\text{in Newtons}), \quad (3-48)$$

where P is the axle load.

The dimensionless coefficient representing all other influences normally falls in the range of 0.8 to 0.9. However, an empirical function has been developed to quantify the effects of temperature, curvature, track modulus, and rail stiffness. This expression is

$$\Gamma = \left[1 - \beta S \Delta\theta \left(1 + \frac{R_o}{R} \right) \right] \left(\frac{U}{U_o} \right)^{1/8} \left[\frac{\epsilon (EI)^{1/4}}{(EJ)^{1/8}} \right] \quad (3-49)$$

where

R = curve radius, m

S = rail section area, m^2

$\Delta\theta$ = temperature change above neutral, $^{\circ}C$

U = track modulus, N/m^2

EI = rail lateral bending stiffness, $N\cdot m^2$

EJ = rail vertical bending stiffness, $N\cdot m^2$.

The reference values and constants used for Equation (3-49) are

$$\beta = .125 \text{ m}^{-2} \text{ per } ^{\circ}C$$

$$R_o = 800 \text{ m.}$$

$$U_o = 2 \times 10^7 \text{ N/m}^2 \text{ (mediocre track)}$$

$$\epsilon = 0.225 \text{ N}^{-1/8} \text{ m}^{-1/4}$$

The lateral bending stiffness of the track frame is also a key to track lateral stability, but it has not been used as a design parameter to achieve a desired lateral stability. A track frame does not act at all as a beam with a constant stiffness factor "EI" against lateral bending when the rails are free to rotate in a horizontal plane. Theoretically, the lateral stiffness of two rails spaced at standard gauge and fastened rigidly to the ties could be as high as 68×10^{10} lb-in² [3-35]. In practice, however, EI values are typically between 3.4×10^8 and 6.8×10^9 lb-in² [3-35], indicating much room for improvement. Increased lateral stability can be obtained by using a rail fastener to restrain rail rotation.

It is evident that considerable additional work is needed in order to develop a rational procedure for evaluating track behavior under combined vertical and lateral loads. In order to evaluate the effects of design changes, an analytical procedure backed by experimental data is needed to relate track behavior to the characteristics of individual track components such as rail fastener restraint, tie geometry, tie weight, ballast type, and the dimensions of the ballast section.

3.4.3 Rail Rollover

The ratio of lateral to vertical wheel loads is the principal factor in determining rail lateral deflections that can cause derailments by either increasing gauge sufficiently to allow the inside wheel to drop off the rail or by displacing the outside rail to a point of total collapse. The resistance to lateral forces depends on a complex combination of lateral bending and torsion of the rail combined with the restoring moment from the vertical forces of adjacent wheels. However, if a simplified model consisting of one truck on a section of rail with loose joint bars is assumed so that the rail torsional restraint can be neglected, the overturning stability depends only on the rail geometry (ratio of base to height). For conventional rail, this criteria indicates that a ratio of the lateral to vertical wheel forces on one side of a truck in excess of about 0.5 can lead to rail rollover. Of course, this margin is increased considerably by the additional restraint from sound spikes or a good fastener.

3.4.4 Wheel Derailment

Wheel derailment due to the wheel flange climbing the rail is the limiting condition for a train derailment if the track has sufficient strength. Consequently, the loading condition resulting in the wheel flange climbing the rail represents an upper bound for track lateral strength requirements, since any capability in excess of this would be unnecessary.

The condition for wheel climb is a complex function of the wheel angle of attack, the local wheel-rail geometry under flange contact, surface conditions which govern friction forces, and the loading dynamics. However, a derailment quotient (ratio of lateral to vertical wheel force L/V) of 0.8 is used as a minimum safety limit by the Japanese National Railways. Derailment quotients as high as 1.0 are often considered acceptable by others, particularly if the loading is more of an impact rather than steady-state loading. Since it takes a finite amount of time for a wheel to climb the rail, steady-state lateral loads are more dangerous than short-duration impacts.

The capability of maintaining a lateral displacement (gauge widening) of no more than 1/4 inch under simultaneous equal lateral and vertical loads ($L/V = 1.0$) up to the maximum static vehicle wheel load was used by AREA [3-24] as the basis for determining lateral rail fastener requirements for concrete ties. Therefore, fasteners satisfying this requirement could be expected to maintain gauge and resist rail rollover when subjected to lateral wheel loads as high as those which might cause wheel derailment.

3.4.5 Wheel Flange Clearance

Wheel flange clearance is another important factor influencing track lateral forces, as well as wheel and rail wear and riding comfort. Birmann [3-41] indicates that on tangent track the lateral forces at the axle bearings increase markedly with increased flange clearance and running speed. In Germany, the flange clearance for track and wheels in new condition is 10 mm (4 inches). Since 1956 this has been reduced to 7mm (2-3/4 inches), first as an experiment, and from 1961 officially, by a reduction of the gauge from 1435 to 1432 mm (4 ft. 8-1/2 in.). After extensive measurements on test sections which were under

observation for years, it has been shown that lateral rail wear in curves with varying radii, and also on tangent track, is noticeably less than on tracks with the standard gauge.

Birmann also points out the importance of the flange clearance for tight curves. For many years it was the opinion in the railroad industry that the gauge should be widened for curves below $R = 500$ to 600 meters (1640 to 1970 feet) to avoid constraining truck rotation and the resulting increase in rail and wheel wear. However, Birmann indicates that these assumptions are really only valid for curves below about $R = 200$ m (656 ft), because the wear increases due to the increased angle of attack permitted by an increase in gauge. As a result, a new regulation has been adopted in Germany whereby only curves with radii less than 200 meters are widened.

A brief review of the U. S. rapid transit practice reported in [3-18] indicates considerable variation and experience related to gauge adjustments. The NYCTA reports that tightening the gauge by $1/4$ inch on tangent track reduces rail and wheel flange wear, whereas the Chicago Transit Authority reports the opposite results. It is possible that this difference is due to the use of cylindrical wheel treads in Chicago.

Some transit properties widen track by $1/4$ inch gauge on all curves less than 125 foot radius. Other properties widen gauge by $1/4$ inch for curves with radii less than 1500 feet, and they increase it by $1/2$ inch for curve radii less than 500 feet. This considerable variation in practice indicates a need for a more complete evaluation of the effect of wheel flange clearance. An evaluation of this type should combine the effects of vehicle curving characteristics with a procedure for predicting rail wear that includes wheel angle of attack and wheel tread contour.

4.0 DISCUSSION OF CURRENT TRACK PROBLEMS AND RECOMMENDATIONS FOR FUTURE RESEARCH

The identification of the major modes of track deterioration and behavior which results in unsatisfactory performance was an important task in this program. Information obtained from available literature was supplemented by discussions with track design and maintenance personnel during informal visits to several rapid transit operating properties. The results of this review and recommendations for future research related to specific track problems are discussed in the following sections.

4.1 LITERATURE SURVEY

Although there is a large quantity of literature pertinent to the technical aspects of specific track problems, both for railroad and rapid transit properties, data on the relative importance of the different problems is quite limited. A 1971 survey report by the MITRE Corporation [4-1] for the Urban Mass Transportation Administration (UMTA) includes a compilation and analysis of the data obtained through written questionnaires and interviews with the rapid transit operating properties and the major suppliers of transit equipment. These results were used to identify fruitful research areas pertinent to all types of industry problems, rather than being limited to track related problems, which is the principal topic for this report.

The major problem categories identified from this survey [4-1] are listed in Table 4-1 in descending order according to priority.

TABLE 4-1. PRIORITY RANKING OF RAPID TRANSIT
INDUSTRY PROBLEMS [4-1]

-
- (1) Noise (including wheel screech)
 - (2) Vandalism and Security
 - (3) Ride Quality (including truck development and track tolerances)
 - (4) Reliability and maintenance (especially electronic components)
 - (5) Fare Collection
 - (6) Propulsion, braking, and power distribution
 - (7) Training of personnel
-

TABLE 4-1. (Continued)

-
- (8) Fire and Safety
 - (9) Derailment
 - (10) Passenger Information Systems
 - (11) Heating and Air-Conditioning
-
-

The research categories in this survey that were related to track performance are noise, ride quality, and derailment. A brief summary of the conclusions for these topics is given in the following sections.

4.1.1 Noise

It was evident that noise problems were of the highest priority for nearly every property. This included noise control in vehicles, terminals, tunnels, and aerial structures. Wheel screech is the major concern. This is most noticeable on tight radius curves, but it can also occur during braking or acceleration if adhesion is inadequate.

The noise related research topics suggested in this survey were:

- (a) Wheel screech reduction
- (b) Environmental noise control
- (c) Vehicle noise assessment
- (d) Track fastener development
- (e) Acoustic materials for tunnel walls
- (f) Field studies of vibration and noise
- (g) Cost effectiveness of methods to reduce wheel screech.

It was also recognized that noise is related to the condition of the track and wheels so that noise, ride quality and track and vehicle maintenance are interactive. Many of these noise research topics are included in current programs being sponsored by the UMTA, under the technical direction of the DOT/TSC.

4.1.2 Ride Quality

A subjective evaluation of vehicle ride indicates that vertical ride quality of modern vehicles with air springs is quite good whereas the lateral response from truck hunting, response to normal track irregularities and transient "lurching" needs further development. The research topics suggested for this subject were:

- (a) Vehicle ride quality assessment
- (b) Rail-wheel wear research
- (c) Rail-wheel profile studies
- (d) Truck modifications to improve ride
- (e) Track condition studies
- (f) Effect of track conditions on suspension requirements
- (g) Ride quality standards
- (h) Advanced suspension development.

Rail corrugations were also identified as a problem and corrugated rail contributes to excessive noise, poor ride and increased maintenance. The development of a track measuring system for use with revenue cars was considered highly desirable by the properties, and this task is being pursued under the UMTA rapid rail research program. Wheel flats and wheel spalling are also major vehicle maintenance problems which affect noise, ride quality, and track maintenance.

4.1.3 Derailment

Train derailment was identified as an important safety problem. However, the diversity of opinions in the rapid transit industry indicates that derailments must be relatively infrequent, and they don't have nearly the priority that they do for railroads, where derailments occur more frequently.

The activities recommended by the rapid transit properties for derailment research were:

- (a) Techniques for predicting derailment from track condition
- (b) Parametric studies of the effect of vehicle weight, truck weight, velocity, draw bar location, gauge tolerance, wheel-rail profile, wheel base, etc., on derailment.

- (c) Evaluation of the use of guard and restraining rails and other protection devices.
- (d) Development of portable equipment to assist in re-railing a vehicle in a tunnel.
- (e) Investigation of the use of scale models for derailment studies rather than using full size vehicles.

The differences in priority assigned to car derailment by the rapid transit and railroad properties reflects several of the basic differences in their operation. The rapid transit industry has a relatively small amount of track with high usage by short trains of light cars operating at well-regulated speeds. Track deterioration results in reduced ride comfort and increased noise and vibration for the passengers and the community. Consequently, track deterioration will be quite objectionable before it reaches the state where it would be unsafe, which is the principal concern of the railroads for their predominantly freight traffic. Therefore, it is generally recognized that urban rail track is maintained in better condition than much of the railroad track in the U.S.

Furthermore, derailments on the railroads are often caused by the lateral component of high coupler forces which are caused by the longitudinal dynamics of very long trains operating over curves and hills. These high lateral forces can produce derailments due to rail roll-over, gauge widening, lateral shift of the track, or the wheel climbing over the rail. The reduction of derailments due to longitudinal train dynamics and train handling is an objective of the current AAR-RPI-FRA Track Train Dynamics Program. Fortunately, the short rapid transit trains are not subjected to this type of derailment problem

4.2 PRIORITY RANKING OF URBAN RAIL TRACK PROBLEMS

4.2.1 Industry Interviews

Informal visits were made to several rapid transit operating properties and other selected individuals in order to supplement and update the information about current track problems that is available in the literature.

These discussions with track design and maintenance personnel were quite beneficial in revealing the practical aspects of track design and track problems and in insuring that this program would emphasize the problems which were most important for the industry.

The operating properties and other organizations which were visited are listed in Table 4-2. The operating properties were selected to provide a reasonable sampling of typical operating conditions, and the meetings were quite informal. This task was not intended to be a comprehensive survey using prepared questionnaires, and therefore did not include all of the major operating properties or the many other organizations which undoubtedly could have provided equally valuable information.

Table 4-3 lists in descending order the priority ranking of track problems. This ranking is based on a review and tabulation of the topics discussed during the interviews and the previous experience of the Battelle-Columbus (BCL) research staff. It should be cautioned that this ranking represents the subjective response of track design and maintenance personnel rather than a quantitative criteria based on maintenance costs, safety, or community acceptance. For example, it is quite possible that track geometry maintenance may require the largest part of the maintenance budget. However, it is so much a part of the normal routine that community and passenger complaints about noise from rail corrugations may be a greater "annoyance" factor to the track supervisors, so that this problem would be given a higher subjective rating based on discussions with track design and maintenance personnel.

The first seven items in Table 4-3 are definitely significant track related problems for the rapid transit industry, whereas the last three items are either of less importance or do not exactly qualify as a track problem. Concrete ties, for example, were only tried on 2 of the 4 operating properties that were interviewed, and the current opinion is that their performance is acceptable. However, both properties had difficulties with initial manufacturing quality, and available concrete ties have not been designed for convenient attachment of restraining rail or a third rail. Similarly, the major complaints about track maintenance equipment, such as excessive noise and incompatibility with subway clearances, are caused by the way the rapid transit operating procedures and environment differ from those of the railroads for which the maintenance equipment has been designed.

TABLE 4-2. ORGANIZATIONS AND PERSONNEL INTERVIEWED
ABOUT TRACK DESIGN AND TRACK PROBLEMS

| Organization | Personnel |
|---|---|
| Port Authority Transit Corporation (PATCO) Camden, New Jersey | Mr. Donald Wolfe Mr. J. William Vigrass |
| New York City Transit Authority (NYCTA) New York, New York | Mr. William F. Tiedeman Mr. Chester Marczeski Mr. William Bulis Mr. Martin Kornstan Mr. A. J. Wolf Mr. Tony Paolillo |
| Chicago Transit Authority (CTA) Chicago, Illinois | Mr. Paul Swanson Mr. Thomas L. Wolgemuth Mr. Roy T. Smith |
| Massachusetts Bay Transportation Authority (MBTA) Boston, Massachusetts | Mr. John A. Carey Mr. Alfred J. Parcelli Mr. Harry D. Tietjen |
| Westenhoff and Novick Chicago, Illinois | Mr. Charles F. May |
| Portland Cement Association (PCA) Chicago, Illinois | Mr. John W. Weber |
| Shaker Heights Rapid Transit Lines Shaker Heights, Ohio | Mr. Robert J. Landgraf |

TABLE 4-3. PRIORITY RANKING OF TRACK STRUCTURE PROBLEMS

-
-
- (1) Rail Joints (Standard and Insulated)
 - (2) Rail Wear and Noise on Curves
 - (3) Rail Fasteners, Bolts and Spikes
 - (4) Rail Corrugation
 - (5) Rail Field Welds
 - (6) Track Geometry Maintenance
 - (a) Curve alignment
 - (b) Joint settlement
 - (c) Bridge approaches
 - (7) Community Noise and Vibration (tangent track)
 - (8) Track Buckling
 - (9) Concrete Ties
 - (a) Manufacturing quality
 - (b) Alignment difficulty
 - (c) Third rail and restraining rail attachment
 - (d) Rail fasteners
 - (10) Track Maintenance Equipment
-
-

It is also obvious that the solutions to many of the high priority track problems are closely related. For example, the significance of rail joint problems could be reduced considerably by more extensive use of continuous welded rail (CWR). Installation of CWR, however, is discouraged by a need for a more reliable field welding procedure that can be used successfully by unskilled persons and by the high rail wear rates on curves that requires frequent rail swapping and replacement--a process that is much easier with bolted joints.

Similarly, rail corrugations are a significant source of noise and vibration on tangent track. And rail joint problems contribute to both noise and vibration as well as the rapid degradation of the track profile in the vicinity of the joint. More detailed evaluations of these high priority track problems are included in the following sections.

4.3 RAIL JOINTS

Bolted rail joints are used to join together standard lengths of rail by means of a joint bar on each side of the rail web. Joint bars range in length from 24 inches (4 bolts) to 36 inches (6 bolts). The standard rail lengths were originally 33 feet, but are now 39 feet. This size was determined by the length of the available cars that could be used for transporting rails.

The bolted rail joint is somewhat weaker than continuous rail even when the joint is new and the bolts are tight. This situation is worsened by the fact that one of the major maintenance problems for rail joints is that the bolts continually loosen and must be retightened. Corrosion and wear at the contact surfaces between the rail and joint bar are recognized as the major cause of loose bolts and loose joints [4-2] despite the use of AREA recommended bolt tensions and spring washers.

Insulated joints are an even more challenging design problem because materials with adequate electrical insulation properties such as wood, rubber, and fiber composites are poor structural materials. Insulated joints are a more important problem for transit properties than for railroads because more of them are required for the shorter signaling block lengths which are typically

about 1000 feet long. The most frequent failure mode for insulated joints is a short circuit caused by the degradation of the fiber end blocks that are positioned vertically in the gap between the rail ends. A failure of this type gives a false occupied block signal which delays train operations and becomes an immediate maintenance problem. It is not unusual to have to rebuild insulated joints as frequently as every 3 months, and the flexibility of these joints, as well as standard bolted joints, contributes to track settlement near the joint, rail end batter, and increased noise, vibration and wheel/rail dynamic loads.

Fortunately, new transit systems and new lines on old systems can be designed with a different type of signalling system called "Audio Frequency Overlay" which eliminates the need for insulated rail joints except at switches and other special trackwork. But existing systems using bolted rail and isolated track circuits have a continuing need for improved standard and insulated bolted rail joints.

Some equipment suppliers are now providing new types of insulated joints. One example of this is the development by Portec, Inc. of a thermoplastic material with fiberglass reinforcement in the bushings and end posts to replace fiber insulators [4-3]. The most important claim for this new material is that it is impervious to moisture and that it has superior insulating properties resulting in a service life from 5 to 10 times that of the fiber material. The development work for this joint included static and dynamic loading tests of the material and rolling load tests of the complete joint.

Another new insulated joint design that is currently being evaluated by 3 out of the 4 properties interviewed is the I-Bond* joint manufactured by Intma Industries under a German license. This joint is normally delivered in 11 to 39 foot lengths using standard or heat-treated rail so that it is installed either by cutting the existing rail and welding the insulated joint assembly into CWR track, or by replacing a standard length of bolted rail in bolted track. This type of joint is referred to as "frozen" because the glass epoxy insulation and all other parts are adhesively bonded into a relatively solid joint.

* Trademark of Intma Industries

The manufacturer claims this is the only rail joint having a 3 year warranty, and this warranty is valid as long as the rail temperature does not exceed 210°F.

The manufacturer indicates that over 200,000 I-Bond joints have been installed in Europe since it was designed in 1956. Data from a rolling load test by the AAR [4-4] using a wheel load of 44,400 pounds on an I-Bond with 132-pound rail indicates that the adhesive bond was in good condition after 2 million cycles and that the electrical insulation was maintained. Although the rolling load test applies both positive and negative bending moments to the joint, it does not include longitudinal forces, dynamic impact effects, or environmental conditions. Also, similar results for joint deflection and rail end batter from other types of joints are needed for at least a comparative basis of evaluation. A comparison of the stiffness for a continuous section of 132-pound rail, a standard bolted joint, and the insulated joint under the rolling load test condition would be a valuable basis for comparison.

The railroads are also becoming interested in using bonded joints, and Union Pacific reports [4-5] that they have about 500 miles of track in which all insulated and standard joints are bonded. Joints capable of withstanding the higher wheel loads of railroads should provide good reliability for rapid transit use.

Because of the high priority held by rail joint problems in the rapid transit industry, this topic was selected for a somewhat more detailed review. The results of this evaluation are discussed in the following section.

4.3.1 Technical Evaluation

The principal deficiencies of bolted rail joints are that they are more flexible than continuous rail, joint bolts require continual retightening, insulated joints need frequent refurbishing, and rail fractures frequently occur at the joint bolt holes when a joint becomes loose.

The reduced stiffness of the rail joint results from the difficulty in maintaining a uniform bending stiffness from one rail end to the other. In Europe, the rail joints on the two rails in a track are usually opposite each other (square), and the ties are usually spaced closer together near the joint

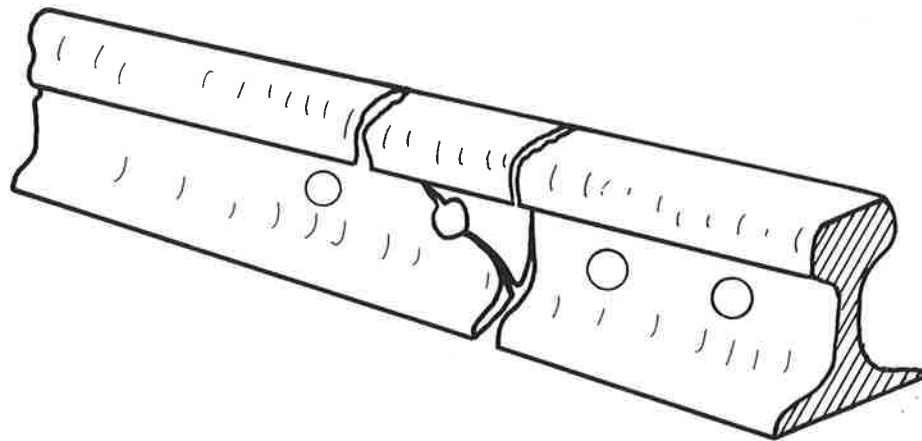


FIGURE 4-1. TYPICAL FAILURE AT RAIL JOINT
THROUGH THE FIRST BOLT HOLE

to provide a better support. In the United States, the joints are usually staggered and a fixed tie spacing is used for the entire track. While the 30-inch tie spacing that is frequently used for the lighter wheel loads in Europe makes variable spacing possible, the approximately 20-inch spacing used for U.S. railroads cannot be reduced without interfering with the 10-inch minimum clearance needed between ties for automatic tamping equipment. The somewhat wider tie spacing now being used with concrete ties on transit track does provide some freedom for variable tie spacing, particularly when the joints are square so that the increased number of ties is minimized. The change in tie spacing needed to improve the joint support should be based on achieving a constant rail seat load for the entire track to minimize differential settlement at the joints, rather than designing to a constant bending stress level in the rail and joint bars based on their differences in section modulus.

The most important and dangerous failure mode for standard bolted joints is a brittle fracture that starts from a fatigue crack in the first "running-on" bolt hole as shown in Figure 4-1. This type of joint failure is caused by the high cyclic transverse shear stresses that are produced in the rail web by the dynamic wheel loading on a loose joint. The danger is that the fatigue cracks do not have to be very large before a complete brittle fracture is possible. A derailment where 49 people were killed in England was caused by a brittle fracture where the fatigue crack was only 1/8-inch long before the accident [4-6]. The analysis of the rail stresses in the vicinity of the joint are discussed in the following sections.

4.3.1.1 Rail Joint Analysis

The beam on elastic foundation analysis can be used to predict rail deflections and bending moments as shown by Equations (3-2) and (3-3). The maximum bending moment in the rail for a single wheel load P is given by

$$M_0 = \frac{P}{4\beta} = \left(\frac{EI}{64U} \right)^{1/4} P \quad (4-1)$$

If there is a break in the continuity of the rail, such as at a rail joint, the resulting deflections and bending moments will depend upon the structural capability of the joint. The resisting moment developed in the joint bars at the rail end may be less than that developed in the rail. The range in the ratio, ρ , of the resisting moment at the middle of the joint to that developed in the rail under similar conditions of loading will vary from 0 to 1.0.

If the conditions of rail support are assumed to be the same as those used in the analysis of continuous rail, for a wheel load P applied directly over the joint, the deflection is given by [4-7]

$$y = \frac{e^{-\beta x}}{2\beta^3 EI} \left[\frac{P}{2} \cos \beta x - \beta \rho M_0 (\cos \beta x - \sin \beta x) \right] \quad (4-2)$$

The slope α of the rail at the joint is obtained by differentiating Equation (4-2) with respect to x , and this slope will be useful later in determining the dynamic load at a joint.

$$\alpha = \left(\frac{dy}{dx} \right)_{x=0} = \frac{-1}{(4\beta^2 EI)} (P - 4\beta \rho M_0) \quad (4-3)$$

Figure 4-2 shows the bending moment and rail deflection for a single wheel load, P , acting at the joint for several values of the ratio ρ ranging from 0 to 1.0. The value of ρ characterizing actual field joints varies from joint to joint and is strongly dependent on bolt tension. For 130-pound P. S. rail, it was found from tests on the Pennsylvania Railroad [4-8] that ρ varied from 0.41 for joints with a low bolt tension of 2,000 pounds to $\rho = 0.87$ for very high bolt tension. In laboratory tests of statically loaded rail joints [4-9], it has been found that the stresses at bolt holes in a loosely bolted joint were nearly twice the stresses in a tight joint. From the moment diagram in Figure (4-2) one is led to conclude that these high stresses are due to the interaction of the rail and the joint bar rather than the bending stresses in the rail.

It has long ago been demonstrated [4-10] that elementary strength of materials methods of determining rail stresses provide quite accurate results

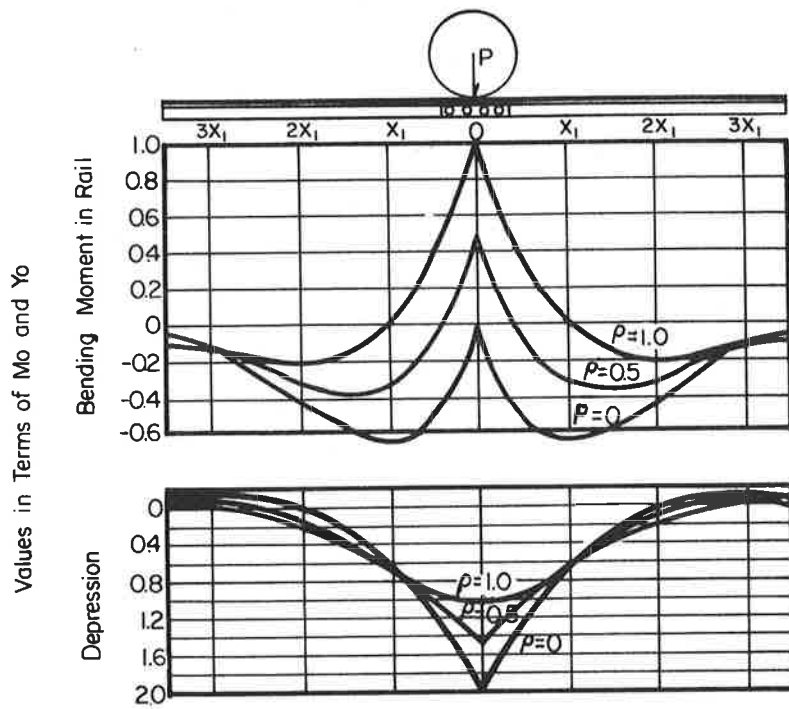


FIGURE 4-2. BENDING MOMENT AND RAIL DEPRESSION FOR A SINGLE WHEEL LOAD AT A JOINT [4-10]

if the correct moment and shear at a particular section in the rail can be determined. An exception to the above is in determining the complex stress distribution in the vicinity of the bolt holes at a joint.

Consider that a wheel load is applied directly over a joint so that the distribution of the bending moment is approximately as shown by Figure 4-3. Unless the joint is tight enough to prevent all relative motion, the joint bar and the rail will not bend together along their length. Instead, the joint bars will act as simple beams with the loads applied as shown in Figure 4-4. The left-hand side of this figure illustrates the shape of the actual contact stress distributions acting between the two members. The right side of the figure shows the static resultants R_1 and R_2 of these stresses applied through the centroids of the loaded areas. In this diagram the reaction "S" is the load resulting from tightening the bolts, and H_1 and H_2 are the shearing reactions caused by incipient shear between the rail and the joint bar.

Figure 4-5 shows the effect of bolt tension on the joint bar stresses at the midsection of a bolted joint, [4-10]. This figure shows that high initial bolt tension can significantly reduce the stress from a lateral bending moment. For a bending moment of 60,000 in-lbs., the minimum necessary bolt tension was found to be 5,000 pounds for the rail and joint bar considered. This type of information is needed for all of the rails and joint bars in present day use to determine if the bolt torque specifications are adequate for the maximum expected loads.

4.3.1.2 Analysis of Stresses at Rail Bolt Holes

To determine an upper bound for the stresses at the bolt holes in the rail, assume that the joint bar is completely removed and the transverse shear at the bolt hole location is solely due to the wheel loading, as shown in Figure 4-6. This figure shows a cantilevered beam of rectangular cross section having a hole of radius R at a distance "a" from the clamped end, and the beam is loaded with a shear force Q across the end. It can be shown [4-11] that the hoop stress at the edge of the hole for the above problem is given by

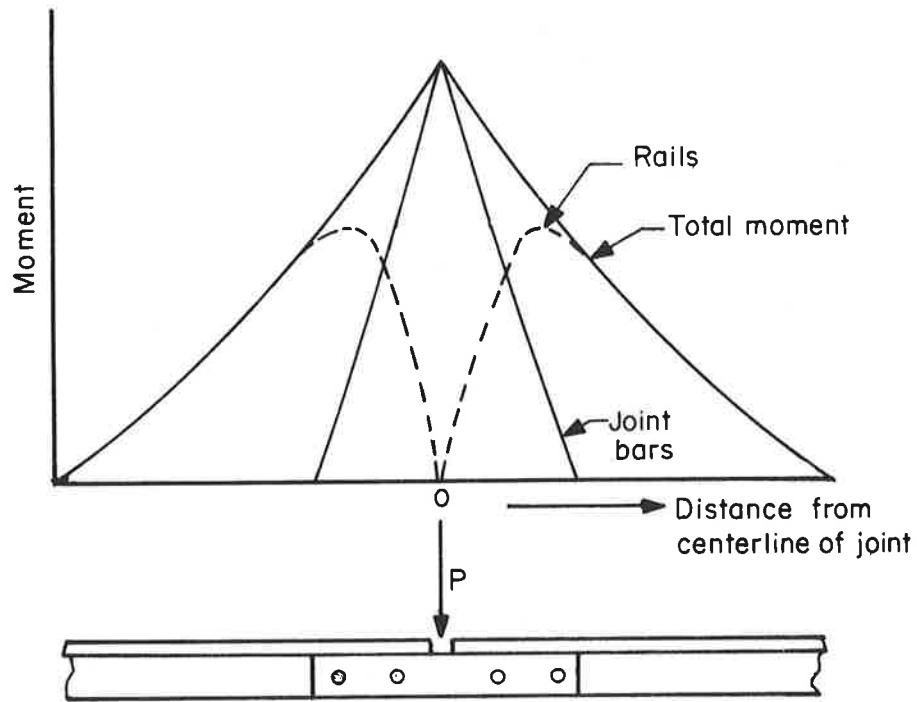


FIGURE 4-3. DIVISION OF MOMENT BETWEEN RAIL AND JOINT BARS

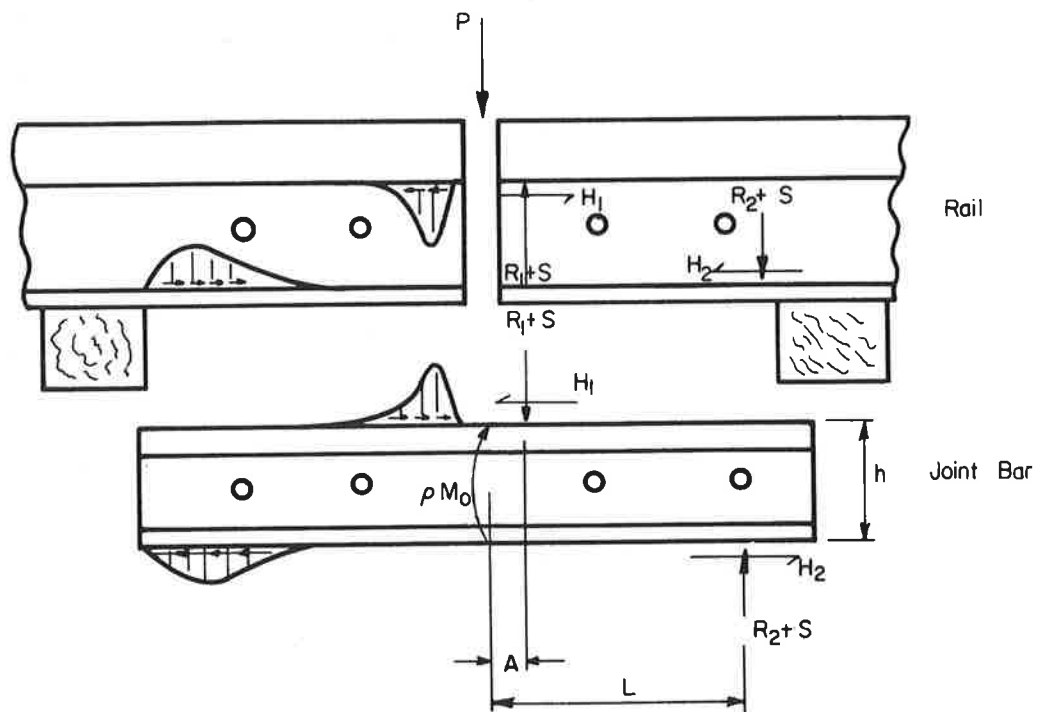


FIGURE 4-4. ILLUSTRATION OF STRESSES ACTING BETWEEN JOINT MEMBERS

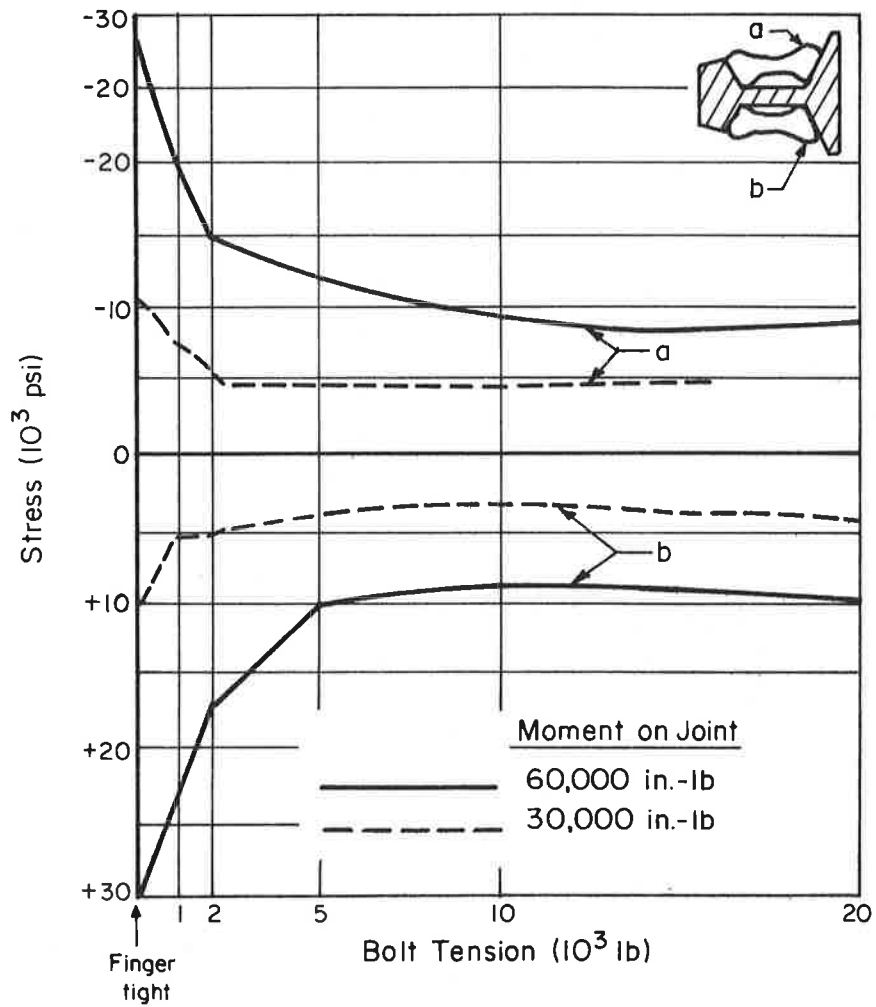


FIGURE 4-5. EFFECT OF BOLT TENSION ON JOINT BAR STRESSES FOR LATERAL BENDING MOMENTS [4-10]

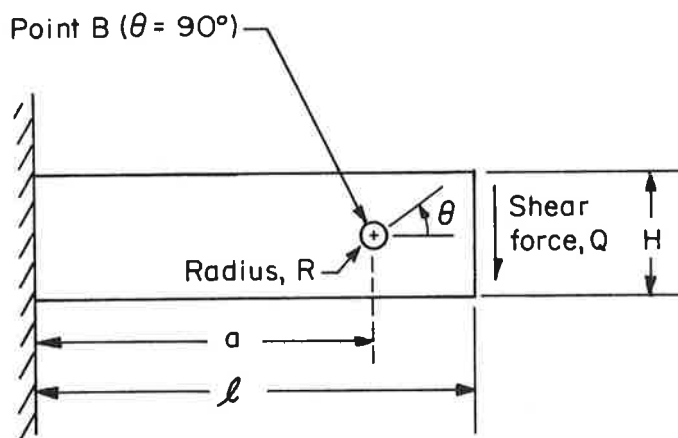


FIGURE 4-6. CANTILEVERED BEAM WITH A HOLE

$$\sigma_{\theta} = \frac{Q(\ell-a)R}{I} (\sin\theta - \sin 3\theta) + \frac{Q}{I} \left[(2H^2 - R^2)\sin 2\theta + R^2\sin 4\theta \right] \quad (4-4)$$

where θ is the angle from horizontal and I is the moment of inertia of the beam.

The first term on the right-hand side of Equation (4-4) is the stress induced by the bending moment at that section. The bending stress at a hole very near the free end of the beam will be small relative to the stress from the transverse shear; therefore, the bending stress has been neglected for the following approximate analysis.

It is convenient to obtain a stress concentration factor, K_{θ} , for the hole by dividing the second term in the right side of the equation (4-4) by the absolute value of the transverse shearing stress, τ , evaluated for a solid beam (no hole) at a distance R from the neutral axis (represents the hole edge at $\theta = 90^{\circ}$ as shown by point B in Figure 4-6). The equation for this stress concentration factor is

$$K_{\theta} = \left(\frac{Q}{I} \right) \frac{[(2H^2 - R^2)\sin 2\theta + R^2\sin 4\theta]}{|\tau|} \quad (4-5)$$

where

$$|\tau| = \left(\frac{Q}{I} \right) \left[\frac{H^2 - 4R^2}{8} \right] \quad (4-6)$$

Since the distribution of the transverse shearing stress in a rail web is very similar to the shear stress at the center of a rectangular beam section, the stress concentration factor for the beam with a hole is a good approximation for the hoop stress around rail bolt holes. Figure 4-7 shows a plot of the stress concentration factor for typical dimensions of a rail web and bolt hole, $R=1$ inch and $H=5-3/4$ inches.

The analytical formulation assumes that the wheel load is applied to the rail as a uniform shearing force across the end section of the beam. To test the validity of this assumption, a 0.4x photoelastic scale model of a 115-pound RE rail was made. The model shown in Figure 4-8 was three dimensional in order to produce the same stress field at the bolt holes as is present in the actual rail. Two-dimensional photoelastic analysis techniques could be used for the web section, however, since the stress state is plane stress.

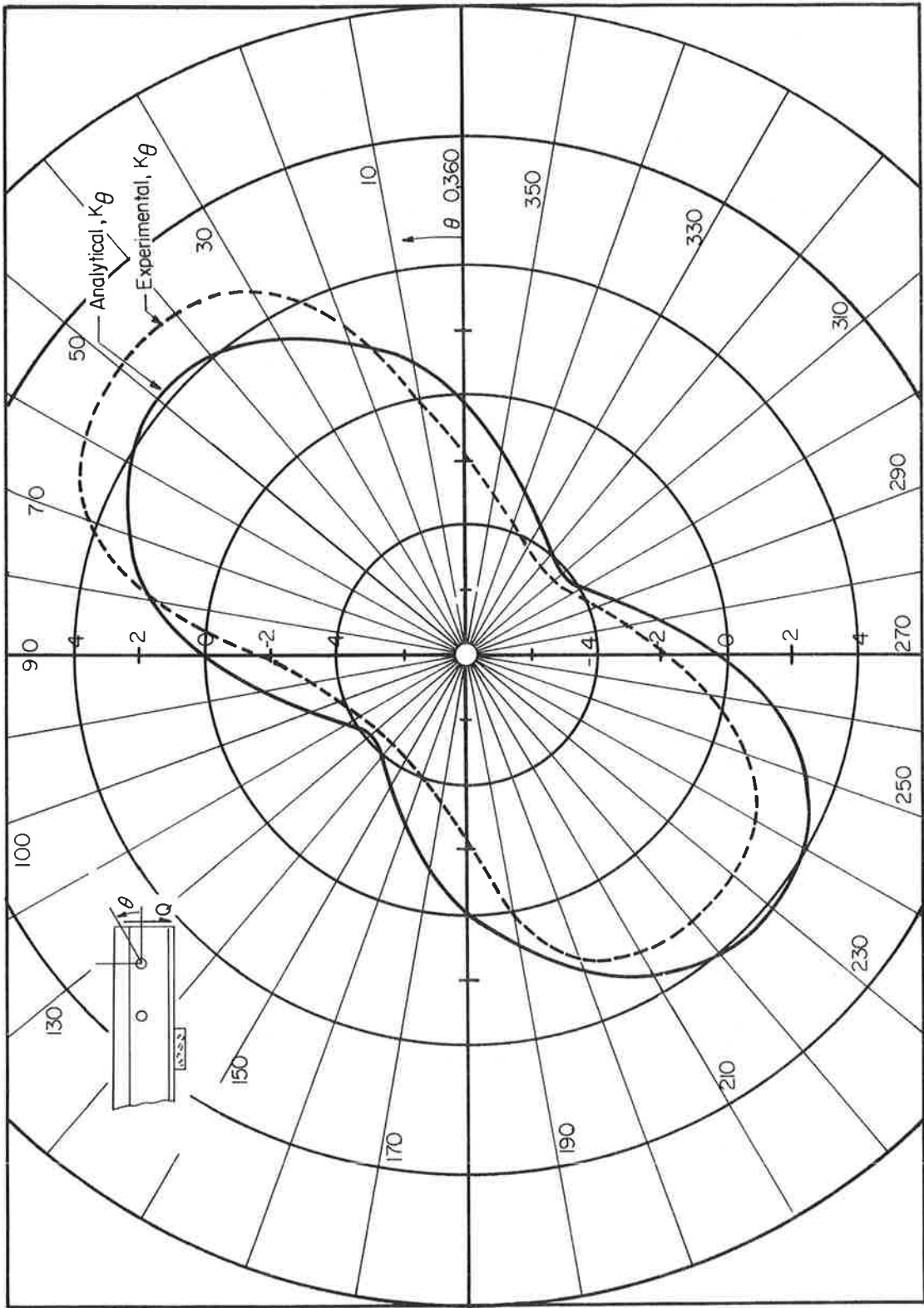
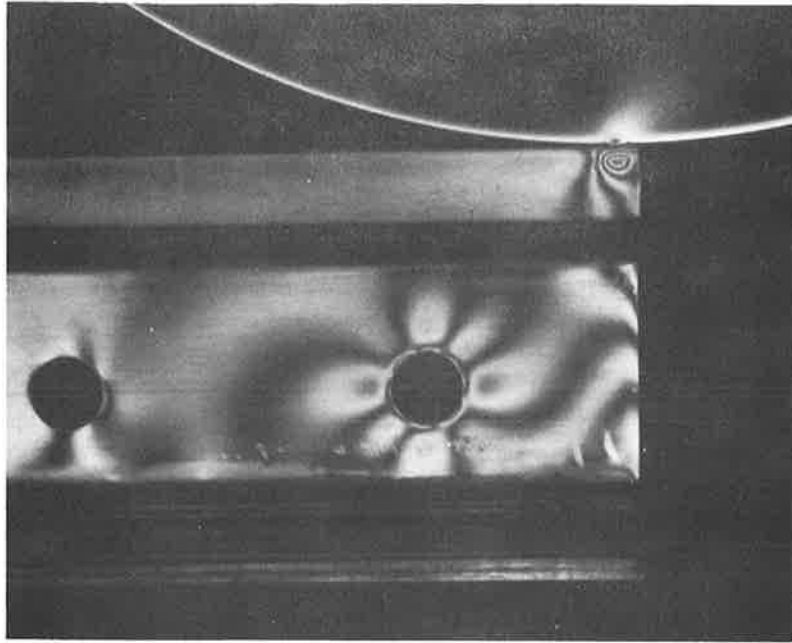
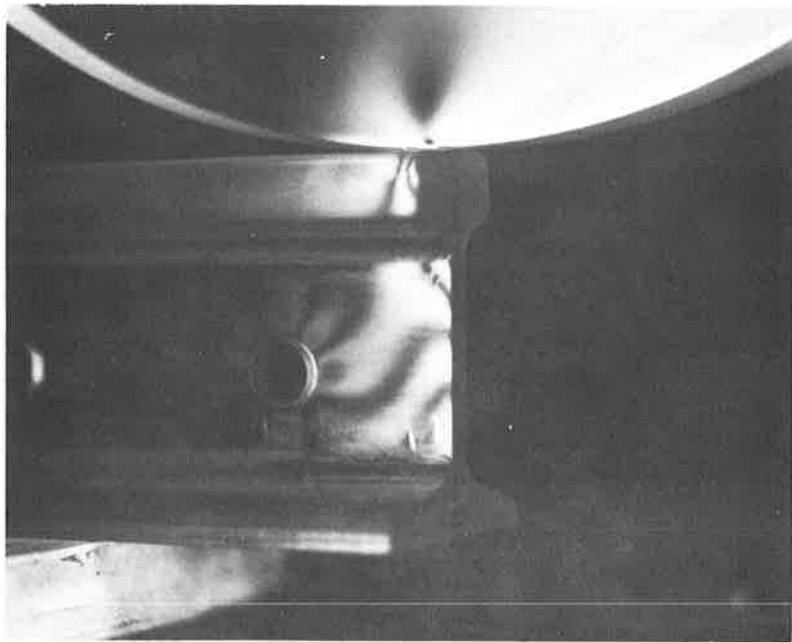


Figure 4 7. Stress Concentration Factor Around a Bolt Hole



(a) Side View of Photoelastic Model



(b) Partial End View of Photoelastic Model

FIGURE 4-8. PHOTOELASTIC MODEL OF LOADED RAIL END

The wheel load was applied to the end of the rail as shown in Figure 4-8. The tie spacing was assumed to be 21 inches with the tie located 10-1/2 inches from the rail end. The fringe patterns shown in Figures 4-8 and 4-9 were analyzed around the first bolt hole to determine the hoop stress fields. This experimentally determined hoop stress distribution around the bolt hole was then nondimensionalized by dividing by the calculated value for the transverse shearing stress in a solid beam at the location of the top of the bolt hole. This experimentally determined distribution is plotted in Figure 4-7 with the theoretical distribution. These results show that whereas the analytical formulation predicted a maximum value of $K_{\theta} = 4.3$, the experimental values yield a higher result of $K_{\theta} = 4.9$. The higher stresses at the bolt hole are due to the influence of the concentrated wheel load.

As discussed earlier, failures at bolt holes nearly always originate at the lower 45° position of the hole ($\theta = 315$ deg., Figure 4-7). It has been determined experimentally and analytically that at this location compressive stress state exists under static load. It is, therefore, necessary to consider the dynamic loading conditions of the rail joint in order to evaluate the cause for failures, since compressive stresses would not be expected to initiate fatigue cracks.

4.3.1.3 Dynamic Loads Due to Impact

When a wheel passes over a joint, the wheel load causes the rail joint to dip, and the wheel impacts the run-on rail. Investigations conducted by the British Railways indicate that dipped rail joints, either by deflection or by wear, constitute the most severe class of readily discernible vertical track irregularities [4-12].

From a simple analysis assuming (a) perfect impact of the wheel with the run-on rail, (b) symmetric profile of the running surface at the joint, i.e., no end batter, and (c) that the joint and the wheel can be characterized by a simple spring-mass system, the dynamic force, P , developed can be expressed [4-13] as

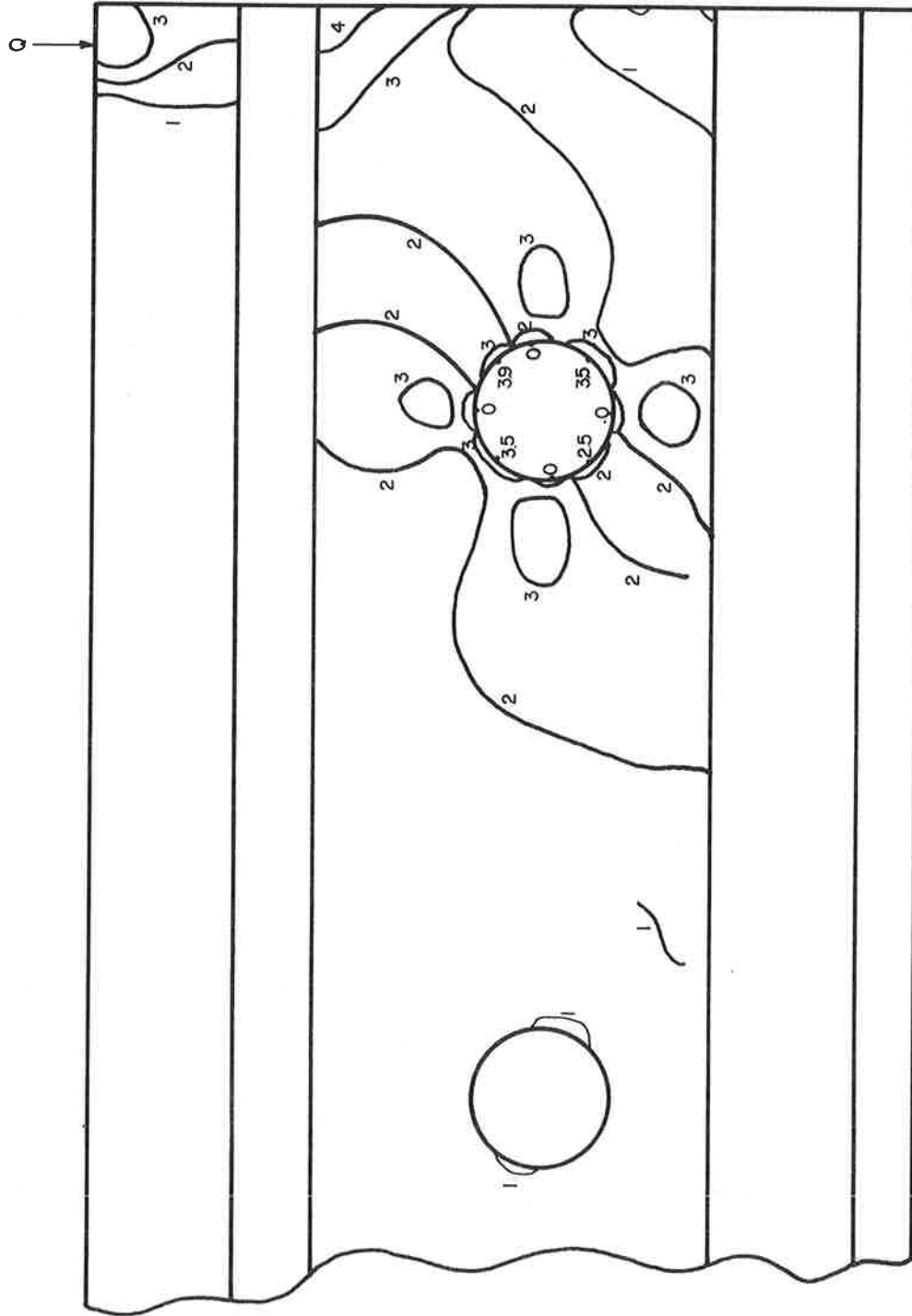


FIGURE 4-9. SKETCH OF FRINGE ORDERS ON PHOTOELASTIC MODEL OF RAIL END. FRINGE CONSTANT IS 160 PSI/FRINGE, THE LOAD Q IS 130.9 LB

$$P = P_o + 2\alpha V \sqrt{\frac{K_R W}{g}} \quad (4-7)$$

where

- P_o = the static wheel load
- α = slope of the rail at the joint (See Equation 4-3)
- V = velocity of the vehicle
- K_R = effective track stiffness at joint
- g = gravitational constant
- W = unsprung weight.

The values of K_R are obtained by using the different joint deflections obtained under known static loads. Typical values for K_R are 100,000 lbs/in. to 500,000 lbs/in. Values of W are usually derived by adding the total weight of wheelset and axle boxes to a portion of the weight of springs, linkages, and traction motor (if axle-hung), and dividing by two. This assumes that the vehicle secondary suspension is very much softer than the wheel disk and the track, and that the suspension characteristics will exert only a minor influence on the effective unsprung weight.

Although more sophisticated analyses have been performed [4-14], the simplified analysis has been shown to give good agreement with experimental tests for wheels with negligible flexibility and with low vehicle velocities (in the literature for $V < 49$ mph). When the flexibility of the wheels cannot be neglected, or when high vehicle velocities are expected, the more refined model should be used. At higher vehicle velocities the wheel leaves the track and free falls across the dipped or battered rail ends. The dynamic load from this action does not increase as rapidly as predicted by Equation (4-7).

The impact of the wheels with the run-on rail has been shown to initiate oscillatory motion of the rail joint and the stresses can reverse from compression to tension. In the case of a compromise joint used to join 130-pound and 140-pound rail, the oscillatory motion was found [4-15] to occur at 330 Hz as shown in Figure 4-10. This reference does not indicate where on the rail these stresses were measured. No measured data on the magnitude of the dynamic stresses at rail bolt holes or the effects of various track parameters (tie spacing, rail size, joint-bar size, foundation modulus) were found in the literature.

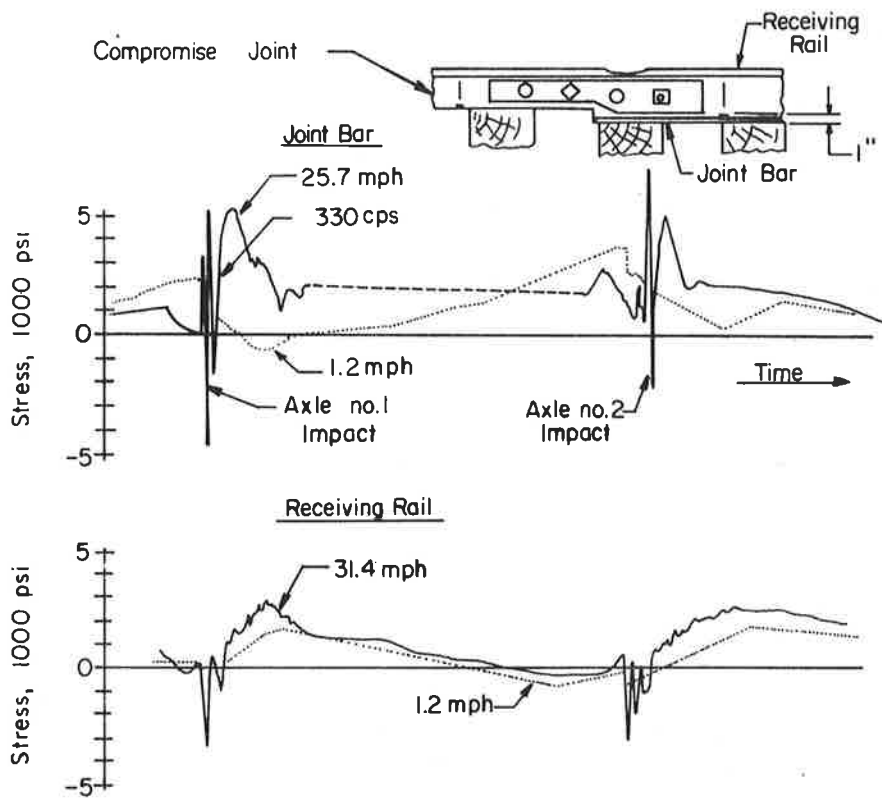


FIGURE 4-10. JOINT BAR AND RECEIVING RAIL IMPACT-LOAD COMPARISON AT LOW AND HIGH SPEED, COMPROMISE JOINT [4-15]

In order to further evaluate the factors which affect joint performance, the following research tasks are recommended:

- (1) Determine a statistical description of joint loading using instrumented joints under train traffic with new track construction. Use this loading to evaluate the performance of current joint configurations using controlled laboratory tests. This evaluation should include the effect of bolt preload on rail deflection, contact surface wear, joint stresses, and longitudinal slip force.
- (2) Make a series of model or full scale studies to better define the interaction between the rail and joint bars.
- (3) Develop and evaluate modified joint design concepts for improving joint life. Concepts to be considered should include:
 - (a) Alternate rail support methods such as reduced tie spacing.
 - (b) The use of wear resistant inserts or coatings such as ceramics and epoxies or changes in joint bar metallurgy to reduce the wear rate at contact surfaces.
 - (c) A modification of the geometry of the joint bar contact surfaces to improve the stress distribution and reduce wear.
- (4) New commercial designs of insulated and standard joints that promise improved life should be evaluated thoroughly and quickly so their evaluation can be made available to the railroad and rapid transit industries as early as possible. There are several installations of new joints in service now where appropriate instrumentation and a methodical reporting of their performance would provide valuable data.

4.4 RAIL WEAR AND LUBRICATION

The frequent negotiation of small radius curves is another example of how the rail rapid transit operation differs considerably from railroad operations. Minimum curve radii of about 90 feet are used in the older subway lines, and even the newer constructions have curve radii as short as 150 to 200 feet. The guidance forces for negotiating these short radius curves result almost entirely from contact between the wheel flanges and the sides of the rail, and this contact is partly responsible for the objectionable wheel squeal noise and for a very high rate of wear on both the gauge side of the outer rails and the wheels.

The importance of rail wear on curves is demonstrated by the need to replace the outside rails as frequently as every 6 months at one 90-foot radius curve on the NYCTA. However, 6 to 9 years appears to be an average rail life for curves compared to a 20 to 40 year life on tangent track [4-16]. The criteria for rail replacement on most properties is an allowable sidewear or headwear of $5/8$ to $3/4$ inches.

In order to reduce rail wear on curves, restraining rails are usually positioned with a flangeway clearance of $1-3/4$ to 2 inches inside the inner (low) running rail so that the restraining rail contacts the back side of the wheel flange. In this way the restraining rail shares the lateral force required to negotiate a curve with the outer (high) running rail. Criteria for the use of restraining rails varies from all curves with radii less than 2600 feet for the Toronto system to all curves of less than 300 feet radius for the Chicago system [4-16].

Similar criteria are used for locating rail lubricators to lubricate the sides of the restraining rail and the outer running rail. The primary reason cited by the operating properties for lubricating rails is to reduce wheel squeal on curves, but lubrication also helps to reduce rail wear as discussed in Section 3.2.2.2. Rail lubricating equipment has been designed for railroad use, and several of the persons interviewed indicated lubricators were poorly designed and require considerable maintenance. One of the most frequent problems is that excessive lubrication applied to the side of the rail gets on the running surface. This reduces the adhesion needed for traction and braking and causes signalling problems.

In the design of a rail joint against fatigue, the effect of two or three cycles of reversed stress due to each expected wheel impact should be included. In the absence of any dynamic stress analysis of rail joints, it is not possible to exactly predict the stresses at the bolt holes. Until such analyses are available, it would appear reasonable to assume that the stresses at the bolt holes are cyclic in nature, with an absolute magnitude equal to the stress induced by the dynamic load of Equation (4-7). To calculate the stress at the bolt hole, the dynamic load is assumed to be applied statically at the end of the rail. The stress concentration factor K_{θ} is then applied to the resulting transverse shearing stress at the hole.

4.3.2 Summary of Conclusions and Recommendations

The major problems with standard bolted rail joints are caused by the inability of bolted joint bars to transmit the wheel loads without incurring relative motion at the contact surfaces between the rail and the joint bars. This relative motion is responsible for wear, and the low angles of the tapered contact surfaces used for a wedging effect amplify the wear displacement by as much as 16:1 when it is resolved into a horizontal motion along the bolt axis. The compliance of even coil spring washers is insufficient to maintain a high bolt tension for very long under these conditions. The reduced bolt loads lead to a rapidly increasing rate of degradation of the joint and the support capability of the ties and ballast near the joint.

Increasing bolt tension sufficiently so that the wheel loads are transmitted by shear without relative motion between the contact surfaces should substantially reduce the wear rate. However, further analysis and tests are needed to determine the minimum bolt tension required for specific joints and the resulting increase in longitudinal rail force required to activate the joint to relieve thermal loads. This function of permitting motion between the rail ends conflicts with the need for reducing wear at the contact surfaces, but a limited number of thermal movements under higher contact stresses may not be an insurmountable wear problem.

Furthermore, there are considerable differences in opinion regarding what is the best lubricant, and these suggestions include solid lubricants, greases, and water-mist.

Although there are several possibilities for improving rail wear on curves and reducing noise, the negotiation of relatively short radius curves is such an important requirement for the rail rapid transit industry that improvements in vehicle guidance should be considered. It is clear that flange guidance is relied upon entirely by the transit systems in Chicago, Cleveland, and San Francisco where cylindrical wheel treads are used and the 20:1 and 40:1 tapered wheel profiles used by the other systems reflect railroad practice and are of little value for negotiating curves having radii less than about 3000 feet. The British Railways is doing considerable work on developing wheel profiles which provide the primary guidance forces for negotiating curves as tight as a 400 foot radius without flange contact for their Advanced Passenger Train (APT); but, here again, the minimum curve radius requirement is much less severe than it is for a rapid transit system. It certainly appears that the development of improved truck designs for rail rapid transit vehicles would be a rewarding achievement contributing to improved ride quality, reduced noise, higher average train speeds and reduced vehicle and track maintenance.

4.4.1 Technical Evaluation of Rail Wear and Lubrication

Rail wear has a number of characteristics including abrasion, plastic deformation, corrosive wear, and surface cracking or crazing [4-17]. By far, the most severe wear occurs on the gauge side of the high rail on curved track (lateral wear), and this is the result of sliding contact between the wheel flange and the rail. Wear of the top surface of the track (vertical wear) also occurs on curves as well as on tangent track. This vertical wear results from the inherent combined sliding-rolling condition which exists at the elastic contact between the wheel and the rail.

In general, wear results in a change in rail contour [4-18] and a change in the wheel-rail contact conditions. Wear on tangent track can be accelerated when corrosion conditions are optimum and a corrosion-wear process takes place.

Vertical rail wear on tangent track is subject to considerable variation. Wear measurements made on British railroads show a range between 0.010 inches per million axles to over 0.100 inches per million [4-18]. Corrosion appears to be a large factor in the data scatter. For instance, rail wear tends to be higher than average in deep cuts where vegetation promotes humid conditions, and it is usually lowest in tunnels on electric lines. A comparison between vertical rail wear value for U.S. and British railroads shows U.S. specific wear values to be much lower than British. This is attributed to the higher carbon content of U.S. rail steel and the higher relative humidity of the atmosphere in Britain [4-18].

The condition of wear combined with corrosion has long been recognized in the field of wear science as an accelerated wear process. The removal of corrosion products by the wear process increases the corrosion rate owing to the loss of surface protection. In addition, the corrosion process weakens surface layers and increases the rate of material removal by abrasion.

4.4.1.1 Rail Wear Analysis

It has been observed by Reynolds [4-19] that the slip occurring between the wheels and rail during rolling is mainly responsible for wear and that plastic deformation is also involved in changes which occur in rail contour. Russian observations indicate that variation of the rail section was 70-75 percent wear (material removal) and 25-30 percent plastic deformation [4-20].

Attempts have been made to develop analytical approaches to predict vertical rail wear. One theory assumes that wear is proportional to the frictional energy resulting from wheel slip. Another assumes that rail wear is a linear function of total distance of sliding and that a wear coefficient can be derived from wear measurements [4-21]. Plastic deformation is accounted for by the use of coefficients in the wear formula. Experimental work in Germany has been directed at using wear data from a bench type wear test (pin-on-disk) to develop analytical techniques for predicting rail wear.

Wear science has developed a general relationship for wear resulting from sliding contact,

$$d = \frac{K WL}{P_m} \quad (4-8)$$

where

d = wear depth

W = contact pressure

L = sliding distance

P_m = compressive yield strength

K = wear coefficient

This relationship can be used to compare a variety of materials in various sliding wear conditions by means of a wear coefficient derived from laboratory tests which simulate operating conditions such as surface chemistry and temperature. For estimating the side wear of a rail head on a curve, sliding distance L should be changed to total number of wheel passes and contact pressure can be related to the average lateral flange force (assuming the contact geometry is the same for all wheels). The yield properties P_m of the rail steel would be a function of the amount of frictional heating in the contact area, and it is difficult to evaluate this effect.

Another approach for developing an equation for estimating rail wear is based on the concept that wear is the result of surface plastic deformation resulting from ploughing of high points on one surface (wheel) through the material of the mating surface (rail). The wear would then be a function of the energy expended in deforming and separating material from the surface. Glagolev [4-22] suggests that the work of friction forces leads to plastic alteration of the surface layer of a rigid body. His experiments show that the ratio between plastic deformation and wear is approximately constant. He assumes then, that rail wear can be related to frictional work. An equation of the following form might be developed from this approach:

$$d = \alpha (fNV)^n \quad (4-8a)$$

where

d = wear in inches penetration
 α = proportionality constant
f = friction coefficient
N = normal contact force
v = sliding velocity
n = coefficient (probably between 0.5 and 1.0).

Some of the elements of these wear theories appear in the wear equations reviewed in Section 3.2.2.2. The Couard method is based on an equation of the form

$$W_s = 1.6D_c(1 + 0.1U_b + 0.23g^{1.7}) 5 \times 10^{-6} BV + 0.0025, \quad (4-9)$$

where

W_s = side head wear, inches for 140 lb rail
B = load, MGT/yr
 U_b = unbalanced upper elevation, inches
V = speed, mph
g = track gradient
 D_c = degree of curve (degrees).

However, several significant factors associated with rail conditions which do not appear in Equation (4-9) are rail steel composition, environment (dry or wet, corrosive, abrasive), and lubrication. Data reported in Section 3.2.2.2 shows that the currently available methods for estimating rail wear on curves are not entirely satisfactory. However, an improved procedure could be developed using an empirical relation similar to the Couard formula and modifying the results with corrective factors. This empirical relation should be verified and modified based on data from wear test experiments on typical wheel and rail steels. The following procedure is suggested:

- (1) Establish a maximum allowable wear (in./year)
- (2) Establish a base wear value for a given gross weight/year traffic density moving at a given average velocity for a standard rail steel (≈ 0.5 percent C)
- (3) Modify these results for the degree of curvature
- (4) Multiply by an environmental factor

- (5) If the predicted wear is too high, estimate the amount of wear reduction that could be obtained by alloying using the relation that wear is reduced about 8 percent for every 0.1 percent increase in carbon or carbon equivalent. Carbon equivalent equals percent carbon plus $1/3$ (percent manganese plus percent chromium).
- (6) Apply a factor for lubrication if further reduction in wear is desired or if alloy steel is undesirable. Wear life can be increased considerably by lubrication. (See Table 3-5)

Effect of Rail Materials. Rail wear can be reduced on curves by the use of heat treated or alloy rail steel. Most rapid transit properties use this technique, and a number of alloys have been evaluated in the U.S. and abroad.

The selection of a rail alloy requires some compromise between the high hardness needed for wear resistance and the toughness needed to reduce the chance of brittle fracture. There is much controversy concerning criteria for selection of the best rail steel alloys. In fact, there is a "general lack of data to aid in the selection of the correct rail for given circumstances" [4-23]. It is possible to increase wear resistance and toughness with proper alloy balance. Steel cleanliness is also an important factor that is overlooked in the attempt to make low-cost rails.

In the USSR, it is reported [4-24] that chromium steels (0.5 - 1 percent chromium) having a carbon + $1/4$ manganese content exceeding 0.88 percent exhibit less wear, show less shelling failure, have a reduced tendency for corrugations and can be made straighter. In addition, experience has shown that with increasing carbon content, the phosphorous content must be kept low (less than 0.04) to maintain toughness.

As far back as 1911, the effect of chromium-nickel, manganese and titanium additions to steel on rail wear on curves was being investigated [4-25]. Although the results were quite variable, it was apparent then that the manganese steels consistently showed superior wear resistance. The abrasion resistance of manganese steels is also well known in the mining industry. In a British report, a special high-manganese steel [4-26]

having 13 percent manganese was found appropriate for very heavy wear conditions, particularly side cutting. However, this steel has high notch sensitivity and cannot be welded to standard rail.

Other alloy steels investigated have not shown as consistently good wear resistance as the high manganese steels. For instance, chromium-nickel steels show a tendency for breakage. High silicon steels (0.7 - 0.8 carbon, 0.14 silicon) have been reported promising [4-27], but not enough data exists for a definite conclusion. Currently, it appears that if a special alloy for wear resistance is desirable, the following composition would be acceptable.

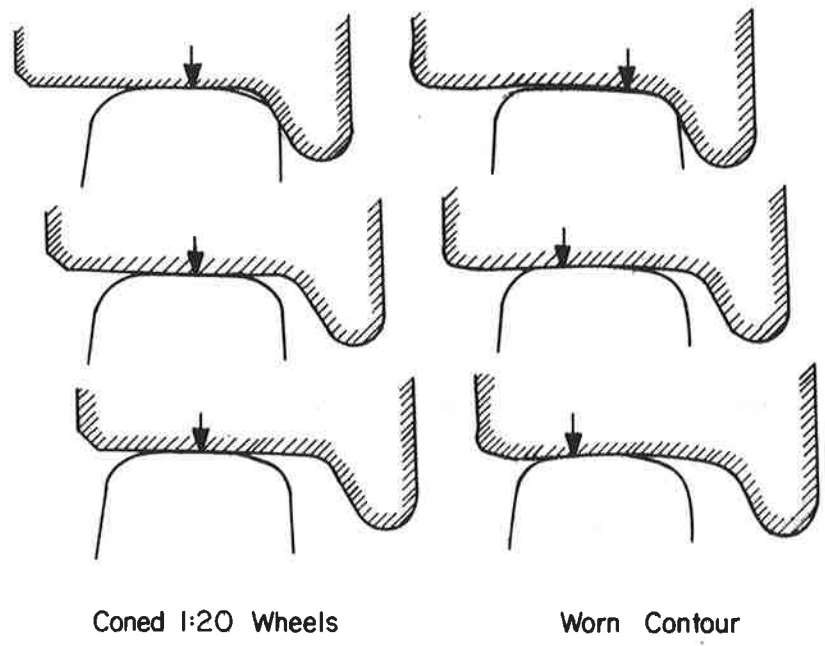
carbon = 0.5 to 0.6 percent

chromium = 0.5 to 1.0 percent

manganese = 1.0 to 2.0 percent

Heat-treatment of carbon steel rails has been the subject of investigation by U.S. railroads for some time. The most practical way used to heat-treat rails is flame hardening. This produces a case hardness of about 35 R_c in 0.6 - 0.7 percent carbon rail steel, and provides a hard surface that is highly resistant to wear and plastic deformation while maintaining a tough, fracture-resistant core. Evaluation of track performance has demonstrated that service life on curves can sometimes be increased by a factor of 6 when heat-treated rails are used to replace conventional non-heat-treated rails [4-28].

Effects of Wheel Contouring. One method of reducing wheel wear is "wheel contouring". In 1913, Heumann [4-29] introduced the idea of designing wheel surfaces in the shape of a worn contour to improve wheel guidance and to reduce both wheel and rail wear. Heumann pointed out what he considered the irrationality of the then prevailing (and still maintained in this country) conical wheel profiles [4-30]. Heumann's wheel profile theoretically contacted the rail at one point only, regardless of lateral position. This geometry demonstrated less wear, lower contact stress, reduced tractive resistance, and improved riding qualities [4-31] over the conventional 2 points of contact coned wheel designs, Figure 4-11.



Coned 1:20 Wheels

Worn Contour

FIGURE 4-11. CONVENTIONAL CONED AND WORN CONTOUR WHEELS

Heumann and his student have published a great number of papers on the subject of wheel contouring [4-32 through 4-41]. The British Railways have found the worn profile to be very effective in reducing wheel wear [4-42]. Performance of the worn contour wheels in Britain also has been reported by King [4-43] and again by Koffman and Bartlett [4-44]. From these investigations, it has been found that after a relatively short running period, a wheel profile which was originally conical becomes hollowed out and worn in the region where it normally contacts the rail head. The wear shape is largely independent of the original profile and the strength of the wheel material. Mueller [4-41] concludes from this that an optimum rail-wheel profile is achieved naturally. He further proposes a wheel profile which combines features from Heumann's profile with these from other worn wheel profiles.

4.4.1.2 Rail Lubricants

Lubricants are used on curves in order to reduce wear and noise caused by sliding contact between the rail and the wheel flange. One important requirement for a rail lubricant is that it stays in place so that it does not contaminate the running surfaces of the rail head and wheels and cause traction and braking problems. Because of this requirement, solid lubricants have been tried in several rail lubrication applications. Problems with the application and replenishment of solid film lubricants, however, have made this form of lubrication unpopular on the railroads.

The most popular method for rail lubrication is the rail lubricator, a stationary dispensing device actuated by the passage of car wheels over a treadle bar. This assembly consists of a trackside grease reservoir, internal pump, hose lines to the rail and rail mounted wiper bars. As each wheel activates the lubricator, a metered amount of grease is applied to the wheel flange by a pressurized system fed by a gear pump.

Most rail lubricant greases have a calcium soap mineral oil base with a graphite filler. The greases are formulated to resist wash out by water, to be pumpable at minimum expected trackside temperatures, have a high dropping point to resist bleeding and be resistant to separation and

decomposition over long storage periods in the temperature range expected for the geographical location. A number of commercial rail and flange lubricants that are available include:

| <u>Lubricant</u> | <u>Graphite Content</u> |
|---------------------------------|---|
| Texaco 904 Grease | 11.5 percent |
| Texaco 975 Rail Curve Grease EP | 11.0 percent; E.P. additive |
| Mobil Curve Grease 1105 | 12.0 percent |
| Fiske's Curve Grease No. 15 | 12.0 percent |
| Fiske's Curve Grease No. 3 | 12.0 percent; stiffer than Fiske's No. 15 |
| Citgo Railroad Curve Grease | 11.0 percent |

All of these greases are calcium soap lubricants. Although this type of grease is inexpensive and resistant to mixing with water, calcium soap greases separate or melt at relatively low temperatures and could offer some problems in long term storage at temperatures above 150°F. Lithium soap greases are more resistant to thermal softening and separation.

Another formulation characteristic common to all of the listed greases is fortification with graphite. The graphite is included as an anti-wear agent capable of sustaining heavy contact stress. Unfortunately, graphite can separate out from suspension in the grease, and it often plugs lubricators or the lines leading from the reservoir to the lubricators.

There is no doubt that grease lubrication is effective in reducing rail and flange wear on curves. However, it should be used as sparingly as possible--especially in areas where it can collect abrasive particles or where it can be carried down the track and foul electrical switch and signal equipment. There have been many effective greases developed in recent years by the military and aerospace industry, and some of their properties might significantly improve the performance of rail lubrication.

Optimum distribution of grease to the rail areas requiring lubrication requires correct placement of lubricators and selection of the amount to be metered for each wheel passage. Lubricator spacing is based on a factor known as "the length of effective carry". Although it is realized that this length is determined mostly by the wheel flange pressure against the rail

head, it has been recognized [4-45] that each lubricator location is a separate problem and no adequate procedures are available to relate lubricator spacing to curve geometry, operating speed, etc.

Temperature can also have a significant effect on rail lubrication since it influences the flow rate of grease through the supply lines. Measurements made on a lubricator with its reservoir temperature controlled have shown that the rate of delivery can vary by a factor of 5 [4-46] over the temperature range of -40°F to 70°F . Experiments with various greases in a rail lubricator indicate that grease delivery rates do vary considerably--not only for various temperature levels but also for rail greases obtained from different suppliers. Therefore, it is evident that the establishment of a fixed setting on a curve lubricator is virtually impossible--especially if it must operate over a wide temperature range. The development of an improved rail lubricator would be a valuable asset to the rapid transit industry.

Solid lubricants have been applied to wheel flanges of locomotives by means of solid sticks of lubricant pressed against the flange under spring pressure. When the stick wears away it has to be replaced. Tests have shown that there is enough transfer of solid lubricant from the wheel flange to influence rail wear. Limited experiments with rapid transit systems [4-47] have been inconclusive. One problem encountered was difficulty in mounting dry lube sticks. Experiments with smearing a slurry of MoS_2 on rails for the Chicago Transit System showed some limited success in reducing noise, but the effect was short lived. The average life of MoS_2 sticks has been quoted as only 2,000 miles by the Reading Railroad [4-48].

It is obvious that solid lubricants have some decided advantages to offer for rail curve lubrication. They provide the resistance to penetration by high contact stress intended by the addition of graphite to grease; they do not collect sand and dust; they do not creep onto the rail running surfaces; and they are potentially more controllable as to the amount applied to a rail or flange surface irrespective of temperature, wheel speed, pressure, etc. It is also obvious that more development work must be done to improve the application method before these advantages can be fully utilized.

4.4.2 Summary of Conclusions and Recommendations

The noise and wear of both wheels and rails that results from operating rapid transit vehicles on tight curves is a high priority problem. The negotiation of short radius curves is such an important requirement for the rail rapid transit industry that the development of improved vehicle design concepts to eliminate guidance by flange contact should be a high priority objective. The wear and noise problems on curves are so intimately related to flange guidance that a relatively major change in vehicle design appears justified. This would include the development of wheel profiles based on modern techniques for contact stress analysis to optimize the profile geometry for minimum wear and maximum flange-free guidance. Vehicle truck designs must also be refined to achieve improved curve negotiation while maintaining dynamic stability (freedom from truck hunting).

Current methods available for predicting rail wear on curves are inadequate and do not include the important parameters with sufficient accuracy to evaluate the effect of design changes to the truck or train. Several recommendations related to wear prediction and the reduction of wear include:

- (1) Improved analytical procedures for predicting rail wear should include the wheel/rail contact stresses, traffic density, frictional energy, curve conditions, rail material, vehicle characteristics, operating speed, environmental conditions and lubrication.
- (2) Wear data obtained from a simulated wheel-rail contact condition should be used to develop improved wear prediction techniques and evaluate their accuracy.
- (3) The lubricants now used for curve lubrication do not reflect recent progress in lubrication science. A lubricant evaluation program combining field and laboratory measurements is recommended to determine the properties for an improved lubricant.
- (4) Wheel and rail lubricators are not sufficiently reliable for rapid transit use. Design improvements are needed to maintain constant lubricant delivery rates for a wide range of temperatures and lubricant properties.

- (5) Solid lubricants have important advantages, but improved application procedures are needed to make solid lubricants economically attractive.

4.5 RAIL FASTENERS

Rail fasteners are considered to be a major source of track maintenance problems for existing systems. Their design is also one of the most important factors for new track construction where the rail is being fastened directly to concrete in the form of concrete ties, or to concrete slabs in subways, on bridges, or at grade level.

The conventional rail spike used to fasten rail to wood ties on ballast or to wood stub ties embedded in concrete in subways has the important advantage of being easy to install and remove. The primary task of the spike is to maintain the lateral position of the rail base in constructions where the rail is laid directly on the tie, or to maintain the lateral position of a tie plate when these are used. The spikes are not expected to provide vertical restraint and, in fact, the AREA Manual [4-49] specifies that there should be a gap of 1/8 to 3/16 inches between the under side of the head of the spike and the top of the rail base when the spikes are installed. Satisfying this requirement prevents the spike head from being deformed by being driven against the rail base and it also allows the rail a free "uplift" as a train wheel approaches without imposing large tension forces on the spikes. It would not be surprising if the specified gap were based on experience where the spikes soon became raised by this amount if they were initially installed flush against the rail base.

Spikes used with wood ties do become loose under traffic and aging of the tie, and there is a limit to how many times the rail can be moved by plugging the spike holes and re-spiking. However, the rail spike has been a relatively reliable fastener, and it has been difficult to include many of its advantageous features in rail fasteners designed for direct fixation or concrete ties. The most frequent complaints from track design and maintenance personnel about currently available rail fasteners used for these applications are:

- (a) Materials used for rail pads and bolt collars rapidly lose their electrical insulation properties (formerly provided by the wood tie).

- (b) Fasteners need lateral adjustment capability for initial alignment, and gage adjustment to compensate for rail sidewear on curves.
- (c) Fastener bolts rapidly become loose under traffic, and the method used to attach fasteners to the concrete are frequently inadequate.
- (d) Fasteners are needed to locate restraining rail and guard rails, which is a unique requirement with the rapid transit industry.
- (e) Fasteners utilizing fixed studs protruding from the concrete make it difficult to replace or swap rails.
- (f) Fasteners providing sufficient longitudinal restraint to replace rail anchors make it necessary to loosen a large number of fasteners in order to adjust the rail for thermal expansion.

A more detailed evaluation of rail fastener design requirements and performance is given in Section 3.2.3. The important conclusions and recommendations from this are included in the following section.

4.5.1 Summary of Conclusions and Recommendations

The design requirements for improved rail fasteners are quite complex, and the development of rail fasteners which combine both the practical requirements and the technical requirements in a fastener design that is economical and durable is a challenge. Fastener specifications have been developed which include a series of static and dynamic loading tests for fastener evaluation. For example, fastener repeated load tests are currently based on average expected wheel loads and include the equivalent of 6 million wheel passages. This represents a service life of only about 6 years using the 12.2 MGT/year traffic density assumed for the WMATA track design (Table 3-7), but these repeated load tests are not intended to simulate service conditions with sufficient accuracy for establishing service life.

It is apparent that the analysis of rail fastener loads discussed in Section 3.2.3 can provide basic design requirements, but a better definition of fastener loading in service is needed to establish fatigue loading and to

provide realistic input data for accelerated life tests on prototype fasteners. For example, Figure 4-12 shows a servo controlled machine that was designed at Battelle-Columbus to reproduce the rail motions and loading for evaluating rail anchors. The control inputs for this machine were obtained from field measurements of anchor loading, tie plate loading and rail deflections relative to the tie plate and tie. This provided a very realistic reproduction of the complex loading caused by train wheels, and it represented a substantial improvement in the capability for developing and evaluating production and prototype designs in the laboratory.

A machine that is similar in principal, but which would be considerably more complex in design, is needed to allow accelerated life testing of rail fasteners under conditions representing actual transit track service. This machine would have to include vertical, lateral and longitudinal loads at the fastener and the rocking motion of the rail caused by wheel passage. The use of a rolling load machine, where the loading from actuators is transmitted through a rolling wheel to the rails should also be considered as a way to simulate the complex loading condition that would be determined from field measurements of fastener loads.

4.6 RAIL CORRUGATION

It was notable that rail corrugation, a wavy wear pattern which develops on the running surface of the rail, was mentioned as a track problem by all of the properties that were interviewed. Rail corrugations are responsible for causing a "roaring" noise and annoying vibration in both the vehicle and the ground adjacent to the track. It is also generally acknowledged that the vibration from rail corrugations increases wheel/rail dynamic forces and contributes to increased wear and maintenance of vehicle wheels and truck mounted equipment.

Complaints due to excessive noise and vibration are the justification for some properties to replace rail, while other properties periodically use rail grinding equipment to remove the corrugations. However, the experience of the Chicago Transit Authority has been that corrugations with a depth of

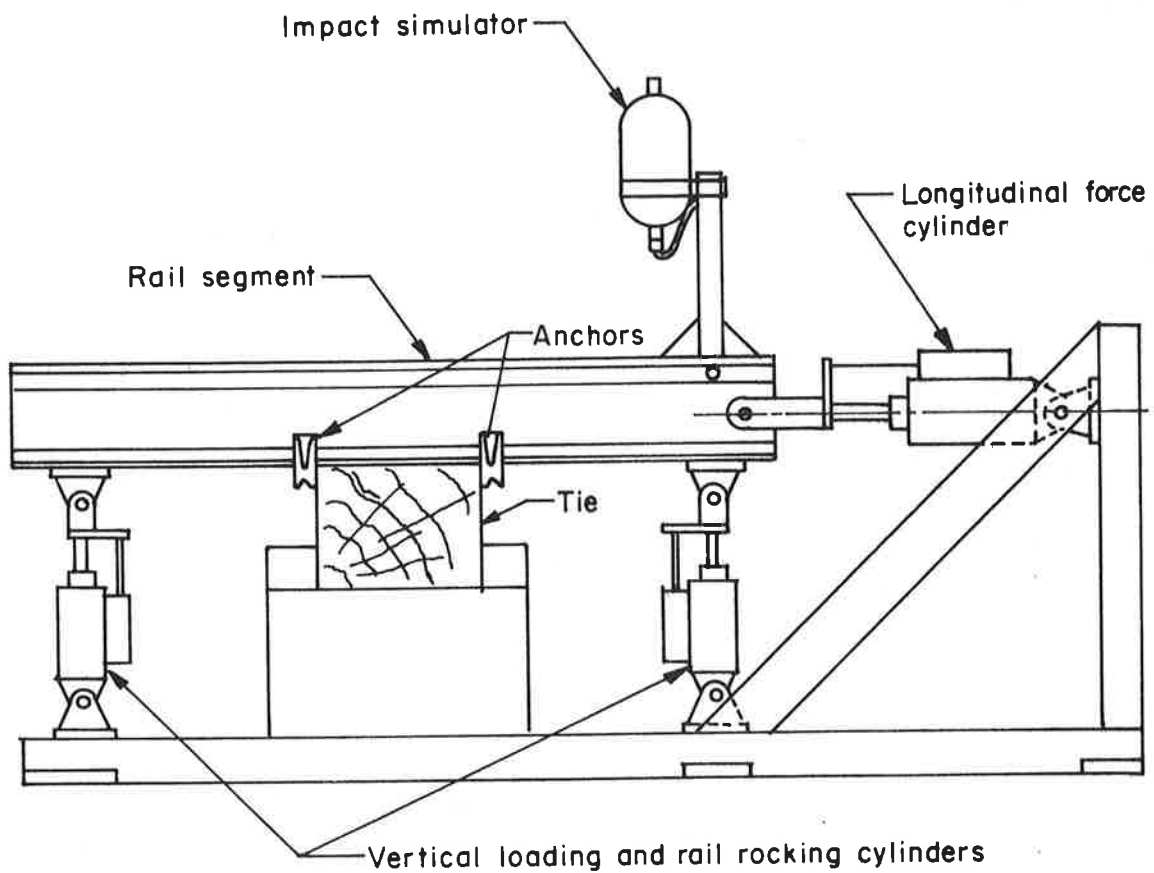


FIGURE 4-12. SERVOCONTROLLED LABORATORY MACHINE TO PRODUCE BOTH VERTICAL LOADING AND LONGITUDINAL ROCKING OF THE RAIL, FOR EVALUATING RAIL ANCHORS

only 1 to 2 mils produce noticeable noise and vibration, and these reoccur as soon as 6 months after the rail has been ground.

It was interesting that there is considerable diversity of opinion about both the origin and the locations on the track where corrugations are most prevalent. Curves are generally acknowledged as the most severe locations and the low rail is often cited as being worse than the high rail, but the high rail does corrugate. The braking areas at station approaches are also frequently cited as locations for severe corrugation. However, on the basis of several similar interviews one can conclude that corrugations occur almost everywhere. This includes both subway and at-grade track, long sections of welded rail where the effect of joints is eliminated, and on systems where there is a considerable variation in vehicles operating on the same track, including light rail and rapid transit vehicles having different suspensions and wheel profiles.

While rail corrugations are recognized as an important track problem, there are no provisions in the design procedures for either track or rail vehicles that pertain to predicting the initiation of, or reducing the occurrence of, rail corrugations. However, some relatively recent theoretical research on contact vibrations may provide the basis for identifying the mechanisms for the initiation and development of corrugations and the role of vehicle and track elements--the first step needed to develop designs to eliminate corrugation.

4.6.1 Technical Evaluation

Rail corrugation is a form of surface wear characterized by bright, hard spots, and the rail surface is deformed to take on a wavy structure as shown in Figure 4-13. The corrugation wave length in railroad and transit track has been found to vary between 1-1/2 to 10 inches [4-50, 4-51]. The phenomenon of corrugation has also been observed in other areas of engineering such as gear teeth [4-52], ball-bearings [4-53], and earth roads [4-54].

The causes and prevention of corrugation have been investigated both here and abroad, and studies of the problem have been reported as early as 1924 [4-55]. In 1940, the AREA Committee on Rail started a long-term program,



FIGURE 4-13. TYPICAL RAIL CORRUGATIONS

and some of the results are contained in Volume 46 (1945) of the Proceedings of the AREA. This volume presents 15 papers on rail corrugation by railroad engineers across the United States and Australia. It is interesting to note that while some papers agreed on one or two points, the total result was about 15 different opinions as to the cause of rail corrugations. This investigation was discontinued in 1946 because it was concluded that corrugation was not a safety problem since it does not lead to rail fractures.

In 1945, it was reported by Cramer [4-56] that a major cause of corrugation in rail was due to slippage. Such slippage has been recently theorized [4-57] to introduce a surface phase change phenomenon (by frictional heating) by which a hard, abrasion-resistant phase (untempered martensite) is produced on the track surface. This process depends on the frictional temperature exceeding the transformation temperature, which is about 1300 °F for steel.

A high coefficient of friction and a low thermal diffusivity tend to increase the tendency to form surface martensite. Although martensite formation in rail surfaces has been investigated [4-58], the true relationship between the formation of martensite and the development, or growth, of corrugation is still unclear. It is quite likely that any phase transformation occurring on the corrugation peaks are accelerating factors in the corrugation process, rather than being a necessary condition to initiate corrugations.

Corrugation formation has been attributed to steel properties, rail defects, rail joints, vertical oscillation of rail or wheels, and wheel set hunting [4-58,4-59]. There is however, increasing experimental and analytical support [4-60] for the belief that corrugation is a contact phenomenon in which deterioration of the rail surface results from dynamic stresses developed during vibratory contact. As a result of work by Carson and Johnson [4-61] sponsored by the British Railway Board (1971), corrugations were spontaneously generated on dry surfaces under laboratory conditions. These corrugations were caused by vibrations excited by rolling contact. The principal mode of vibration was that of "contact resonance" in which the disks oscillate on the spring provided by their elasticity in the vicinity of their contact area.

Extending an approach by Gray and Johnson [4-62], Nayak and Tanner [4-63] analytically investigated the free and forced contact vibrations of a railway wheel and a rail due to surface irregularities (roughness). Their

approach accounts for the fact that when a wheel rolls on a rail having a randomly wavy surface, the random waviness represents a displacement input for the wheel and rail with high-frequency ($f > 100\text{Hz}$) spectral content. This displacement input excites the contact resonance of the system, wherein the mass of the wheel and an "equivalent mass" of the rail vibrates on the nonlinear contact spring. It was found in this investigation that loss of contact between the wheel and rail is predicted when the static load is low and the standard deviation of the dynamic contact force is high. Such a condition may form regions of stick slip or initiate wear deformations on the rail surface.

When both the static wheel load and the standard deviation of the dynamic contact force are high, the probability of developing plastic deformations on the rail surface is also high. When these deformations occur in clusters, they cause a significant local change in the rail roughness in precisely that frequency band in which the initial response from the contact resonance was large. The response of a subsequent wheel is, therefore, larger than that of the first one, causing the deformation in a cluster to deepen as well as causing the cluster to elongate. This unstable process rapidly leads to the formation of severe corrugations once it has been initiated.

In the formulation of the Nayak and Tanner approach to the theory of corrugations, no mention is made of tractive forces in the contact region. However, it has been shown by Johnson and Jefferis [4-64] that such surface tractions may significantly influence the geometry of plastic deformations as well as the normal load at which they occur. Surface tractions are also an important mechanism affecting the wear process.

4.6.1.1 Field Observations

During this program, an inspection of corrugated rail was made on the Shaker Heights transit system (Cleveland suburb) in order to obtain some additional, first-hand data to supplement the literature review. The Shaker Heights transit system is reputed to have severe corrugations which are often attributed to the resilient wheels used on the PCC cars (street cars). The PCC cars have only a 5300 pound wheel load (empty car), which is

about 50 percent of the weight of most rapid transit cars. In sections where the PCC cars and the Cleveland Transit cars share the same track, the rail is corrugated badly, whereas corrugations are not a major problem on rail which is only used by the heavier transit cars.

On the Shaker Heights system, rail corrugations were observed on tangent track, on the high and low rails on curves, and on rails in both acceleration and deceleration zones near stations. Visual inspection of the rail showed that fretting and sliding had taken place on the corrugation peaks. Hardness measurements made along the running surface revealed that the hardness varied considerably. In the valleys between high spots, the hardness ranged between 23 R_c and 28 R_c , whereas on the high shiny spots, the hardness was found to range between 32 R_c and 50 R_c . The surface of the high spots, when observed through a 5X magnifier glass, showed areas of local heating (blue to orange discoloration), while the surface of the low valley areas appeared undamaged.

Corrugation wavelengths and rail surface profile measurements were made on severely corrugated areas. The profile measurements were made using a dial indicator attached to a beam which was clamped on the rail, Figure 4-14. Typical corrugation profile measurements are shown in Figure 4-15 and 4-16. It was found that the bright shiny spots observed visually on the rail surface were not always individual corrugation peaks, because the shiny spots are worn areas of sliding that often occur in pairs--one spot on the leading edge and one spot on the trailing edge of a high corrugation plateau. Two examples of this are shown in Figures 4-15 and 4-16.

One of the important conclusions from the contact resonance theory for rail corrugations is that the resonant frequency is relatively constant for a particular rail and wheel combination. If this is true, the corrugation wave length should be directly proportional to vehicle speed. This relationship is shown in Figure 4-17 for several assumed resonant frequencies above 100 Hz.

Measurements of corrugation wave length at Shaker Heights, Figure 4-18 showed that the wave length did vary at locations where the estimated vehicle speed was different. The characteristic frequency was between 106 and 215 Hz, which is reasonable for contact resonant frequencies. Some of the apparent scatter in this data may be due to errors in the estimated vehicle

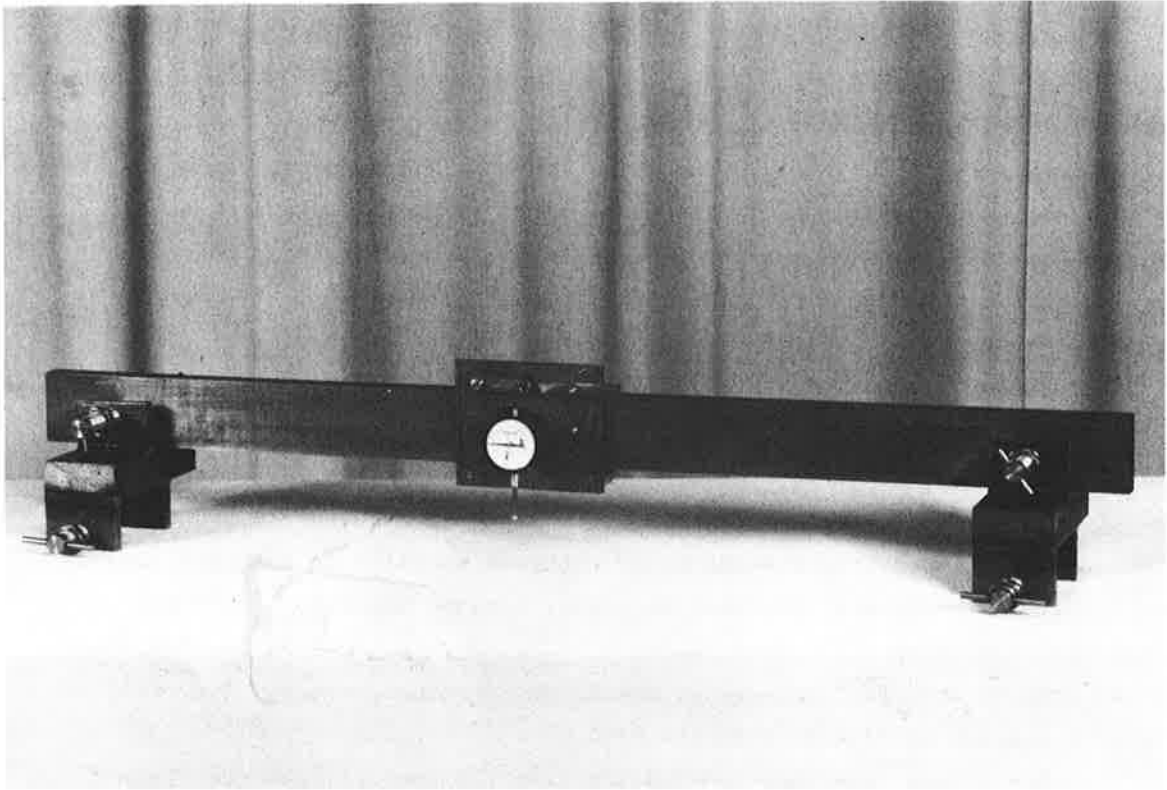


FIGURE 4-14. RAIL PROFILE MEASUREMENT APPARATUS

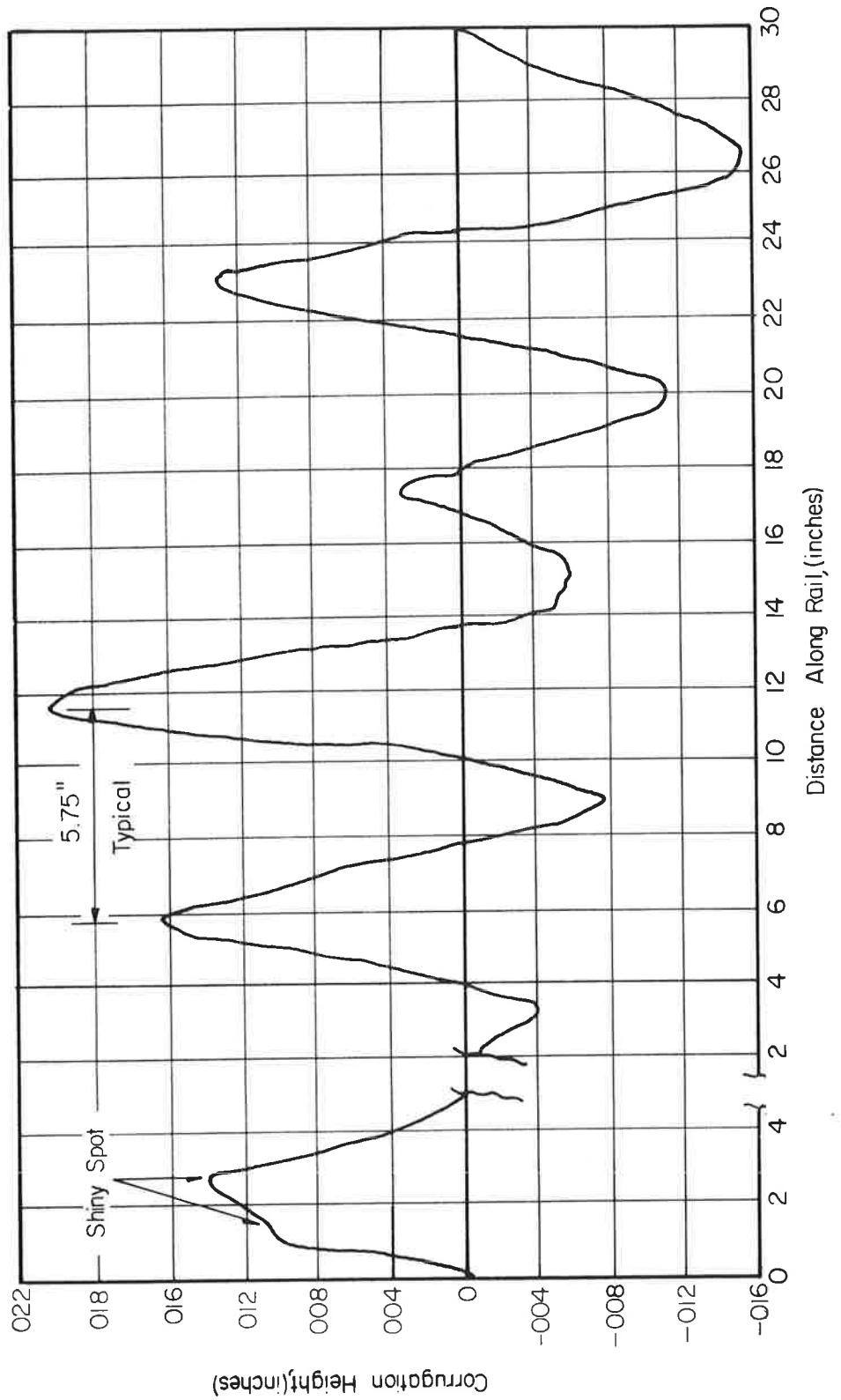


FIGURE 4-15. PROFILE OF TYPICAL CORRUGATIONS ON SHAKER HEIGHTS RAPID TRANSIT LINES. East Bound Track Located East of Lee Station, 35 MPH Region.

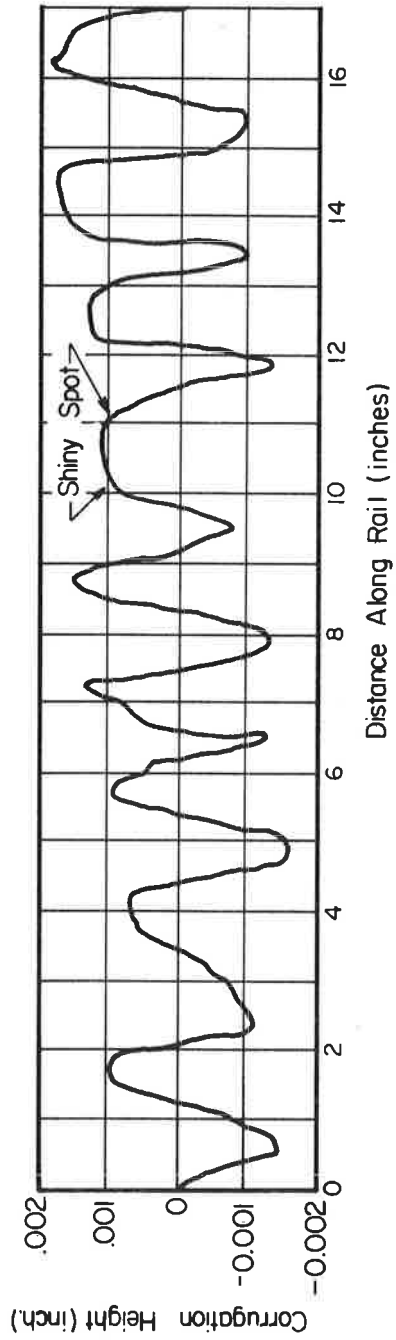


FIGURE 4-16. PROFILE OF CORRUGATIONS ON SHAKER HEIGHTS RAPID TRANSIT LINES.
West Bound Track East of Lee Station, 25-30 MPH.

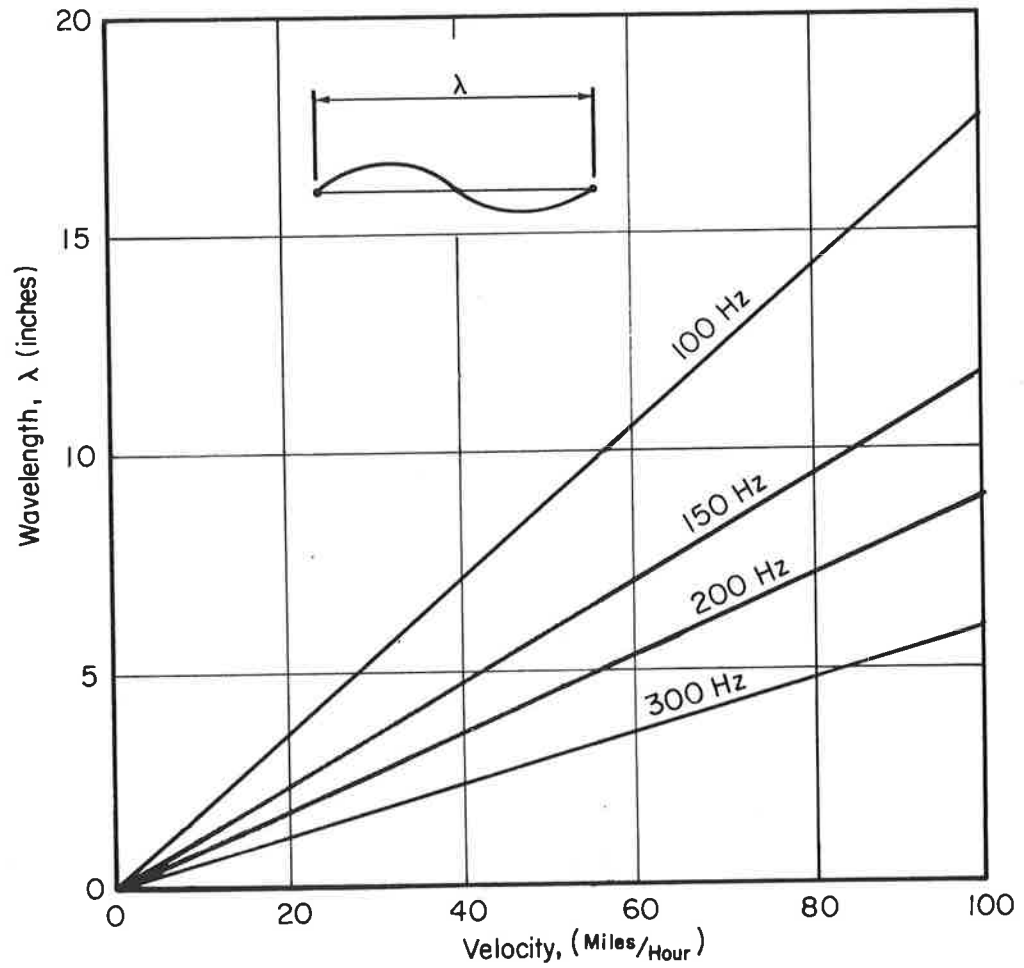


FIGURE 4-17. EFFECT OF TRAIN VELOCITY ON CORRUGATION WAVELENGTH FOR TYPICAL CONTACT RESONANT FREQUENCIES

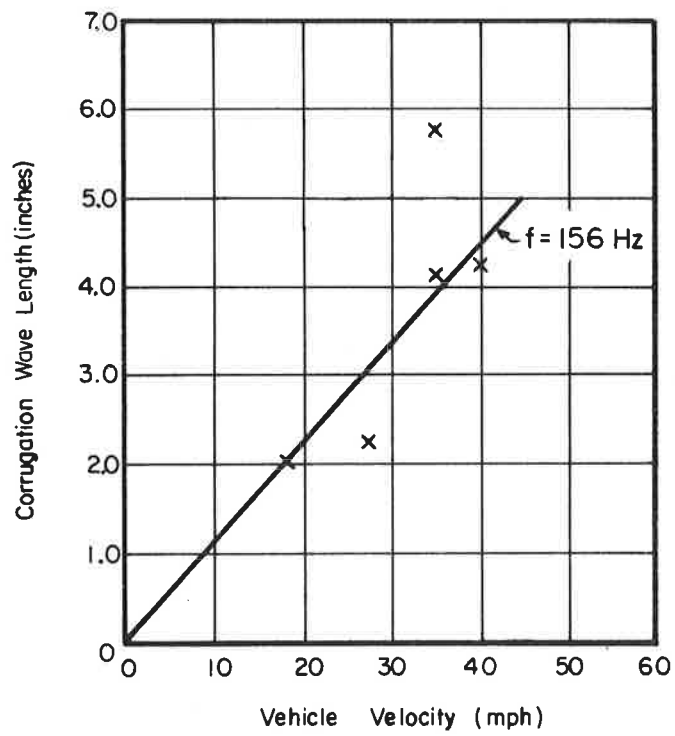


FIGURE 4-18. SUMMARY OF CORRUGATION WAVELENGTH VERSUS ESTIMATED TRAIN SPEED MEASUREMENTS AT SHAKER HEIGHTS

speed and to differences in the effective rail stiffness caused by variations in the contact geometry and/or rail bending flexibility. Some of the rail was badly worn 80-lb rail where the thickness of the rail head was considerably less than that of a new rail.

4.6.2 Summary of Results and Conclusions

Although the contact resonance theory is the most promising model available to explain the initiation and development of corrugations, it is necessary to validate this model before it can be used to define the requirements for reducing or eliminating corrugations by changing track or vehicle design procedures. The contact resonance model developed by Nayak and Tanner is based on determining the conditions required for plastic deformation with purely normal loads, and the effects of surface tractions are not considered. However, data from laboratory tests indicate that corrugations can be formed when the stresses from the normal loads are well below the yield point. Furthermore, the presence of surface tractions can effect both the mechanism of surface wear under reduced normal loading and the mechanism of plastic deformation. Plastic deformation can occur under combined normal and tractive stresses when the normal stresses alone would be below the yield point.

A research program to identify the critical mechanisms for the initiation of corrugation should include:

- (1) An evaluation of the effect of vehicle traffic on rail surface profile (roughness) starting with new track and continuing through the development of a well-defined pattern of corrugation. Track locations should be selected where all traffic consists of identical vehicle design and the operating speed is relatively constant. Track locations should include curves and constant speed tangent track covering both low speeds and high speeds to better identify the relation between vehicle speed and corrugation wavelength. The track should be instrumented sufficiently to monitor all operating parameters which might effect corrugation development.

- (2) A study of the formation of corrugations using controlled laboratory tests to identify the critical parameters and evaluate the effectiveness of design changes to prevent the initiation of corrugations. Determining the combined effect of normal loads and shear loads on the deformation and wear mechanisms should be a major objective of this task.
- (3) Metallurgical analyses of corrugated rail should be made in support of (1) and (2) to identify the role of wear, plastic flow and material phase changes on corrugation development.
- (4) The effectiveness of proposed design changes should be evaluated by full scale demonstration tests on test sections of track in operating transit systems where corrugations are a current problem.

4.7 RAIL FIELD WELDS

Welding is used extensively for many different purposes in constructing and maintaining urban rail transit systems. However, the availability of an effective method of field welding sections of rail together to eliminate bolted rail joints is particularly important because bolted rail joints are such an important source of track-related problems (see Section 4.3). The results from interviews indicated that it is possible to obtain satisfactory field welds using the thermit process. However, obtaining welds with a high degree of reliability requires skill and experience which often exceeds the capabilities of track construction and maintenance personnel. Some specific comments were that it was difficult to eliminate vertical and lateral kinks and end mismatch. This indicates there is excessive tolerance in maintaining rail alignment during welding. It has also been noted that the weld collar formed by excessive metal on the rail base often prohibits the placement of a tie at that location unless the excess material is removed by grinding.

The thermit welding process is attractive for use on transit track where space limitations restrict the use of large, special equipment because the weld kit, furnished by the supplier for each weld, is the only equipment needed. The weld kit includes the molds which align the rail ends and hold

them in position while the joint is heated. The heat is produced by an exothermic reaction based on the alumino-thermic reduction of iron from iron oxide. This reaction produces heat, slag and iron, and various additives are used to produce the mechanical properties desired for a particular rail stock.

The static strength properties obtained from the thermit process are usually adequate, but the principal deficiency in the process is that the welds have a lower fatigue strength than the rail steel or other types of welds. Weld and heat-affected zone toughnesses are low, and under traffic, fatigue induced transverse fractures frequently originate from defects in the heat-affected zone.

4.7.1 Conclusions and Recommendations

Based on the previous discussion, it appears that the thermit process is capable of producing welds with sufficient strength for use by the rapid transit industry. However, the weld kits and procedures should be evaluated to determine if they can be modified to improve the reliability of obtaining good welds using unskilled labor. The first phase of this program should include a controlled investigation of those factors which produce variations in rail end alignment and weld quality. An evaluation of joint integrity would include the mechanical properties of the joint and a determination of important defects (voids, cracks) in the weld and heat-affected zones. The results of this investigation would be used to develop recommendations for modifications needed to obtain improved performance.

It is also recommended that new processes be investigated to identify those concepts which might provide rapid, economical and reliable methods for field welding rail. However, considerable research will be required to fully evaluate the applicability of any new process for joining rails in the field.

New processes for welding rails should have the following characteristics:

- (1) High joint strength and fatigue resistance
- (2) Reproducible, relatively inexpensive, and amenable to non-destructive evaluation

- (3) Low capital investment for equipment
- (4) Suitable for unskilled labor
- (5) Convenient for on-site repair.

4.8 TRACK GEOMETRY

The principal track geometry parameters are gauge, alignment (lateral position), and surface (vertical rail profiles and track cross-level). Track geometry has a strong influence on vehicle ride quality. Consequently, track maintenance is often initiated as a result of the degradation in ride at specific track locations as well as from visual observations made during daily inspection by track walkers.

A review of track geometry maintenance practices in the rapid transit industry [4-16] and discussions with industry personnel indicate a wide variation in the frequency of scheduled maintenance. The Toronto system track is surfaced and lined twice a year, Boston (MBTA) tracks are lined and surfaced every 4 to 7 years depending on local conditions, and Chicago (CTA) is now covering their system once every two years. Other properties only maintain track geometry on an as-needed basis.

An interesting aspect of track geometry maintenance is that until very recently none of the transit properties used specifications for track geometry tolerances as a basis for scheduling maintenance. This was also true for railroads until the Federal Railroad Administration (FRA) published the Track Safety Standards [4-65]. A committee of the rapid transit industry then proceeded to prepare guidelines for minimum track geometry standards [4-66], for four classes of track covering operating speeds up to 80 mph. A brief comparison of the track geometry tolerances indicates the rapid transit standards are somewhat tighter than those in the FRA Track Safety Standards. This agrees with observations made during interviews at the transit properties where it was frequently stated that rapid transit track would meet the FRA standards with little difficulty.

The particular areas of track geometry maintenance that were identified during BCL interviews as significant track problems were curve alignment, track settlement at joints, and track settlement in the vicinity of structures such as bridges. Track settlement at bridges is a difficult problem for at-grade track because some settlement relative to the fixed bridge structure is inevitable, and this causes a very abrupt change in track surface and stiffness.

Highway designers are faced with the same problems, and personal experience indicates that no complete solution has been achieved for the highway problem at this time. The transition in going from one type of track to another was considered in the design of the Kansas Test Track [4-67] and reinforced concrete slabs with a tapered thickness were installed below the ballast to provide a more gradual transition zone. A similar approach should be practical for bridge approaches and at the junctions of other types of permanent structures encountered in rail track systems.

The review of current track design practice indicated that although track geometry is a key parameter in track performance, there are no design criteria directly related to the degradation of track geometry which results from differential settlement along the track route. A review of the literature indicated that very little work has been done on track settlement except for the development of an analytical roadbed model by TRW. A brief review of this work and some of the pertinent technical aspects of track settlement are discussed in the following sections.

4.8.1 Technical Evaluation

The track structure settlement model and computer program developed in the TRW study [4-68, 4-69] were based on a nonlinear finite element model for the roadbed. The ties, ballast, and soil were represented by a series combination of a linear spring, a hysteretic spring, and a damped hysteretic spring, respectively. The train loading included a static wheel load plus as many as three sinusoidal components to represent wheel dynamic loads, but all coupling between the track and vehicle response was neglected to simplify the analysis. The computed results included the residual settlement of the ballast and subgrade for a single train passage. The cumulative effect of several trains was then determined as a function of the settlement for a single train.

The roadbed model utilized a very approximate model for the transient and residual deformation of the ballast and subgrade under repetitive loads. The ballast model was based on data for course gravel, because no data were available for actual ballast materials. The load-settlement models were admittedly quite simplified and they were not expected to give accurate

predictions of track settlement. However, they were judged to be adequate for parametric studies of the relative effects of different track stiffnesses, vehicle suspensions, weights, speeds, etc.

This settlement model was only used to predict the uniform settlement for uniform track properties. Therefore, some simplified assumptions were made to relate differential settlement (track roughness) to the calculated uniform settlement because of the lack of available data relating the probable variation of soil and ballast properties along typical track. In this way it was possible to estimate a roughness versus wavelength relationship. Although it was not included in the program, this type of result could be used in an iteration process to modify the wheel dynamic forces based on transfer functions relating vehicle dynamic response to track roughness.

Although it is not clear from the TRW report [4-69] if the effects of long-term track settlement were superimposed with the predicted settlement for train loading, a discussion of long-term settlement was included. The long-term settlement included three basic processes which result from the weight of the track structure and embankment

- (1) An immediate deformation that takes place as the track is built
- (2) A consolidation which is a time-dependent settlement caused by compressing the voids in the material under the track
- (3) A viscoelastic deformation which is probably caused by the slow reorientation of the cohesive particles in the solid portion of soil.

Because of the lack of any real soil data, simplified assumptions of a one-dimensional soil model and the use of elastic theory to predict stresses after the soil deformation started were used to complete the predictions.

In summary, it appears that the TRW study represents a reasonable start on the development of procedures for evaluating the effects of vehicle and track design on the degradation of track geometry. It is also evident that considerable additional work is needed on modeling the deformation of ballast and subgrade materials, and this must be based on material performance

measured under realistic conditions for track structures.

There has been considerable research on soil modeling and soil properties under cyclic loading which was evidently not considered in the TRW study, and some of this work is reviewed in Appendix E to provide a more complete description of the state-of-the-art on this subject. The conclusions and recommendations from this review follow.

4.8.2 Conclusions and Recommendations

The basic mathematical formulations of the response of soil materials to simplified dynamic loading have been established and numerical analysis methods and other solution techniques are currently available for these analyses. However, considerable additional research is needed to generalize these formulations to include the complex state of stress and service conditions found in track structure.

The analysis of the settlement of track structures including ballast, subgrade, and embankment requires (1) an improved analysis of the state of stresses and displacements; (2) determination of the constitutive equations describing the response of the appropriate materials; and (3) measured data on track settlement to determine the validity of theoretical assumptions, and to correlate with the results of theoretical analyses. The results of analyses of soil settlement under dynamic loads indicate that peak stress amplitude, strain or displacement amplitude, pulse duration and the rate of loading affect the settlement process. The soil characteristics such as strength, modulus, and state of saturation influence the magnitude of observed settlement.

The determination of track settlement under dynamic load requires further research on the characterization of ballast and subballast materials subjected to repeated loadings. The material characterization and development of constitutive equations for ballast and subballast response must be based on simulated field states of stress. The effect of dynamic confining pressures, pore pressure, and dynamic normal and shear stresses on the material response needs further detailed investigation. In addition, the analysis program must recognize the effect of time-dependent degradation and weakening of the ballast

material. The freeze and thaw cycles to which the roadbed materials are exposed leads to time-variation of material constitutive equations.

Extensive field instrumentation, in situ material characterization and reevaluation are needed to properly correlate theory and observations. The statistical variability of dynamic and static soil response should be determined using nondestructive field techniques for measuring dynamic response.

4.9 COMMUNITY NOISE AND VIBRATION

The high priority of all aspects of noise from rail rapid transit systems, and some of the relationships between noise and other track problems such as rail corrugations and rail wear on curves were discussed in previous sections. Other track related noise problems include impact due to rail joints and wheel flats, and groundborne vibration. Joint noise is particularly objectionable on aerial structures where the structure is an efficient source of radiated noise. Wheel flats caused by wheel sliding during braking are an important source of community noise and vibration as well as being responsible for increasing the dynamic forces transmitted to both the track and the vehicle.

There has been considerable research on the effect of different types of track construction, and particularly the advantages of resilient rail fasteners, for attenuating community noise and vibration. The Washington Metropolitan Area Transit Authority (WMATA) is utilizing floating slab designs at critical locations in subways to attenuate ground vibrations, and a 200-foot test section of floating slab is being constructed by the NYCTA. Data from these installations should be quite useful in evaluating the effectiveness of this type of track construction. Results from these field installations should be thoroughly evaluated and documented so they can be used throughout the industry.

4.10 TRACK BUCKLING

Track buckling due to thermal loads is considered to be a relatively minor maintenance problem for the rapid rail transit industry. However, track buckling does sometimes occur in new constructions, and one or more trials

at shortening rail lengths may be required to eliminate buckling.

The effects of thermal stresses in CWR on steel bridges and elevated structures is an important design problem that should be solved, because the elimination of bolted rail on elevated structures would reduce the maintenance and noise problems caused by rail joints. Railroad bridges often consist of steel beam spans supporting wood ties. The wood ties are joined together longitudinally by a timber beam that serves as a vehicle guard and a tie spacer. The steel beams are free to move under the ties but the concern is for the loads transmitted to the wood guard beams.

The AREA design rules used for predicting thermal stresses and deflections in rails are based on a free expansion analysis of unrestrained rail. This model should be relatively accurate for conventional wood tie and ballast track, but the longitudinal restraint provided by rail fasteners used on concrete ties or concrete slabs can be quite significant. An important design criterion for rail fasteners used on elevated structures is that their maximum longitudinal force capability must be limited to avoid over stressing CWR rail due to thermal movements of the aerial structure. An accurate prediction of these stresses requires a detailed analysis of the elevated structure including realistic longitudinal load-deflection characteristics for the fasteners.

4.11 TRACK MAINTENANCE EQUIPMENT

Although track maintenance equipment has not been identified as a high priority track problem, there are several important differences between rapid transit and railroad operations that make it difficult to utilize equipment designed for railroads. Several of these differences are

- (1) Most rapid transit track maintenance must be done between the hours of 1 to 5 AM, or on weekends. The noise levels from much of the track maintenance equipment are excessive.
- (2) Space restrictions by the third rail, restraining rail, guard rails, and by subway tunnels prohibit the use of many types of equipment.

- (3) The weight of heavy work trains and maintenance equipment often exceeds the weight of rapid transit vehicles and the track must be designed accordingly. Concrete ties have been particularly susceptible to failure from center binding during track construction.
- (4) The handling of welded rail on a transit system is particularly difficult and has inhibited its use. However, the Chicago Transit Authority has successfully transported two 468-foot lengths of 100-pound rail through 185-foot radius curves using a train of old passenger cars.

4.12 RAIL FAILURES

The literature on rail problems includes an extensive list of different types of rail defects. Many of these can be considered as surface failures resulting from the very high local stresses in the wheel-rail contact zone. Most of these defects are significant problems for the railroad industry, but many of them are relatively unimportant for the rapid transit industry because of the reduced wheel loads of rapid transit cars. The most important rail problems for the rapid transit industry, namely rail corrugation, rail wear, and rail joints, have been reviewed in previous sections of this report. Therefore, this section includes only a very brief description of the different types of rail defects and some additional detail on rail shelly failures because this is of some concern for rapid transit properties.

4.12.1 Rail Shelling

Shelly failures are usually described as small shell-like pieces that have broken away from the top surface or sides of a rail head after some period of service. Shelly spots are generally located on the top gauge corner of high rails on curves, but they are also sometimes found on tangent track. They consist of individual pieces of broken-out metal from 1 to 6 inches long, 1/4 to 1-1/2 inches wide and from 1/8 to 1/2-inch deep as shown in Figure 4-19.

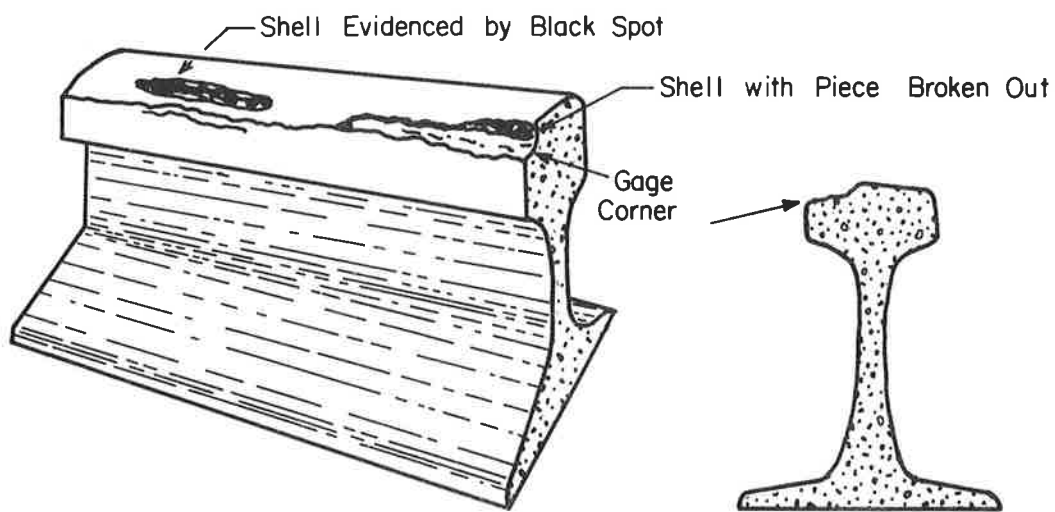


FIGURE 4-19. TYPICAL SHELLY FAILURES

They first appear as dark spots in the running surface, indicating a separation in the metal a slight distance underneath the surface. The plane of separation can be regular or irregular, and may extend as much as 1/2 inch below the upper corner on the gauge side of the rail head. Although shelling may be visible in some cases, shelly rail fractures can occur before the defect becomes noticeably visible on the surface.

There is a large amount of literature about rail shelling in the United States. The most voluminous is in the AREA Proceedings starting in 1942. The AAR and AISI jointly sponsored a 15-year investigation by R. B. Cramer at the University of Illinois in which test rails were subjected to rolling loads in the laboratory. Perhaps the most significant aspect of this study is the lack of fundamental information developed regarding the shelling failure mechanism. Metallurgical defects and plastic flow were cited as causes, but a failure theory was not developed.

In the recent literature, many different types of failures in the form of cracking of the rail head have been referred to as shelly failures. It is generally agreed that, depending upon the type of wheel loading, fatigue failures may have either surface or subsurface origins. Failures initiated from subsurface origins are most representative of the previously mentioned shelly definition.

It is generally believed that heavy wheel loads are a direct cause of shelly failures. In Britain, where wheel loads are less than they are in the United States, Dearden [4-70] of the British Railways states that shelly failures of the rail surfaces are not nearly as severe as the problems that exist in this country. In the case of heavily loaded wheels, the shearing stresses developed within the rails may exceed the elastic limit by as much as a factor of 2.5 [4-71]. In these cases, the material in the contact region deforms plastically, and the contact area increases until the stresses are reduced below the yield point. The relaxation of the loads is elastic, and it was pointed out by Archard [4-72] that subsequent loading would cause only elastic deformation. It has been found [4-73] that this is not exactly correct and, in fact, every cycle brings an additional increment of plastic deformation. The increment does, however, become progressively less.

High stress area may also be developed due to misalignment between rails and wheels. Johns [4-74] points out that failures due to misalignment may occur very near the surface if contact occurs near the corner radius of the wheel. The same effect would be caused by contacting the gauge corner of a rail. Due to this action, high normal contact stresses cause a region of high shearing stress just beneath the contact surface near the corner radius. These stress distributions have been verified experimentally; [4-75] however, no correlation between the resulting stress concentrations and shelly failures has been attempted.

To summarize, there have been significant contributions to the basic understanding of fatigue failures of rolling contact, but most of the work has been directed toward the study of the fatigue mechanisms in gear and bearing steels. There remains a definite need for similar efforts to be made toward developing a basic understanding of the shelly mechanism. Effects of surface tractions, misalignment, micro structure, surface chemistry, and lubrication must be considered. Recent advances in analytical capabilities for predicting the state of stress in arbitrarily shaped three dimensional bodies with surface loading represent an important advantage for evaluating the mechanism for shelly failures. Further, an effort must be made to relate the rolling contact behavior to basic material properties that can be determined experimentally.

A research program of this type should include

- (1) A comprehensive analysis of the rail stresses due to wheel contact to evaluate the effect of wheel-rail misalignment and surface tractions.
- (2) An evaluation of available fatigue failure criteria to determine which criteria give the best correlation for rail steels.
- (3) A program of rolling load fatigue tests to provide data for correlating the predicted fatigue results with the results from tasks (1) and (2).

4.12.2 Transverse Fissures

A transverse fissure is a progressive, crosswise fracture which starts from a crystalline center, or nucleus, inside the rail head. It then

spreads outward as a smooth, bright or dark, round or oval surface at an almost right angle to the rail length. The features shown in Figure 4-20 which distinguish a transverse fissure from other types of fractures or defects are the crystalline center and the nearly smooth surface of the development which surrounds it.

In the early 1900's, the transverse fissure was the most serious defect for open-hearth steel rails. Transverse fissures can be caused by contact stresses which propagate a crack that starts from an internal flaw or inclusion in the steel. This source of transverse fissures has been virtually eliminated by the use of control-cooled rail.

Transverse fissures may also occur from hot-torn steel, which is the tearing of steel during rolling when a portion of the rail bloom has been reheated too hot for successful rolling. This leaves a porous condition in the rail head. Most of the failed rails from this cause were rolled before 1944.

4.12.3 Engine-Burn Fractures

An engine-burn fracture is a progressive fracture which originates in a spot where driving wheels have slipped on top of the rail head. They occur most frequently where trains start, such as near stations, crossings, signals, etc. The spinning of the drive wheels creates sufficient heat to melt the steel in a local area. As a result of the intense heat, thermal cracking often propagates downward from the burned area. Unless the rail is removed from the track, the failure will progress until complete rupture occurs. Engine-burn fractures can seldom be located visually, but they can be found by detector cars.

4.12.4 Horizontal Split Head

A horizontal split head is a horizontal crack which originates inside the rail head, usually 1/4 inch or more below the running surface, and propagates horizontally in all directions as shown in Figure 4-21a. These failures are usually accompanied by flat spots on the running surface as shown in Figure 4-21b.

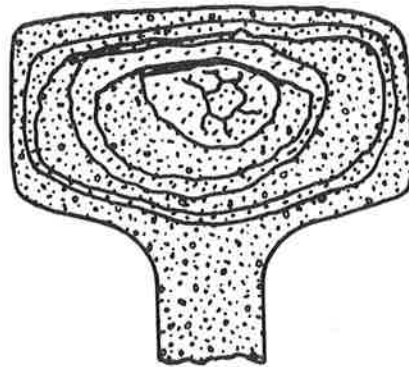
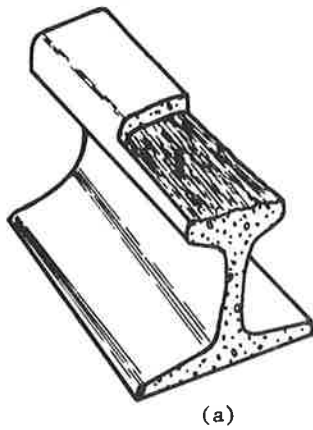
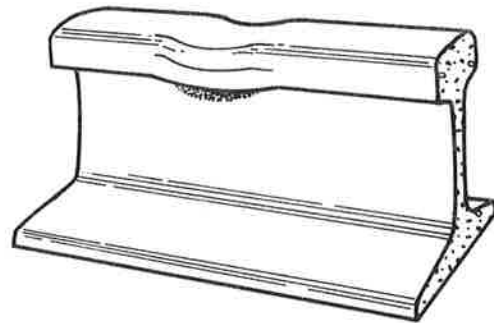


FIGURE 4-20. RAIL HEAD SHOWING TRANSVERSE FISSURE DEFECT [4-81]

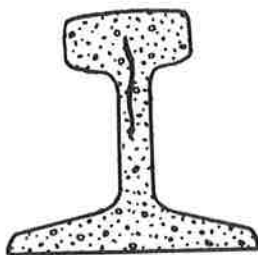


(a)

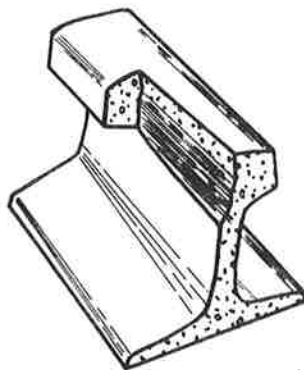


(b)

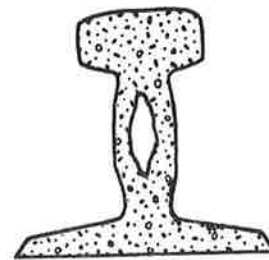
FIGURE 4-21. HORIZONTAL SPLIT-HEAD DEFECT [4-81]



(a) split head



(b) split head



(c) piped rail

FIGURE 4-22. VERTICAL HEAD AND WEB DEFECTS [4-81]

They appear as a longitudinal crack when the crack reaches the side of the rail head. The crack origin is usually an internal longitudinal seam, a segregation, or an inclusion. They tend to occur at several places in the same rail, since the seam or segregation may exist throughout the rail.

4.12.5 Vertical Split Head

A vertical split head is a vertical longitudinal crack near the middle of the rail head as shown in Figures 4-22a and 4-22b. A crack or streak of rust may appear under the head close to the web. Its origin is usually an internal longitudinal seam, a segregation, or an inclusion. It is rarely visible on the surface until it has grown to a length of several feet.

4.12.6 Piped Rail

A piped rail is one with a vertical split, usually in the rail web as shown in Figure 4-22c. It is theorized that it is caused by the failure of the sides of the shrinkage cavity to unite during the rolling process. Heavy loads will eventually cause it to spread, or open up, in a crosswise direction and cause a bulge in the web. This defect is seldom found in modern rail.

4.12.7 Compound Fissure

The compound fissure is a progressive fracture in the rail head which usually starts as a horizontal separation and then turns up or down, or in both directions, to form a transverse separation at nearly right angles to the running surface. If the horizontal separation is long enough to reach the surface and cause a flat spot on the running surface of the rail head, its growth will be very rapid.

4.12.8 Weeping Cracks

Weeping cracks are fatigue cracks which occur at the rail surface and grow inward laterally and longitudinally. The cracks are often found at rail

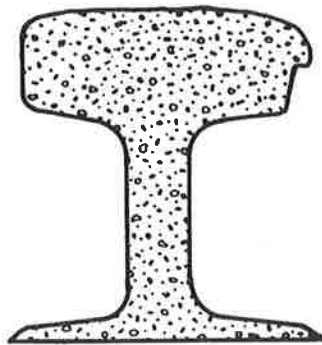


FIGURE 4-23. FLOWED HEAD AND HEAD CHECK

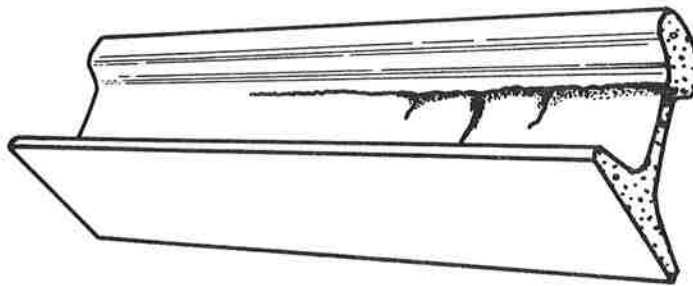


FIGURE 4-24. HEAD AND WEB SEPARATION

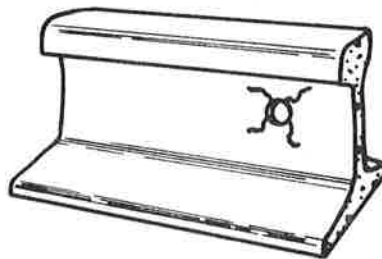


FIGURE 4-25. SPLIT WEB ORIGINATING AROUND BOLT HOLES

ends. Because these cracks allow the entry of water, rust is carried to the surface; hence, the term "weeping cracks". In the recent literature, these cracks are frequently called shelling [4-76] because of the appearance of the fracture surface.

4.12.9 Flowed Head and Head Check

When a rail is loaded excessively, there may be considerable plastic flow of material as shown in Figure 4-23. The material is displaced downward and toward the gauge corner of the rail which results in an overhanging lip. The rail material is work hardened, and a progressive fracture often starts at the gauge corner of the rail head. This has also been referred to as a shelly failure in some literature [4-77].

4.12.10 Head and Web Separation

A head and web separation is a fracture which propagates longitudinally to separate the rail head and web at the fillet under the head as shown in Figure 4-24. This type of failure is usually found in rails which are laid through highway crossings where materials hold moisture and promote corrosion along the rail head fillets. Through the use of photoelastic models, Frocht (1954) [4-78] and the Japanese National Railway (1961) [4-79, 4-80] have found that the thickness of the rail web and the angle formed by the fishplate at its point of contact strongly influence the stresses in the fillet.

4.12.11 Split Web and Bolt Hole Crack

The split web is a progressive fracture which develops in a longitudinal or transverse direction through the web. The origin of these fractures is often a seam or damage in the web, but split webs sometimes start where heat numbers are stamped into the web.

In the past, fractures which originated at bolt holes in the web were included in a single category of split web failures, but bolt hole cracks, as shown in Figure 4-25, are now often considered a separate category. Because of

the frequency of this mode of failure, the British Railways Research Department has made many stress measurements [4-9] at the critical positions around the bolt holes. A more detailed discussion of the rail stresses around bolt holes can be found in Section 4.3.

REFERENCES

Section 3.0

- 3-1. Hetenyi, M., Beams on Elastic Foundations, University of Michigan Press, 1946, pp 1,29.
- 3-2. Progress Reports of the Special Committee on Stresses in Track, AREA Proceedings, Vol. 19, 21, 24, 26, 31, 35, 42, American Railway Engineering Association, Chicago, Illinois.
- 3-3. Timoshenko, S. and Langer, B. F., "Stresses in Railroad Track", ASME Transactions, 54 (1932), pp 277-293.
- 3-4. Clarke, C. W., "Track Loading Fundamentals, Parts 1-7", Railway Gazette, 106 (1957), London, England.
- 3-5. Kerr, A. D., "The Continuously Supported Rail Subjected to An Axial Force and a Moving Load", Report No. S-70-2, NYU-AA-70--03, New York University, April, 1970.
- 3-6. Kerr, A. D. "A Modeling Study for Vertical Track Buckling", Report No. NYU-AA-71-31, New York University, October, 1971.
- 3-7. Hay, W. W., Railroad Engineering, Vol. 1, John Wiley and Sons, Inc., 1953.
- 3-8. Kurzweil, L., "Dynamic Track Compliance", Report No. TSC-GSP-067, DOT/Transportation Systems Center, Cambridge, Massachusetts, May, 1972, pp 13-14.
- 3-9. "Trackwork Study-Volume II - Recommended Trackwork Standards", prepared by DeLeuw, Cather and Co., for the Washington Metropolitan Area Transit Authority, August, 1968.
- 3-10. Bycroft, G. N., "Forced Vibrations of a Rigid Circular Plate on a Semi-Infinite Elastic Space and on an Elastic Stratum", Philosophical Transactions of the Royal Society of London, Series A, 248 (1950), pp 327-368.
- 3-11. Meacham, H. C., Voorhees, J. E., and Eggert, J. G., "Study of New Track Structure Design-Phase II", Report No. FRA-RT-72-15 prepared by Battelle Memorial Institute for the Federal Railroad Administration, August, 1968.
- 3-12. Srinivasan, M., "Modern Permanent Way", Somaiya Publications, Bombay, India, 1969, pp 134-136.
- 3-13. Schramm, G., "Permanent Way Technique and Permanent Way Economy", Trans. by H. Lange, 1961, Otto Elsner Verlagsgesellschaft, Darmstadt, Germany.
- 3-14. Magee, G. M., "Calculation of Rail Bending Stress for 125-Ton Tank Cars", AAR Research Center, Chicago, Illinois, April, 1965.

REFERENCES (Continued)

- 3-15. Proceedings of the American Railway Engineering Association, 58 (532), November, 1956, Chicago, Illinois, pp 359-360.
- 3-16. Reiner, I. A., and Law, C. W., "The Selection of an Economical Rail Section", B&O-C&O Research, Services Planning Department, Reports 1 and 2, Baltimore, Maryland, 1963.
- 3-17. Meacham, H. C. and Prause, R. H., "Studies for Rail Vehicle Track Structures", Report No. FRA-RT-71-45 prepared by Battelle Memorial Institute for the DOT, April 1970.
- 3-18. Dunn, R. H., "Trackwork Study-Volume I-Trackwork Practices of North American Rapid Transit Systems", Prepared by DeLeuw, Cather and Co. for the Washington Metropolitan Area Transit Authority, November, 1967.
- 3-19. Railway Track and Structures, Chicago, Illinois, May, 1973.
- 3-20. Manual for Railway Engineering-Volume I, American Railway Engineering Association, Chicago, Illinois, pp 7-1-19.
- 3-21. Roark, R. J., Formulas for Stress and Strain, 4th Edition, McGraw-Hill Book Company, 1965, p 417.
- 3-22. Weber, John W., "Concrete Crossties in the United States", Journal of the Prestressed Concrete Institute, 14 (1), February 1969, pp 46-61.
- 3-23. "On the C&O/B&O: Main-Line Test of Concrete Crossties", Railway Track and Structures, January, 1969, pp 22-24.
- 3-24. "Preliminary Specifications for Concrete Cross Ties (and Fastenings)", AREA Bulletin, 73 (634), September-October, 1971, pp 100-139.
- 3-25. "Data Collection and Analysis Report, Track and Roadbed Investigations for Test Track Program of San Francisco Bay Area Rapid Transit District", Report No. 64-25-R prepared by Kaiser Engineers, May, 1964, Section VII.
- 3-26. Proceedings of the American Railway Engineering Association, Vol. 67, Chicago, Illinois, p 622.
- 3-27. Bulletin of the International Railway Congress Association, December, 1965, London, England, p 881/61 f.
- 3-28. Salem, M. T. and Hay W. W., "Vertical Pressure Distribution in the Ballast Section and on the Subgrade Beneath Statically Loaded Ties", University of Illinois, Department of Civil Engineering, July, 1966.
- 3-29. "Advanced Transport Technology", A presentation by the British Railways to the U.S. Department of Transportation, March, 1972.

REFERENCES (Continued)

- 3-30. Yoder, E. J., Principles of Pavement Design, John Wiley and Sons, Inc., New York, 1959, p 227.
- 3-31. Oglesby, C. H., Highway Engineering, John Wiley and Sons, Inc., New York, 1963, p 439.
- 3-32. Maclean, D. J., editor, Soil Mechanics for Road Engineers, Her Majesty's Stationary Office, London, 1952.
- 3-33. Heath, D. L., Shenton, M. J., Sparrow, R. W., Waters, J. M., "Design of Conventional Rail Track Foundations", Proceedings of the Institute of Civil Engineers (Britain), 51(K), 1972, pp 251-267.
- 3-34. Proceedings of the American Railway Engineering Association, 72 (629), Chicago, Illinois, September-October, 1970. pp 95-104.
- 3-35. "Lateral Stability of Rails, Especially Long Welded Rails", ORE, International Union of Railways, Question D14, Interim Report No. 1, April, 1965, Utrecht, Netherlands.
- 3-36. Magee, G. M., "Welded Rail on Bridges", Railway Track and Structures, November, 1965, Chicago, Illinois, pp 24-26.
- 3-37. Koci, L. F., and Marta, H. A., "Wheel and Rail Loadings from Diesel Locomotives", Electro-Motive Division of General Motors, LaGrange, Illinois.
- 3-38. Sonnevile, R. and Bentot, A., "Elastic and Lateral Strength of the Permanent Way", Bulletin of the International Railway Congress Association, Vol. 32, No. 3, March 1955, pp 184-208.
- 3-39. Novion, F. F., "An Investigation of the Railway Vehicle Suspension at High Speeds", reference unknown.
- 3-40. Amans, F. and Sauvage, R., "Railway Track Stability in Relation to Transverse Stresses Exerted by Rolling Stock - A Theoretical Study of Track Behavior", Bulletin of the International Railway Congress Association, November, 1969, pp 685-716.
- 3-41. Birmann, F., "Track Parameters, Static and Dynamic", Proceedings of the Institute of Mechanical Engineers, Volume 180 (3F), Paper 5.
- 3-42. Meacham, H., et al, "Study of New Track Structure Design - Phase I", 3, Report No. FRA-RT-72-12 prepared by Battelle Memorial Institute for the Federal Railroad Administration, September, 1966, pp 89-94.

Section 4.0

- 4-1. McGean, Thomas, J., "Research Requirements Survey of the Rapid Rail Industry" prepared by MITRE Corporation for the Urban Mass Transportation Administration, UMTA-TRD-90-71 (PB204438) June, 1971.

REFERENCES (Continued)

- 4-2. Railway Track and Structures Cyclopedia, 8th Edition, 1955, p 325.
- 4-3. "Plastic Insulation for Rail Joints", Railway Track and Structures, Chicago, Illinois, September, 1973, p 37.
- 4-4. "Rolling Load Test of an Intma International I-Bond Insulated Rail Joint", AAR Research Center Report No. LT-323, August, 1972.
- 4-5. "M/W Efficiency on Union Pacific", Railway Age, June 11, 1973, pp 38-41.
- 4-6. "Railway Track After Hither Green", Engineering 10, November, 1967, pp 737-738.
- 4-7. Timoshenko, S., Strength of Materials, Part II, Third Edition, D. Van Nostrand Company, Inc., New York, 1956, p 12.
- 4-8. "Proceeding of American Railway Engineering Association", Volume 35, 1934, pp 156.
- 4-9. Babb, A. S., "Experimental Stress Analysis of Rails", Proc. Inst. Machine Engineer, Volume 180, Part I, No. 41.
- 4-10. "Proceedings of American Railway Engineering Association", Volume 31; 1930.
- 4-11. Savin, G. N., Stress Concentrations Around Holes, Pergamon Press Oxford, 1961, p 90.
- 4-12. Gilchrist, A. O., "Results of a Survey of Rail Joints Irregularities Using Matisa Records", B. R. Research Department Internal Report, DYN/15, December, 1965.
- 4-13. Nield, B. J., Goodwin, W. H., "Dynamic Loading At Rail Joints", Railway Gazette, August 15, 1969.
- 4-14. Bjork, J., "Dynamic Loading At Rail Joints - Effects of Resilient Wheels", Railway Gazette, June 5, 1970.
- 4-15. Yontar, M., "Research on the Operating Stresses in PATH Railcar Axles, Drive Systems, Wheels, and Rail Joints", 9th Joint ASME-IEEE Railroad Conference May, 1966, Paper No. 66RR-6.
- 4-16. Dunn, R. H., "Trackwork Study - Volume I - Trackwork Practices of North American Rapid Transit Systems" prepared by DeLeuw, Cather and Company for the Washington Metropolitan Area Transit Authority, November 1967, (PB204212).
- 4-17. Kilburn, K. R., "An Introduction to Rail Wear and Rail Lubrication Problems", Wear (7), 1964, pp 255-269.

REFERENCES (Continued)

- 4-18. Dearden, J., "Wear and Corrosion of Rails", The Railway Gazette, June 1, 1965, pp 18-21.
- 4-19. Reynolds, O., "On Rolling Friction", Philos. Trans, Roy Soc., London, 116, 1876, p 1.
- 4-20. Glagoley, N. I., "Rolling Friction and Wear", Friction and Wear in Machinery, 19, 1965, pp 144-171.
- 4-21. Archard, J. F., "Wear", NASA Symposium on Interdisciplinary Approach to Friction and Wear, November, 1967, pp 5.1-5.60.
- 4-22. Glagolev, N. I., "Rolling Friction and Wear", Friction and Wear in Machinery, Vol. 19, 1969, Translation by ASME from Russian.
- 4-23. "Rail Steels, Stronger, Harder, or Tougher?", Railway Gazette International, December, 1972, pp 471-472.
- 4-24. "Effectiveness of Alloying Rail Steel with Chromium", D. S. Kazarovskii et al, Stalin English, Metal Working and Heat Treatment, September, 1969, pp 823-825.
- 4-25. Engineering News, "The Wear of Rails of Different Grades of Steel", Volume 66, No. 18, 1911, p 538.
- 4-26. Patterson, A., "Matching the Track to the Head", Railway Gazette International, February, 1972.
- 4-27. AREA Bulletin No. 605, Volume 68, February, 1967, p 476.
- 4-28. AREA Bulletin No. 577, Volume 64, February, 1963, p 531.
- 4-29. Heumann, H., "Zum Verhalten von Eisenbahnfahrzeugen in Gleisbogen", (Comments on the Behavior of Railroad Cars on Curves) Organ f. d. Fortschritte d. Eisenbahnwesens, (1913), pp 104, 118, 136, 158.
- 4-30. Heumann, H., "Zur Frage des Radreifen-Umrisses", (Comments on the Question Relative to the Wheel tread Contour), Organ, September 15, 1934.
- 4-31. Koffman, J. L., "Tractive Resistance and Riding of Railcars", Diesel Railway Traction, November, 1963.
- 4-32. Heumann, H., "Zum Schlingern von Eisenbahnfahrzeugen", (Comments on the Irregular Oscillation of Railroad Cars), Organ, August 1943, pp 221-235.
- 4-33. Heumann, H., "Grundzüge der Führung der Eisenbahnfahrzeugen", (Basic Features of the Guiding of the Railroad Vehicles), Lectures at T. H. Munich, Verlag Raw, Munich, 1947.

REFERENCES (Continued)

- 4-34. Heumann, H., "Grundzüge der Führung der Schienenfahrzeuge", (Basic Features of the Guiding of Cars on Rails), R. Oldenburg, Munich, 1954.
- 4-35. Heumann, H., "Journal Inst. Loco. Engineers", No. 295, 1963-1964, pp 517-529.
- 4-36. Nothen, G., "ABC der Spurführung" ("Glassers Annalen") (ABC of Gauge Guiding) August, September, 1957.
- 4-37. Pflanz, K., "Lauf und Entgleisungssicherheit von Schienenfahrzeugen", (Running Safety and Protection Against Derailing of Cars on Rails), Oesterreichische Bundesbahn, Lehrbehelf, Nr 22.
- 4-38. Müller, C. Th., "Der Eisenbahnradatz", (The Railroad Wheel Set), Glassers Annalen, September, 1953, pp 264-281.
- 4-39. Danner, W., et al., "Einführung in die Spurführungsmechanik der Schienenfahrzeuge", (Introduction To the Track Guiding Mechanics of Cars on Rails), Archiv für Eisenbahntechnik, Nr. 2, January 1953, pp 1-28.
- 4-40. Bontefoy, M. G., "Running of Bogies Through Curves, the Heumann Method", French Rlwy, Techniques, No. 4, 1964, pp 225-232.
- 4-41. Müller, C. Th., "Radreifenverschleiss und Fahrzeuglauf", (Wheel tread Wear and Running of the Car), Osterreichische Ingenieur-Zeitschrift, Volume 7, No. 7, 1964, pp 215-224.
- 4-42. Koffenran, J. L., "Heumann Type Profile Tests on British Railways", Railway Gazette, April 1965, pp 279-283.
- 4-43. King, H. L., "New Type Profiles for British Railways", Railway Gazette, January 1968, pp 60-64.
- 4-44. Koffman, J.L. , Bartlett, D. L., "An Appreciation of the Practical Problems: A Survey of the Problems and Their Importance", Proc. I. Mech. Engr., Volume 180, Part 3 F, 1965, p 2.
- 4-45. AREA Proceedings, Track Committee Report, Volume 42, 1940, p 628.
- 4-46. Smith, F. W. and Dufault, R. J. A., "Rail Curve Lubricants - A Partial Correlation Between Apparent Viscosity and Delivery", National Research Council, Ottawa, Canada, Report MP-37, August, 1965.
- 4-47. Private communication with R. G. Bielenberg, NALCO.
- 4-48. Railway Age, "Reading Adds Years to Curve Rail Life With New Lubricant", November 10, 1958, p 21.
- 4-49. Manual for Railway Engineering, American Railway Engineering Association, Volume I, 1971, pp 5-5-3.

REFERENCES (Continued)

- 4-50. Meacham, H. C., Ahlbeck, D. R., "A Computer Study of Dynamic Loads Caused by Vehicle-Track Interaction", Trans. ASME, J. of Engineering for Industry, 69-RR-1, January, 1969.
- 4-51. British Railways, "Bibliography on Corrugation of Rails", B. R. Research Department, Derby, 1954.
- 4-52. Landen, E. W., "Slow Speed Wear of Steel Surfaces by Thin Oil Films", Trans. ASME, 11 (6), 1968.
- 4-53. Palmgren, A., "Ball and Roller Bearing Engineering", SKF Industries, Philadelphia, 1945.
- 4-54. Mather, K. B., "The Cause of Road Corrugations and the Instability of Surfaces Under Wheel Action", Civil Eng. Public Works Rev., 617, 1962, p 781.
- 4-55. Diehl, A., "Zerstörungsformen bei Schienen im Eisenbahntrieb", (Destruction Forms in Rails in Railroad Operation), Stahl und Eisen, 38, September 18, 1924, pp 1148-1149.
- 4-56. Cramer, R. E., Proc. 45th Annual Convention AREA, Volume 47, 1946.
- 4-57. Van Erdman Stolte, "The Formation and Stability of Marionsite Layers on Rail Steels", Stahl und Eisen, 22. October 1963, pp 1363- 1368.
- 4-58. Spiekir, V. W., Kohler, H., Kuhlmeier, M., "Investigations Into the Formation of Corrugations of Rails in Trial Tracks Under Conventional Conditions of Traction", Stahl und Eisen, 91, December, 1971, pp 1470-1478.
- 4-59. "Data Collection and Analysis Report. Track and Roadbed Investigation for Track Program of San Francisco Bay Area Rapid Transit District", Report by Kaiser Engineers to Parsons, Brinckerhoff, Tudor, Bechtel, May, 1964.
- 4-60. Nayak, P. R., "Contact Vibrations", J. Sound Vibr., 22 (2), 1972.
- 4-61. Carson, R. M., Johnson, K. L., "Surfact Corrugations Spontaneously Generated in a Rolling Contact Disc Machine", Wear, 17 (59-72), 1971.
- 4-62. Gray, G. G., and Johnson, K. L., "The Dynamic Reponse of Elastic Bodies in Rolling Contact to Random Roughness of Their Surfaces", J. Sound Vibr. 22 (3), 1972, pp 323-342.
- 4-63. Nayak, P. R., Tanner, R. B., "Frictional and Vibratory Behavior of Rolling and Sliding Contacts", FRA-RT-73-13, 1972.
- 4-64. Johnson, K. L., Jefferis, J. A., "Plastic Flow and Residual Stress in Rolling and Sliding Contact", Proc. Inst. Mech. Engr. Symposium on Fatigue, 1963.

REFERENCES (Continued)

- 4-65. Track Safety Standards, Federal Railroad Administration, Reprinted from Railway Track and Structures, February, 1973, containing modifications as published in the Federal Register on January 5 and January 15, 1973.
- 4-66. "Moving People Safely-Safety Guidelines for Urban Rapid Transit Systems", Prepared by Passenger Safety Committee of the Institute for Rapid Transit, Washington, D.C., May, 1972.
- 4-67. McLean, F. G., Williams, R. D., and Turnbull, R. C., "The Kansas Test Track, Nonconventional Track Structures-Design Report", prepared for the Federal Railroad Administration by Westenhoff and Novick, Inc., September, 1972, (PB212358).
- 4-68. "High-Speed Ground Transportation Systems Engineering Study--High Speed Rail Systems", Report No. FRA-RT-70-36 prepared for the U.S. Department of Transportation by TRW Systems Group, Redondo Beach, California, February, 1970.
- 4-69. "High-Speed Ground Transportation Systems Engineering Study--Supporting Studies for HSGT System Reports", prepared for the U.S. Department of Transportation by TRW Systems Group, Redondo Beach, California, June, 1970.
- 4-70. Dearden, R., "Rail Failures on British Railways", Railway Gazette, February 19, 1965, p 150.
- 4-71. Ito, Atsushi, "Contact Pressure Between Wheel and Rail and Its Influence on Mechanical Properties of Rail Steel", Quarterly Report on Railway Technical Research Institute (RTRI) of Japanese National Railway, Volume 3, No. 1, March, 1962, pp 21-25.
- 4-72. Archand, J. F., "Elastic Deformation and the Loss of Friction", Proc. Roy. Soc., A 243, 1957, p 190.
- 4-73. Martin, G. C., Hay, W. W., "The Influence of Wheel-Rail Contact Forces on the Formation of Rail Shells", Trans. ASME, 72-WA/RT-8, 1972.
- 4-74. Johns, T. G., et al., "Design Analysis of Roller-Track System for Large Steerable Antenna", Report to U.S.N.R.L., by Battelle Memorial Institute, May 11, 1973.
- 4-75. Kannel, J., "Comparison Between Predicted and Measured Pressure Distributions for Cylinders", ASME Paper No. D3-71, to be published, Journal Lubrication Tech., 1973.
- 4-76. Nakumura, R., et al., "The Rail Shelly Crack in Japan", Quarterly Report RTRI, Volume 6, No. 3, 1965, pp 34-44.

REFERENCES (Continued)

- 4-77. Cramer, R., AREA Bulletin, 584, Proc. Volume 65, February, 1964.
- 4-78. Frocht, M. M., "A Three Demensional Photoelastic Study of Contact Stresses in the Head of a Model of a Railroad Rail", Proc. S.E.S.A., Volume 14, No. 1, April, 1955.
- 4-79. Saska, N., Kakisawa, M., "Experiments on Local Stresses of Rails in Principal Use in Several Countries", JNR, Quarterly Report, Volume 2, No. 3, September, 1961.
- 4-80. Miyairi, M., Sasaki, N., "Two-Dimensional Photoelastic Experiments on Several Rail Sections", JNR, Volume 2, No. 3, September, 1961.
- 4-81. Rail Defect Manual, compiled by Sperry Rail Service, Automation Industries, Inc., Danbury, Connecticut.

APPENDIX A

RAIL PRODUCTION DATA

In the United States, rail sections selected for new urban transit track should be limited to the rail sizes recommended by the American Railway Engineering Association. There are currently six recommended rail sections [A-1]: 100#RE, 115#RE, 119#RE (formerly 119#CF&I), 132#RE, 136#RE, and 140#RE. Of these six, the two heaviest sections (136#RE and 140#RE) exceed the requirements for most urban rail transit systems. That leaves four rail sections that are of particular interest: 100#RE, 115#RE, 119#RE, and 132#RE. Table A-1 shows a breakdown of the quantities of these four rail sections rolled in the U. S. and Canada since 1962, and relative percentage data are plotted in Figure A-1 to illustrate production trends. With the possible exception of 100#RE rail which has a relatively low production rate, there should be no availability problems for these four rail sections and their related special trackwork such as switches, frogs, turnouts, etc.

The 119#RE rail section represents the most recent design in wide usage in this country today. This section was developed in the 1950's and differs from the other RE sections by providing a larger radii on the upper fillets and lower corners of the head as well as a deeper head section. This design was influenced by the advent of continuous welded rail and its corresponding increase in potential life of the rail.

Another interesting aspect of the 119#RE rail section is that the rail failures tabulated by the AREA Committee 4 on Rail show that this section has two to three times fewer rail failures per 100 track-mile-years than other rails of similar weight. However, care must be used when drawing conclusions from these data, as there are many factors that could be contributing to these results, e.g., region of country in which this rail is used, type of traffic, relative level of maintenance, etc.

TABLE A-1. QUANTITIES OF AREA RECOMMENDED RAIL SECTIONS ROLLED
IN NORTH AMERICA FROM 1962 TO 1971

| Year | 100#RE | | 115#RE | | 119#RE | | 132#RE | |
|------|--------|-----|---------|------|---------|------|---------|------|
| | Tons | %* | Tons | % | Tons | % | Tons | % |
| 1962 | 41,487 | 7.6 | 112,260 | 20.5 | 30,780 | 5.6 | 63,706 | 11.6 |
| 1963 | 7,110 | 1.2 | 146,302 | 23.7 | 24,101 | 3.9 | 113,600 | 18.4 |
| 1964 | 5,628 | .8 | 144,222 | 20.3 | 56,162 | 7.9 | 122,361 | 17.2 |
| 1965 | 12,237 | 1.6 | 174,206 | 23.2 | 53,382 | 7.1 | 110,960 | 14.8 |
| 1966 | 17,385 | 1.7 | 299,277 | 29.0 | 79,661 | 7.7 | 156,443 | 15.2 |
| 1967 | 9,893 | 1.1 | 250,049 | 27.9 | 49,948 | 5.6 | 157,009 | 17.5 |
| 1968 | 9,903 | 1.0 | 209,777 | 20.6 | 113,841 | 11.2 | 260,940 | 25.7 |
| 1969 | 9,182 | .8 | 274,384 | 24.7 | 81,000 | 7.3 | 274,264 | 24.7 |
| 1970 | 93,720 | 8.0 | 212,025 | 18.0 | 116,079 | 9.9 | 378,502 | 32.1 |
| 1971 | 13,372 | 1.1 | 219,374 | 17.8 | 143,223 | 11.7 | 337,703 | 27.5 |

* Percentage of total rail rolled during indicated year.

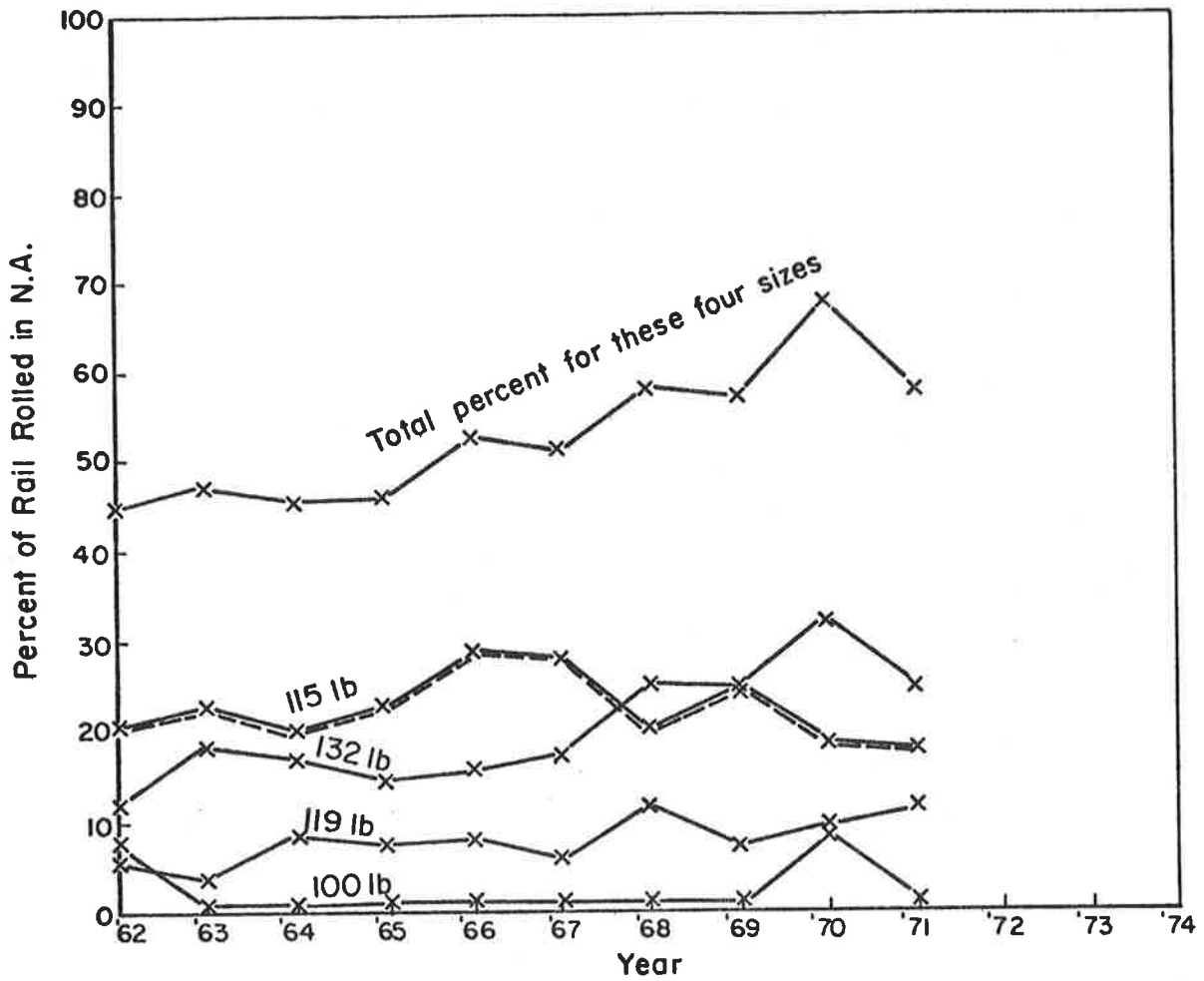


FIGURE A-1. PERCENTAGE OF TOTAL RAIL ROLLED IN NORTH AMERICA BY YEAR FOR THE FOUR RAIL SECTIONS OF MAJOR INTEREST

Table A-2 compares the properties of the four rail sections discussed previously with other rail sections from many parts of the world. Figure A-2 plots the data from Table A-2 and reveals the relative "efficiency" of the rail sections with respect to vertical stiffness. These data indicate that the RE rail sections have greater vertical stiffness for a given weight than any of the foreign rail sections tabulated.

TABLE A-2. RAIL SECTION PROPERTIES

| Rail Size | Weight, lb/yd (K _g /m) | Area, A in. ² (cm ²) | Moment of Inertia | |
|----------------|--------------------------------------|--|---|-------------------------|
| | | | I _x in. ⁴ (cm ⁴) | I/A in. ² |
| BR 98 | 98.1 (48.7) | 9.61 (62.00) | 40.7 (1695) | 4.24 |
| S 49 | 99.6 (49.4) | 9.76 (62.97) | 43.7 (1819) | 4.48 |
| 100 RE | 101.5 (50.4) | 9.95 (64.19) | 49.0 (2039) | 4.92 |
| SNCF 50 | 102.2 (50.7) | 10.00 (64.50) | 48.5 (2019) | 4.85 |
| JNR 50T | 107.5 (53.3) | 10.52 (67.90) | 54.8 (2280) | 5.21 |
| S54(IEV)/BR109 | 109.7 (54.4) | 10.75 (69.34) | 56.4 (2346) | 5.25 |
| 115 RE | 114.7 (56.9) | 11.25 (72.58) | 65.6 (2730) | 5.83 |
| 119 RE | 118.8 (58.9) | 11.65 (75.16) | 71.4 (2972) | 6.13 |
| S 60 (IEV) | 121.8 (60.4) | 11.91 (76.86) | 73.4 (3055) | 6.16 |
| JNR 60 | 122.6 (60.8) | 12.01 (77.50) | 74.2 (3090) | 6.18 |
| S 64 | 130.8 (64.9) | 12.82 (82.70) | 78.1 (3252) | 6.09 |
| 132 RE | 132.1 (65.5) | 12.95 (83.55) | 88.2 (3671) | 6.81 |
| 136 RE | 136.2 (67.6) | 13.35 (86.13) | 94.9 (3950) | 7.11 |

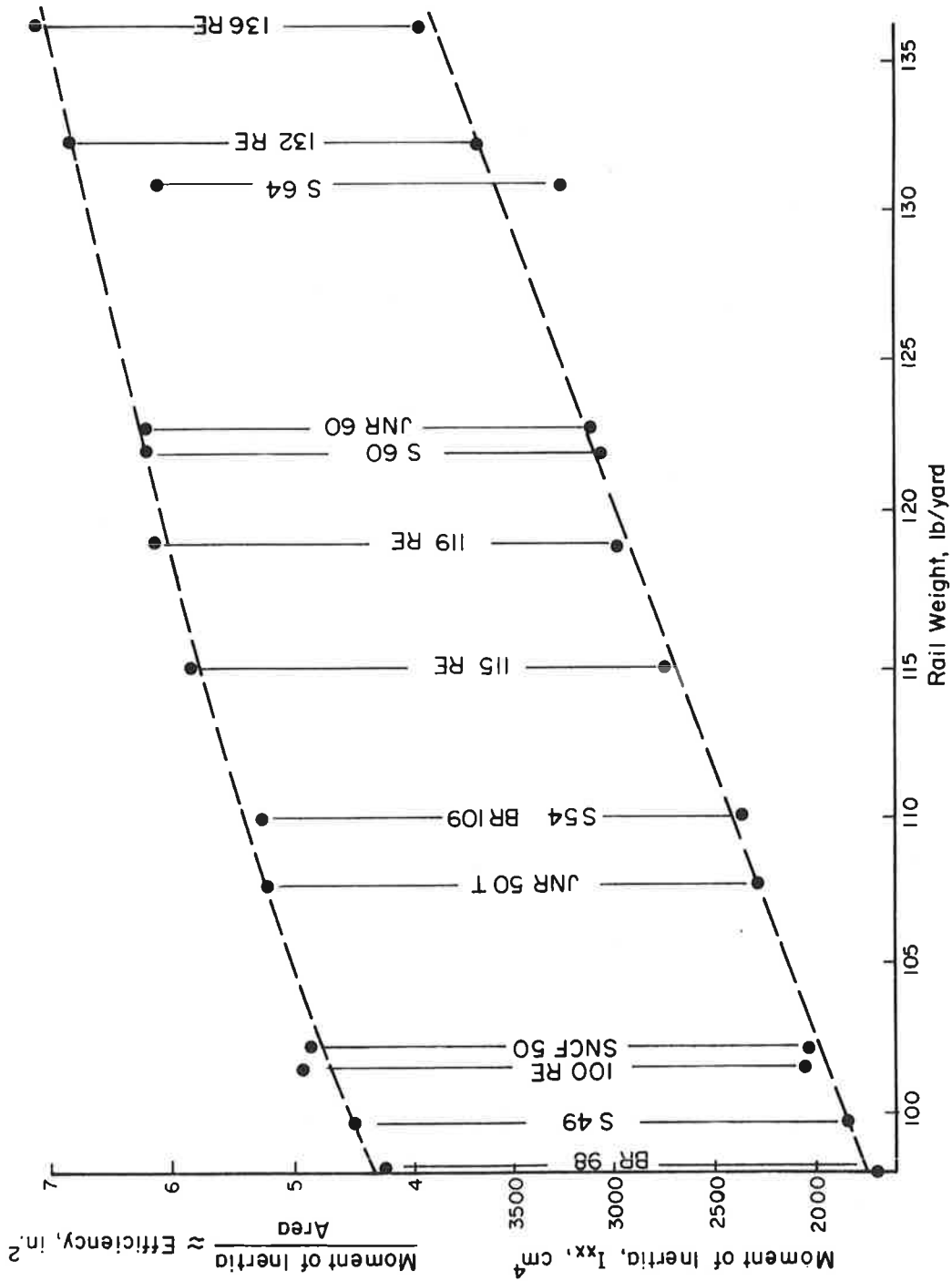


FIGURE A-2. BENDING STIFFNESS AND RELATIVE EFFICIENCY OF VARIOUS RAIL SECTIONS

REFERENCES

- A-1 Proceedings of the American Railway Engineering Association, 74 (641),
January-February, 1973, pp 335.

APPENDIX B

BEAM ON ELASTIC FOUNDATION ANALYSIS OF TIE DEFLECTIONS AND BALLAST PRESSURES

INTRODUCTION

The theory for a beam on an elastic foundation has long been used to determine the rail stresses and deflections and the average pressure of the tie on the ballast along the length of the track. Little attention, however, has been given to determining the pressure distribution on the ballast underneath the entire length of a tie. As a first step toward developing a more comprehensive analysis of this tie-ballast interaction, the beam on an elastic foundation model has been used to determine the tie deflections, ballast pressure and tie bending moment distributions.

It was found from this study that for most combinations of ballast and tie materials in common use, the pressure on the ballast varies considerably along the tie length. This will inevitably result in rutting, i.e., a flow of the ballast material from beneath the rail seat toward the center and ends of the tie.

ANALYSIS

In the theory for the bending of beams on an elastic foundation, it is assumed that there exists a direct proportionality between the displacement of the beam and the mean pressure per unit length [B-1]. It was noted by Galin [B-2], however, that the geometry of the contacting beam on the elastic foundation had much to do with how the foundation reacted against the beam. It follows, therefore, that the effective foundation modulus, k , is not a function of the elastic properties of the foundation (or ballast) alone, but it is a function of the beam (or tie) geometry as well.

Galín shows that for a beam on an elastic foundation, Figure B-1, the reactive pressure on the foundation is given by

$$\sigma_z(x,y) \Big|_{z=0} = \sigma_o(x) (1 - \eta^2)^{-1/2} \quad , \quad (B-1)$$

where

$$\sigma_o(x) = \frac{2P(x)}{\pi b} \quad ,$$

$$\eta = \frac{2y}{b} \quad ,$$

and $P(x) = kW(x)$ is the variation of the reactive force per unit length along the length of the tie.

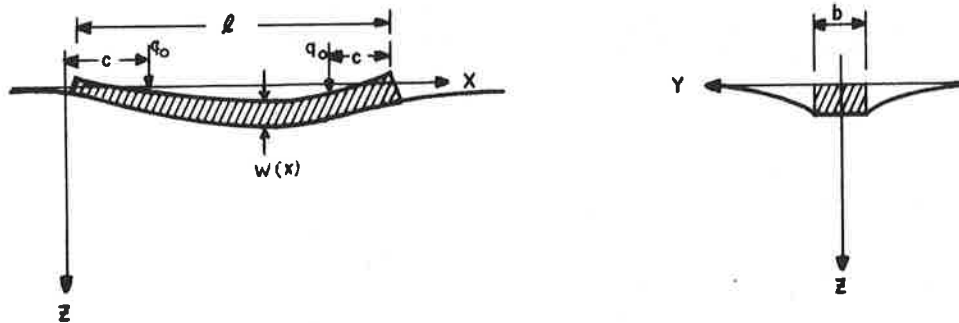


FIGURE B-1. ILLUSTRATION OF A BEAM ON AN ELASTIC FOUNDATION

The effective foundation modulus is given by

$$k = \frac{\pi E}{2(1-\nu^2) \ln(l/b)} \quad (B-2)$$

Noting, however, that the foundation modulus is sometimes given by

$$k_o = \frac{E}{2(1-\nu^2)} \quad , \quad (B-3)$$

the effective modulus can then be given by

$$k = \frac{\pi k_o}{\ln(l/b)} \quad . \quad (B-4)$$

The well-known differential equation for the deflection curve, W , of a beam supported on an elastic foundation, Figure B-1 is given by

$$E_b I \frac{d^4 W}{dx^4} = -kW + q_o \left[\delta(c) + \delta(l-c) \right] \quad , \quad (B-5)$$

where

E_b = the beam (tie) modulus of elasticity,

I = bending moment of inertia of the beam (tie)

$\delta(X)$ = Dirac's delta function $\begin{cases} 1 & X = 0 \\ 0 & X \neq 0 \end{cases}$

q_o = the load applied to the tie by each rail.

The solution to Equation B-5 is obtained by first solving the problem of an infinite length beam and then removing the moments and shearing forces at the ends of a finite length beam by superimposing the opposite reactions at those locations. These formulations have been developed by Hetenyi [B-3], and only the solutions will be given here.

Due to the rail seat forces, q_o , on a tie of infinite length, the moment $M_1(x)$ and deflection $W_1(x)$ are given by the following equations:

$$M_1(x) = \frac{q_0}{4\lambda} \left\{ e^{-\lambda|x-c|} \left[\cos\lambda|x-c| - \sin\lambda|x-c| \right] + e^{-\lambda|x-\ell+c|} \left[\cos\lambda|x-\ell+c| - \sin\lambda|x-\ell+c| \right] \right\}, \quad (B-6)$$

$$W_1(x) = \frac{q_0\lambda}{2k} \left\{ e^{-\lambda|x-c|} \left[\cos\lambda|x-c| + \sin\lambda|x-c| \right] + e^{-\lambda|x-\ell+c|} \left[\cos\lambda|x-\ell+c| + \sin\lambda|x-\ell+c| \right] \right\},$$

where,

$$\lambda = \left[\frac{k}{4E_b I} \right]^{1/4}.$$

Due to the superposition of shear forces, P_o , caused by the rail forces at the tie ends, the moment $M_2(x)$ and deflection $W_2(x)$ is developed. These are expressed as follows:

$$M_2(x) = \frac{P_o}{8\lambda} \left\{ e^{-\lambda x} (\cos\lambda x - \sin\lambda x) + e^{-\lambda|x-\ell|} \left[\cos\lambda|x-\ell| - \sin\lambda|x-\ell| \right] \right\}$$

$$W_2(x) = \frac{P_o\lambda}{4k} \left\{ e^{-\lambda x} (\cos\lambda x + \sin\lambda x) + e^{-\lambda|x-\ell|} \left[\cos\lambda|x-\ell| - \sin\lambda|x-\ell| \right] \right\} \quad (B-7)$$

where

$$P_o = 4G \left[Q_A(1+D) + \lambda M_A(1-A) \right]$$

$$G = \frac{1}{2(1-D^2) - (1-A)(1+C)}$$

$$A = e^{-\lambda\ell} (\cos\lambda\ell + \sin\lambda\ell)$$

$$B = e^{-\lambda\ell} (\sin\lambda\ell)$$

$$C = e^{-\lambda\ell} (\cos\lambda\ell - \sin\lambda\ell)$$

$$D = e^{-\lambda\ell} (\cos\lambda\ell)$$

$$Q_A = \frac{q_0}{2} \left[e^{-\lambda\ell} \cos\lambda c + e^{-\lambda(\ell-c)} \cos\lambda(\ell-c) \right]$$

$$M_A = \frac{q_0}{4\lambda} \left\{ e^{-\lambda c} \left[\cos\lambda c - \sin\lambda c \right] + e^{-\lambda(\ell-c)} \left[\cos(\lambda-c) - \sin(\lambda-c) \right] \right\}.$$

Due to superposition of moments, M_o , caused by the rail forces at the tie ends, the moment $M_3(x)$ and deflection $W_3(x)$ are developed. These are expressed as follows

$$M_3(x) = \frac{M_o}{2} \left[e^{-\lambda x} \cos \lambda x + e^{-\lambda |x-l|} \cos \lambda |x-l| \right] ,$$

$$W_3(x) = \frac{M_o \lambda^2}{K} \left[e^{-\lambda x} \sin \lambda x + e^{-\lambda |x-l|} \sin \lambda |x-l| \right] ,$$
(B-8)

where

$$M_o = \frac{2G}{\lambda} \left[Q_A (1+C) + 2\lambda M_A (1-D) \right] .$$

The actual moment $M(x)$ and deflection of the beam (or tie) is then the superposition of the above, or

$$M(x) = M_1(x) + M_2(x) + M_3(x) \quad (a)$$
(B-9)

$$W(x) = W_1(x) + W_2(x) + W_3(x) \quad (b)$$

To determine the loading $P(x)$ on the ballast underneath the tie one simply multiplies $W(x)$ by the foundation modulus. It follows then from Equation (B-1) that the ballast pressure under the tie is given by

$$\sigma_z = \frac{2k}{\pi b} W(x) (1-\eta^2)^{-1/2} .$$
(B-10)

Computational Results

The ballast pressure from Equation (B-10) was calculated for various ballast and tie material combinations. The rail seat load in each case was assumed to be $q_o = 17,500$ pounds. Figure B-2 shows the pressure distribution along the center line of the tie ($\eta = 0$) for a wood (oak) tie ($E_b = 1.15 \times 10^6$ psi) and several different values of ballast modulus. The pressure distribution is seen to vary greatly along the length of the tie, and in each case the pressure is highest beneath the rails.

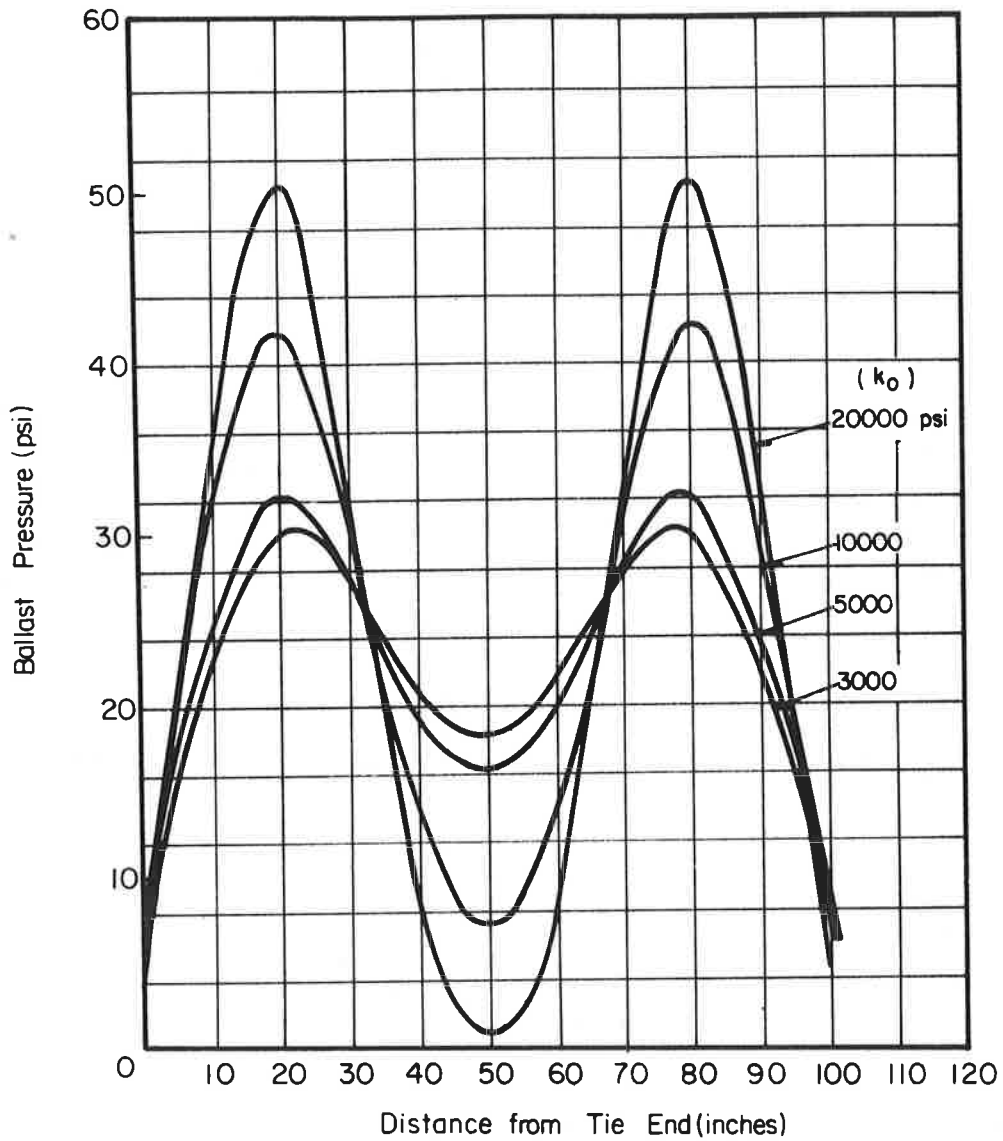


FIGURE B-2. BALLAST PRESSURE UNDER AN OAK TIE (6' x 8' x 8'6", $E_b = 1.15 \times 10^6$ psi) FOR VARIOUS VALUES OF BALLAST FOUNDATION MODULUS, k_o . THE RAIL SEAT LOAD $q_o = 17,500$ LBS.

In Figure B-3 the ballast pressure distribution along the length of the tie is shown again for a constant ballast foundation modulus ($k_o = 5000$ psi) and several values of tie modulus. For wood ties the pressure distribution varies greatly along the length of the tie; however, for a stiffer concrete tie ($E_b = 5.0 \times 10^6$ psi), this variation, as well as the maximum pressure, on the ballast is seen to be reduced.

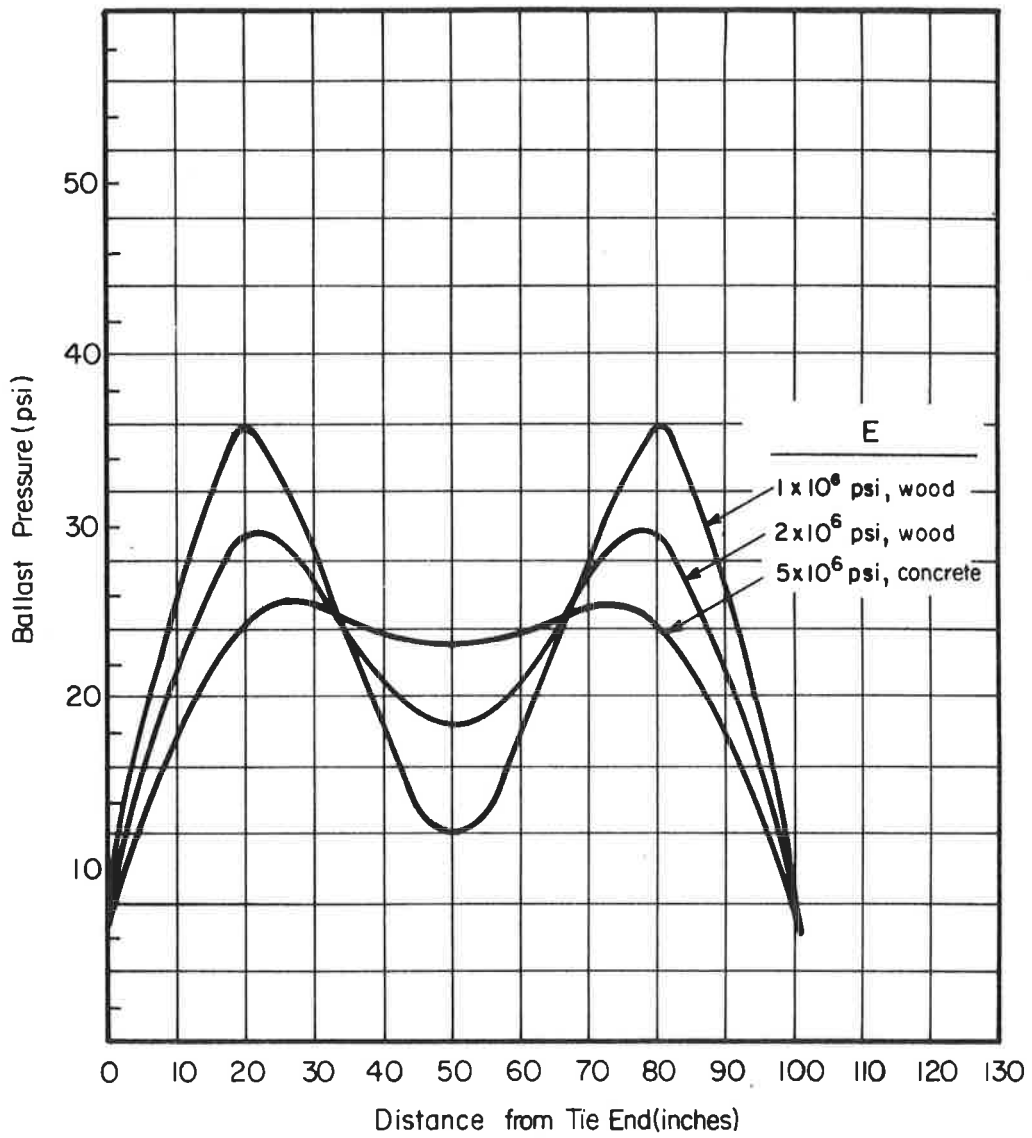


FIGURE B-3. BALLAST PRESSURE UNDER 6' x 8' x 8'6" WOOD AND CONCRETE TIES. BALLAST FOUNDATION MODULUS $k_o = 5000$ psi AND THE RAIL SEAT LOAD $q_o = 17,500$ LBS.

REFERENCES

- B-1. Winkler, E., Die Lehr von der Elastizität und Festigkeit, (The Theory of Elasticity and Strength), Prague, 1867, pp 182-184.
- B-2. Galin, Contact Problems in the Theory of Elasticity (in Russian) Moscow-Leningrad 1953. Available in English Translation Ed. I. N. Sneddon, North Carolina State College NSF G16447, 1961.
- B-3. Hentenyi, M., Beams on Elastic Foundation, Oxford University Press, London, 1946, p.41.

APPENDIX C

BALLAST PYRAMID MODEL

Although there are several pyramid models that attempt to describe ballast behavior, none of these have the capability of predicting both pressure distributions and stiffness using realistic material properties. To improve this situation, a modified pyramid model was developed using the experimental pressure data [C-1] for a load on a single 7" x 9" x 8'6" wood tie. Typical values for ballast properties were obtained from various sources, and these data were included in a simplified analysis of the ballast pressure variation as a function of ballast depth and effective tie bearing area.

The initial simplifying assumption in any pyramid model is that the pressure at any depth h below the tie bottom is constant over the bearing area so that

$$P(h) = \frac{q_0}{A(h)} \quad (C-1)$$

where $P(h)$ is the pressure, q_0 is the rail seat load, and $A(h)$ is the effective area.

The equation for the effective area using only the top pyramid in the model shown in Figure C-1 is

$$A(h) = (ch + b)(ch + L) \quad (C-2)$$

where $c = 2 \tan \theta$ (C-3)

and b is the tie width, L is the effective bearing length of the tie, and θ is the angle of internal friction for the ballast.

Figure C-2 shows a typical pressure distribution by Talbot [C-2] which indicates that the effective friction angle changes considerably at a depth of about 6 inches below the tie. Consequently, the ballast has

C-1 Salem, M. T., and Hay, W. W., "Vertical Pressure Distribution in the Ballast Section and on the Subgrade Beneath Statically Loaded Ties", University of Illinois, Department of Civil Engineering, July, 1966.

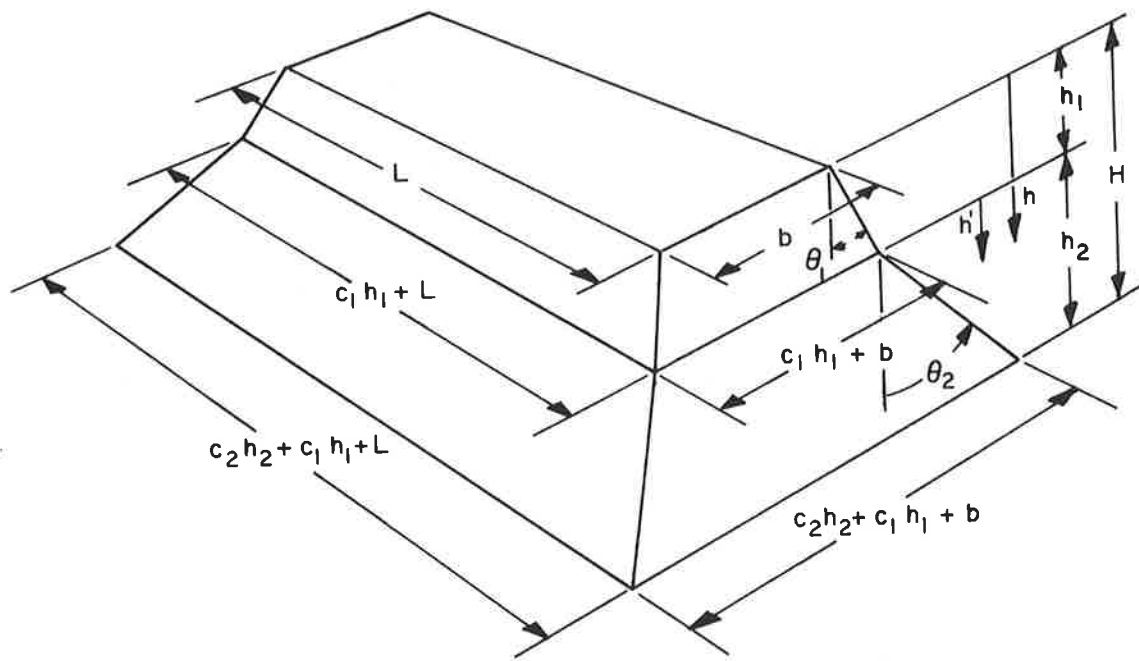


FIGURE C- 1 BALLAST PYRAMID MODEL

been divided into two sections, each having a different friction angle in order to include this effect in the pyramid model (see Figure C-1).

The equations for the effective area are then given by

$$A(h) = (c_1 h + b)(c_1 h + L) \quad 0 \leq h \leq h_1 \quad (C-4)$$

$$A(h) = (c_2 h' + c_1 h_1 + b)(c_2 h' + c_1 h_1 + L) \quad h_1 \leq h \leq H. \quad (C-5)$$

where

$$h' = h - h_1 \quad (C-6)$$

Data from Salem and Hay indicated that the effective areas under a 7" x 9" x 8'6" wood tie (see Figure C-3) were $A(h_1) = 575 \text{ in}^2$ at a depth of 6 inches, and $A(h_2) = 1155 \text{ in}^2$ at a depth of 12 inches ($h_2 = 6$ inches). Using $b = 9$ inches and $L = 34$ inches results in the following values of friction angle needed to fit Equations (C-4) and (C-5) to this experimental data:

$$\begin{aligned} c_1 &= .93 & \theta_1 &= 25^\circ \\ c_2 &= 1.52 & \theta_2 &= 37^\circ \end{aligned}$$

This indicates that a relatively small friction angle exists under the tie, which agrees qualitatively with the results shown in Figure C-2. The angle of 37° at greater depths agrees with other data reported by Schramm [C-3] that the ballast friction angle varies from 30° for poor ballast to about 40° for excellent ballast, with a typical value of 36° .

The stiffness of the total pyramid will be the effective stiffness of two springs in series

$$K_b = \frac{K_1 K_2}{K_1 + K_2} \quad (C-7)$$

and it can be shown that the stiffness of each spring can be determined from:

-
- C-2 Second Progress Report of Special Committee on Stresses in Track, AREA Proceedings, Volume 21, 1920, p 806.
 - C-3 Schramm, G., Permanent Way Technique and Permanent Way Economy, translated by H. Lange, 1961, Otto Elsner Verlagsgesellschaft, Darmstadt, Germany.

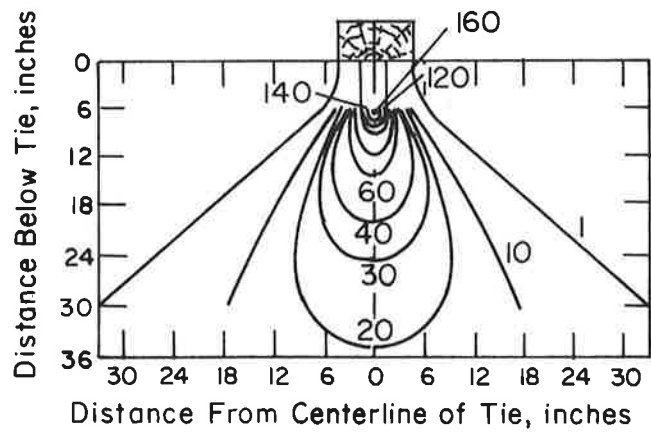


FIGURE C-2. LINES OF EQUAL VERTICAL PRESSURE IN BALLAST FOR A SINGLE LOADED TIE [C-2]

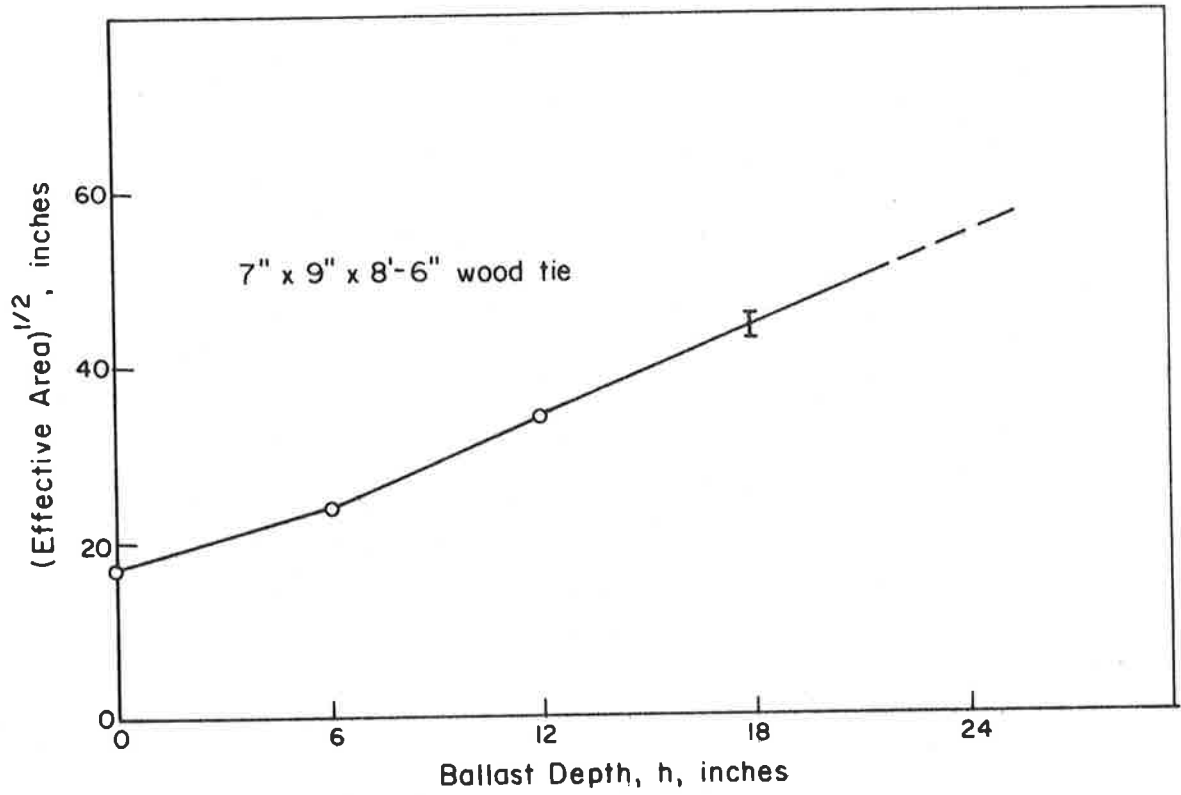


FIGURE C-3. EFFECTIVE BEARING AREA AS A FUNCTION OF BALLAST DEPTH BENEATH TIE BASE

$$K_1 = \frac{c_1 (L - b) E_b}{\ln_e \left[\frac{L(c_1 h_1 + b)}{b(c_1 h_1 + L)} \right]} \quad (C-8)$$

$$K_2 = \frac{c_2 (L - b) E_b}{\ln_e \left[\frac{(c_1 h_1 + L)(c_2 h' + c_1 h_1 + b)}{(c_1 h_1 + b)(c_2 h' + c_1 h_1 + L)} \right]} \quad (C-9)$$

and E_b is the modulus of elasticity of the ballast.

Using the parameters of $b = 9$ inches and $L = 34$ inches for a 7" x 9" x 8'6" tie,

$$K_1 = 70.5 E_b$$

for $h_1 = 6$ inches, and

$$K_2 = 136.5 E_b$$

for a total ballast depth of 12 inches ($h_2 = 6$ inches).

This gives a total ballast stiffness of

$$K_b = 46.5 E_b$$

For a typical value of $E_b = 17,100$ psi, $K_b = 795,000$ lb/in which is reasonable when compared to the range of 280,000 lb/in to 1,680,000 lb/in given by Birmann [C-4].

It should be noted that an increase in total ballast depth h reduces ballast stiffness, but the total track stiffness is usually increased because of the increased area over which the subgrade is loaded.

G-4 Birmann, F., "Track Parameters, Static and Dynamic", Proceedings of the Institute of Mechanical Engineers, Volume 180 (3F), Paper 5.

APPENDIX D

SOIL CLASSIFICATION

A railroad track is invariably supported directly or indirectly on earth materials, and therefore soil is one of the most important components of a track structure. Soils are generally classified by particle size and there are several different classification procedures in current use. The American Society for Testing and Materials (ASTM) recommends the classification given in Table D-1, and Table D-2 gives a summary of the soil components defined by the United Soil Classification System (USCS) of the U. S. Corps of Engineers. There are many other soil classifications recommended for highway and airport runway design, so it is important to identify the classification system used to describe soil specimens from particular construction sites.

The AREA Manual for Railway Engineering, Section 1-1, includes additional information about soil classifications and a useful summary of the physical properties of soils that affect their performance under applied loads. The important physical properties are

(1) Internal Friction is the resistance to motion of particles of soil in contact caused by the roughness of their surfaces and the shape and size of the individual grains. It varies with applied pressure. Internal friction is high in sands and relatively low in clays.

(2) Cohesion is the resistance to forces tending to separate two or more soil particles held together by minute moisture films, possible supplemented by the natural stickiness of colloids. It is independent of applied pressure. Cohesion is very low in sands and relatively high in clays. Cohesion and internal friction between the soil particles make up the shearing strength of a soil. Shearing strength is a property which enables soil to maintain equilibrium on a sloping surface of a cut or fill and which greatly influences the bearing capacity of a foundation soil.

TABLE D-1. ASTM SOIL CLASSIFICATION [D-1]

| Soil | Grain Size, Millimeters |
|----------------|-------------------------|
| Gravel | Larger than 2.0 |
| Sand, coarse | 2.0 - 0.42 |
| Sand, fine | 0.42 - 0.074 |
| Silt | 0.074 - 0.005 |
| Clay | Smaller than 0.005 |
| Colloidal clay | Smaller than 0.001 |

TABLE D-2. SOIL COMPONENTS-USCS SYSTEM [D-2]

| Component | Size Range |
|-------------------------|--|
| Cobbles | Above 3 in. |
| Gravel | 3 in. to No. 4 sieve (4.76 mm) |
| Coarse gravel | 3 in. to 3/4 in. |
| Fine gravel | 3/4 in. to No. 4 sieve (4.76 mm) |
| Sand | No. 4 sieve (4.76 mm) to No. 200 sieve (0.074 mm) |
| Course sand | No. 4 sieve (4.76 mm) to No. 10 sieve (2.0 mm) |
| Medium sand | No. 10 sieve (2.0 mm) to No. 40 sieve (0.42 mm) |
| Fine Sand | No. 40 sieve (0.42 mm) to No. 200 sieve (0.074 mm) |
| Fines (silt or clay) | Finer than No. 200 sieve (0.074 mm) |

(3) Compressibility represents the change in the volume of soil produced by pressure. The compressibility of a soil is a function of the decrease in volume of voids. If the voids are filled with water, compression can occur only as a result of escape of water from the voids. The compressibility of sands in which the grains bear almost directly on adjacent grains is slight. It is much larger in clays where the minute scale-like grains are separated by water which is squeezed out and the volume of voids is decreased.

(4) Elasticity is the property of soil to rebound after removal of load. It is almost entirely absent in sand with its bulky and rather rigid grains; it is present to varying degree in undisturbed clay, due principally to the scale-like, flexible particles and to a flocculated, honey-comb arrangement of the particles. Elasticity, due to a spongy structure, is present in some soils containing organic matter.

(5) Permeability determines the rate of consolidation of soils. All soils contain continuous voids and are thus said to be permeable. However, there are large differences in the degree of permeability of various earth materials. Highly permeable soils such as sands will consolidate under loads very rapidly because excess water can escape from the voids quite readily. A saturated clay which has low permeability will require more time for the excess water to squeeze out and consequently will consolidate over a long period of time.

(6) Capillarity in soils is a phenomenon which tends to draw or retain moisture above the water table. It is caused by the surface tension of water and its molecular attraction to the walls of the hair-fine tubes or spaces between the soil particles. The void spaces of sands are too large to act as capillaries except to a slight degree. Higher capillarity, such as clays possess, contributes to the properties of cohesion, compressibility, and elasticity. Capillarity is an important contributing factor in the frost heaving of soils.

The AREA Manual, Section 1-1, also describes a penetration test that is used to identify soil condition. This test is performed by dropping a 140-pound weight on a soil sampling spoon from a height of 30 inches. The sampling spoon is usually seated about 6 inches into the soil, and the number

of blows required to penetrate the next one foot of soil is used to determine the relative density of sand soils and the relative strength of clay soils from Table D-3. The data for unconfined compressive strength represent the maximum axial stress at which unconfined prismatic or cylindrical specimens of the soil fail in a simple compression test.

TABLE D-3. SOIL STRENGTH AND DENSITY FOR PENETRATION TEST [D-3]

| Sands | | Clays | | |
|---------------------------------------|---------------------|---------------------------------------|-------------|--|
| No. of Blows for 1 Ft. Penetration | Relative Density | No. of Blows for 1 Ft. Penetration | Consistency | Unconfined Compressive Strength (tons/sq ft.) |
| 0 - 4 | Very Loose | 0 - 2 | Very Soft | Less than 0.25 |
| 4 - 10 | Loose | 2 - 4 | Soft | 0.25 - 0.50 |
| 10 - 30 | Medium | 4 - 8 | Medium | 0.50 - 1.00 |
| 30 - 50 | Dense | 8 - 15 | Stiff | 1.00 - 2.00 |
| Over 50 | Very Dense | 15 - 30 | Very Stiff | 2.00 - 4.00 |
| | | Over 30 | Hard | Over 4.00 |

REFERENCES

- D-1 American Railway Engineering Association, Manual for Railway Engineering (Fixed Properties of AREA), Vol. I, p 1-1-37.
- D-2 Yoder, Principles of Pavement Design, John Wiley & Sons, 1959, p 168.
- D-3 American Railway Engineering Association, Manual for Railway Engineering, (Fixed Properties of AREA), Vol. I, p. 1-1-42.1.

APPENDIX E

TRACK STRUCTURE SETTLEMENT

INTRODUCTION

To formulate design procedures and requirements for track structure with regard to the foundation, it is necessary to study in depth the mechanism contributing to roadbed settlement and the possible means for alleviating this problem. Under a given track structure, which in general consists of ballast, subballast, subgrade, embankment and natural soil, the state of stresses is represented by a static state upon which a dynamic stress condition is superimposed. In general, one might divide the settlement of track structure into the following broad categories:

- (1) Densification and/or rutting of ballast, subballast, subgrade, embankment and natural soil foundation due to repeated load application
- (2) The immediate elastic settlement of the embankment or foundation due to the weight of the embankment and track
- (3) Time-dependent, consolidation settlement of the foundation due to the weight of the embankment and track.

In the discussion of settlement presented in this section, shear failure associated with either bearing capacity or liquefaction of sandy soils has not been included.

With respect to the mechanics of settlement, the observed deformation phenomena consists of the following categories:

- (1) Instantaneous of time-dependent volumetric change associated with densification and deformation under load
- (2) Instantaneous of time-dependent shear distortion associated with static and dynamic loads.

To determine the magnitude and rate of settlement that is expected to occur under typical track structure, the state of stress existing under the subgrade and foundation must be known. This state of stress can be considered as a superposition of the effects of static and cyclic stresses. An element of soil beneath the track structure is subjected to a static vertical stress, σ_v , horizontal stress, σ_h , and shear stress, τ . These stresses are a combination of the stresses for a rest state of the soil media and the stress caused by static loads. The soil element is also subjected to dynamic stresses consisting of vertical stress $\pm\Delta\sigma_v$, horizontal stresses, $\pm\Delta\sigma_h$, and cyclic shear $\pm\Delta\tau$, which are due to the dynamic loads induced by traffic.

SETTLEMENT DUE TO CYCLIC STRESSES

Foundations subjected to vibratory loadings often show settlements many times larger than those corresponding to static loads of equal magnitude. Progressive settlement under cyclic loading occurs more frequently in foundations of noncohesive soils. Although analyses of soil based on static loading concepts often indicate a high resistance to deformation, much larger deformations result from cyclic loading.

There has been considerable research work carried out on the subject of soil dynamics and soil behavior under repeated loading, and the results have been well documented in the literature [E-1 through E-5]. The investigation of dynamic shear strength and damping characteristics of soil media has also been carried out by several investigators [E-6 through E-9].

The experimental data indicate that the confining pressure, impulse, and sustained stresses influence the response of soils under dynamic loading. The relation between measured axial strain and the number of pulse applications is shown in Figure E-1. In this Figure, the impulse stress and the sustained stress are expressed in terms of a percent of the deviatoric stress which results in specimen failure during normal strength experiments. The data presented in Figure E-1 correspond to experiments conducted under a sustained stress of 50 percent of the soil's normal strength. The magnitude of impulse stress greatly influences the axial strain and the number of pulses required

to failure. However, the confining pressure, ranging from 14.2 to 60.0 psi, has only a small, random effect on the dynamic strength of cohesive soils. This small effect may well be within the error limits for the test.

An increase in the cyclic strain or stress amplitude decreases the observed modulus and increases the material damping. At low strain levels, the soil exhibits a high modulus and low damping characteristics and its response can be approximated by the elastic media. On the other hand, the increase in material density (or its packing) only slightly increases the modulus response.

Extensive work has been carried out on the use of vibration for soil compaction. The effect of magnitude of load, frequency and number of load repetitions on soil densification or compaction has been investigated [3-11, E-12 and E-13].

Theoretical Models of Soild Under Cyclic Loads

In most analyses of soil under cyclic loading, the theory of elasticity has been employed. However, it should be noted that the elastic approach has severe limitations where progressive and irrecoverable (inelastic) deformations are involved. Recently, the elastic-plastic theory was used to account for the accumulation of permanent deformation.

To explain some of the fundamental concepts in the elastic-plastic behavior of soils, consider a typical response of the material shown in Figure E-2. Within the segment from 0 to the proportional limit A, the material is linearly elastic and is reversible. Above A, the deformation is partly irreversible so that unloading from C to zero stress would leave a permanent plastic strain. Reloading from a point such as E proceeds along path EFGH.

The gradual change in slope of the stress-strain curve with increasing strain is termed work-hardening. With further idealization, in which work-hardening is absent and plastic deformation takes place under constant stress, the material is said to be elastic, perfectly plastic. A stress-strain diagram for such a material is shown in Figure E-3, where OA represents the linear

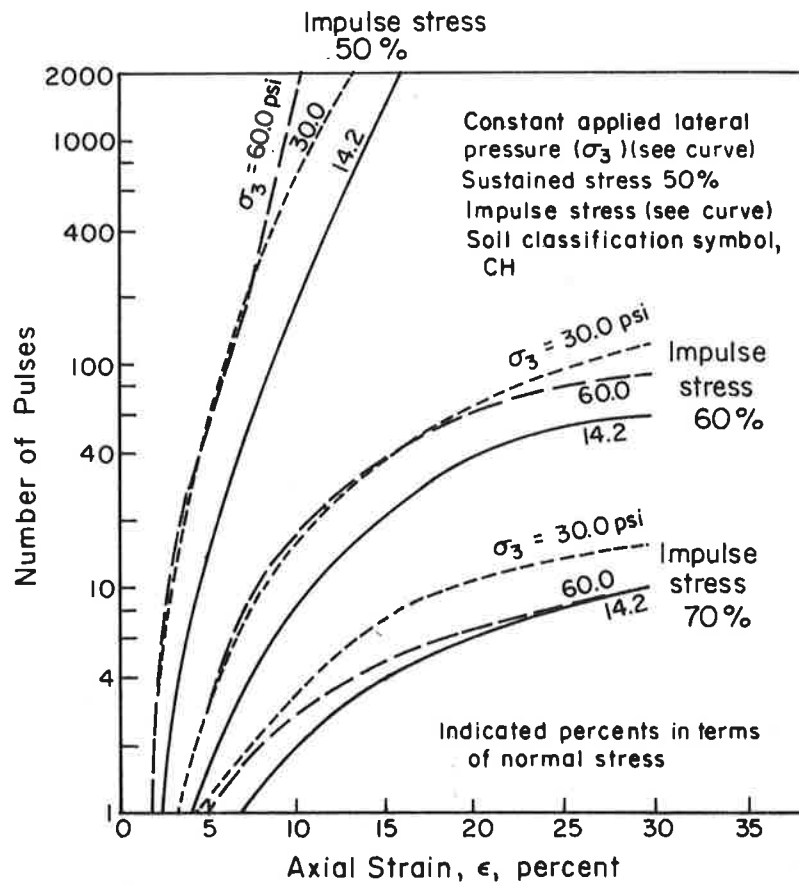


FIGURE E-1. EFFECT OF CONFINING PRESSURE AND NUMBER OF LOAD CYCLES ON THE AXIAL STRAIN [E-10]

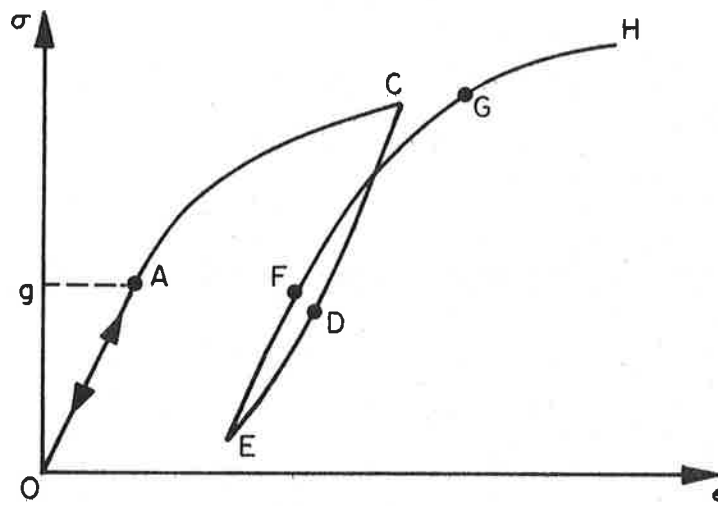


FIGURE E-2. TYPICAL STRESS-STRAIN CURVE FOR A SOIL

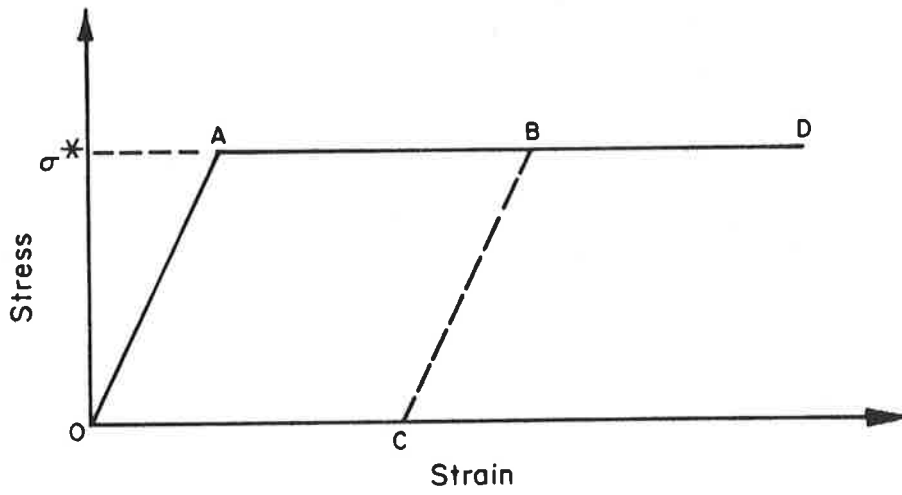


FIGURE E-3. STRESS-STRAIN DIAGRAM OF AN ELASTIC, PERFECTLY PLASTIC MATERIAL

relationship between stress and strain. At the critical stress, σ^* , the material flows plastically as shown by the portion ABD.

Various models have been presented in the literature to account for the accumulation of permanent deformation of soils. These mathematical models are: (1) the Drucker, Gibson, and Henkel formulation; (2) the Cambridge model by Roscoe and co-workers; (3) the MIT formulation; and (4) the DiMaggio and Sandler model [E-14, E-15]. All these models would only give the plastic strain after yielding occurs and do not predict the time-dependent effect. A review of these four models by Khosla [E-16] concluded that, for dry sand under static and dynamic loading, the second and fourth models are the best, with the fourth effectively predicting the strains for both static and cyclic loading.

In addition to the elastic-plastic models developed for sand and ideal granular material, extensive work has also been carried out on the behavior of clay soils under repeated loading. Majidzadeh and Guirguis have presented a rutting model based on micro-rheological consideration of soil response under static and repetitive loads [E-17, E-18].

It has been documented that the cumulative deformation and failure response of materials under repeated loading are very similar to that of the creep-rupture phenomena. It has been, therefore, asserted that the principles of static and dynamic rupture are identical and that the observed difference in the life of specimens is due to the rate of cumulative damage and relaxation between load applications. Figure E-4 shows a typical deformation-time relation for a soil specimen under repeated loading in which the variation of cumulative permanent deformation, γ_p , with the number of load applications is presented. It is noted that similar to creep-rupture phenomena, the cumulative permanent deformation-time relation might be divided into three distinct regions.

- (1) Initially, the deformation increases rapidly but with a decreasing rate with the number of cycles of loading; densification may occur here and involves the decrease in air void content of the soil by the progressive rearrangement of the particles relative to each other.

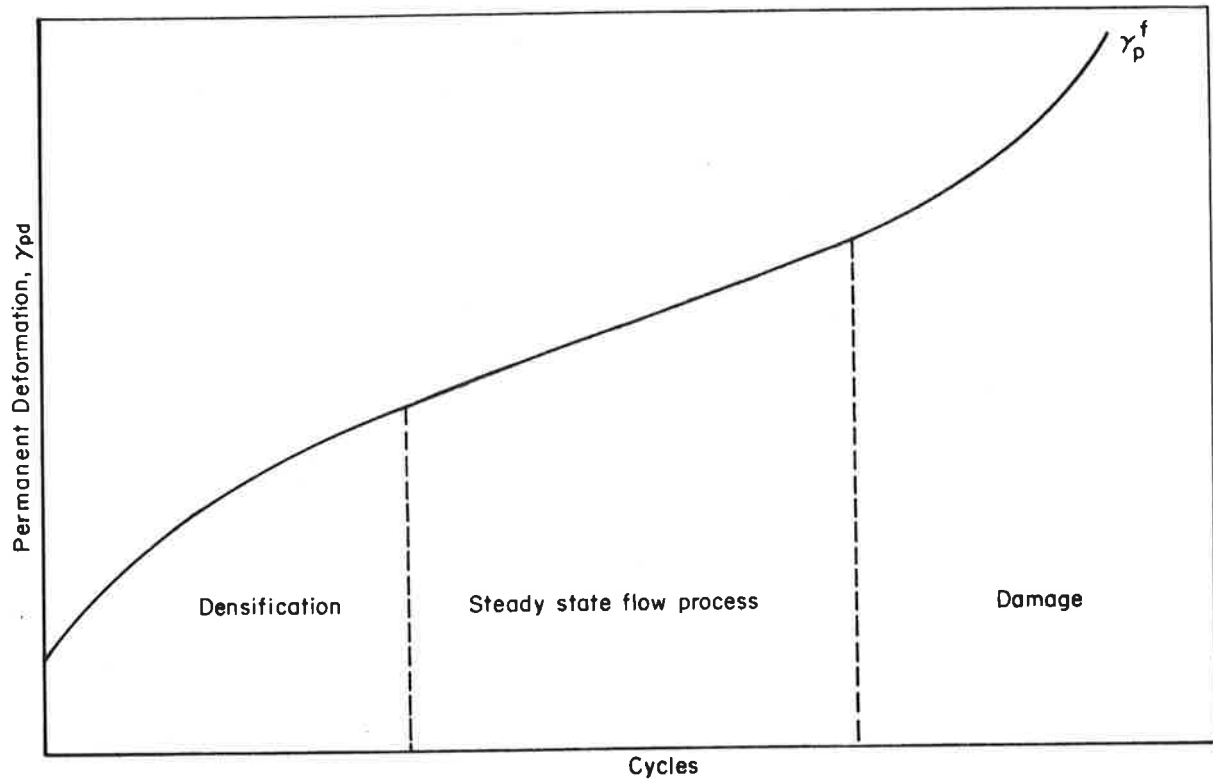


FIGURE E-4. TYPICAL DEFORMATION-LOAD CYCLES, N , CURVE

- (2) The second stage involves the time-dependent arrangement of the particles. It is an irrecoverable flow process and is effected by the successive yielding and deformation of particle contacts. The resulting deformation is in accordance with the postulates of the rate process theory: with the rate of permanent deformation expressed in terms of the number of load applications instead of the time of load applications. The rate of deformation and volume change are considerably reduced, which is consistent with the idea that particles flow into the vacated voids and rearrange as opposed to a translation of particles.
- (3) This stage is characterized by an increase in the rate of deformation leading ultimately to failure. Failure is due to an accumulation of damage resulting from the formulation and growth of plastic zones at points of local overstressing and the enlargement of voids and weak boundaries in the soil structure under repeated loading.

The mechanistic model presented by Majidzadeh and Guirguis utilizes the rate process theory concepts to explain the accumulation of permanent deformation of stages 1 and 2 for clay specimens under repeated loadings. Extensive laboratory investigations have lead to the conclusion that the mechanisms of compacted clay deformation under static and dynamic conditions are very similar, if not the same. The possibility exists, therefore, of being able to predict dynamic response from static tests and vice versa. In addition, the effect of cyclic and repetitive loading on the modulus of clay soil has also been investigated. In this case it has been noted that the sinusoidal loading functions used to determine a dynamic modulus is an oversimplification of the actual loading pattern occurring in railroad tracks and highways. To better simulate field loading patterns in the laboratory, experiments must be conducted using pulsating dynamic loads of varying frequency and rest periods.

From the review of the state of the art presented in the foregoing sections, it is apparent that the prediction of soil settlement under repeated loading is a major concern to the engineering profession. The settlement analysis for roadbed and track structures involves two main tasks for future research in this area. First, the exact nature of induced dynamic stresses and strains in the roadbed system should be determined analytically and verified by field observations. Second, the material response, involving a wide range of materials such as ballast, subballast, clay and sandy soils, etc, should be determined under realistic loading conditions. This would require an extensive laboratory investigation of the response of ballast materials to cyclic and pulsating axial and lateral stresses. Utilizing such a material characterization procedure and the mathematical models developed, the verification of the rutting and permanent deformation exhibited in the field should then be carried out.

SETTLEMENT DUE TO STATIC LOADS

The observed settlement of roadbed and track structures is partly due to the static loads resulting from the weight of the embankment and the track structure. In order to conduct a detailed analysis of immediate settlement and primary and secondary consolidation, an accurate determination of stresses and displacements in the subgrade soil is necessary. The distribution of stresses due to long elastic embankments has been carried out previously by various approximations of the real problem [E-19, E-20, E-21]. The Schwartz-Christoffel transformation has been suggested as a means of transforming the embankment surface into straight lines and subsequently obtaining an analytical solution [E-22]. The finite difference method has been used by Zienkiewicz to obtain solutions for the stress-distribution of an elastic embankment and the analysis was further extended to a special case where embankment material modulus and subgrade modulus differed [E-23]. The finite element method has also been used by Zienkiewicz, Clough, and Finn for similar analyses [E-24, E-25]. These numerical methods present the best available methods of analysis.

In addition, a closed form solution has been developed by Perloff and Baladi [E-26]. to predict the stress distribution within and under an elastic embankment. The assumption of plain strain is used in this analysis, and the solution is found by transferring the region of the embankment where the solution is unknown into a half-space where the solution is easily found. The Cauchy integral formula is used for the determination of stresses.

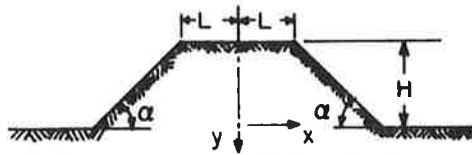
A typical stress distribution within and under an embankment is shown in Figure E-5. In this figure, the contours of the vertical normal stress in dimensionless form, $\sigma_y/\gamma H$ for a typical embankment with, $\alpha = 45^\circ$, $L/H = 3$, and $\mu = 0.3$ are shown. These contour lines only show the effect of embankment weight. The two dashed lines in this figure are stress contours representing the normal loading approximation frequently used for analysis. It should be noted that the stress distribution using this normal loading approximation is independent of Poisson's ratio, μ , whereas the elastic-embankment analysis is dependent upon μ . However, the vertical stresses are extremely insensitive to variations of Poisson's ratio.

From a knowledge of the stress distribution, the material characteristics and the geometrical variables, the total settlement due to static loads can be calculated. The total settlement of roadbed structures due to head load can be divided into an immediate initial settlement and a time-dependent settlement [E-27, E-28] which are discussed in the following sections.

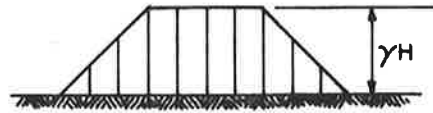
A. Initial Settlement

The application of static or dynamic forces on soil media results in an immediate settlement of the foundation. The initial settlement, as was pointed out earlier, might constitute an important part of the total long-term settlement of the structure. In some instances the initial settlement might exceed the critical limits which can be tolerated by the structure or it might lead to the failure of the soil media.

Various methods of predicting and determining initial settlement have been developed. The analysis for initial settlement requires development of a theory which considers the local yielding condition as well as an appropriate selection of constitutive equations describing the soil responses.



(a) Long symmetric elastic embankment continuous with foundation



(b) Normal loading approximation

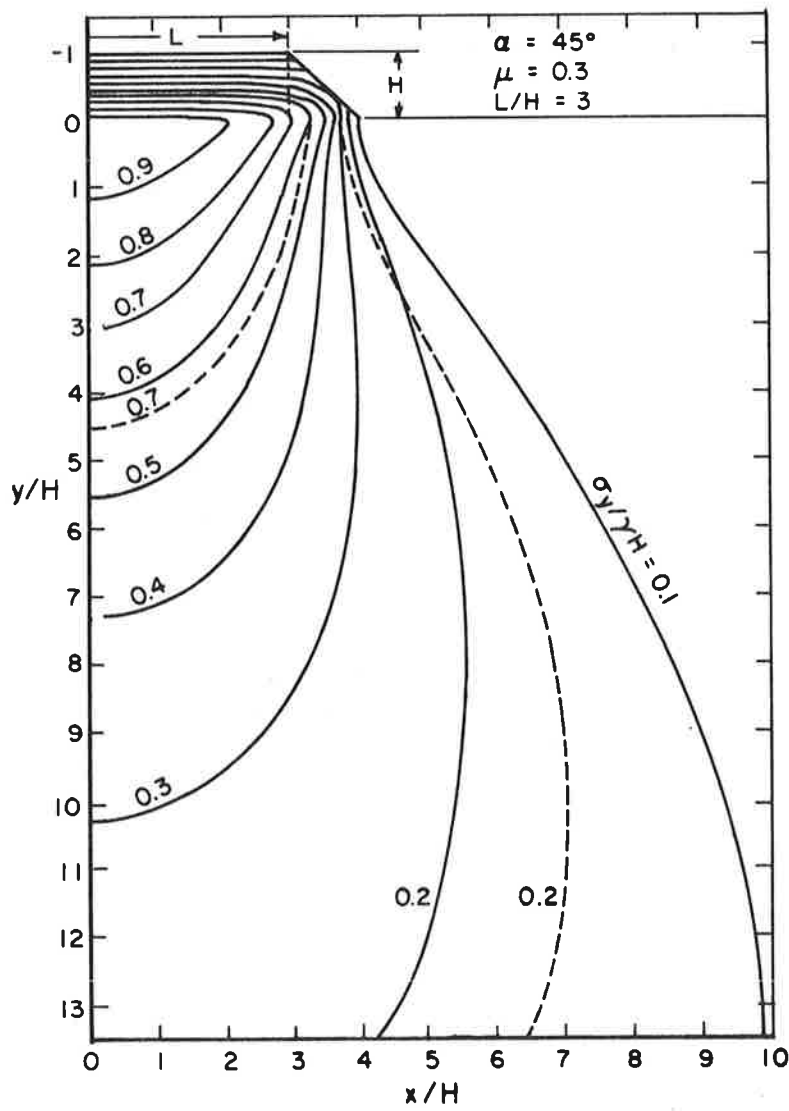


FIGURE E-5. CONTOURS OF VERTICAL STRESS [E-25]

Several approaches have been taken. One approach to a soil deformation model selected for initial settlement analysis is shown in Figure E-6. The model consists of three segments. The analysis pertaining to segment OA is based upon a linear-elastic assumption, whereas segment AB corresponds to local yielding or plastic flow. The part BC of the load settlement diagram is associated with the ultimate failure of the foundation.

For the linear portion of settlement load condition, the initial settlement analysis can be predicted using the elastic theory. Numerous solutions have been presented by Boussinesq, Taylor, Poulos, and Giroud [E-21, E-29 through E-33]. However, the limitation of these elastic analyses is associated with the validity of the assumption pertaining to soil isotropy, homogeneity, and linearity.

In addition to the elastic method of analysis, the stress-path method and finite element methods are often used to predict the initial settlement of soil media. The stress-path method put forward by Lambe [E-34] can indirectly take into consideration the nonlinearity in the stress-strain characteristics of soil. The basis of the stress-path method is that if a laboratory sample is subjected to the same initial stresses and the same stress changes as a soil element in the field, the laboratory sample will experience the same strains as the field element [E-35].

The application of the stress-path method requires the determination of in-situ state of stress and stress changes resulting from the induced loading. Then the laboratory stress-path experiments can be conducted in which field conditions are duplicated to determine the extent of field initial settlement. However, if the stress-strain characteristics of the soil are not known, the in-situ state of stress cannot be determined and the stress-path analysis cannot be carried out effectively.

The finite element method used by Christian [E-36, E-37] might be considered as an extension of the stress-path method and it is applicable to non-linear elastic-plastic systems. In this model, the soil is assumed to be bilinear elastic and exists in an anisotropic state of stress. The analysis requires input information with regard to material characteristics. It is assumed that laboratory measured soil properties can adequately define in-situ soil conditions.

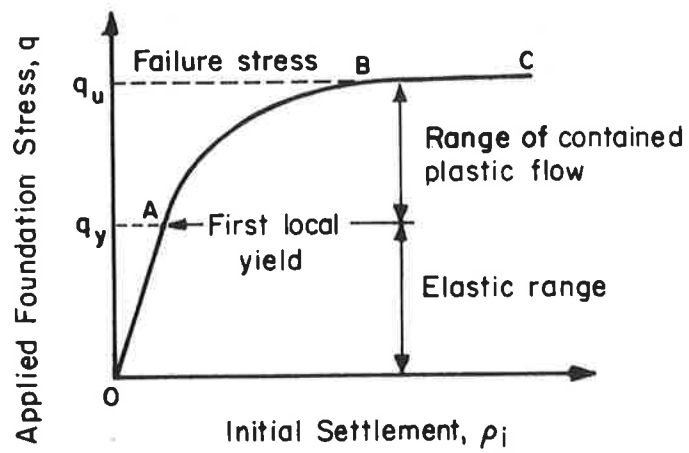


FIGURE E-6. IDEALIZED LOAD-INITIAL SETTLEMENT CURVE

In the finite element method of analysis, all of the material properties of the continuum are retained in the individual elements substituted for the continuum. In this method, as compared to other analyses or solution techniques, the boundary condition, soil properties, and spatial distribution of soil media can be more rationally incorporated in the analysis. It should be noted, however, that these have been two-dimensional models. But three-dimensional finite element capability is currently being developed and this will be quite useful for this type of analysis.

B. Time-Dependent Settlement

The time-dependent settlement is a part of the total settlement of subgrade soil which occurs gradually over an extended period of time. This settlement, or change of volume, which occurs as a result of dissipation of excess water pressure and drainage of water from pore space is known as consolidation. The soil consolidation has been traditionally divided into primary and secondary stages, although in reality and in some recent mathematical models the consolidation process is considered as a continuous phenomena [E-38 through E-41].

In general, the total settlement of a soil media might be expressed as

$$\rho_T = \rho_i + \rho_c$$

where the ρ_i is the initial settlement which was discussed previously. The term ρ_c corresponds to final magnitude and ultimate settlement under consolidation conditions. It is obvious that not only the magnitude of the ultimate settlement is important, but also, the rate of settlement observed that governs the time required to achieve a given degree of consolidation.

The ultimate settlement and the rate of settlement can be determined from the assumptions of consolidation theory. The traditional consolidation theory, credited to K. Terzaghi [E-40], is based on one-dimensional state of volume change. The basic assumptions of Terzaghi's theory of consolidation are: (1) the soil behaves elastically, and the variation of void ratio with pressure is linear, (2) the soil is fully saturated and the water phase is

incompressible, (3) the one-dimensional flow follows Darcy's law, (4) the parameters defined as coefficient of permeability, coefficient of consolidation, etc., are material constants for induced stress increments.

To increase the reliability of settlement analysis, firstly the variability in the material properties should be incorporated in the analysis. The finite element method of analysis is an analytical technique which is capable of incorporating variable material properties. Secondly, these parameters should be presented as probability distribution functions. Monte Carlo simulation can be used to develop an appropriate distribution function for settlement analysis.

Theoretical Models of Consolidation

Two of the most significant approximations of the consolidation theory are the assumption of one-dimensional settlement and the assumption of linear elastic response for soil. A review of published data and documents associated with field observations indicates that the actual rate of consolidation in the field is much faster than predicted by the theory of one-dimensional analysis [E-30]. It is obvious that in many practical cases the geometric conditions are far from one dimensional and that the horizontal dissipation of pore pressure causes an increase in the rate of settlement. These limitations of one-dimensional theory have been noted for a long time, but the use of three-dimensional theory for practical foundation problems appears to have been hindered by a shortage of theoretical solutions covering an adequate range of practical situations.

Davis and Poulos [E-30, E-42] have presented a theoretical approach for three- and two-dimensional consolidation problems which retains the assumptions of linear elastic response, Darcy flow, and isotropy of permeability coefficient. Biot [E-43] has presented a more complete theory of consolidation. The Biot theory also considers in detail the problem of the rate of settlement of a foundation resting on anisotropic elastic materials. It has been reported that three-dimensional effects influencing the rate of settlement are numerous and in many instances, due to the complexity of the problem, these factors have only been treated for the one-dimensional case.

Recently, Sandhu [E-44] has developed a finite element program for the analysis of soil consolidation using Biot's formulations. Postulating a variational principle, he has developed appropriate field equations for fluid flow in saturated porous elastic media. The procedure permits the analysis of consolidation of saturated elastic media for nonhomogenous material properties, complex geometry and boundary conditions. The problems of partial saturation, nonlinear material properties, and incremental loading conditions can also be utilized in this analysis technique. Figures E-7 and E-8 show a comparison of the theoretical methods and the finite element method.

Recent analysis of the consolidation process indicates that although traditionally the consolidation is divided into primary and secondary effects, the process is actually a continuous phenomena. It is commonly noted that during the primary stage of consolidation the settlement is accompanied by dissipation of pore pressure and change of volume, whereas secondary consolidation is characterized by creep under constant effective stress. As a continuous, time-dependent deformation process, the consolidation is affected by the viscous mechanism of soil-water structure, structural viscosity and soil thixotropic effects. The acceptance of a rheological model for the consolidation process dates back to the late 1930's and early 1940's when Merchant and Taylor [E-45, E-46] presented models for soil deformation process.

The rheological treatment of soil media based on effective stress concepts considers two fundamental and interlinked time effects; namely, hydrodynamic lag and viscous creep of the soil skeleton. It should be noted that due to the fact that during consolidation the pore pressure (and hence the effective stresses) varies depending on the distance from the drainage boundaries, the rheological approach requires the treatment of infinitesimal strains in which each element response is integrated over the sample height. This procedure, i.e., integration of the element, was adopted by Taylor and Merchant, Gibson and Lo, and others [E-45, E-47, E-48].

The rheological models presented by these investigators follow the assumption of small strain, linear viscoelasticity. The corresponding mechanical models are shown in Figure E-9. With regard to these model analyses, the most common method of representation assumes an elastic volumetric response accompanied

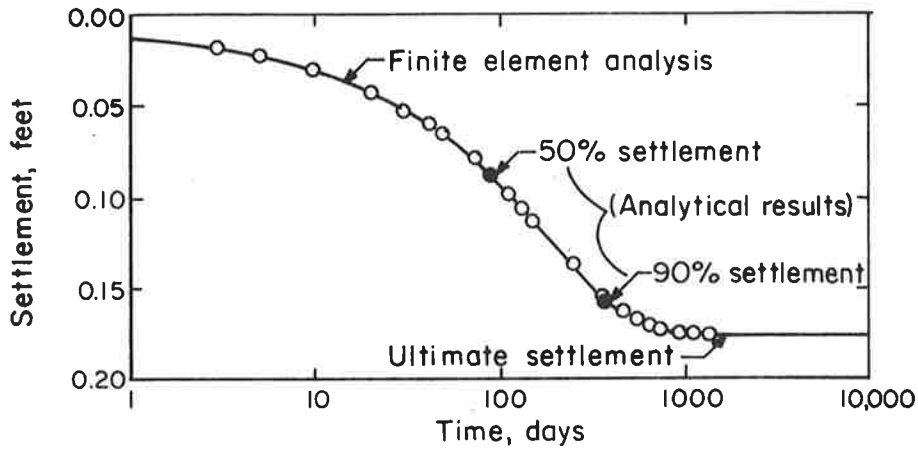


FIGURE E-7. TERZAGHI'S PROBLEM - ONE DIMENSIONAL CONSOLIDATION

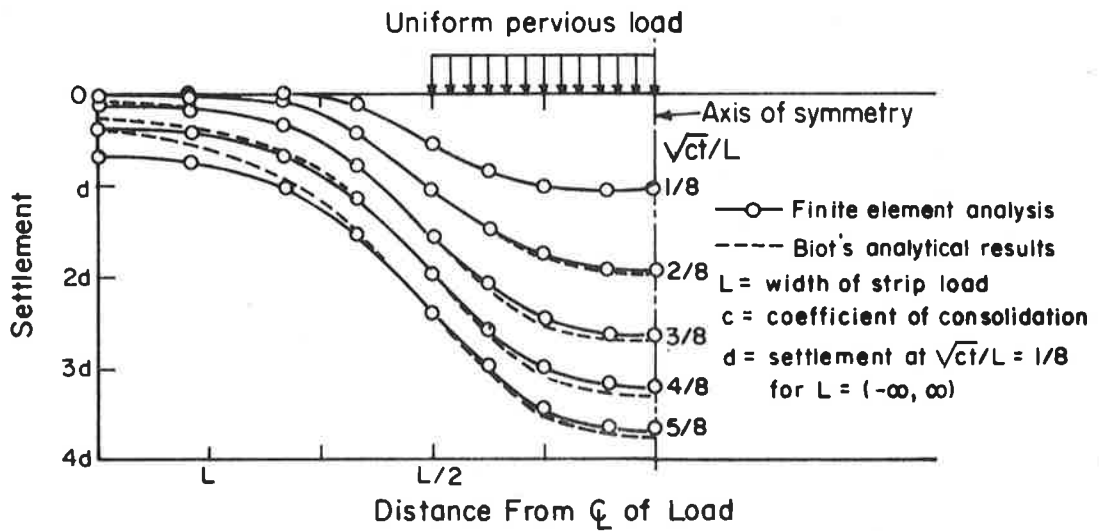


FIGURE E-8. BIOT'S PROBLEM -- PREVIOUS STRIP LOAD ON HALFSPACE (SPATIAL DISTRIBUTION OF SURFACE SETTLEMENTS) [E-44]

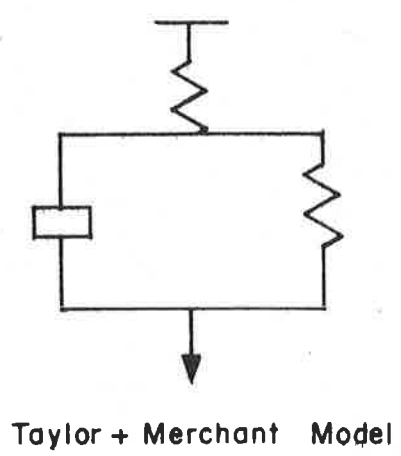
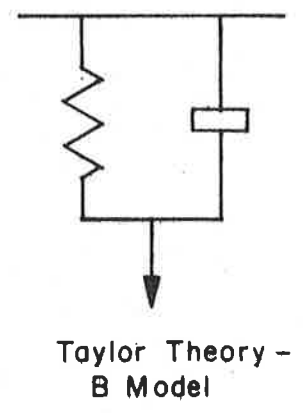
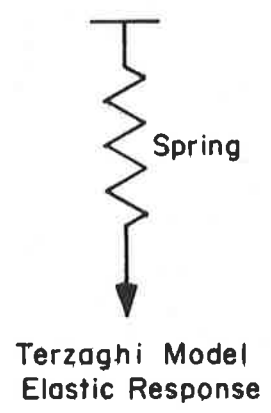
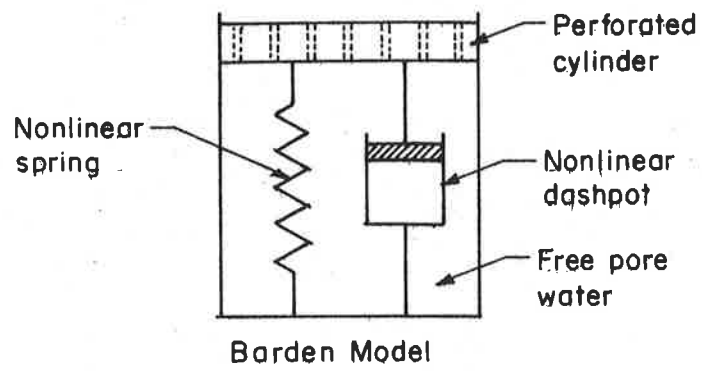


FIGURE E-9. VISCOELASTIC AND ELASTIC MODELS FOR SOIL CONSOLIDATION
E-19

by a deviatoric response represented by a Maxwell element. Other proposed models include a spring in series with a Kelvin, or n-Kelvins in series, or even an infinite number of parameters are used to represent the soil consolidation process.

A more elaborate model has been presented by Barden [E-38] which consists of a nonlinear spring to account for the nonlinear void ratio versus effective stress relation. This model also incorporates a nonlinear viscous element, or dash pot, which is associated with the structural viscosity and thixotropy of the soil-water system.

A detailed analysis of these models indicates that a Kelvin spring (viscoelastic solid) representation initially presented by Taylor-Merchant [E-45, E-46] is too simple to account for the secondary consolidation process as well as the effect of load increment. The multiparameter model consisting of a series of Kelvin elements and a degenerated Kelvin element proposed by Schiffmann [E-47] is aimed at estimating instantaneous settlement of the soil skeleton under effective stresses. The nonlinear Kelvin model, on the other hand, as presented by Barden, results in encouraging agreement with theoretical data and published experimental results.

REFERENCES

- E-1 Barkan, D. D. Dynamics of Bases and Foundations, McGraw-Hill Book Company, New York, 1962.
- E-2 Bazant and Dvorak. "Effect of Vibration on Sand and Measurement of Dynamic Properties", Proceedings of the Sixth International Conference on Soil Mechanics and Foundation Engineering, 1965.
- E-3 Bernhard, R. K. "Static and Dynamic Soil Compaction", Proceedings of the Highway Research Board, XXXI, pp 563-592, 1952.
- E-4 Hardin, B. O. and Mossbarger, W. A., Jr. "The Resonant Column Technique for Vibration Testing of Soils and Asphalts", Proceedings Instrument Society of America, October, 1966.
- E-5 Hardin, B. O. and Music, J. "Apparatus for Vibration of Soil Specimens During the Triaxial Test", American Society for Testing and Materials, STP 392, 1965.
- E-6 Seed, H. B. and Lee, K. L. "Liquefaction of Saturated Sand During Cyclic Loading", Journal of Soil Mechanics and Foundation Engineering, ASCE, Vol XCII, SM6, pp 105-134, 1966.
- E-7 Seed, H. B. and Lee, K. L. "Cyclic Stress Conditions Causing Liquefaction of Sand", Journal of Soil Mechanics and Foundation Engineering, ASCE, Vol XCIII, SM1, pp 47-70, 1967.
- E-8 Seed, H. B. and Idriss, I. M. "Analysis of Soil Liquefaction: Niigata Earthquake", Journal of Soil Mechanics and Foundation Engineering, ASCE, Vol 93, No. SM3, 1967.
- E-9 Seed, H. B. and Lee, K. L. "Dynamics Strength of Anisotropically Consolidated Sand", Journal of Soil Mechanics and Foundation Engineering, ASCE, Vol CXIII, SM5, pp 169-190, 1967.
- E-10 Ellis, W., "Stability and Performance of Slopes and Embankments", ASCE, Soil Mechanics and Foundations Division Conference, Univ. of Calif., August 22-26, 1966, pp 387-407.
- E-11 Youd, T. Leslie, "Densification and Shear of Sand During Vibrations", Journal of Soil Mechanics and Foundation Engineering, ASCE, Vol. 93, SM3, May, 1970.
- E-12. Watanabe, Takashi, "Compaction of Sandy Ground by Vibration-Vibroflotation and Related Problems", Proceedings of Second Asian Region Conference on Soil Mechanics and Foundation Engineering, Vol. 1, pp 406-410, 1963.
- E-13 D'Appolonia, D. J., Whitman, R. V., and D'Appolonia, E., "Sand Compaction With Vibratory Rollers", Journal of the Soil Mechanics and Foundation Engineering, ASCE, Vol. 95, No. SML, pp 263-284, 1969.

- E-14 DiMaggio, F. L. and Sandler, I. "Material Model for Granular Soils", Journal of Engineering Mechanics, ASCE, p 935, January, 1971.
- E-15 Drucker, D. C. and Prager, W., "Soil Mechanics and Plastics Analysis or Limit Analysis", Quarterly of Applied Mathematics, Nov. 10, 1952.
- E-16 Khosla, V. K. "Behavior of Dry Ottawa Sand under Cyclic Loadings", Ph.D. Dissertation, The Ohio State University, 1972.
- E-17 Guirguis, H. R. "Subgrade Compaction and Its Performance Under Traffic Loads", M. S. Thesis, The Ohio State University, 1970.
- E-18 Majidzadeh, K. and Guirguis, H. R. "Fundamentals of Soil Compaction and Performance", A Paper Prepared for Presentation at the 1973 Annual Meeting of the Highway Research Board in Washington, D.C., 1973.
- E-19 Brown, C. B. "Incremental Analysis of Gravitational Stresses in Embankments and Their Effect Upon the Failure of Earth Structures", Ph.D. Dissertation, University of Minnesota, 1962.
- E-20 Carlton, T. A., Jr. "The Distribution of Gravity Stresses in a Symmetrical Trapezoidal Embankment and Its Foundation", Ph.D. Thesis, University of Texas, 1962.
- E-21 Giroud, Jean-Pierre. "Settlement of an Embankment Resting on a Semi-Infinite Elastic Soil", HRB, 223, p 18, 1968.
- E-22 Finn, W. D. L. "Stresses in Soil Masses Under Various Boundary Conditions". Ph.D. Thesis, University of Washington, 1960.
- E-23 Zienkiewicz, O. C. "Stress Distribution in Gravity Dams", Journal Institution of Civil Engineers, Vol 27, p 247, January 1947.
- E-24 Zienkiewicz, O. C. and Gerstner, R. W. "Foundation Elasticity Effects in Gravity Dams", Proc. Institution of Civil Engineers, Vol 19, p 209, 1961.
- E-25 Clough, T. and Chopra, A. K. "Earthquake Stress Analysis in Earth Dams", Journal Engineering Mechanics Division, Proc. ASCE Vol 92, No. EU2, April, 1966.
- E-26 Perloff, W. H. and Baladi, G. Y. "Stress-Distribution Within and Under-Long Elastic Embankment", HRB Record, No. 181, p 12, 1967.
- E-27 Seed, H. B. "Settlement Analysis, A Review of Theory", ASCE, SM2, p 4247, 1965.
- E-28 D'Appolonia, D. J. and Lambe, T. W. "A Method for Predicting Initial Settlement", Journal of Soil Mechanics and Foundations Division, ASCE, Vol 96, No. SM2, Proc. Paper 7167, March, 1970, p 523-545.

- E-29 Burmister, D. M. "Stresses and Displacement Characteristics of a Two-Layer Rigid Base Soil System: Influence Diagrams and Practical Applications", Proceedings of the Highway Research Board, Vol 35, 1956.
- E-30 Davis, E. H. and Poulos, H. G. "The Use of Elastic Theory for Settlement Prediction Under Three-Dimensional Conditions", Geotechnique, Vol XVIII, No. 1, March, 1968, p 67-91.
- E-31 Davis, E. H. and Taylor, H. "The Surface Displacement of an Elastic Layer Due to Horizontal and Vertical Surface Loading", Proceedings Fifth International Conference on Soil Mechanics and Foundation Engineering, Paris, Vol 1, 1961.
- E-32 Poulos, H. G. "Stresses and Displacements in an Elastic Layer Underlain by a Rough Rigid Base", Geotechnique, Vol XVII, No. 4, December, 1967, p 378-418.
- E-33 Davis, E. H. and Poulos, H. G. "Triaxial Testing and Three-Dimensional Settlement Analysis", Proceedings, Fourth Australia-New Zealand Conference on Soil Mechanics, 1963.
- E-34 Lambe, T. W. "Stress Path Method", Journal of Soil Mechanics and Foundations Division, ASCE, Vol 93, No. SM6, Proc Paper 5613, November, 1967, p 309-331.
- E-35 Lambe, T. W. "Methods of Estimating Settlement", Journal of Soil Mechanics and Foundation Division, ASCE, Vol 90, No. SM5, Proc. Paper 4060, September, 1964, p 43-67.
- E-36 Christian, J. T. "Plane Strain Deformation Analysis of Soils", Thesis presented to MIT Department of Civil Engineering, at Cambridge, Massachusetts, in 1966, in partial fulfillment of the requirements for the degree of Doctor of Philosophy.
- E-37 Christian, J. T. "Undrained Stress Distribution by Numerical Methods", Journal of Soil Mechanics and Foundations Division, ASCE, Vol 94, No. SM6, Proc. Paper 6243, November, 1968, p 1333-1345.
- E-38 Barden, L. "Primary and Secondary Consolidation of Clay and Peat", Geotechnique, Vol 18, No. 1, March, 1973.
- E-39 Christie, I. F. "A Re-appraisal of Merchant's Contribution to the Theory of Consolidation", Vol 14, No. 4, December, 1964.
- E-40 Gibson, R. E., England, G. L., and Hussey, M.J.L. "The Theory of One-Dimensional Consolidation of Saturated Clays-Finite Non-Linear Consolidation of Thin Homogeneous Layers", Geotechnique, Vol 17, No. 3, September, 1967.

- E-41 Terzaghi, K. "Undisturbed Clay Samples and Undisturbed Clays", Boston Society of Civil Engineers, Journal, Vol 28, No. 3, p 211-231. Also published in Boston Society of Civil Engineers. Contributions to Soil Mechanics, 1941-1953, Boston, 1953, p 45-65. Also published as Harvard Soil Mechanics Series 16, 1941.
- E-42 Davis, E. H. and Poulos, H. G. "Date of Settlement Under Two- and Three-Dimensional Conditions", Geotechnique, Vol 22, No. 1, 1972.
- E-43 Biot, M. "General Theory of Three-Dimensional Consolidation", Journal of Applied Physics, Vol 12, February, 1941.
- E-44 Sandhu, R. S. "Finite Element Analysis of Seepage in Elastic Media", ASCE, Engineering Mechanics Division, EM-3, p 6615, June, 1969.
- E-45 Taylor, D. W. and Merchant, W. "A Theory of Clay Consolidation Accounting for Secondary Compression", Journal of Math. Phys. Vol 19, 1940.
- E-46 Taylor, D. W. "Research on the Consolidation of Clays", Serial 82, MIT Publication, 1942.
- E-47 Schiffman, R. L., Ladd, C. C., and Chen, A. J. "The Secondary Consolidation of Clay", Symposium Rheology of Soil Mechanics, p 273, 1964.
- E-48 Wahls. "Analysis of Primary and Secondary Consolidation", Proceedings American Society of Civil Engineering, Vol 88, SM6, 1962.

APPENDIX F
REPORT OF INVENTIONS

This report contains a comprehensive review of reported work on rail track structure design and behavior. After a diligent review of the work performed under this contract, it was found that no new inventions, discoveries, or improvements of inventions were made.

INDEX

- Ballast, 10, 24, 58, 61, 90, 157,
 - B-1, E-1
 - Compaction, 12, 64, E-1
 - Depth, 3, 10, 21, 24, 58, 62,
 - 71, 75, 85, 88, C-6, E-1
- Batter, 105, 119
- Bolt Holes, 106, 108, 111, 116, 123,
 - 169
- Cross Ties, 10, 49, B-1, C-1
 - Concrete, 4, 24, 39, 44, 50, 90
 - 101, 103, 137, B-8
 - Design, 52
 - Movement, 51
 - Spacing, 3, 10, 17, 21, 23, 50,
 - 58, 85, 108
 - Wooden, 23, 24, 49, 71, B-8
- Derailment, 14, 94, 95, 98, 99, 108
- Fasteners, 4, 26, 37, 94
 - Bolts, 103, 138
 - Clips, 39
 - Joint Bars, 29, 94
 - Spikes, 37, 104, 137
 - Spring Washers, 48
- Fissures (Rails), 164
 - Star Cracks, 126
- Heat Treatment, 131
- Insulation, 39, 104
- Lateral Dynamics, 14, 27, 29
- Lateral Shift, 100
- Loading, 71
 - Dynamic, 9, 43, 95, 109, 119, 138
 - 158, E-2
 - Lateral, 5, 41, 48, 88, 92
 - Vertical, 5, 14, 16, 32, 41,
 - 48, 71, 91, 94
- Noise, 3, 6, 97, 98, 126, 149
- Rail
 - Corrugation, 6, 8, 99, 104, 139,
 - 141
 - Deflection, 17, 19, 21, 23, 24,
 - 109
 - Failure, 161, A-1
 - Shelling, 161
 - Splitting, 165
 - Voids, 153
 - Web Defects, 169
- Rail Joints, 6, 94, 103, 104, 108
- Rail Overturning, 5, 100
- Rail Wear, 7, 24, 33, 103, 125
 - Abrasion, 126, 143
- Rapid Transit Systems, 23
- Report of Inventions, F-1
- Ride Quality, 3, 14, 97, 99, 126, 131
- Roadbed, 4, 10, 12, 24, 62, 75, 156, E-1
- Slab, 4, 39, 137, 156
- Soil Mechanics, 76, 157, D-1, E-1
 - Dynamics, 77, 85, E-2
- Stress
 - Bending, 3, 10, 14, 17, 19, 23, 27,
 - 32, 55, 116
 - Contact, 4, 164
 - Rail, 3, 23, 24, 28, 164
 - Tensile, 29
 - Thermal, 16, 32, 160
 - Track, 3
- Stress Distribution, 111
- Tie Plates, 48, 139
- Track
 - Curved, 29, 33, 96, 125
 - Tangent, 29, 33, 95, 126, 145

INDEX (Continued)

Track Buckling, 5, 89, 103, 159
Track Construction, 85
Track Design, 3, 14, 24, 85
Track Geometry, 28
 Crosslevel, 3, 155
 Lateral Profile, 3, 155
 Superelevation, 27
 Track Gauge, 3, 155
 Vertical Profile, 3, 155
Track Maintenance, 6, 101, 104, 137, 152,
 155, 160
 Vegetation, 61, 127
Vertical Dynamics, 14
Wheel-Rail Dynamics, 12, 28, 45, 93, 126,
 136, 149, 144